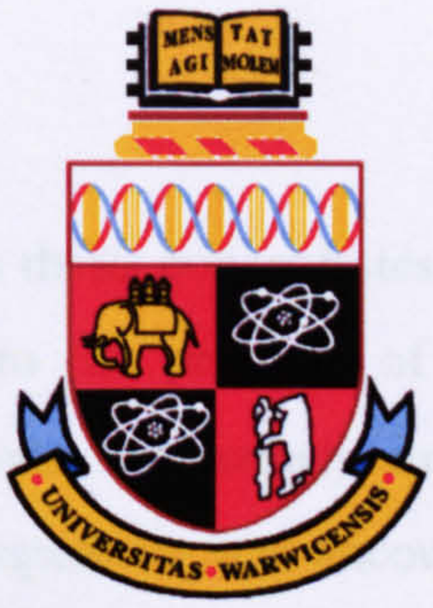

THE UNIVERSITY OF
WARWICK

Congestion management using FACTS controllers

Beatrice Chong

A Thesis submitted for partial fulfilment of the requirements
for the degree of Doctor or Philosophy

University of Warwick, School of Engineering

September 2008

Abstract

The research work described in this thesis concentrates on the application and feasibility of FACTS controllers as a solution to the problem of congestion management. Effective congestion management has become increasingly important since wholesale electricity markets became privatised and competition was encouraged between generation and load (supply) companies. In addition, growth in load demand, planning permission and the need to integrate renewable generation sources will push transmission systems to work closer to their operating limits. Therefore, ensuring future systems are able to sustain these new conditions is a considerable challenge.

The first part of the work focuses on the integration of the bilateral market and steady state FACTS controller models into the interior point optimal power flow (IP OPF) algorithm. The objective is to minimise changes to scheduled bilateral market contracts to provide economic savings for the transmission system operator (TSO) within congested systems. The optimisation technique is able to reduce the level of congestion. Early results identify that congestion is the dominant proportion of the system costs incurred while system losses are of similar levels with and without controller installation. A functional procedure is proposed for fair and easy comparison and a general two-step method is introduced which aims to find optimal location and rating of the installed controller by applying the IP OPF algorithm.

In the latter part, the general two-step method is utilised to assess the performance of FACTS controllers in terms of financial benefits over an average year, and considers daily and seasonal changes in demand. In practice, transmission systems contain thousands of buses therefore a sensitivity-based three-step method is developed to reduce the number of required simulations to find the optimal location and rating of FACTS controllers. The method has been successfully demonstrated on IEEE standard test systems and has the potential to act as a first-step screening technique for practical systems. The last section of this work is concerned with assessing the economic feasibility of FACTS controllers as a congestion management solution by introducing an economic measure - a return index. This measure is used to assess the viability of different locations as it compares the relative cost savings of the TSO to the equipment cost of the controller. In conclusion, the results show that with appropriate location choice, installation of specified FACTS controllers are able to provide a solution to the congestion management problem with realistic payback periods.

Table of contents

Chapter 2: Bilateral electricity market model and the interior point OPF method

Chapter 3: FACTS controllers and the interior point OPF method

Acknowledgements

I would like to thank my primary academic supervisor Dr. Xiao-Ping Zhang for his guidance and supervision during my PhD studies. He has given me the chance to learn in great depth about an ever-changing and interesting subject. He has provided the required foundation to the work presented by the support he has given. I am grateful for the time and opportunity to study and work under his supervision.

I would also like to express my appreciation to my co-supervisor Professor Keith Godfrey for his advice and encouragement during both my postgraduate and undergraduate studies at the University of Warwick.

I am grateful for the support given by AREVA T&D to complete my PhD project. In particular I am indebted to industrial experts, Dr. Liangzhong Yao and Mr. Masoud Bazargan (AREVA T&D) for their invaluable suggestions and the opportunity to have numerous discussions throughout my time as a PhD research student.

Primary financial support was supplied by University of Warwick from funds provided by the Engineering and Physical Science Research Council (EPSRC) Doctoral Training Account, which maintained my academic fees and living expenses. AREVA T&D. provided financial support allowing me to attend international conferences and workshops.

Finally I would like to show appreciation to my parents, my boyfriend Darren and all my friends for their constant support and patience for the entire duration of my PhD studies.

Declaration

Parts of the work contained in this Thesis have been published and or presented in the proceedings of conferences and reports for AREVA T&D:

1. Chong, B., Zhang, X. P., Godfrey, K. R., Yao, L. and Bazargan, M., (2008), "Planning for efficient electricity transmission: Optimal location of Unified Power Flow Controller (UPFC) for congestion management", to be presented at *CIGRE 2008 Session*, Paris, France, 24-29 August.
2. Zhang, X. P., Chong, B., Godfrey, K. R., Yao, L., Bazargan, M. and Schmitt, L., (2007), "Management of congestion costs utilizing FACTS controllers in a bilateral electricity market environment", in *Proceedings of IEEE International Power Tech Conference*, Lausanne, Switzerland, 1-5 July.
3. Chong, B., Zhang, X. P., Yao, L., Godfrey, K. R. and Bazargan, M., (2007), "Congestion management of electricity markets using FACTS controllers", in *Proceedings of IEEE Power Engineering Society (PES) General Meeting*, Tampa, Florida, USA, 24-28 June.
4. Chong, B., Zhang, X. P. and Godfrey, K. R., (2007), "Modelling and methodology developments for solutions of network congestion", report for AREVA T&D, Stafford, April.
5. Chong, B., Zhang, X. P. and Godfrey, K. R., (2006), "A review on congestion management of electricity networks with embedded wind farms", report for AREVA T&D, Stafford, March.
6. Chong, B., Zhang, X. P. and Godfrey, K. R., (2006), "Grid code review", report for AREVA T&D, Stafford, February.
7. Zhang, X. P., Yao, L., Chong, B., Sasse, C. and Godfrey, K. R., (2005), "FACTS and HVDC technologies for the development of Future Power Systems", in *Proceedings of the 1st International Conference on Future Power Systems*, Amsterdam, Netherlands, 14-16 November.
8. Chong, B., (2005), "The impact of wind power on the operation of electricity transmission grids", poster presented at *SET (Science, Engineering & Technology) for Britain, Britain's Younger Engineers at the House of Commons*, London, UK, 6 December.

List of figures

List of tables

List of acronyms and abbreviations

a.c.	Alternating Current
BETTA	British Electricity Transmission and Trading Arrangements
CSC	Converter Static Compensator
d.c.	Direct Current
DNO	Distribution Network Operators
FACTS	Flexible Alternating Current Transmission System
FSC	Fixed Series Capacitor
GA	Genetic Algorithm
GB	Great Britain
GTO	Gate Turn-Off
HVDC	High Voltage Direct Current
IGBT	Insulated Gate Bipolar Transistor
IGCT	Insulate Gate Commutated Thyristor
IP	Interior Point
KKT	Karush-Kuhn-Tucker
NETA	New Electricity Trading Arrangements
OPF	Optimal Power Flow
PC	Active power flow control
PE	Power Exchange
PI	Performance Index
PWM	Pulse Width Modulation
QC	Reactive power flow control
RI	Return Index
RSC	Reduction in System Cost
SO	System Operator
Spec	Specified value
SSR	Subsynchronous Resonance
SSSC	Static Synchronous Series Compensator
STATCOM	Static Synchronous Compensator
SVC	Static Var Compensators
TCPAR	Thyristor-Controlled Phase Angle Regulator
TCSC	Thyristor Controlled Series Compensator
TSO	Transmission System Operator
UK	United Kingdom
UPFC	Unified Power Flow Controller
VSC	Voltage Source Converter

Companies and Organisations

CIGRÉ	International Council on Large Electric Systems
CEC	California Energy Commission
DTI	Department of Trade and Industry
EPRI	Electric Power Research Institute
GBSO	Great Britain System Operator
GE	General Electric
IEEE	Institute of Electrical and Electronic Engineers
OFGEM	Office of Gas and Electricity Markets
PES	Power Engineering Society
SAGD	Siemens AG Database
SP	Scottish Power
S&SE	Scottish and Southern Electric
TEN-E	Trans-European Energy Network

Chapter 1

Introduction

1.1 Background introduction

Growth in load demand, a widening generation mix and an increase in the number of market transactions will put strain on electricity transmission systems. The push to increase the mix of generation to include more renewable energy sources within a competitive market framework will lead to transmission systems functioning closer to their operational limits and increase the probability of system bottlenecks. Therefore, ensuring the transmission system is flexible enough to meet new and less predictable power supply and demand conditions is an inevitable challenge. Figure 1.1 shows a prediction of the future electricity systems, where central and distributed generators will share system operation [Sasse (2006)].

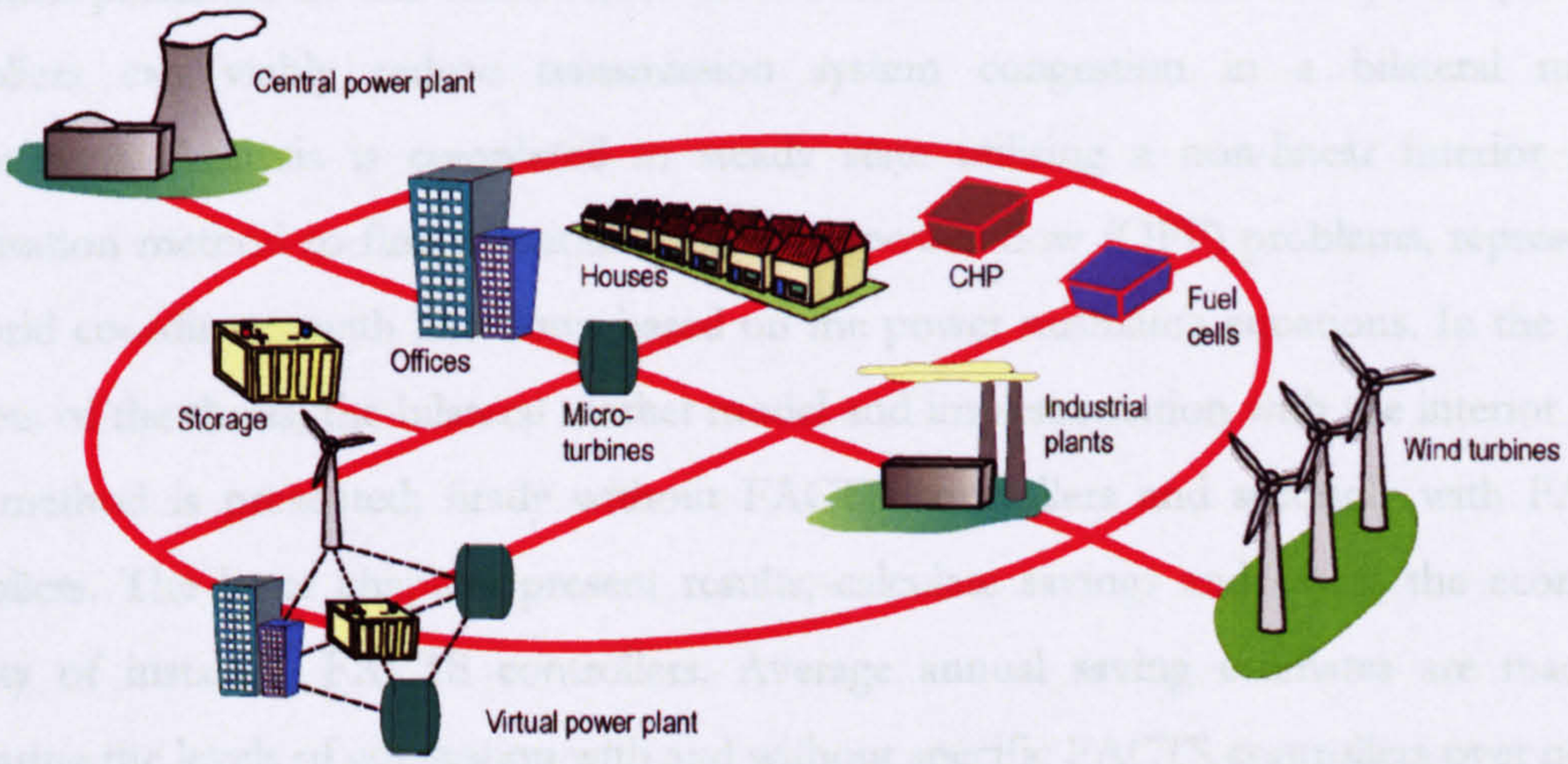

Figure 1.1: Prediction of future electricity systems [Sasse (2006)].

Congestion management has become an increasingly important subject for transmission system operators (TSOs) since the start of privatisation, which in Britain was in the 1990s. At present, as well as adjusting to the deregulated market environment, there is pressure for generation sources to become "greener" to achieve low carbon generation targets and reduce emissions. In the United Kingdom (UK) the aim is to supply 20% of electricity by renewable sources by 2020 [DTI, (2003)] and reduce carbon dioxide emissions by 20% by 2010 [White (2004)] and by 60% [The Guardian (2006)] compared to the 1990 base line by 2050.

The consequences of becoming more reliant on renewable generation for supply, the aging network infrastructure and expected growth in customer demand give TSOs an increasingly complex control task. In the UK, renewable generation sources are onshore and offshore wind, waves, tidal, solar, hydro and biomass (including waste) [DTI (2006)] which, compared to conventional generation from coal, oil, gas and nuclear are considered small-scale generation sources which are connected in a dispersed manner. Furthermore, the governmental push for wind power means the TSOs have to handle intermittent generation. Originally, many transmission systems were designed to handle a unidirectional flow of electricity, transporting energy from large conventional generating stations to distribution companies and major industrial loads. With the oncoming advent of dispersed generation, there will be a blurring of functions between electricity transmission and distribution functions. There will be an increased need for handling the flow of electricity at the transmission level (bulk power) as well as in a bidirectional manner at distribution level; therefore, major updates to control and communication requirements are needed to achieve balancing and real time price information [Nabuurs and Vaessen (2006)].

The work presented in this thesis shows how Flexible AC Transmission System (FACTS) controllers can viably reduce transmission system congestion in a bilateral market environment. Analysis is completed in steady state utilising a non-linear interior point optimisation method to find solutions to optimal power flow (OPF) problems, represented in hybrid coordinates with line flows based on the power mismatch equations. In the initial chapters of the thesis, the bilateral market model and implementation with the interior point OPF method is presented; firstly without FACTS controllers and secondly with FACTS controllers. The latter chapters present results, calculate savings and assess the economic viability of installing FACTS controllers. Average annual saving estimates are made by comparing the levels of congestion with and without specific FACTS controllers over normal daily and seasonal demand levels. In addition, a method to reduce the number of required simulations to find FACTS controller optimal locations is implemented using a sensitivity-based method.

Chapter 1 provides a comprehensive introduction and literature review on the congestion problem and multidisciplinary issues relating the physical running of electricity transmission systems, the statutory requirements and the financial trading arrangements. In Chapter 2, the implementation of the bilateral market model into the interior point OPF method is

presented. Chapter 3 introduces the FACTS controller models and describes the additional equations required for the interior point OPF algorithm. In Chapter 4 the method previously described is put into practice and average annual congestion costs are calculated at all of FACTS controller locations using a variety of orientations. Chapter 5 presents a decision making process, a sensitivity-based method to predict optimal location for FACTS controllers that reduces the number of simulations to find best locations. In Chapter 6, the economic viability of installing FACTS controllers is assessed against the corresponding savings. In Chapter 7, conclusions are presented and the work evaluated.

The remainder of Chapter 1 is arranged as follows, Section 1.2 describes the congestion problem and details the different ways in which congestion can occur. Section 1.3 explains characteristics of electricity as a unique trading commodity and the problems market trading systems have to overcome. Section 1.4 gives an overview of theoretical electricity market models and some of their tools while Section 1.5 examines the predominant bilateral electricity market presently operating in Britain. Section 1.6 investigates possible solutions to the congestion management problem and highlights FACTS controllers as the method investigated. Section 1.7 looks at methods for finding solutions to OPF problems and discusses types of objective functions applied. Section 1.8 concentrates on the interior point method and underlying principles. Section 1.9 presents proposed work described in this thesis and Section 1.10 outlines the thesis structure.

1.2 The congestion problem

Congestion occurs when transfer limits of transmission systems are exceeded [Christie et al. (2000)]. The change from fewer large generating stations to more dispersed smaller generation sites means the control of electricity flow on transmission and distribution networks may continue to become more complex. Moreover, the regular issues such as generation-demand balance, power system quality and power system stability still need to be regulated within an increasingly constrained system. Consequently, increase in penetration of intermittent renewable power will inevitability increase the probability of congestion on the transmission network. Bompard et al. (2003) give a comprehensive definition, "congestion occurs whenever the system state of the grid is characterised by one or more violations of the physical, operational, or policy constraints under which the grid operates in the normal state or under any one of the contingency cases in a set of specified

contingencies. Congestion is associated with a specified point in time." Subsections 1.2.1-1.2.4 gives a description of each constraint.

Prior to deregulation, congestion was less well defined and considered as part of steady-state security where the objective was to ensure limitations were not exceeded at lowest cost. However, as electricity obeys Kirchhoff's laws and not those specified by market contracts, electricity may flow into areas that affects third party utilities, causing security to be traded off against expenditure [Christie et al. (2000)]. In the present deregulated market environments, rules are applied to deal with the occurrence of congestion between market participants in a fair and structured manner. The technique currently used in Britain is presented in Section 1.5.

1.2.1 Physical constraints

Physical constraints refer to limitations on electricity power system components such as substations, transmission interfaces, units of equipment that ensure reliable operation, and control devices. Components primarily include transmission lines and transformers where the thermal or current capacities are their limiting factor [Scottish Hydro-Electric Transmission Ltd. (2004)]. In addition, to ensure predicted or guaranteed lifespan, components must work within their designed rated values. In terms of transmission interfaces, the stability and voltage limits of generators and FACTS controllers must also be considered [Hrehor and Sytsma (2002)]. In this respect, congestion management is the control of the transmission system to obey transfer limits [Christie et al. (2000)].

1.2.2 Policy constraints

Policy constraints refer to the bilateral contracts held between the generating companies and consumers and are concerned with factors such as meeting the needs of the distribution network operator (DNO) and industrial loads in terms of power delivery and quality. The respective generator and load companies must fulfil their bilateral contracts or pay the pre-agreed fines implemented in the contracts. The transmission system operator (TSO) will be aware of the quantity of power and time of delivery for each bilateral contract, as their consultation is required for transmission capacity information and to ensure that no violations of constraints occur [Bompard et al. (2003)].

1.2.3 Operational constraints

Operational constraints refer to meeting the combination of all constraints in the most efficient manner managed by a central power exchange or TSO. Any deregulated electricity market uses a central power exchange or a TSO who is in charge of coordinating scheduled power flows and transactions. The power exchange or TSO will assess if all transactions are viable at least cost and maximum system benefit. Supposing all transactions are carried out without physical constraints being exceeded then a "feasible operating state" is said to exist, this is also known as dispatch. If a feasible operating state is not found, then an operational constraint has been exceeded and the system operator will adjust the transactions to achieve another feasible operating state at least cost. The operational constraint encompasses physical and policy constraints. Therefore, the central power exchange or TSO is responsible for determining the necessary actions for re-dispatch at least cost [Bompard et al. (2003)].

1.2.4 Contingency cases

The system operator must allow for reasonable unforeseen events, contingencies or contingency cases, for example, when a transmission line, transformer or any other component of the transmission network is out of order for a known or unknown reason and period. Contingencies can be scheduled for maintenance purposes, or unscheduled due to an unforeseen incident, adverse weather conditions or a fault. The two most common contingency cases generally considered are the "n-1" and "n-2" cases, where n represents the total number of buses in the area of consideration; and the following digit is the number of unavailable buses. Developed systems are able to handle frequent component outages by design, making more than two buses unavailable to the system a rare event.

1.3 Trading electricity

Most physically traded resources share common characteristics, allowing commodities to be modelled in a similar financial manner. Energy, in the form of electricity however, is a unique trading commodity with special features [Christie et al. (2000)]:

- Electricity cannot be efficiently stored in large amounts;
- Large demand changes can occur within short periods of time throughout the day and depends on weather and seasonal effects;

- Strict functional and control requirements must be adhered to maintain safe and reliable operation. All transmission system components have voltage and current limits that must accommodate normal and unplanned operation to ensure power system security;
- Transportation of electricity from the suppliers to the consumers is defined by a central operator. In pool markets this is usually a power exchange. In bilateral markets this is usually the TSO;
- Any electrical failure has the potential to cause widespread blackouts interrupting the interconnected system and disrupt normal economic trade, industry, transport, manufacturing and domestic life.

Due to these features, one of the most important dilemmas the power industry has to solve is the "transmission management problem", simultaneously making transactions efficient and avoiding congestion. In Christie et al. (2000) a description of how congestion in the vertically integrated structure was previously handled and the problem of congestion are explained from the point of view of market economics and transmission management. It is vital to realise that transmission management integrates economic principles, high voltage power engineering, and Kirchhoff's Law. Electricity will always take the path of least resistance and cannot follow specific diversion routes like road traffic.

1.3.1 Electricity trading problems

Problems in electricity trading can be broadly categorised into two groups, those due to the defining laws of physics and those from society pressures, for example expected continuous uninterrupted supply. Due to the nature of the problems, there is significant overlap between categories. Examples of problems due to the physics of electricity flow loop-flows, dominant-flow and counter-flows which have lead to the invention of financial instruments called contract paths and the action of wheeling (or third party wheeling). Problems associated with society and statutory demands include power system security and reliability of supply, and power quality.

A. Loop-flows

Non-contracted flows of electricity are called loop-flows. They are unscheduled flows of electricity that do not obey the system operator or private contracts held between generator and load [Hydro One (2004)].

B. Contract paths

The contract held between generator and load will often include a description of the power flow over specified paths, known as the "contract path". However, at the time of delivery the scheduled power flow ordered in the contract may only use small fraction of that path. The remaining power is delivered to the load but via loop-flows that interfere with third parties and who will incur costs [Hogan (1992)] due to transmission loss costs (see wheeling).

C. Dominant-flow and counter-flow

Transactions can cause power flow in the same direction as the net flow or in the opposite direction to the net flow along any one line. The flow in the same direction is "dominant-flow" and the flow in the opposite direction is the "counter-flow" [Gross and Tao (2000)]. Counter-flows are an important phenomenon in power system utility [Chowdhury and Bhuiya (2001)] as they can decrease transmission losses, resulting in cost savings. Within the deregulated market, it is important that all parties benefit from resulting counter flows to maintain fair competition.

D. Wheeling or third party wheeling

Wheeling is a consequence of counter-flows. The following example of wheeling is based on one given by Hydro One (2004), a service provided by a transmission system between a buyer or a seller in different jurisdictions. For example, if a utility in area A wanted to sell to area B, it could request that an independent utility wheel the power to area B. The utility would then receive a wheeling fee for doing this. Wheeling is therefore, the process of transferring electrical energy from one party to another with the use of a third party, usually an independent utility. The definition assumes a contracted agreement, however non-contracted wheeling may also occur. In these cases, wheeling becomes a problem as unknown activity could exceed security limitations within a third or more parties.

E. Power system security and power quality

Interruptions in electricity supply can cause inconvenience to domestic customers, and major disruption and economic loss to areas of industry and trade. Therefore, the design of the transmission system must be robust and withstand faults and losses of equipment. The level of robustness, known as power system security, is dependent on the level of acceptable loss of demand between generator and the transmission system [Knight (2001)].

Power quality is another performance aspect of the power system that refers to the consistency of voltage magnitude and frequency. Systems with high power quality will deliver voltage that does not often suffer from sudden step changes and transients [Knight (2001)].

1.4 Electricity market models

The deregulation of the electricity market from a single private entity to a competitive industry meant that mechanisms for fair competition had to be implemented to help prevent market dominance. The concept of " transmission open access" is defined as "access to the transmission system by generators and loads be managed in a non-discriminatory and equitable manner" [Singh et al. (1998)]. The following market models discussed are competitive non-vertically based market structures. Three dominant electricity market structures seen in developed national economies are based on the Pool model, the Bilateral model and the Hybrid model. A description of each follows with reference to two dominant market s tructures, the spot or centralised market and the forward and futures market

1.4.1 Pool model

The pool model is based on "spot pricing" [Bohn et al. (1984) and Schweppe et al. (1988)]. Nodal or "nodes" refers to buses on the transmission system and the theory of nodal spot pricing takes into account the fact that each bus is situated at a different physical location. The objective of nodal pricing is to adjust energy prices in a pool to reflect their locational values (to account for losses and congestion) [Singh et al. (1998)].

The pool model relies on a central power exchange. The role of the exchange is to coordinate the price bids and electrical quantities given by generators in an efficient manner to meet demand and supply. Therefore, the power exchange must be aware of all energy bids given by the generators and suppliers and all network data from each transmission area.

Before the use of a pool market system, generator cost curves were used to meet the demand required for the loads. Bids from generators and loads replaced the cost curves. The power exchange coordinates electricity and decides on the nodal spot prices with

consideration to system constraints to avoid congestion and pay for transmission losses. A consequence of this action is that nodal spot prices at the consumer locations are generally higher than at the generator locations. The difference in price is the "locational price differential" which acts as a net income or for the power exchange. Therefore, all transactions are dealt with through the power exchange and there is no direct contact between the suppliers and consumers. The power exchange acts as an auctioneer, and is able to charge all consumers who wish to participate.

1.4.2 Spot or centralised markets

The pool model is commonly conducted in a spot or centralised market style. The main advantage is immediacy of transactions. This means the producer can sell exact quantities, and consumers purchase desired amounts. The disadvantages are that this market is susceptible to wild price fluctuations and unpredictable changes in spot price. For example, forecasts can influence spot prices, a sudden new find in gas could send prices of gas plunging in the short term; and subsequently, the lack of natural resources will increase the spot price in the long term. Therefore, forward and futures markets have been developed to minimise these disadvantages, described in Section 1.4.4.

1.4.3 Bilateral model

This model involves private transactions between two individuals, the seller (generator) and buyer (supplier, load). The bilateral model relies on multiple bilateral trades and is based upon the belief that free market competition is the best way to achieve competition in an electricity market [Singh et al. (1998)]. Therefore, prices are independently set and not publicly known.

There are different forms of bilateral trades, for example customised long-term contacts, over-the-counter trading and electronic trading [Kirschen and Strbac (2004)]. Customised long-term contracts usually involve large transactions. These are good for big companies that negotiate thousands of MW over months or years. Generators and consumers commonly use the trading over-the-counter type of bilateral trade. These contracts involve standard amounts of energy delivered at set periods of the day or week. Finally, electronic trading is the fastest of the three. These occur shortly before the market closes, this is when generators and retailers fine-tune their position ahead of the delivery period [Kirschen and Strbac (2004)]. This electronic trading market is automated and is theoretically the most

transparent. Quantities of electricity and prices put forward as bids and offers are available to all participants but the corresponding party remains anonymous. The software used for electronic trading is designed to match appropriate bids and offers and list any outstanding ones. This takes place for all periods and new bids and offers are generated for each period.

Bilateral markets models are considered less transparent than pool market models, which may decrease efficiency. Customised long-term contracts are private, but to increase efficiency independent sources may publish summary information about the prices of the over-the-counter bilateral trades without revealing the identity of any party. Together with electronic trading, these publications aid all participants to form a clear idea of the position and trend of the market

1.4.4 Forward and futures contracts and market

Bilateral contracts can be a form of forward or futures contract and therefore they can play a part in forward and futures markets. These markets are secondary markets where parties can manage exposure to fluctuations in spot prices. Similarities between the terms of bilateral, forward and futures contracts include quantity and quality of commodity to be delivered, date of delivery; date of payment following delivery, penalties if either party fails to honour its commitment and price to be paid which is usually estimated on historical information [Kirschen and Strbac (2004)].

For forward markets to exist, enough companies need to be interested in trading for a commodity in advance. Forward contracts are made when a competitive deal is agreed. Assuming there is a standardisation of contracts forward contracts can be brought or sold to another company within the forward market. Forward contracts are backed by physical delivery of the commodity and therefore are held between parties that actually produce or consume the commodity. Futures contracts are not backed by the physical delivery of the commodity and therefore can be held by any party that wishes to participate in the futures markets.

1.4.5 Hybrid model

The purpose of a hybrid model is to combine the most favourable features from the pool and the bilateral models to maximise market competition. A hybrid model can be seen as a pool model that allows private bilateral transactions and physical bilateral contracts. The

present electricity market structure in Britain is a hybrid model with bilateral market dominance.

1.4.6 Summary of market models

The pool and bilateral market models described above are idealised situations and are not often realised in practice. Competitive market structures implemented around the world are forms of hybrid model that incorporate the some sort of pool market and one or more bilateral markets. Bilateral markets are usually less organised and pool markets with a central operator more organised [Soft (2002)]. For example, in Norway, Sweden and Finland a predominant power pool market is employed, this was also true for England and Wales before 2001 [Electricity Pool (2000)]. In the USA both pool and bilateral markets are used in different electricity regions.

1.5 Electricity markets of Great Britain

There are two main markets in deregulated electricity systems, the retail market and the wholesale market. The retail market exists between the supply companies and domestic customers and allows customers to choose their supplier. In Britain over 19 million customers changed suppliers as a result of competition and lower prices since 1999 [National Grid plc. (2008)]. The wholesale electricity market deals with transactions made between generating companies and suppliers, such as distributed network operators (DNO) and industrial loads. An agent, such as a transmission system operator (TSO) aids transactions on the wholesale market and they oversee and coordinate the electricity transactions on the transmission system to meet the forecast demand on a continuous 24 hour basis.

The wholesale electricity market of Britain was introduced to facilitate competition and maintain non-inflated prices for all customers. A motivation behind this included the fact that before deregulation wholesale costs made up around half of all domestic customers' bills [OFGEM (2005)]. The present trading structure of the electricity market of Britain has a hybrid structure with bilateral market dominance. The British Electricity Transmission and Trading Arrangements (BETTA) set the rules for buying and selling for all market participants and Elexon is a non-profit company which administers the wholesale electricity balancing and settlement arrangements for Britain. They are also responsible for the governance of the market processes under the Balancing and Settlement Code [Elexon (2006)], as the Balance and Settlement Code Company. They e stimated that long-term

bilateral transactions make up about 98% of the total electricity traded and the remaining 2% by an auction method [Elexon (2005)].

BETTA was introduced on 1st April 2005. It was an update from the previous New Electricity Trading Arrangements (NETA) by extension of the predominant bilateral transaction model to include the two Scottish transmission systems with those of England and Wales, forming for the first time a Great Britain (GB) wholesale electricity market where the National Grid plc. became the GB System Operator (SO). It took over the operation of the two transmission networks from the owners in Scotland, Scottish Power (SP) and Scottish & Southern Electric (S&SE) while ownership remained with SP and S&SE. Figure 1.2 gives a market overview of BETTA. The continuous running of the transmission system is managed by dividing time into half hour delivery periods.

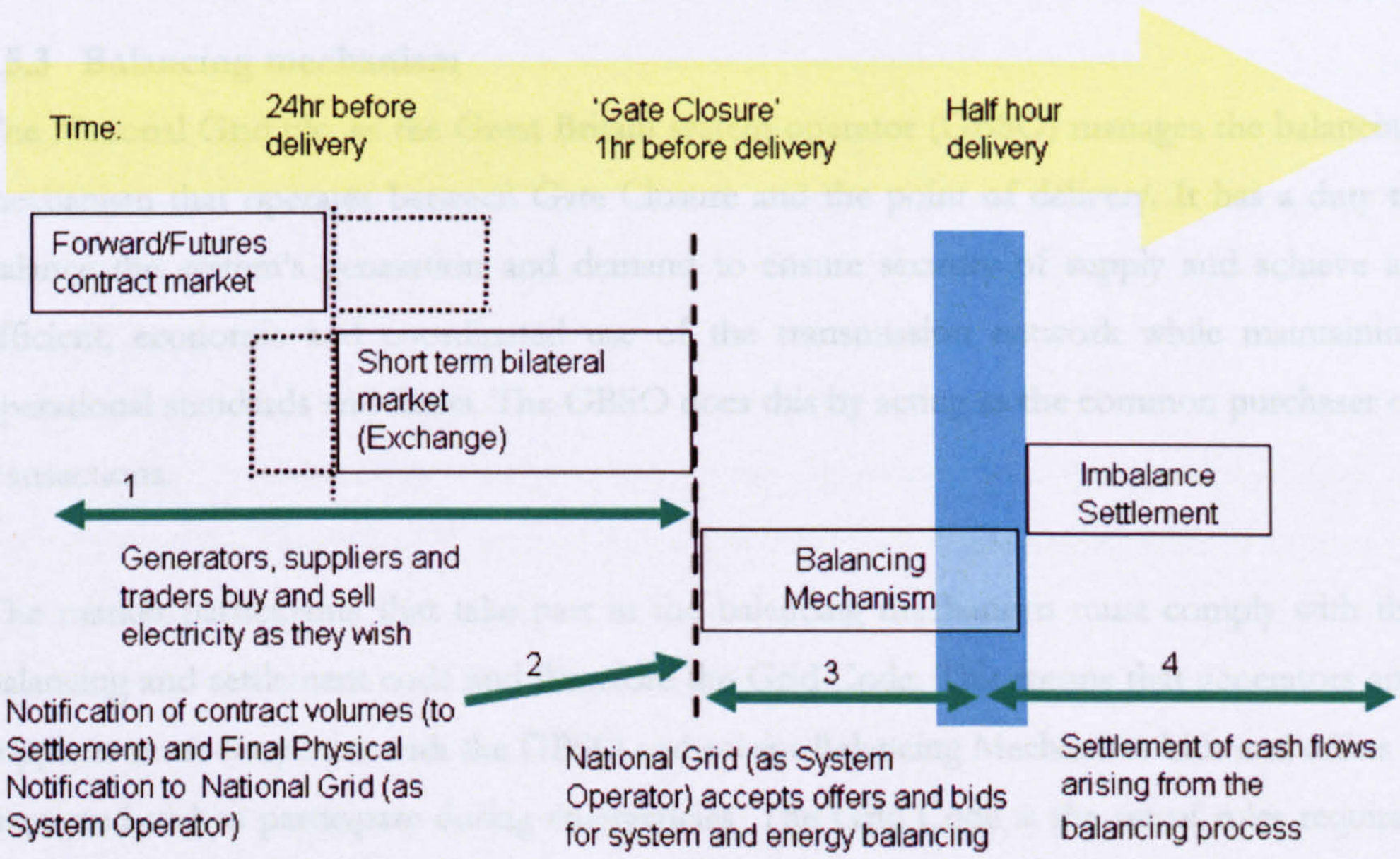

Figure 1.2: Overview of BETTA market structure [National Grid plc. (2007)]

1.5.1 Gate closure

One hour ahead of "real- time" (the point of delivery), gate closure defines the point in time when voluntary market participants notify the SO of their scheduled generation and demand quantities and is the deadline for notification of exiting contracts. In addition, it is the deadline for specified generators to tell the SO their final physical situations.

1.5.2 Bilateral markets

There are two types of bilateral markets, forward and futures market and the short-term bilateral market or power exchanges.

The forward and futures markets typically operate 1 year to 24 hours before point of delivery. These bilateral contracts are made between generators and suppliers to ensure specified quantities of power are transferred at a set price on a specified date. The majority of electricity is traded within this market

Short-term bilateral contracts are generally traded in the period 24 hours before gate closure and operate on an electronic exchange. The quantity of electricity and the time of delivery/consumption are specified with guide prices. This market allows the market participants to ensure that their scheduled supply/demand quantities will be met.

1.5.3 Balancing mechanism

The National Grid plc. as the Great Britain system operator (GBSO) manages the balancing mechanism that operates between Gate Closure and the point of delivery. It has a duty to balance the system's generation and demand to ensure security of supply and achieve an efficient, economic and coordinated use of the transmission network while maintaining operational standards and limits. The GBSO does this by acting as the common purchaser of transactions.

The market participants that take part in the balancing mechanism must comply with the balancing and settlement code and therefore the Grid Code. This means that generators and suppliers must cooperate with the GBSO and accept Balancing Mechanism bids and offers if requested and to participate during emergencies. The Grid Code is the set of rules required by all units, f or example generators, distribution network operators (DNOs) and loads connected to the transmission network.

1.5.4 Imbalances and settlements

Despite the bilateral market contracts, and balancing mechanism efforts to ensure generation meets demand, the contracted and actual amount of power truly transferred may not have been equal. The imbalance quantity is the difference between the contracted and actual quantity delivered/obtained at the load. This results in an imbalance price paid by the

contracted market participants to the GBSO, the price is based on average cost of the marginal 100MWh the GBSO had to purchase to resolve the imbalance at point of delivery [National Grid plc. (2007a)].

1.6 Possible solutions to congestion management

As previously discussed, congestion occurs by any violation of the three types of constraints - physical, policy or operational - therefore any solution to the congestion management problem generally concentrates on one of the constraints while remaining within the limits of the other two. For example, physical constraints are predominantly defined by the equipment limitations and network structure, policy constraints by the market mechanism and model adopted, and operational constraints by the network structure and security limitations.

The limits of operational constraints can depend upon the transmission network structure, which is often dictated by the geography and location of load centres and available generating sites, and security levels by customer demand and statutory requirements. For example the announcement by the EU in 2003 to achieve 10% renewable generation by 2010 [DTI (2003)] required a mandatory update of Britain's Grid Code for renewable generation or "intermittent power sources" such as wind, wave and solar [National Grid plc. (2005)].

As policy constraints are highly dependent on the market structure and market mechanism, ways to reduce congestion by changes in policy are dependent upon the power exchange or TSO of the pool, bilateral or hybrid market respectively. Although hybrid markets consist of bilateral contracts, limitations of the network are also taken into account to prevent over-scheduling and congestion. The ways in which the market can be changed to prevent congestion has been discussed by Christie et al. (2000), where three transmission management approaches in deregulated markets applied around the world are compared. These are the approach used in Britain, Australia, New Zealand, the approach used in Norway, Sweden and Finland, and one approach predominantly used in USA.

One way to overcome physical constraints is by simply adding transmission lines in the areas where congestion occurs, therefore reinforcing the network and increasing the load capacity. However, overhead transmission lines are often perceived as eyesores and damaging to the local environment, therefore planning permission to erect new overhead lines is often difficult to obtain. Another way to overcome physical constraints and simultaneously

improve operational constraints is to use FACTS technology, which is considered a low-environmental impact technology and a viable solution for upgrading transmission system capacity on a long-term cost-effective basis [Hingorani and Gyugyi (2000)] as with time the cost of thyristor valves will continue to decrease [Sood (2004)]. The acronym stands for Flexible AC Transmission System defined as, "alternating current transmission systems incorporating power electronic-based and other static controllers to enhance controllability and increase power transfer capability" [Edris et al. (1997)]. Here, the term "flexible" is defined as "the ability to accommodate changes in the electric transmission system or operating conditions while maintaining sufficient steady-state and transient margins" [Edris et al. (1997)].

1.6.1 FACTS controllers

The integration of FACTS controllers aims to achieve a more flexible power system that can provide control of specific a.c. transmission system parameters. As well as providing increased support in terms of control of the network, FACTS controllers can be built at existing substation sites, therefore requiring less space for construction in comparison to erecting new overhead transmission lines. In addition, they are becoming more compact allowing for modular construction, ease of relocation [Hanson et al. (2002)] and valve units housed in containers result in reduced building costs [Sood (2004)].

The primary control objectives of power systems incorporating FACTS controllers and high voltage direct current or HVDC technologies are [Zhang et al. (2005)],

- to facilitate electricity trading;
- to optimise the overall performance and robustness of the whole electricity system at generation, transmission and distribution levels;
- to react in a timely manner to disturbances to minimise their impact and prevent the system against blackouts and;
- to restore the system to the normal operating level after a disturbance.

Table 1-1 gives an overview of common compensation methods and the proceeding sections provide brief descriptions of each compensation method.

A. Mechanically switched controllers

Mechanical switches operate the connection of passive fixed resistance, inductance or capacitance components. Historically these are the first category of compensators employed

and remain in common use due to their relatively low cost in comparison to FACTS controllers [GE (2000)]. Fixed series capacitor (FSC) compensation and mechanically switched controllers connected in shunt provide direct compensation and can be controlled manually or automatically [Siemens AG (2008) and (2008a)]. These controllers are useful when there are slow changing demand variations, providing steady-state support to control transmission line voltage and decrease overall effective series transmission impedance of the line to increase current and transmitted power respectively. In practice, protection and monitoring of compensators are required. In certain applications mechanically switched capacitors are used in combination with thyristor-based controllers when an acceptable performance can be achieved at lower cost [Mathur and Varma (2002)].

The development of FACTS controllers was motivated in the USA in 1980s because of restrictions on transmission line construction and growth in the amounts of power being exported and imported between regions, and to facilitate transactions between utilities [Song and Johns (1999)]. The two FACTS controller groups listed in Table 1-1 are distinguished by the technology employed. The first group involves thyristor switches and the second, static voltage source power electronic based controllers. FACTS controllers are also composed of fixed resistance, inductance and capacitance components but have more sophisticated control; this allows smaller step changes and the ability to follow a.c. voltage cycles.

Table 1-1: Overview of common compensation methods and FACTS controllers [Zhang et al. (2006)]

Connection type	**Mechanically Switched Controllers (MSC)**	**FACTS controllers**	
	Resistive (R), Inductive (L), Capacitive (C) components and transformers	**Thyristor-based**	**Voltage Source Converter (VSC) based**
Shunt	Switched shunt compensation (L, C)	Static Var Compensator (SVC)	Static Synchronous Compensator (STATCOM)
Series	Switched series compensation (L, C)	Thyristor Controlled Series Compensator (TCSC)	Static Synchronous Series Compensator (SSSC)
Combination shunt and series	-	Phase-shifter	Unified/Interline Power Flow Controller (UPFC/IPFC)

B. Thyristor-based controllers

Thyristor-based controllers are solid-state switching devices, also known as "conventional thyristors" because they have turn-on control capability but no turn-off capability. The

thyristor switches are used for the connection of capacitor and reactor banks composed of fixed components. They can be employed faster than mechanically switched compensators and by control of the on and off periods, the thyristor-based controllers are able to mimic a variable reactive impedance. The switching frequency of thyristor-based controllers is only twice per cycle which limits the speed of achievable control, but they have low switching losses. Unlike the mechanical compensators, the shunt connected Static Var Compensator (SVC) and the series connected Thyristor Controller Series Compensator (TCSC) act indirectly on transmission network. Due to the thyristor switches, the SVC and TCSC are able to respond quicker and return to idle state faster compared to mechanical switches [John (2002)]. The TCSC has several advantages over the FSC including finer and smoother control for compensation, improved protection of capacitor bank and the ability to mitigate subsynchronous resonance (SSR) [Siemens AG (2008b)]. The phase shifter or phase angle regulator aims to maintain the phase angle difference between the sending and receiving-end voltages to increase the actual transmitted power over the line [Song and Johns (1999)].

C. Voltage source converter (VSC) based controllers

Self-commutated, voltage-sourced switching converters based on gate turn-off (GTO) thyristors convert d.c. to a.c. and employ Insulated Gate Bipolar Transistors (IGBT) or Insulated Gate Commutated Thyristors (IGCT). Unlike the thyristor-based controllers they are able to exchange real power directly with a.c. system and are able to control voltage magnitude and phase more precisely than thyristor-based controllers as they have higher switching frequencies, but at the cost of higher switching losses. The high switching frequencies are obtained by use of pulse width modulation (PWM), which allows the controller output to contain only low order harmonic and eliminates higher order harmonics.

The shunt connected STATCOM is analogous to the thyristor-controller SVC. The STATCOM uses input from a d.c. source (charged capacitors or some other energy storage device) and outputs a 3-phase a.c. voltage output that matches the a.c. system in synchronism and in phase. The connection between the controller and transmission system is through a coupling transformer. The series connected SSSC is analogous to the TCSC, in being connected by a series connected transformer so that it is able to inject voltage in parallel with the line voltage to reduce the effective line reactance (by increasing the line-reactance voltage). By combining the STATCOM and SSSC, another controller, the unified power flow controller (UPFC) can be made. The combination of shunt-series connection allows control

of active and reactive power flow in transmission lines. The interline power flow controller (IPFC) is another combination controller that employs two or more SSSC each providing series compensation for a different line and connected by a common d.c. link. The IPFC, similarly to the UPFC, is able to control active and reactive power flow in the compensated line, but in addition it also has the advantage of being able to provide multiple line compensation [Gyugyi (1999) and Zhang (2003a)].

At present, compared to thyristor-based controllers, VSC power levels for application are lower and require higher installation costs. However, with the expected demands on transmission systems it is predicted that costs will improve and technological advances will allow higher voltage and power ratings [Zhang et al. (2006)]. In light of this, this work concentrates on VSC based FACTS controller for the mitigation of congestion.

1.7 Optimal power flow (OPF)

The idea of Optimal Power Flow (OPF) was first discussed in the early 1960s [Carpentier, (1962)]. Initially it was an extension to the conventional economic dispatch problem, where the active power generation balance equation, demand plus losses equals sum of power flows, $\left(P_d + P_{LOSS} - \sum_{i=1}^{N} P_i = 0\right)$ this was extended to include the entire set of system power flow equations; the active power generation limits $\left(P_{g\min} < P_g < P_{g\max}\right)$, and reactive power and voltage magnitudes of buses, generators and other system components. It aimed to determine the optimal values for control variables with consideration to the operational, statutory and control constraints [Dommel and Tinney (1968)]. Operational constraints relate to the electricity network and include power flow constraints, real and reactive generation capacity limits, transmission line capacity limits, generation voltage control, bus voltage limits, transformer tap-ratio control, load shedding, security constraints, and other limits depending on the equipment within the system. Statutory constraints that relate to safety, and legal requirements enforced by relevant governments include contingency constraints endorsed during and after system faults. The term OPF is used as a generic name for a large series of related network optimisation problems [Momoh (2001)]. OPF problems are generally solved iteratively using numerical techniques that stop at a solution that satisfies all stipulated constraints. Digital technology and computer programming has allowed increased speeds for OPF convergence.

There is a variety of solution techniques for solving OPF problems. Each aims to find a solution to a specified objective function by seeking more commonly the minimum, or occasionally the maximum feasible solution point. Examples of the application of OPF include, [Wood and Wollenberg (1996) and Zhang et al. (2006)]

- finding optimum generation pattern for minimum generation cost;
- finding optimal power flow for minimum transmission losses;
- finding optimal power flow for maximisation of total transfer capability;
- finding optimal setting for transmission system components to achieve voltage control transformer tap-ratio adjustments, static VAR compensators, FACTS controllers and other devices;
- assisting planning studies of power networks;
- calculating marginal cost of power at each network bus;
- in deregulated markets, assisting TSO or market operator to;
    - balance system generation and demand,
    - choose the optimal bids and offers from generators and suppliers,
    - obtain market clearing prices,
    - maximise social welfare for all customers.

Since Carpentier proposed his method to solve economic dispatch with bus voltage constraints in 1962, the OPF problem has been defined as an extension to the economic dispatch problem, where the solution seeks the best combination of control variables within the system constraints. A number of OPF techniques exist: the reduced gradient method [Dommel and Tinney (1968)]; linear programming method [Stott and Marinho (1979) and Alsaç et al. (1990)]; quadratic programming methods [Burchett et al. (1984), and Glavitsch and Spoerry (1983)]; Newton methods [Dommel and Tinney (1968), Sun et al. (1984) and Monticelli and Liu (1992)]; and interior point methods [Granville (19940 and Wu et al. (1994)]. The best use of each technique is dependent upon the exact OPF problem. Several OPF review papers have been published [Momoh (1993), Huneault and Galiana (1991) and Chowdhury and Rahman (1990)], a more extensive list can be found in [Zhang et al. (2006)]. The method employed in this work is the interior point programming method.

1.7.1 Interior point programming method overview

The interior point method is so called because it searches for an optimal point through the interior of the feasible solution region [Yan (1997)]. There are three key components to

interior point methods; the Fiacco-McCormick logarithmic barrier method for conversion of a minimisation problem with inequality constraints to an equivalent problem with only equality constraints; the Lagrange minimisation for conversion of a minimisation problem with equality constraints into an unconstrained minimisation problem; and the Newton method for solving the non-linear unconstrained minimisation equations.

Interior point methods can be classified into different variations; the projective method, the affine scaling method, the potential reduction method, and the logarithmic barrier (path following) method [Yan (1997)]. Karmarkar (1984) used the projective method, an affine-scaling method is used in Ponnambalam (1992), the potential reduction method is used in Anstreicher (1991), and the logarithmic barrier methods in Quintana and Torres (1999). The interior point methods have been applied to solve linear, non-linear, convex and non-convex optimisation problems [Quintana et al. (2000)].

One specific strand of the interior-point logarithmic barrier method is the interior point primal-dual method where the logarithmic barrier method is applied to the primal and dual problems simultaneously [Yan (1997)]. The interior-point primal-dual methods can be further subdivided into categories for solving the OPF problem. They are the linear primal-dual interior point OPF, the nonlinear primal-dual interior point OPF, and the predictor-corrector primal-dual interior point OPF.

The primal-dual interior point methods have been applied to linear problems [Marsten et al. (1990), Astfalk et al. (1992), Lustig et al. (1994)] and non-linear problems, [El-Bakry et al. (1996)] and to the electricity OPF problem [Granville et al. (1996)]. A direct primal-dual method, able to solve the inequality and equality constraints simultaneously using the Karush-Kuhn-Tucker (KKT) conditions and Newton method was proposed in Wu et al. (1994), Granville (1994) and Granville et al. (1996). The direct non-linear primal-dual methods has been applied to a variety of problems, including OPF problems with FACTS controllers [Zhang and Handschin (2001) and Zhang et al. (2001)]; minimisation of load shedding [Granville et al. (1996)]; and maximum loadability OPF problem [Irisarri et al. (1997)]. The predictor-corrector primal-dual interior point OPF method is an extension to the primal-dual method. It was developed to reduce the number of iterations for solution convergence but is more computationally complex relative to the other methods stated

[Mehrotra (1992), Ponnambalam et al. (1992) and Irisarri et al. (1997)]. In this thesis, the non-linear primal-dual interior point method is applied to the OPF problem.

1.8 Principles of the interior point method

The interior point method was first proposed by [Karmarkar (1984)] for solving linear optimisation problems, after which it has been applied to a wide variety of problems by adapting it to solve for particular problems. The approach applied here is based on the method applied by Wu et al. (1994), Granville (1994) and Petoussis (2006). There are three key components to interior point methods; the Fiacco-McCormick logarithmic barrier method; the Lagrange minimisation method; and Newton method for solving the non-linear unconstrained minimisation equations.

1.8.1 Fiacco-McCormick barrier method

This method was first proposed in 1960s [Fiacco and McCormick (1968)] but not utilised until the mid-1980s when the interior point method was developing. It converts a minimisation problem with inequality constraints to an equivalent problem with only equality constraints.

Consider the optimisation problem:

$$\min\ f(x)\ \text{subject to}\ x > 0 \tag{1.1}$$

Transform into equivalent problem using Fiacco-McCormick barrier method:

$$\min\ F_\mu(x) = f(x) - \mu \sum_{j=1}^{N_h} \log\left(sl_{x_j}\right) \tag{1.2}$$

$$\text{subject to: } x - sl_{x_j} = 0 \text{ where } sl_{x_j} > 0$$

where,

x is the system variable,

μ is the barrier parameter,

N_h is the total number of inequalities,

sl_{x_j} is the slack variable related to inequality j of system variable x,

j inequality number $j = 1, 2, ..., N_h$.

By adding a non-negative slack variable sl_{x_j} the inequality constraint $x>0$ of problem (1.1) can be converted into an equality constraint. The logarithmic term forces the solution process to begin from a point well within the feasible region while obeying the inequality. The term $\log\left(sl_{x_j}\right)$ will also force the objective function above the limit, $x>0$ when x approaches zero. The contribution of barrier logarithmic term of the objective function $F_\mu(x)$ against the value of the real objective function $f(x)$ is balanced with the barrier parameter μ. As the algorithm reaches its solution the barrier parameter is minimised, that is when $x_j = x^*$, $\mu \approx 0$. At the solution the barrier objective function equals the real objective function, $F_\mu(x) = f(x)$.

1.8.2 Lagrange minimisation with equality constraints

The Lagrange method applied transforms optimisation problems subject to equality constraints into an equivalent unconstrained optimisation problem. Consider an optimisation problem with equality constraints:

$$\textit{Minimise} \qquad F_\mu(x) = f(x) - \mu \sum_{j=1}^{N_h} \log\left(sl_{x_j}\right) \tag{1.3}$$

$$\text{subject to:} \quad x - sl_{x_j} = 0$$

$$g_j(x_j) = 0$$

Equivalent problem in the form of a Lagrange function:

$$L_\mu = F_\mu(x) - \sum_{j=1}^{N_p} \lambda_j g_j(x_j) \tag{1.4}$$

where,

$g_j(x_j)$ is the set of equality constraints,

x vector of primal variables,

λ_j vector of dual variables,

N_p is the total number of primal variables.

Derive Karush-Kuhn-Tucker (KKT) conditions to minimise Lagrange function:

$$\frac{\partial L_\mu}{\partial x_j} = \frac{\partial F_\mu(x)}{\partial x_j} - \sum_{j=1}^{N_p} \lambda_j \frac{\partial g_j(x_j)}{\partial x_j}$$

$$\frac{\partial L_\mu}{\partial \lambda_j} = \frac{\partial F_\mu(x)}{\partial \lambda_j} - \sum_{j=1}^{N_p} g_j(x_j) = 0 \qquad (1.5)$$

The set of minimised unconstrained equations is solved using Newton's method. A simple example for power flow analysis using a typical 3 bus system follows.

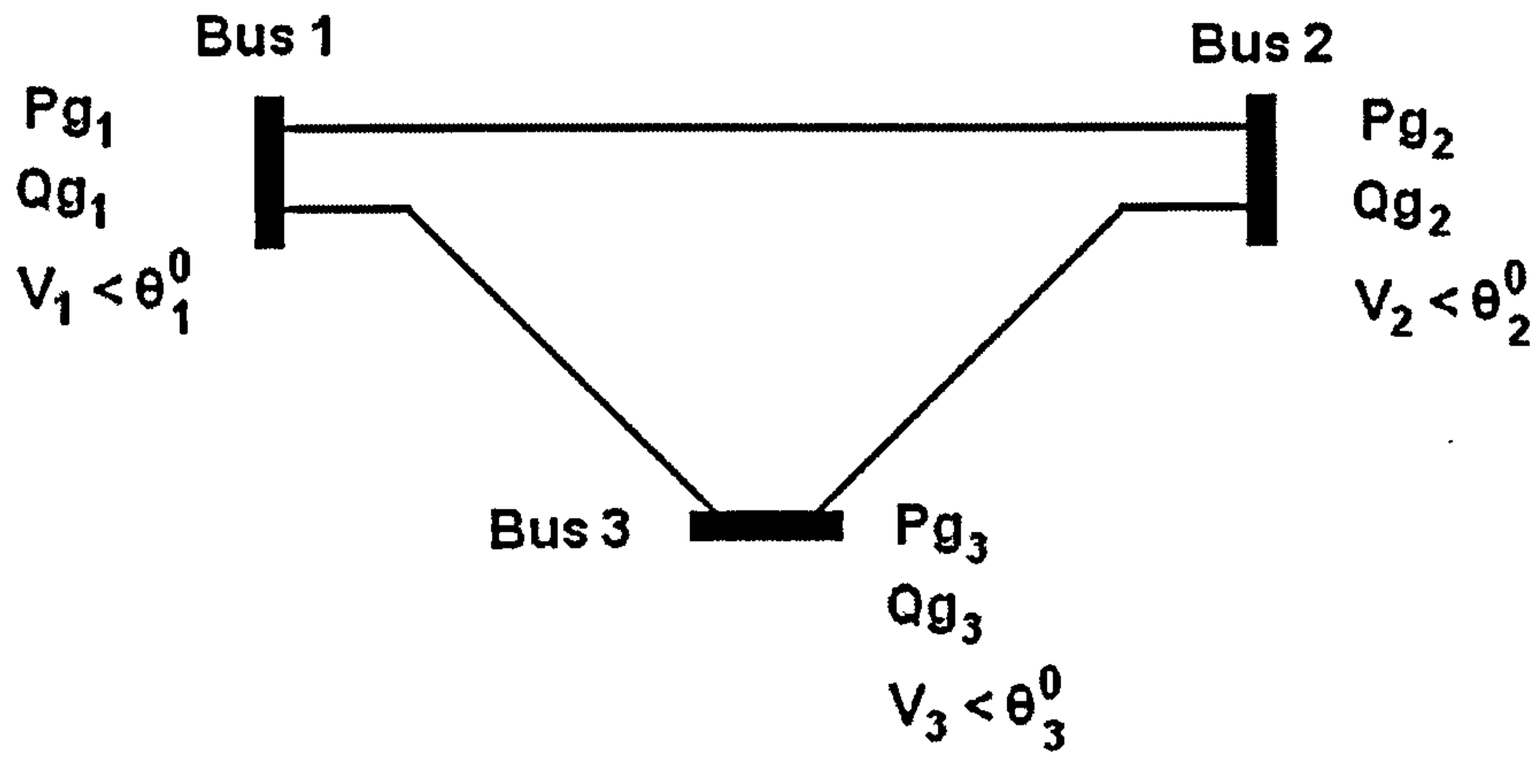

Figure 1.3: 3 bus system

Where system variables correspond to optimisation problem variables in the following manner, with reference to bus 1:

primal variables $x_1 = \left[Pg_1, Qg_1, V_1, \theta_1^0 \right]$

equality constraints $g_j(x_j) = \left[\Delta P_1 , \Delta Q_1 \right]$

slack variables $sl_j = \left[sl_{Pg1}^{\min}, sl_{Pg1}^{\max}, sl_{Qg1}^{\min}, sl_{Qg1}^{\max}, sl_{V1}^{\min}, sl_{V1}^{\max} \right]$

dual variables $\lambda_j = \left[\lambda_{\Delta P_1}, \lambda_{\Delta Q_1}, \lambda_{Pg1}^{\min}, \lambda_{Pg_1}^{\max}, \lambda_{Qg_1}^{\min}, \lambda_{Qg_1}^{\max}, \lambda_{V1}^{\min}, \lambda_{V1}^{\max} \right]$

1.8.3 Newton's method for solving unconstrained minimisation

Newton's method solves the resulting set of equations through approximations using first order derivatives or Jacobian matrix elements. The following approximation attempts to find the solution of $a(x) = 0$, for an initial estimate of x_0:

$$x_{c+1} = x_c - \frac{a(x_c)}{a'(x_c)} \tag{1.6}$$

for $c = \ ,1,2,..,|a(x_c)| < \varepsilon$

where c is the iteration count and ε is a very small number.

Now consider a case where there are several equations with a number of unknowns:

$$a(x) = \begin{bmatrix} a_1(x) \\ a_2(x) \\ \vdots \\ a_n(x) \end{bmatrix}$$

where x is a set of variables $[x_1, x_2, x_3, ..., x_n]$

Elements of the Jacobian matrix are:

$$J(x) = \frac{\partial a_i(x)}{\partial x_j} \tag{1.7}$$

Substitute into (1.6), the Newton method approximation becomes,

$$x_{c+1} = x_c - J^{-1}(x_c)a(x_c) \tag{1.8}$$

Let $x_{c+1} - x_c$ equal to dx then (1.8) becomes,

$$J(x_c)dx = -a(x_c) \tag{1.9}$$

This technique can be applied iteratively to solve a sequence of simultaneous equations. The approximation applied in (1.9) can be applied to an unconstrained minimisation problem. Consider the optimisation problem,

$$\min \ f(x) \qquad \text{subject to } g_j(x_j) = 0$$

The corresponding Lagrange function is,

$$L_\mu = f(x) - \lambda_j g_j(x_j) \tag{1.10}$$

To minimise L_μ consider $a(x)$ from (1.9), set to $a(x) = \frac{\partial L_\mu(x)}{\partial x, \lambda}$ and apply Newton. Assume L_μ is a function of z, where $z = [x, \lambda]$, then the set of equations for Newton's method $a(x)$ is,

$$\begin{aligned}
\frac{\partial L_\mu(z_1)}{\partial z_1} &= \frac{\partial f(z_1)}{\partial z_1} - \lambda_j \frac{\partial g_j(z_1)}{\partial z_1} \\
&\vdots \quad\quad \vdots \quad\quad \vdots \\
&\vdots \quad\quad \vdots \quad\quad \vdots \\
&\vdots \quad\quad \vdots \quad\quad \vdots \\
\frac{\partial L_\mu(z_n)}{\partial z_n} &= \frac{\partial f(z_n)}{\partial z_n} - \lambda_j \frac{\partial g_j(z_n)}{\partial z_n}
\end{aligned} \tag{1.11}$$

Then, the Newton approximation for solving the unconstrained minimisation problem is,

$$\begin{aligned}
\nabla_{z_1}^2 L_\mu(z_1) dz_1 &= -\nabla_{z_1} L_\mu(z_1) \\
&\vdots \quad\quad \vdots \quad\quad \vdots \\
&\vdots \quad\quad \vdots \quad\quad \vdots \\
&\vdots \quad\quad \vdots \quad\quad \vdots \\
\nabla_{z_n}^2 L_\mu(z_n) dz_n &= -\nabla_{z_n} L_\mu(z_n)
\end{aligned} \tag{1.12}$$

where,

n variable number $n = 1, 2, ..., N$ and N total number of system variables,

$\nabla_z L_\mu$ is the gradient of $L_\mu(z)$,

$\nabla_z^2 L_\mu$ is the Hessian of $L_\mu(z)$.

Rearranging (1.12) into matrix form, it can be solved using sparse matrix techniques,

$$\begin{bmatrix}
\nabla_{z_1}\nabla_{z_1} L_\mu & \cdot & \cdot & \cdot & \nabla_{z_1}\nabla_{z_n} L_\mu \\
\cdot & & \cdot & & \cdot \\
\cdot & & & \cdot & \cdot \\
\nabla_{z_n}\nabla_{z_1} L_\mu & \cdot & \cdot & \cdot & \nabla_{z_n}\nabla_{z_n} L_\mu
\end{bmatrix}
\begin{bmatrix} dz_1 \\ \cdot \\ \cdot \\ dz_n \end{bmatrix} =
\begin{bmatrix} -\nabla_{z_1} L_\mu(z_1) \\ \cdot \\ \cdot \\ -\nabla_{z_n} L_\mu(z_n) \end{bmatrix} \tag{1.13}$$

1.8.4 Summary of interior point method

The three key components of the interior point method are as follows,

1. the initial optimisation problem is transformed from a problem with inequality constraints to an equivalent problem with equality constraints using the Barrier method;
2. the problem is then transformed again into an unconstrained optimisation problem using the Lagrange function;
3. the Newton method is applied to solve the series of non-liner unconstrained minimisation equations (1.13) to obtain the final optimal solution.

The iterative technique requires an update of variables after each iteration count,

$$\begin{aligned}
x^{(c+1)} &= x^{(c)} + \alpha_p \Delta x \\
y^{(c+1)} &= y^{(c)} + \alpha_d \Delta y
\end{aligned} \tag{1.14}$$

where,

x is the vector of variables of the primal problem,

y is the vector of variables of the dual problem,

c is the iteration count number,

α_p is the primal step length,

α_p is the dual step length.

Iteration stops after specified parameters reach their tolerance values. The parameters will include the barrier parameter μ and the complementary gap amongst others (defined in Chapter 2, equations (2.87) and (2.88) respectively).

1.9 Work presented in this thesis

The research described in this thesis surrounds finding a solution for optimal location and rating of a FACTS controller to minimise congestion in a bilateral market environment. To achieve this, essential foundation work, implementing a bilateral market model into the interior point OPF algorithm is necessary, after which quantitative results are estimated. The latter part of the thesis deals with a method to predict optimal location, and an assessment of economic viability of FACTS controllers as a practical solution to the congestion management problem.

1.9.1 Bilateral market model implementation using interior point OPF method with FACTS controller models

The minimum cost due to congestion and real power system losses are found with the aid of a non-linear interior point based algorithm, proposed to solve the bilateral electricity market model with full a.c. network representation. Based on the a.c. transmission model the algorithm takes into account all operating aspects including real and reactive power generation capacity limits, bus voltage limits, real and reactive transmission line constraints, system losses, transformer tap-ratio control and FACTS controller real and reactive power and bus voltage limits. The overall amount of demand and generation can be specified at the start of every iteration.

This allows for direct comparison between systems pre and post FACTS controller installations at a variety of demand levels, permitting analysis at a single instant in time and

for extension to typical daily and seasonal load changes. Extrapolation of these results can give an average performance over an annual period.

1.9.2 Generalised two-step method for finding optimal location and rating of FACTS controller

A standard system set-up procedure and generalised method for finding the optimal location and rating of a specified FACTS controller is proposed and implemented in Chapters 2 and 3. The set-up accounts for reasonable levels of generation with respect to the demand required and the system losses. This gives initial generation quantities for the reference system. The generalised method is simple and effective. It is able to identify the location of congested transmission lines, system costs, differentiate between contributions from congestion and system losses, identify attributes at individual buses and lines and give the necessary FACTS controller output power rating, voltage magnitude and angle at individual demand levels.

1.9.3 Sensitivity analysis for optimal FACTS controller location

The disadvantage of the simple generalised method is that it is unable to identify the optimal FACTS controller installation location without testing all feasible system sites. Extension of this method to the three-step method incorporating sensitivity analysis allows fast determination of FACTS controller location by elimination of whole system areas and gives a significant reduction in the number of simulations. The method applied in the second step, acts as a screening process, and only requires a single simulation of system base case at the specified demand level. It has been successful for indicating locations that require series compensation with a combined series-shunt controller.

1.9.4 Economic analysis of FACTS controller investment costs

A general economic analysis framework is presented using the "Return Index" (RI). The RI indicates a period of time that relates the congestion cost savings made by FACTS controllers with the cost required due to equipment rating. Three independent, commonly cited sources form the basis of the applied FACTS controller price information; these were published by IEEE Power Engineering Society (PES), Siemens, and the California Energy Commission. Economic benefit is often disregarded in theoretical analyses, as firm quantitative benefits are difficult to measure, although a few attempts have been made, for example in EPRI (1999) and Mwanza et al. (2007). In the case studies presented here, a measure of congestion cost

savings is known, therefore, the RI acts as the final decision making factor for optimal FACTS controller location.

1.9.5 Major contributions of this work

The major contributions of this work can be summaries as follows:

a) Implementation of bilateral market objective function into non-linear interior point algorithm using a.c. power flow network model, hybrid coordinates and a reduced Newton matrix with FACTS controller steady state models;
b) Determination of the impact of FACTS controllers on congestion and real power system loss costs within a bilateral electricity market environment over daily, seasonal and annual time periods;
c) Proposal of a generalised two-step method for finding optimal FACTS controller location and rating for minimisation of congestion and real power system loss costs;
d) Proposal a sensitivity-based three-step method for finding optimal FACTS controller location and rating for minimising congestion and real power system loss costs to reduced the number of required simulations;
e) Determination of a method to assess the economic viability of FACTS controller equipment costs for solving the congestion management problem.

A. Advantages of primal-dual interior point method

The primal-dual non-linear interior point method has been applied to solve a wide variety of OPF problems, and on large scales. Several primal-dual methods have been performed that show that primal-dual logarithmic barrier method is possibly one of the top methods in comparison to the other interior point methods [Petoussis (2006)]. In addition, it is able to find optimal results efficiently and accurately [Astfalk et al. (1992)]. The biggest advantage of the interior point methods in general, is that it can handle large sets of equality and inequality constraints [Irisarri et al. (1997)] and converge within a sensible number of iterations [Wood and Wollenberg (1996)].

B. Advantages of a.c. model representation

Full a.c. electricity network and FACTS controller representation is preferred over simplified d.c. representation because some basic electricity network properties are overlooked when the d.c. power flow approximation model is applied [Hogan (1993)]. As the d.c. model can

only provide a linear approximation to the true behaviour of the electricity network, the advantages of implementing the a.c. model are:

- Realistic a.c. transmission network line flows;
- Reactive power generation and reactive line flows;
- Real and reactive transmission network losses;
- Bus voltage limits, bus voltage control and voltage regulations;
- Real and reactive generation and transmission line capacity limits;
- Modelling of transformer tap-ratio control.

References using d.c. power flow models [Singh et al. (1998) and Yuen and Lo (2003)] are unable to represent reactive power and control functions such as voltage control, transformer tap-ratio control and network losses because transmission line inductance and capacitance are not considered.

The proposed non-linear interior-point algorithm and the bilateral market model has the potential for use in several practical applications, a few examples are summarised here.

i. The model would be of interest to TSOs for rapidly identifying congested transmission lines once amounts of power delivery agreed in bilateral contracts are made known, therefore allowing time for balancing adjustments. It also has the capability to assess a wide combination of demand and generation schemes at individual bus and system levels.

ii. The model is useful for FACTS controller manufacturers by assessing the impact of controllers in theoretical and real situations during the steady state. It is able to identify the changes experienced at all buses and give an indication of required rating for power flow control.

iii. The model is of interest to TSOs and manufacturers simultaneously as the sensitivity-based analysis is a useful first step screening technique. It is able to assess the viability of FACTS controllers on any transmission network suffering from congestion problems.

iv. The proposed methods can be useful for predicting likely locations of FACTS controller on expected future power systems with integration of renewable generation sources.

C. Advantages of investigating a variety of load levels

Studies applying steady state analysis often refer to a single specified instant in time, after all transients have cleared. Analysis applied here extends single instants to multiple ones and

each demand level is compiled to assess the characteristics of Britain's system over typical daily load curves experienced in the summer and winter seasons. This gives refined details and further extrapolation has allowed estimates indicating annual savings.

D. Advantages of the sensitivity-based method

Application of sensitivity analysis to the base case system allows for rapid elimination of the majority of FACTS controller installation locations. Furthermore, only one simulation is required at each specified demand level. A practical approach, it has use as a first step screening process, especially applicable for large-scale system.

1.10 Structure of thesis

The remaining chapters are arranged as follows:

In Chapter 2 the bilateral market model and implementation with interior point OPF method is presented. It includes an explanation of the bilateral market model characteristics and assumptions made with reference to the market trading system of Britain. This is followed by a description of the three main components of the interior point OPF method namely Fiacco and McCormick's barrier method for eliminating inequalities, Lagrange function for optimisation with equalities, and Newton's method for solving non-linear equations. The chapter also includes definition of terms used for assessing the case studies presented at the end of Chapter 2 and in subsequent chapters.

Chapter 3 introduces three main voltage sourced converter (VSC) based FACTS controllers; the shunt connected Static Compensator (STATCOM), series connected Static Synchronous Series Compensator (SSSC) and the combination, shunt-series connected Unified Power Flow Controller (UPFC). An overview of the features of each controller, functional models and steady state equivalent circuit diagrams are given. The steady state equivalent circuit models allow derivation of power flow equations and constraints. The inclusion of FACTS controller models increases the size and complexity of the previously presented OPF problem, therefore a description of the additional variables are highlighted with respect to the inequalities, equalities, Lagrange function and Newton equations. Finally, the FACTS controller models are tested on a small 4 bus system and the IEEE 14 bus system to show that costs due to increased load demands can successfully be reduced.

In Chapter 4, the initial results presented in Chapter 3 are extended to test the ability of FACTS controllers to reduce costs on an annual, seasonal and daily demand basis based on the load profiles of Britain in 2004/5. The STATCOM is tested at three locations at all viable system transmission line locations *i-j*; firstly at the ends of the lines at bus *i*; secondly at the opposite end at bus *j* and finally at the midpoint of the transmission line *i-j*. The UPFC is tested at four sites on each transmission line namely shunt branch connected to bus *i*, shunt branch connected to bus *j*, series branch connected to bus *i*, and series branch connected to bus *j*. The main conclusion is that significant congestion mitigation is made when the FACTS controller is appropriately sited.

Chapter 5 is concerned with the decision making process of FACTS controller allocation for congestion and cost minimisation. A method of sensitivity analysis is applied to attempt to predict the optimal location for FACTS controllers for optimal congestion mitigation. The aim of the analysis is to reduce the number of system simulations required to identify the optimal location. The method successfully identifies the area in which the UPFC can reduce congestion by change in transmission line impedance.

Chapter 6 explores the financial constraints of installing FACTS controllers to reduce system congestion. After a brief literature review, an averaged equipment price is assumed and cost is calculated by the required controller ratings. A measure called the Return Index (RI) is used to evaluate the most economical FACTS controller solution by comparing the annual savings made by congestion mitigation and equipment cost of the controller. In addition to the sensitivity measure applied in Chapter 5, this eases the decision making process required for investment choices.

In Chapter 7, the conclusions, main contributions of work and the potential for further work are described.

Finally, in the Appendices, the analytical mathematical formulae required for the applied methods presented in Chapters 2 to 5 are detailed.

Chapter 2

Bilateral electricity market model and the interior point optimal power flow method

2.1 Introduction

This Chapter introduces the bilateral market model applied to all case studies in this thesis and the implementation of the model into the interior point optimal point flow (OPF) algorithm. The interior point OPF (IP OPF) algorithm has been adapted to minimise the cost of congestion in a bilateral electricity market environment. The transmission system model includes standard equipment found on a transmission network; transmission lines, transformers, generators and loads. This chapter forms the foundations to the implemented algorithm and results.

In Section 2.2 the bilateral market employed on the electricity transmission system of Britain; first introduced in Chapter 1, is summarised. Section 2.3 introduces the bilateral market model and characteristics of the model discussed, include active power generation changes, calculation of system loss, system congestion and relationship with the total system cost incurred. In Section 2.4 the necessary steps to implement the bilateral market model into the IP OPF method are described and Section 2.5 discusses implementation issues. Section 2.6 provides numerical results involving test systems, a 4 bus system and IEEE 14 bus system. Finally in Section 2.7 conclusions are drawn.

2.2 Bilateral market

In a bilateral market, buyers and sellers of a commodity trade independently of a third party. Electricity trading in Britain is performed by a predominant bilateral trading system defined by BETTA (British Electricity Transmission and Trading Arrangements) [Elexon (2005)]. Due to this, an objective function that reflects the characteristics of a bilateral market is used. The objective function allows the simulation to produce results that can be analysed from the perspective of the transmission system operator (TSO), who is in charge of balancing generation and demand while minimising congestion costs, the process is also known as re-dispatch, [Bompard et al. (2003)].

In wholesale bilateral electricity markets the TSO is the centrepiece of electricity trading on the transmission system. Its role is to ensure that all demand is met in the most efficient manner. The priority is to maintain all bilateral contracts to prevent having to pay generators to change their scheduled output levels. Electricity is a unique commodity because the transmission system it is transported upon has a finite capacity and strict safety regulations. The use of storage is not standard procedure. Therefore, some electricity bilateral transactions must be changed near to the time of delivery to ensure demand is constantly met. Within BETTA this is done using the "Balancing Mechanism" which operates between the time of Gate Closure and point of delivery (real-time) and is run by the National Grid plc. as its role as Great Britain System Operator (GBSO) [National Grid (2007a)].

2.3 Mathematical model

In order to balance system generation and demand the TSO will pay generators to change their future generation output to avoid congestion. This debit is considered to be the congestion cost. The mathematical model to represent a bilateral market is simultaneously a measure of congestion and system loss costs. The model is linear and defined by,

$$\min f(x) = \sum_{i}^{Ng}\left[Cg_i^{+}Pg_i^{+}\right] + \sum_{i}^{Ng}\left[Cg_i^{-}Pg_i^{-}\right] \tag{2.1}$$

where,

$f(x)$ bilateral market objective function, system cost, unit: \$/h,

x vector of system variables $x = \left[t_i, P_{g_i}^{+}, P_{g_i}^{-}, Q_{g_i}, \theta_i, V_i\right]$,

$P_{g_i}^{+}$ per unit (p.u.) increase in MW generation from generator at bus i, $P_{g_i}^{+} \geq 0$,

$P_{g_i}^{-}$ per unit (p.u.) decrease in MW generation from generator at bus i, $P_{g_i}^{-} \geq 0$,

$C_{g_i}^{+}$ cost per unit (price) for increase in MW generation, \$/MWh, $C_{g_i}^{+} \geq 0$,

$C_{g_i}^{-}$ cost per unit (price) for decrease in MW generation, \$/MWh, $C_{g_i}^{-} \geq 0$,

N_g total number of system generator buses,

i bus index number 1, 2, …, N_g.

2.3.1 Incremental active power generator changes at individual bus *i*,

At each generator bus i, there can only be one of three situations,

1. No change in scheduled generation: $P^{+}_{g_i} = P^{-}_{g_i} = 0$,

2. Increase in scheduled generation: $P^{+}_{g_i} > 0$ and $P^{-}_{g_i} = 0$,

   - active power output: $Pg_i = Pg_i^0 + Pg_i^+$, (2.2)

3. Decrease in scheduled generation: $P^{+}_{g_i} = 0$ and $P^{-}_{g_i} > 0$,

   - active power output: $Pg_i = Pg_i^0 - Pg_i^-$, (2.3)

where, Pg_i^0 is the scheduled MW generation from generator at bus i, $P^{0}_{g_i} \geq 0$.

When there is no system congestion only situations one or two can exist, and when there is system congestion only situations two and three exist.

2.3.2 System active power generation changes

For the system base case, with no FACTS controller, there are two conditions; system without congestion and system with congestion. For the system as a whole, the individual changes at each generator bus are summed from bus i to N_g.

P_{g_i} - per unit MW generation

The system active power generation output P_g after changes from scheduled generation is the total MW generation at each generator bus i,

$$\sum_{i}^{N_g}\left[P_{g_i}\right] = \sum_{i}^{N_g}\left[P^{0}_{g_i}\right] + \sum_{i}^{N_g}\left[P^{+}_{g_i}\right] - \sum_{i}^{N_g}\left[P^{-}_{g_i}\right] \quad (2.4)$$

$P^{+}_{g_i}$ - per unit increase in MW generation

The system active power generation increase P_g^+ is the increase in MW generation at each generator bus i. The total system increase in MW from output to scheduled generation is,

$$\sum_{i}^{N_g}\left[P^{+}_{g_i}\right] = \sum_{i}^{N_g}\left[P_{g_i}\right] - \sum_{i}^{N_g}\left[P^{0}_{g_i}\right] \quad (2.5)$$

It is related to system loss and system congestion by the following equation,

$$\sum_{i}^{N_g}\left[P_{g_i}^{+}\right] = P_{LOSS} + P_C \tag{2.6}$$

$P_{g_i}^{-}$ - per unit decrease in MW generation

The system active power generation decrease P_g^- is the decrease in MW generation at each generator bus *i*. The total system decrease in MW from scheduled generation is shown in equation (2.7). It also defines whether congestion is present on the system, as the magnitude of system active power generation decrease is equal to the amount of system congestion P_C.

$$\sum_{i}^{N_g}\left[P_{g_i}^{-}\right] = \sum_{i}^{N_g}\left[P_{g_i}^{+}\right] - P_{LOSS} \tag{2.7}$$

Substitute equation (2.5),

$$\sum_{i}^{N_g}\left[P_{g_i}^{-}\right] = \sum_{i}^{N_g}\left[P_{g_i}\right] - \sum_{i}^{N_g}\left[P_{g_i}^{0}\right] - P_{LOSS} \tag{2.8}$$

$$\left|\sum_{i}^{N_g}\left[P_{g_i}^{-}\right]\right| = P_C \tag{2.9}$$

Table 2-1 summarises the relationships between objective function, congestion, loss, system cost, per unit MW generation increase and decrease.

Table 2-1: System active power generation and system cost relationship.

Condition 1: No congestion	**Condition 2: With congestion**
No congestion $P_C = 0$	Congestion $P_C > 0$
$f(x) > 0$	$f(x) > 0$
$P_{LOSS} > 0$	$P_{LOSS} > 0$
$\sum_{i}^{N_g}\left[P_{g_i}^{+}\right] > 0,\ \sum_{i}^{N_g}\left[P_{g_i}^{+}\right] = P_{LOSS}$	$\sum_{i}^{N_g}\left[P_{g_i}^{+}\right] > 0,\ \sum_{i}^{N_g}\left[P_{g_i}^{+}\right] = P_{LOSS} + P_C$
$\sum_{i}^{N_g}\left[P_{g_i}^{-}\right] = 0$	$\sum_{i}^{N_g}\left[P_{g_i}^{-}\right] > 0,\ \left\lvert\sum_{i}^{N_g}\left[P_{g_i}^{-}\right]\right\rvert = P_C$

P_C - per unit MW system congestion

System congestion P_C is defined by the per unit incremental MW change required to meet system demand excluding system losses. It is the system per unit incremental MW increase

minus the per unit system MW loss, which is equal in magnitude to the incremental MW decrease. The sum of MW generation is conserved because demand is constant.

$$P_C = \sum_{i}^{N_g}\left[P_{g_i}^{+}\right] - P_{LOSS} = \left|\sum_{i}^{N_g} P_{g_i}^{-}\right| \tag{2.10}$$

P_{LOSS} - per unit MW system loss

The per unit system loss is defined by the per unit system MW generation P_g subtracted by the per unit system MW demand P_d,

$$P_{LOSS} = \sum_{i}^{N_g}\left[P_{g_i}\right] - \sum_{i}^{N_d}\left[P_{d_i}\right], \tag{2.11}$$

where, system MW generation is defined by equation (2.4), and N_d is the total number of loads on the system. For most systems, only transmission lines and transformers contribute to system loss as it is assumed that other components are fewer in number and therefore do not supply a significant contribution.

2.3.3 Objective function characteristics and assumptions

Equation (2.1) is the bilateral market objective function implemented to minimise system cost, composed of system congestion and loss. On a real system there will always be system loss. Therefore, the system cost will always be positive unless the sum of scheduled generation has already accounted for system losses.

When there is system congestion, the system cost to the TSO is dependent on incremental increase in generation to overcome congestion and system losses,

$$\sum_{i}^{N_g}\left[Cg_i^{+} Pg_i^{+}\right] + \sum_{i}^{N_g}\left[Cg_i^{-} Pg_i^{-}\right] \geq 0 \tag{2.13}$$

It is assumed that all generators are rational and will charge the TSO more to increase active power output than to decrease,

$$Cg_i^{+} > Cg_i^{-} \tag{2.14}$$

This assumption extends to include all generating units on the system, therefore,

$$\sum_{i}^{N_g}\left[Cg_i^+ Pg_i^+\right] > \sum_{i}^{N_g}\left[Cg_i^- Pg_i^-\right] \tag{2.15}$$

2.4 Application of bilateral market model into interior point OPF method

The basic task of any OPF method is to obtain a viable optimised steady state solution of an electric power system, and at the same time to minimise or maximise a chosen objective function subject to physical and operational constraints. Usual objective functions include mathematical expressions for the minimisation of the total generating cost, the active power losses or the maximisation of the total transfer capability and the social welfare [Zhang and Handschin (2001)]. In the following formulations for the non-linear IP OPF an objective function for the minimisation of the total operating cost in a bilateral market is employed. The objective function is as first stated in equation (2.1):

$$\min\ f(x) = \sum_{i}^{N_g}\left[Cg_i^+ Pg_i^+\right] + \sum_{i}^{N_g}\left[Cg_i^- Pg_i^-\right] \tag{2.16}$$

where, $x = \left[\theta_i, V_i, P_{g_i}^+, P_{g_i}^-, Q_{g_i}, t_i\right]^T$ vector of system variables,

θ bus voltage angle,

V bus voltage magnitude,

$P_{g_i}^+$ bus per unit increase in MW generation,

$P_{g_i}^-$ bus per unit decrease in MW generation,

Q_{g_i} bus per unit reactive power generation,

t_i transformer tap ratio.

(2.16) is subject to the following constraints: non-linear equality constraints, vector $g(x)$,

$$\Delta P_i(x) = P_{g_i}^0 + P_{g_i}^+ - P_{g_i}^- - P_{d_i} - P_i(\theta, V) = 0 \tag{2.17}$$

$$\Delta Q_i(x) = Q_{g_i} - Q_{d_i} - Q_i(\theta, V) = 0 \tag{2.18}$$

where, $\Delta P_i(x)$ bus active power mismatch equations,

$\Delta Q_i(x)$ bus reactive power mismatch equations,

$P_{g_i}^0$ bus per unit scheduled MW generation,

P_{d_i} bus per unit MW demand,

Q_{d_i} bus per unit reactive power demand,

$P_i(\theta,V)$ active power injection at bus i,

$Q_i(\theta,V)$ reactive power injection at bus i,

and (2.16) is subject to non-linear inequality constraints,

$$h_j^{\min} \le h_j(x) \le h_j^{\max} \tag{2.19}$$

where, $h(x)$ is a vector of functional inequality constraints including line flow and voltage magnitude constraints, simple inequality constraints of variables such as generator active power, generator reactive power, transformer tap ratio.

2.4.1 Elimination of inequality constraints

The IP OPF method employs the logarithmic barrier method for optimisation with inequalities proposed by Fiacco and McCormick (1968) and Marsten et al. (1990) to solve the non-linear optimisation problem. The logarithmic barrier method transforms the non-linear inequality constraints into equivalent equality constraints by the addition of non-negative slack variables. The optimisation problem defined by equations (2.16)-(2.19) is transformed into the equivalent optimisation problem defined by equations (2.20)-(2.24):

$$\text{Objective: } \min\left\{ f(x) - \mu \sum_{j=1}^{N_h} \ln(sl_j) - \mu \sum_{j=1}^{N_h} \ln(su_j) \right\} \tag{2.20}$$

Subject to the following equality constraints:

$$\Delta P_i(x) = 0 \tag{2.21}$$

$$\Delta Q_i(x) = 0 \tag{2.22}$$

$$h_j(x) - sl_j - h_j^{\min} = 0 \tag{2.23}$$

$$h_j(x) + su_j - h_j^{\max} = 0 \tag{2.24}$$

where,

N_h total number of system inequalities, j inequality number 1, 2, …, N_h,

$\mu > 0$ barrier parameter, a positive number forced to minimise iteratively,

$sl_j > 0$ lower non-negative slack variable,

$su_j > 0$ upper non-negative slack variable.

2.4.2 Lagrange function for optimisation with equalities

The Lagrange function for an optimisation problem with only equalities is defined by equations (2.20)-(2.25):

$$L_\mu = f(x) - \mu \sum_{j=1}^{N_h} \ln(sl_j) - \mu \sum_{j=1}^{N_h} \ln(su_j) - \sum_{i=1}^{N} \lambda_{p_i} \Delta P_i - \sum_{i=1}^{N} \lambda_{q_i} \Delta Q_i - \sum_{j=1}^{N_h} \pi l_j (h_j - sl_j - h_j^{\min}) - \sum_{j=1}^{N_h} \pi u_j (h_j + su_j - h_j^{\max}) \quad (2.25)$$

The Lagrange method deals with the objective function and equalities by the addition of a Lagrange multiplier for each constraint, where, λ_{p_i}, λ_{q_i}, πl_j, πu_j are the Lagrange multipliers for the constraints of equations (2.21)-(2.25) respectively and N is the total number of system buses, i bus number 1, 2, …, N.

2.4.3 First order KKT conditions

The Karush-Kuhn-Tucker (KKT) first order conditions state that the partial differentials of the Lagrange function with respect the system, slack and Lagrange multiplier variables (x, λ_{p_i}, λ_{q_i}, sl_j, su_j, πl_j, πu_j) are equal to zero.

$$\nabla x_\alpha L_\mu = \nabla x_\alpha f(x) - \sum_{i=1}^{N} \nabla x_\alpha \Delta P_i \lambda_{p_i} - \sum_{i=1}^{N} \nabla x_\alpha \Delta Q_i \lambda_{q_i} - \sum_{j=1}^{N_h} \nabla x_\alpha h_j \pi l_j - \sum_{j=1}^{N_h} \nabla x_\alpha h_j \pi u_j = 0 \quad (2.26)$$

$$\nabla \lambda_{p_i} L_\mu = -\Delta P_i = 0 \quad (2.27)$$

$$\nabla \lambda_{q_i} L_\mu = -\Delta Q_i = 0 \quad (2.28)$$

$$\nabla \pi l_j L_\mu = -\left(h_j - sl_j - h_j^{\min}\right) = 0 \quad (2.29)$$

$$\nabla \pi u_j L_\mu = -\left(h_j + su_j - h_j^{\max}\right) = 0 \quad (2.30)$$

$$\nabla sl_j L_\mu = \mu - sl_j \pi l_j = 0 \quad (2.31)$$

$$\nabla su_j L_\mu = \mu + su_j \pi u_j = 0 \quad (2.32)$$

where,

$$x_\alpha = [x, \lambda_{p_i}, \lambda_{q_i}, sl_j, su_j, \pi l_j, \pi u_j]$$

α system variable number $= 1, 2, ...2N + 3N_g + N_t$,

N total number of system buses,

N_g total number of generator buses,

N_t is the total number of transformers.

First order KKT conditions (equations (2.26) - (2.32)) formulae are listed in Appendix I and a corresponding list of first and second order derivatives is presented in Appendix V.

2.4.4 Newton's method for solving nonlinear equations

The power flow problem is defined by non-linear equations and is thus a non-linear problem. To utilise Newton's method the first order KKT equations (2.26)-(2.32) need to be linearised. The Taylor series expansion is applied. In general this can be expressed as,

$$f(w) = f(w_o) + f'(w_o)\Delta w + f''(w_o)\Delta^2 w + f'''(w_o)\Delta^3 w + ... \tag{2.33}$$

If: $f(w) = \rho'(w)$

and $\rho'(w) = \left[\nabla_x L_\mu, \nabla_{\lambda_{p_i}} L_\mu, \nabla_{\lambda_{q_i}} L_\mu, \nabla_{\pi l_j} L_\mu, \nabla_{\pi u_j} L_\mu, \nabla_{s l_j} L_\mu, \nabla_{s u_j} L_\mu\right]$

By ignoring terms higher than the second order, equation (2.33) becomes,

$$\rho'(w) = \rho'(w_o) + \rho''(w_o)\Delta w \tag{2.34}$$

From the 1st order KKT conditions equation (2.34) is equal to zero,

$$\rho'(w) = \rho'(w_o) + \rho''(w_o)\Delta w = 0 \tag{2.35}$$

so, $$-\rho'(w_o) = \rho''(w_o)\Delta w \tag{2.36}$$

Applying this relationship to equations (2.26) to (2.32) results in the following expressions for the Newton equation:

$$-\nabla_{x_\alpha} L_\mu = \left[-\sum_{i=1}^{N} \nabla_x (\nabla_x \Delta P_i)\lambda_{p_i} - \sum_{i=1}^{N} \nabla_x (\nabla_x \Delta Q_i)\lambda_{q_i} - \sum_{j=1}^{N_h} \nabla_x (\nabla_x h_j)\pi l_j - \sum_{j=1}^{N_h} \nabla_x (\nabla_x h_j)\pi u_j \right]\Delta x$$

$$-\sum_{i=1}^{N} \nabla_{x_\alpha} \Delta P_i \Delta\lambda_{p_i} - \sum_{i=1}^{N} \nabla_{x_\alpha} \Delta Q_i \Delta\lambda_{q_i} - \sum_{j=1}^{N_h} \nabla_{x_\alpha} h_j \Delta\pi l_j - \sum_{j=1}^{N_h} \nabla_{x_\alpha} h_j \Delta\pi u_j \tag{2.37}$$

$$+\sum_{i=1}^{N_g} \nabla_x \nabla_x f(x)\Delta x$$

$$-\nabla \lambda_{p_i} L_\mu = -\sum_{i=1}^{N} \nabla_x \Delta P_i \Delta x \tag{2.38}$$

$$-\nabla \lambda_{q_i} L_\mu = -\sum_{i=1}^{N} \nabla_x \Delta Q_i \Delta x \tag{2.39}$$

$$-\nabla \pi l_j L_\mu = -\sum_{j=1}^{N_h} \nabla_x h_j \Delta x + \Delta s l_j$$

$$-\nabla \pi u_j L_\mu = -\sum_{j=1}^{N_h} \nabla_x h_j \Delta x - \Delta s u_j \tag{2.40}$$

$$-\nabla \pi u_j L_\mu = -\sum_{j=1}^{N_h} \nabla_x h_j \Delta x - \Delta s u_j \tag{2.41}$$

$$-\nabla_{sl_j} L_\mu = -sl_j \Delta \pi l_j - \pi l_j \Delta s l_j \tag{2.42}$$

$$-\nabla_{su_j} L_\mu = su_j \Delta \pi u_j + \pi u_j \Delta s u_j \tag{2.43}$$

The formulae for the elements in the matrix set of Newton equations ((2.37) - (2.43)) are listed in Appendix I and a corresponding list of first and second order derivatives is presented in Appendix V.

The linearisation means that the Newton equations (2.37)-(2.43) can then be expressed in a symmetrical matrix form, as suggested by Granville (1994).

$$\begin{bmatrix} Sl^{-1}\Pi l & 0 & I & 0 & 0 & 0 & 0 \\ 0 & -Su^{-1}\Pi u & 0 & -I & 0 & 0 & 0 \\ I & 0 & 0 & 0 & -\nabla h & 0 & 0 \\ 0 & -I & 0 & 0 & -\nabla h & 0 & 0 \\ 0 & 0 & -\nabla h^T & -\nabla h^T & H & -Jp^T & -Jq^T \\ 0 & 0 & 0 & 0 & -Jp & 0 & 0 \\ 0 & 0 & 0 & 0 & -Jq & 0 & 0 \end{bmatrix} \times \begin{bmatrix} \Delta sl \\ \Delta su \\ \Delta \pi l \\ \Delta \pi u \\ \Delta x \\ \Delta \lambda p \\ \Delta \lambda q \end{bmatrix} = \begin{bmatrix} Sl^{-1}\nabla_{sl} L_\mu \\ Su^{-1}\nabla_{su} L_\mu \\ -\nabla_{\pi l} L_\mu \\ -\nabla_{\pi u} L_\mu \\ -\nabla_x L_\mu \\ -\nabla_{\lambda p} L_\mu \\ -\nabla_{\lambda q} L_\mu \end{bmatrix} \tag{2.44}$$

where,

H is the matrix of second order differential terms with respect to vector x,

$$H(x, \lambda p, \lambda q, \pi l, \pi u) = \nabla_x \nabla_x f(x) - \sum_{i=1}^{N} \nabla_x \left(\nabla_x \Delta P_i(x)\right) \lambda_{p_i} - \sum_{i=1}^{N} \nabla_x \left(\nabla_x \Delta Q_i(x)\right) \lambda_{q_i} - \sum_{j=1}^{N_h} \nabla_x \left(\nabla_x h_j(x)\right) \pi l_j - \sum_{j=1}^{N_h} \nabla_x \left(\nabla_x h_j(x)\right) \pi u_j \tag{2.45}$$

J_p and J_q are the Jacobian matrices of first order partial derivatives,

$$J_p(x) = \left[\frac{\partial \Delta P_i(x)}{\partial x}\right] = \nabla_x \Delta P_i(x) \tag{2.46}$$

$$J_q(x) = \left[\frac{\partial \Delta Q_i(x)}{\partial x}\right] = \nabla_x \Delta Q_i(x) \tag{2.47}$$

$Sl = diag(sl_j)$ diagonal matrix of lower slack variables (2.48)

$Su = diag(su_j)$ diagonal matrix of upper slack variables (2.49)

$\Pi l = diag(\pi l_j)$ diagonal matrix of lower dual variables (2.50)

$\Pi u = diag(\pi u_j)$ diagonal matrix of upper dual variables (2.51)

The Hessian matrix, H can also be expressed in matrix form:

$$\begin{bmatrix} H_{t_i t_i} & 0 & 0 & 0 & H_{t_i \theta_i} & H_{t_i V_i} \\ 0 & H_{P_{g_i}^+ P_{g_i}^+} & 0 & 0 & 0 & 0 \\ 0 & 0 & H_{P_{g_i}^- P_{g_i}^-} & 0 & 0 & 0 \\ 0 & 0 & 0 & H_{Q_{g_i} Q_{g_i}} & 0 & 0 \\ H_{t_i \theta_i} & 0 & 0 & 0 & H_{\theta_i \theta_i} & H_{\theta_i V_i} \\ H_{t_i V_i} & 0 & 0 & 0 & H_{\theta_i V_i} & H_{V_i V_i} \end{bmatrix} \times \begin{bmatrix} \Delta t \\ \Delta P_{g_i}^+ \\ \Delta P_{g_i}^- \\ \Delta Q_{g_i} \\ \Delta \theta_i \\ \Delta V_i \end{bmatrix} = \begin{bmatrix} -\nabla_t L_\mu \\ -\nabla_{P_g^+} L_\mu \\ -\nabla_{P_g^-} L_\mu \\ -\nabla_{Q_g} L_\mu \\ -\nabla_{\theta_i} L_\mu \\ -\nabla_{V_i} L_\mu \end{bmatrix} \tag{2.52}$$

where,

$$x = \left[t_i, P_{g_i}^+, P_{g_i}^-, Q_{g_i}, \theta_i, V_i\right]$$

Note that the bilateral market objective function is a linear function.

$$f(x) = \sum_i^{Ng}\left[Cg_i^+ Pg_i^+\right] + \sum_i^{Ng}\left[Cg_i^- Pg_i^-\right]$$

from which,

$$\frac{\partial f(x)}{\partial P_{g_i}^+} = C_{g_i}^+ \text{ and } \frac{\partial f(x)}{\partial P_{g_i}^-} = C_{g_i}^- \tag{2.53}$$

Therefore, all second order derivatives with respect to $P_{g_i}^+$ and $P_{g_i}^-$ are equal to zero,

$$H_{P_{g_i}^+ P_{g_i}^+} = \frac{\partial^2 L_\mu}{\partial P_{g_i}^+ \partial P_{g_i}^+} = 0 \text{ and } H_{P_{g_i}^- P_{g_i}^-} = \frac{\partial^2 L_\mu}{\partial P_{g_i}^- \partial P_{g_i}^-} = 0 \tag{2.54}$$

All equations for each element of the Newton matrix are presented analytically in Appendix I and Appendix V. The derivations of power mismatch equations are presented in Appendix II.

2.4.5 Operational constraints

The bilateral market IP OPF has a total of five double-sided inequality constraints, having both upper and lower limits and one single-sided inequality constraint, having an upper operational limit only. They are,

1. per unit incremental MW generation increase $P_{g_i}^{+}$: $h_{P_{g_i}^{+}}^{\min} \le P_{g_i}^{+} \le h_{P_{g_i}^{+}}^{\max}$,
2. per unit incremental MW generation decrease $P_{g_i}^{-}$: $h_{P_{g_i}^{-}}^{\min} \le P_{g_i}^{-} \le h_{P_{g_i}^{-}}^{\max}$,
3. reactive power generation Q_{g_i}: $h_{Q_{g_i}}^{\min} \le Q_{g_i} \le h_{Q_{g_i}}^{\max}$,
4. bus voltage V_i: $h_{V_i}^{\min} \le V_i \le h_{V_i}^{\max}$,
5. transformer tap ratio t_i: $h_{t_i}^{\min} \le t_i \le h_{t_i}^{\max}$,
6. transmission line capacity constraint S_{ij}^2: $S_{ij}^2 \le h_{S_{ij}^2}^{\max}$,

where, $h_j^{\min}(x)$ and $h_j^{\max}(x)$ are the lower and upper limits for each set of constraints. The constraints of reactive power generation Q_{g_i}, tap ratio t_i and bus voltage V_i are simple inequality constraints as they are constrained by constant values of Q_{g_i}, t_i and V_i respectively.

The constraints of the per unit incremental MW generation increase and decrease are functions of the active power generation inequality constraint, $h_{P_{g_i}}^{\min} \le P_{g_i} \le h_{P_{g_i}}^{\max}$ or $P_{g_i}^{\min} \le P_{g_i} \le P_{g_i}^{\max}$.

For $P_{g_i}^{+}$: $h_{P_{g_i}^{+}}^{\min} = 0$ and $h_{P_{g_i}^{+}}^{\max} = P_{g_i}^{\max} - P_{g_i}$,

For $P_{g_i}^{-}$: $h_{P_{g_i}^{-}}^{\min} = 0$ and $h_{P_{g_i}^{-}}^{\max} = P_{g_i} - P_{g_i}^{\min}$.

The transmission line capacity constraint is also a functional constraint as it is a squared function of the real and imaginary voltage components of both buses i and j forming the branch ij. Refer to Appendix II for the derivation of the functional transmission line capacity constraint, S_{ij}^2. It is important to realise that the formulation may not be able to guarantee a feasible solution in all cases.

2.4.6 Formulating the reduced Newton equation

The Gaussian Elimination technique is applied to reduce the dimensions of the Newton matrix to reduce computation time in comparison to solving the complete Newton matrix. The reduced form involves only bus voltages, associated dual variables and functional constraint variables. This compact form is similar in structure to the system admittance matrix. This method was proposed by Granville (1994) and Wu et al. (1994) and utilised in subsequent publications [Zhang et al. (2001)].

A. Elimination of slack variables

To eliminate the slack variables sl_j and su_j from Newton equation (2.44), rearrange equations (2.42) and (2.43) to make Δsl_j and Δsu_j the subject respectively,

$$\Delta sl_j = \pi l_j^{-1}\left(\nabla_{sl_j} L_\mu - sl_j \Delta \pi l_j\right) \tag{2.55}$$

$$\Delta su_j = \pi u_j^{-1}\left(-\nabla_{su_j} L_\mu - su_j \Delta \pi u_j\right) \tag{2.56}$$

Substitute into equations (2.40) and (2.41) to update the set of Newton matrix equations.

$$\begin{aligned} -\nabla_{x_\alpha} L_\mu = &\left[-\sum_{i=1}^{N} \nabla_x (\nabla_x \Delta P_i) \lambda_{p_i} - \sum_{i=1}^{N} \nabla_x (\nabla_x \Delta Q_i) \lambda_{q_i} - \sum_{j=1}^{N_h} \nabla_x (\nabla_x h_j) \pi l_j - \sum_{j=1}^{N_h} \nabla_x (\nabla_x h_j) \pi u_j \right] \Delta x \\ &- \sum_{i=1}^{N} \nabla_{x_\alpha} \Delta P_i \Delta \lambda_{p_i} - \sum_{i=1}^{N} \nabla_{x_\alpha} \Delta Q_i \Delta \lambda_{q_i} - \sum_{j=1}^{N_h} \nabla_{x_\alpha} h_j \Delta \pi l_j - \sum_{j=1}^{N_h} \nabla_{x_\alpha} h_j \Delta \pi u_j \\ &+ \sum_{i=1}^{N_g} \nabla_x \nabla_x f(x) \Delta x \end{aligned} \tag{2.57}$$

$$-\nabla \lambda_{p_i} L_\mu = -\sum_{i=1}^{N} \nabla_x \Delta P_i \Delta x \tag{2.58}$$

$$-\nabla \lambda_{q_i} L_\mu = -\sum_{i=1}^{N} \nabla_x \Delta Q_i \Delta x \tag{2.59}$$

$$-\nabla^*_{\pi l_j} L_\mu = \left(-\sum_{j=1}^{N_h} \nabla_x h_j\right) \Delta x - sl_j \pi l_j^{-1} \Delta \pi l_j \tag{2.60}$$

$$-\nabla^*_{\pi u_j} L_\mu = \left(-\sum_{j=1}^{N_h} \nabla_x h_j\right) \Delta x + su_j \pi u_j^{-1} \Delta \pi u_j \tag{2.61}$$

where, $-\nabla^*_{\pi l_j} L_\mu$ of (2.60) and $-\nabla^*_{\pi u_j} L_\mu$ of (2.61) update to,

$$-\nabla^*_{\pi l_j} L_\mu = -\nabla_{\pi l_j} L_\mu - \pi l_j^{-1} \nabla_{sl_j} L_\mu \tag{2.62}$$

$$-\nabla^*_{\pi u_j} L_\mu = -\nabla_{\pi u_j} L_\mu - \pi l_j^{-1} \nabla_{su_j} L_\mu \tag{2.63}$$

In matrix form the set of Newton equations (2.57)-(2.61) are,

$$\begin{bmatrix} -\Pi l^{-1} Sl & 0 & -\nabla h & 0 & 0 \\ 0 & -\Pi u^{-1} Su & -\nabla h & 0 & 0 \\ -\nabla h^T & -\nabla h^T & H & -Jp^T & -Jq^T \\ 0 & 0 & -Jp & 0 & 0 \\ 0 & 0 & -Jq & 0 & 0 \end{bmatrix} \times \begin{bmatrix} \Delta \pi l \\ \Delta \pi u \\ \Delta x \\ \Delta \lambda p \\ \Delta \lambda q \end{bmatrix} = \begin{bmatrix} -\nabla_{\pi l_j} L_\mu - \Pi l_j^{-1} \nabla_{sl_j} L_\mu \\ -\nabla_{\pi u_j} L_\mu - \Pi l_j^{-1} \nabla_{su_j} L_\mu \\ -\nabla_x L_\mu \\ -\nabla_{\lambda p} L_\mu \\ -\nabla_{\lambda q} L_\mu \end{bmatrix} \tag{2.64}$$

where,

$$\begin{aligned} H\left(x, \lambda_p, \lambda_q \pi l, \pi u\right) = \nabla_x \nabla_x f(x) - \sum_{i=1}^{N} \nabla_x \left(J_{p_i}(x)\right) \lambda_{p_i} - \sum_{i=1}^{N} \nabla_x \left(J_{q_i}(x)\right) \lambda_{q_i} \\ - \sum_{j=1}^{N_h} (+\pi u_j) \nabla_x \left(\nabla_x h_j(x)\right) \pi l_j - \sum_{j=1}^{N_h} \nabla_x \left(\nabla_x h_j(x)\right) \pi u_j \end{aligned} \tag{2.65}$$

$$J_{p_i}(x) = \left[\frac{\partial \Delta P_i(x)}{\partial x}\right], \; J_{q_i}(x) = \left[\frac{\partial \Delta Q_i(x)}{\partial x}\right] \tag{2.66}$$

Using back substitution and the result from equation (2.64), the values of Δsl_j and Δsu_j can be found by equations (2.55) and (2.56).

B. Elimination of dual variables

To eliminate the dual variables $\Delta \pi l_j$ and $\Delta \pi u_j$ from (2.64) a similar procedure is followed.

Rearrange equations (2.60) and (2.61) to make $\Delta \pi l_j$ and $\Delta \pi u_j$ the subject respectively,

$$\Delta \pi l_j = -\pi l_j sl_j^{-1} \left(\left[\sum_{j=1}^{N_h} \nabla_x h_j \right] \Delta x - \nabla_{\pi l_j} L_\mu \right) + sl_j^{-1} \nabla_{sl_j} L_\mu \tag{2.67}$$

$$\Delta\pi u_j = \pi u_j su_j^{-1}\left(\left[\sum_{j=1}^{N_h}\nabla_x h_j\right]\Delta x - \nabla_{\pi u_j} L_\mu\right) + su_j^{-1}\nabla_{su_j} L_\mu \tag{2.68}$$

Substitute into equation (2.57) to update the set of Newton matrix equations,

$$\begin{aligned}-\nabla^*_{x_\alpha} L_\mu = H\Delta x + \sum_{i=1}^{N_g}\nabla x\nabla x f(x)\Delta x - \sum_{i=1}^{N}\nabla_{x_\alpha}\Delta P_i\Delta\lambda_{p_i} - \sum_{i=1}^{N}\nabla_{x_\alpha}\Delta Q_i\Delta\lambda_{q_i} \\ +\pi l_j sl_j^{-1}\sum_{j=1}^{N_h}\nabla_x h_j\nabla_x h_j\Delta x - \pi u_j su_j^{-1}\sum_{j=1}^{N_h}\nabla_x h_j\nabla_x h_j\Delta x\end{aligned} \tag{2.69}$$

$$-\nabla_{\lambda_{p_i}} L_\mu = -\sum_{i=1}^{N}\nabla_x\Delta P_i\Delta x \tag{2.70}$$

$$-\nabla_{\lambda_{q_i}} L_\mu = -\sum_{i=1}^{N}\nabla_x\Delta Q_i\Delta x \tag{2.71}$$

where,

$$H = \left[-\sum_{i=1}^{N}\nabla_x(\nabla_x\Delta P_i)\lambda_{p_i} - \sum_{i=1}^{N}\nabla_x(\nabla_x\Delta Q_i)\lambda_{q_i} - \sum_{j=1}^{N_h}\nabla_x(\nabla_x h_j)\pi l_j - \sum_{j=1}^{N_h}\nabla_x(\nabla_x h_j)\pi u_j\right] \tag{2.72}$$

and $\nabla^*_{x_\alpha} L_\mu$ the right hand side of equation (2.69) update to,

$$\begin{aligned}\nabla^*_{x_\alpha} L_\mu = -\nabla_{x_\alpha} L_\mu + sl_j^{-1}\sum_{j=1}^{N_h}\nabla_{x_\alpha} h_j^T\left(\pi l_j\nabla_{\pi l_j} L_\mu + \nabla_{sl_j} L_\mu\right) \\ -su_j^{-1}\sum_{j=1}^{N_h}\nabla_{x_\alpha} h_j^T\left(\pi u_j\nabla_{\pi u_j} L_\mu + \nabla_{su_j} L_\mu\right)\end{aligned} \tag{2.73}$$

Newton equations (2.69)-(2.71) in matrix form without slack and dual variables are reduced to the compact form,

$$\begin{bmatrix} H^* & -J_p^T & -J_q^T \\ -J_p & 0 & 0 \\ -J_q & 0 & 0 \end{bmatrix}\times\begin{bmatrix}\Delta x \\ \Delta\lambda_p \\ \Delta\lambda_q\end{bmatrix} = \begin{bmatrix}-\nabla^*_x L_\mu \\ -\nabla_{\lambda_p} L_\mu \\ -\nabla_{\lambda_q} L_\mu\end{bmatrix} \tag{2.74}$$

where,

$$H^* = \left[-\sum_{i=1}^{N} \nabla_x (\nabla_x \Delta P_i) \lambda_{p_i} - \sum_{i=1}^{N} \nabla_x (\nabla_x \Delta Q_i) \lambda_{q_i} - \sum_{j=1}^{N_h} \nabla_x (\nabla_x h_j) \pi l_j - \sum_{j=1}^{N_h} \nabla_x (\nabla_x h_j) \pi u_j \right] + \sum_{i=1}^{N_g} \nabla_x \nabla_x f(x) + \sum_{j=1}^{N_h} \nabla_x h_j \nabla_x h_j \left(\pi l_j s l_j^{-1} - \pi u_j s u_j^{-1} \right) \tag{2.75}$$

$$H^* = H + \sum_{i=1}^{N_g} \nabla_x \nabla_x f(x) + \sum_{j=1}^{N_h} \nabla_x h_j \nabla_x h_j \left(\pi l_j s l_j^{-1} - \pi u_j s u_j^{-1} \right) \tag{2.76}$$

where, H is defined in equation (2.72) and within the square brackets of equation (2.75).

The solution to (2.74) gives values for Δx, then by substitution into equations (2.67) and (2.68) the values of $\Delta \pi l$ and $\Delta \pi u$ can be found. Correspondingly, by substitution into equations (2.55) and (2.56) the values of Δsl and Δsu can be found.

In the compact matrix of Newton equations (2.74) all inequality elements have been eliminated, making the solution computationally easier to solve than previously (2.44). Analytically matrix (2.77) is shown below to give all relevant elements related to bus i.

$$\begin{bmatrix}
H^*_{t_i t_i} & 0 & 0 & 0 & 0 & 0 & -J_{p_i,t_i} & -J_{q_i,t_i} \\
0 & H^*_{P_{gi}^+ P_{gi}^+} & 0 & 0 & 0 & 0 & -J_{p_i,P_{gi}^+} & 0 \\
0 & 0 & H^*_{P_{gi}^- P_{gi}^-} & 0 & 0 & 0 & -J_{p_i,P_{gi}^-} & 0 \\
0 & 0 & 0 & H^*_{Q_{gi} Q_{gi}} & 0 & 0 & 0 & -J_{q_i,Q_g} \\
H^*_{t_i \theta_i} & 0 & 0 & 0 & H^*_{\theta_i \theta_i} & H^*_{\theta_i V_i} & -J_{p_i,\theta_i} & -J_{q_i,\theta_i} \\
H^*_{t_i V_i} & 0 & 0 & 0 & H^*_{\theta_i V_i} & H^*_{V_i V_i} & -J_{q_i,V_i} & -J_{q_i,V_i} \\
-J_{p_i,t_i} & -J_{p_i,P_{gi}^+} & -J_{p_i,P_{gi}^-} & 0 & -J_{p_i,\theta_i} & -J_{q_i,V_i} & 0 & 0 \\
-J_{q_i,t_i} & 0 & 0 & -J_{q_i,Q_g} & -J_{q_i,\theta_i} & -J_{q_i,V_i} & 0 & 0
\end{bmatrix} \times$$

$$\begin{bmatrix} \Delta t \\ \Delta P^{+}_{g_i} \\ \Delta P^{-}_{g_i} \\ \Delta Q_{g_i} \\ \Delta\theta_i \\ \Delta V_i \\ \Delta\lambda_{p_i} \\ \Delta\lambda_{q_i} \end{bmatrix} = \begin{bmatrix} -\nabla^{*}_{t} L_\mu \\ -\nabla^{*}_{P^{+}_{g_i}} L_\mu \\ -\nabla^{*}_{P^{-}_{g_i}} L_\mu \\ -\nabla^{*}_{Q_{g_i}} L_\mu \\ -\nabla^{*}_{\theta_i} L_\mu \\ -\nabla^{*}_{V_i} L_\mu \\ -\nabla_{\lambda_{p_i}} L_\mu \\ -\nabla_{\lambda_{q_i}} L_\mu \end{bmatrix} \tag{2.77}$$

2.5 Implementation

In order to implement the method, set up and exit conditions are required. The initialisation of variables, update of the solution after an iteration step, and an overview of the solution routine are described in the following sections.

2.5.1 Initialisation of solution routine

Initial conditions must satisfy the slack and dual variable properties; $sl_j > 0, su_j > 0$, $\pi l_j > 0$ and $\pi u_j < 0$. The following is a list of initial values for system, slack, dual and the barrier parameter variables.

1. $P^{0}_{g_i} = P_{g_i}$ taken directly from input file, initial values of $P^{+0}_{g_i}$ and $P^{-0}_{g_i}$ set to small values (0.001);
2. slack variable for $P^{+}_{g_i}$: $sl_{P^{+}_{g_i}} = P^{+0}_{g_i}$ and $su_{P^{+}_{g_i}} = P^{\max}_{g_i} - P^{0}_{g_i} - P^{+0}_{g_i}$, corresponding dual variable μ / sl_j;
3. slack variable for $P^{-}_{g_i}$: $sl_{P^{-}_{g_i}} = P^{-0}_{g_i}$ and $su_{P^{-}_{g_i}} = P^{0}_{g_i} - P^{\min}_{g_i} - P^{-0}_{g_i}$, corresponding dual variable $-\mu / su_j$;
4. Q_{g_i} set to average between maximum and minimum;
5. all other slack variables sl_j are set to $h_j - h^{\min}_j$ and dual variables πl_j are set to μ / sl_j;

6. all other slack variables su_j are set to $h_j^{\max} - h_j$ and dual variables πu_j are set to $-\mu / su_j$;
7. dual variables λ_{p_i} are set to 10 and λ_{q_i} are set to zero;
8. barrier parameter μ is set between 0.01-10 depending on the desired convergence performance.

2.5.2 Update solution

With the solution to equation (2.77) and back substitution into equations (2.67), (2.68), (2.55) and (2.56); Δx , $\Delta\lambda_p$, $\Delta\lambda_q$, $\Delta\pi l$, $\Delta\pi u$, Δsl and Δsu are known. The OPF solution is updated by the following equations,

$$sl^{(c+1)} = sl^{(c)} + \sigma\alpha_p \Delta sl \tag{2.78}$$

$$su^{(c+1)} = su^{(c)} + \sigma\alpha_p \Delta su \tag{2.79}$$

$$x^{(c+1)} = x^{(c)} + \sigma\alpha_p \Delta x \tag{2.80}$$

$$\pi l^{(c+1)} = \pi l^{(c)} + \sigma\alpha_d \Delta\pi l \tag{2.81}$$

$$\pi u^{(c+1)} = \pi u^{(c)} + \sigma\alpha_d \Delta\pi u \tag{2.82}$$

$$\lambda p^{(c+1)} = \lambda p^{(c)} + \sigma\alpha_d \Delta\lambda p \tag{2.83}$$

$$\lambda q^{(c+1)} = \lambda q^{(c)} + \sigma\alpha_d \Delta\lambda q \tag{2.84}$$

where,

c is the iteration count,

$\sigma \in [0.995 - 0.99995]$, this factor prevents the solution from reaching the boundary [Marsten (1990)],

α_p is the primal step-length parameter (2.85),

α_d is dual step-length parameter (2.86).

$$\alpha_p = \min\left\{\min\left(\frac{sl}{-\Delta sl}\right), \min\left(\frac{su}{-\Delta su}\right), 1.0\right\} \tag{2.85}$$

$$\alpha_d = \min\left\{\min\left(\frac{-\pi l}{\Delta\pi l}\right), \min\left(\frac{\pi u}{-\Delta\pi u}\right), 1.0\right\} \tag{2.86}$$

The value of the step lengths are dependent upon the conditions that, $\Delta sl < 0$, $\Delta su < 0$, $\Delta \pi l < 0$ and $\Delta \pi u > 0$. The parameter σ ensures slack and dual variables remain within the conditions, $sl_j > 0, su_j > 0$, $\pi l_j > 0$ and $\pi u_j < 0$.

Fiacco and McCormick's barrier function theorem states that the barrier parameter μ must approach zero during the iteration process. The amount that it reduces is dependent upon the performance of the algorithm to converge. The value of the barrier parameter after each iteration is evaluated by,

$$\mu = \frac{\beta * Cgap}{2 * N_h} \tag{2.87}$$

where, $\beta \in [0.01 - 0.2]$ is the centering parameter, C_{gap} is the complementary gap for the non-linear IP OPF. Linear programming techniques set the barrier parameter μ to a value proportional to the duality gap; however, this is not valid for non-linear primal-dual methods. Therefore the barrier parameter μ is dependent upon the predicted decrease of the complementary gap as recommend by Wu et al. (1994) and Granville (1994). The complementary gap is evaluated as,

$$Cgap = \sum_{j=1}^{N_h} \left(sl_j \pi l_j - su_j \pi u_j \right) \tag{2.88}$$

2.5.3 Solution routine for non-linear interior point OPF

The algorithm terminates when the convergence tolerances are met or the maximum number of iterations is reached. Convergence is dependent upon preset values of the active and reactive power mismatch, the complementary gap and the barrier parameter μ. Values used for results gathered in this chapter are,

$$\left|\max \Delta P_i\right| < 10^{-4} \text{ and } \left|\max \Delta Q_i\right| < 10^{-4} \tag{2.89}$$

$$C_{gap} < 5 \times 10^{-4} \tag{2.90}$$

$$\mu < 10^{-5} \tag{2.91}$$

An overview of the solution routine is presented in Figure 2.1.

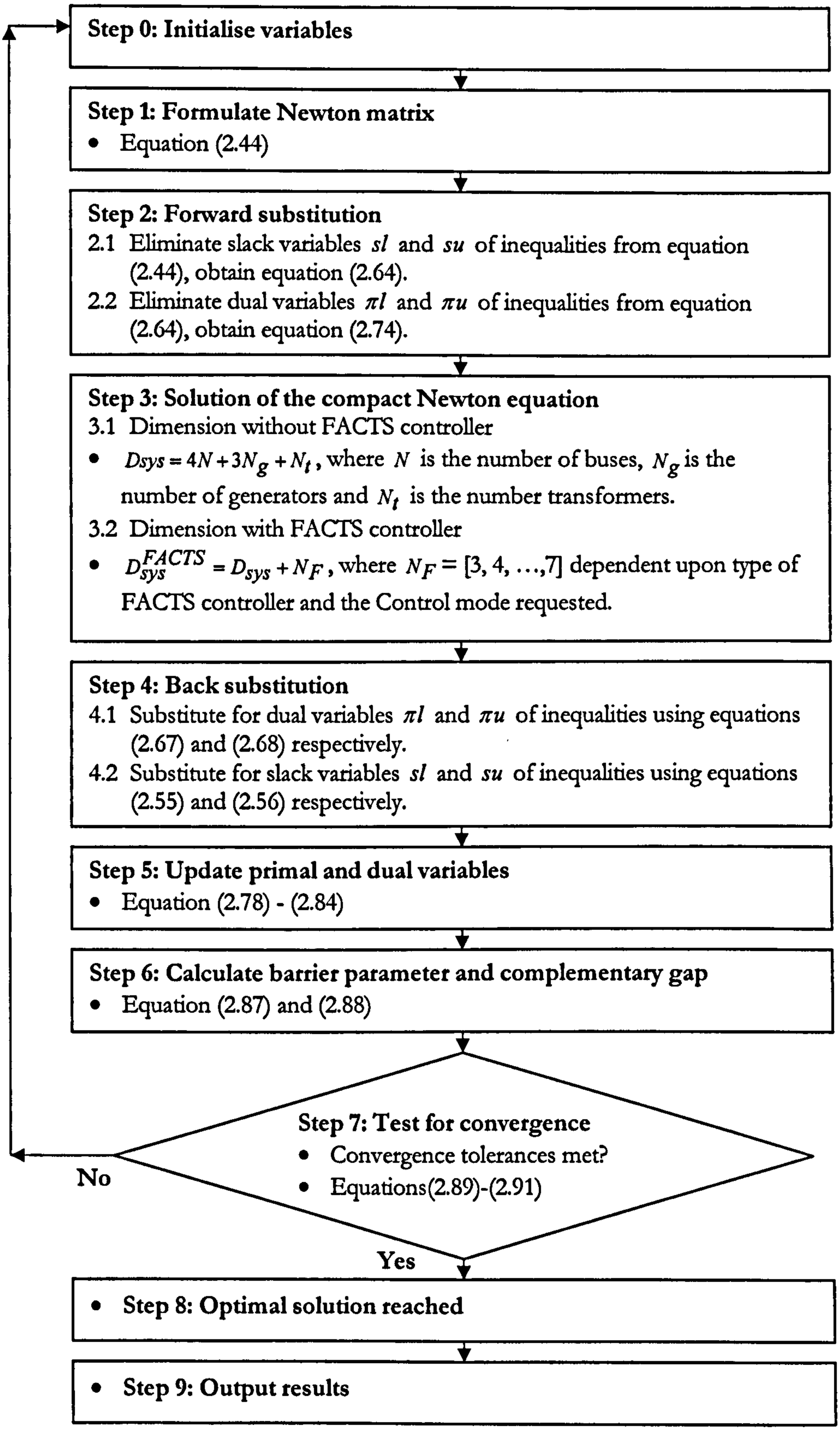

Figure 2.1: Interior point OPF solution routine overview.

2.6 Numerical results

To ensure the bilateral market model implemented with the IP OPF method was successful, a number of numerical examples were examined. The are two general situations of most interest when using the bilateral market model, the first is when there is no system congestion and the second is when congestion is present. The test results show the difference between the situations and explain two methods in which system congestion is modelled. The algorithm was implemented in C language and all power flow equations are represented in hybrid form, where voltage is represented in polar coordinates and impedance represented in rectangular coordinates.

2.6.1 System congestion

There are two ways in which congestion on a system can be caused. First, when a single critical transmission line is out or its capacity reduced and second, when system demand levels are purely due to daily demand fluctuations. The 4 bus and IEEE 14 bus systems are used to test the system under each of the congested situations respectively.

The 4 bus system consists of four buses, four transmission lines, two generators and three loads. The IEEE 14 bus system consists of 14 buses, 20 transmission lines, three online tap changing transformers, five generators and 11 loads. Input data for all test systems in this chapter can be found in Appendix VIII and for the IEEE 14 bus system in University of Washington (2007). Convergence tolerances were set to 1×10^{-4} p.u. for the absolute bus power mismatches, 5×10^{-4} for the complementary gap and 1×10^{-5} for the barrier parameter.

2.6.2 4 bus system

Both generators have generator equal cost coefficient values of $C_{gi}^{+}=20$ \$/MWh and $C_{gi}^{-}=10$ \$/MWh. In the original system there is no congestion (Figure 2.2(a)) and in the congested system, the capacity of transmission line 1-2 is reduced by 60% of that of the original (Figure 2.2(b)). Table 2-2 gives an overview of the system active power generation changes and losses and Table 2-3 details the changes at each generator. In these test cases the initial generation does not account for system losses.

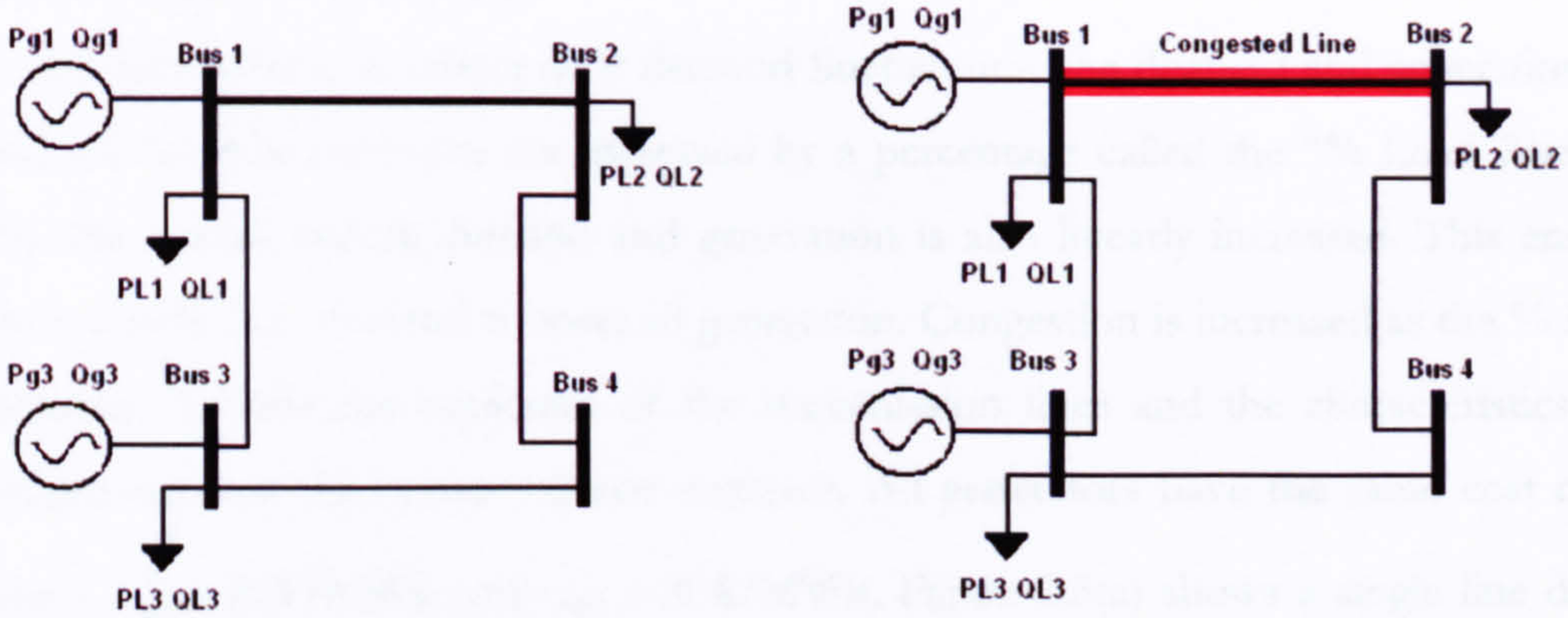

Figure 2.2: 4 bus system (a) no congestion (b) single congested line by reduction of $S_{12}^{2\max}$ by 60%.

Results in Table 2-2 show that when there is no congestion there are no decreases to the initial generation and the system cost is purely due to system losses. The table also shows that when there is congestion the relative system losses increases, there are decreases to the initial generation and cost is predominately due to congestion and partly due to system losses. The more detailed set of generation results in Table 2-3 confirm that at each generator bus there is either increase or decrease in active power generation. The results show the objective function and model is behaving as expected. All of the 4 bus system test results converged in fewer than 15 iterations.

Table 2-2: 4 bus system: System comparison with and without congestion.

4 bus system: System comparison	**Total** $\sum_{i}^{N_g} P^{+}_{g_i}$ **(p.u.)**	**Total** $\sum_{i}^{N_g} P^{-}_{g_i}$ **(p.u.)**	**Total output** $\sum_{i=1}^{N_g} P_{g_i}$ **(p.u.)**	**System losses** P_{LOSS} **(p.u.)**	**System cost** $f(x)$ **$/h**	**% $f(x)$ due to system losses**	**% $f(x)$ due to congestion**
No congestion	0.3	0.0	9.3	0.3	5.2	100%	0%
Congestion	1.0	0.6	9.4	0.4	27.0	30%	70%

Table 2-3: 4 bus system with congestion: Changes at each generator.

4 bus system with congestion	**Initial active power generation** $P^{0}_{g_i}$ **(p.u.)**	**Increase in active power** $P^{+}_{g_i}$ **(p.u.)**	**Decrease in active power** $P^{-}_{g_i}$ **(p.u.)**	**Change in active power generation** $\left(\Delta P^{+}_{g_i} - \Delta P^{-}_{g_i}\right)$ **(p.u.)**	**Active power output** P_{g_i} **(p.u.)**
Pg_1	5	0.00	0.65	-0.65	4.35
Pg_3	4	1.02	0.00	1.02	5.02
System total	**9**	**1.02**	**0.56**	**0.37**	**9.37**

2.6.3 IEEE 14 bus system

In this test system, to reflect daily demand fluctuations, the demand and generation levels at each of the relevant buses are increased by a percentage called the "% Load Rise". In this way the overall system demand and generation is also linearly increased. This ensures that there is sufficient demand to meet all generation. Congestion is increased as the % Load Rise increases because the capacities of the transmission lines and the characteristics of other components on the system remain constant. All generators have the same cost coefficient values $C_{gi}^{+} = 20\,\$/\text{MWh}$ and $C_{gi}^{-} = 10\ \$/\text{MWh}$. Figure 2.3(a) shows a single line diagram of IEEE 14 bus system and Figure 2.3(b) shows the system at 70% Load Rise highlighting the congested lines and showing the order in which the three lines become congested as % Load Rise is increased from 30% to 50% and 70%.

Table 2-4 shows the relative percentage changes in system active power generation incremental increase $P_{g_i}^{+}$, incremental decrease $P_{g_i}^{-}$, output P_{g_i} and system losses with respect to the system initial active power generation $P_{g_i}^{0}$ at each % Load Rise with one, two and three congested lines. Equations (2.92) to (2.95) give the definitions of columns 4 to 7 respectively.

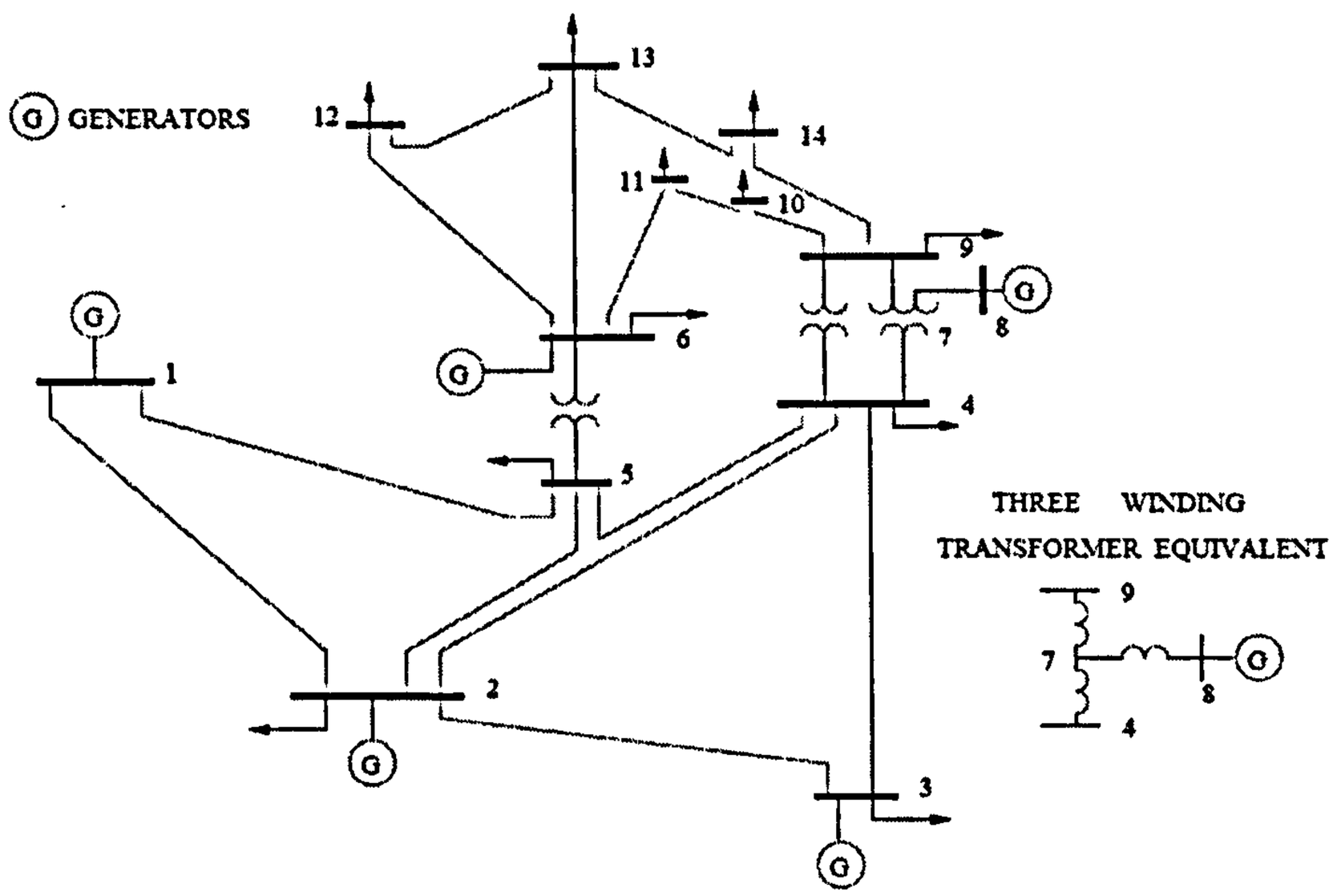

Figure 2.3(a): IEEE 14 bus system.

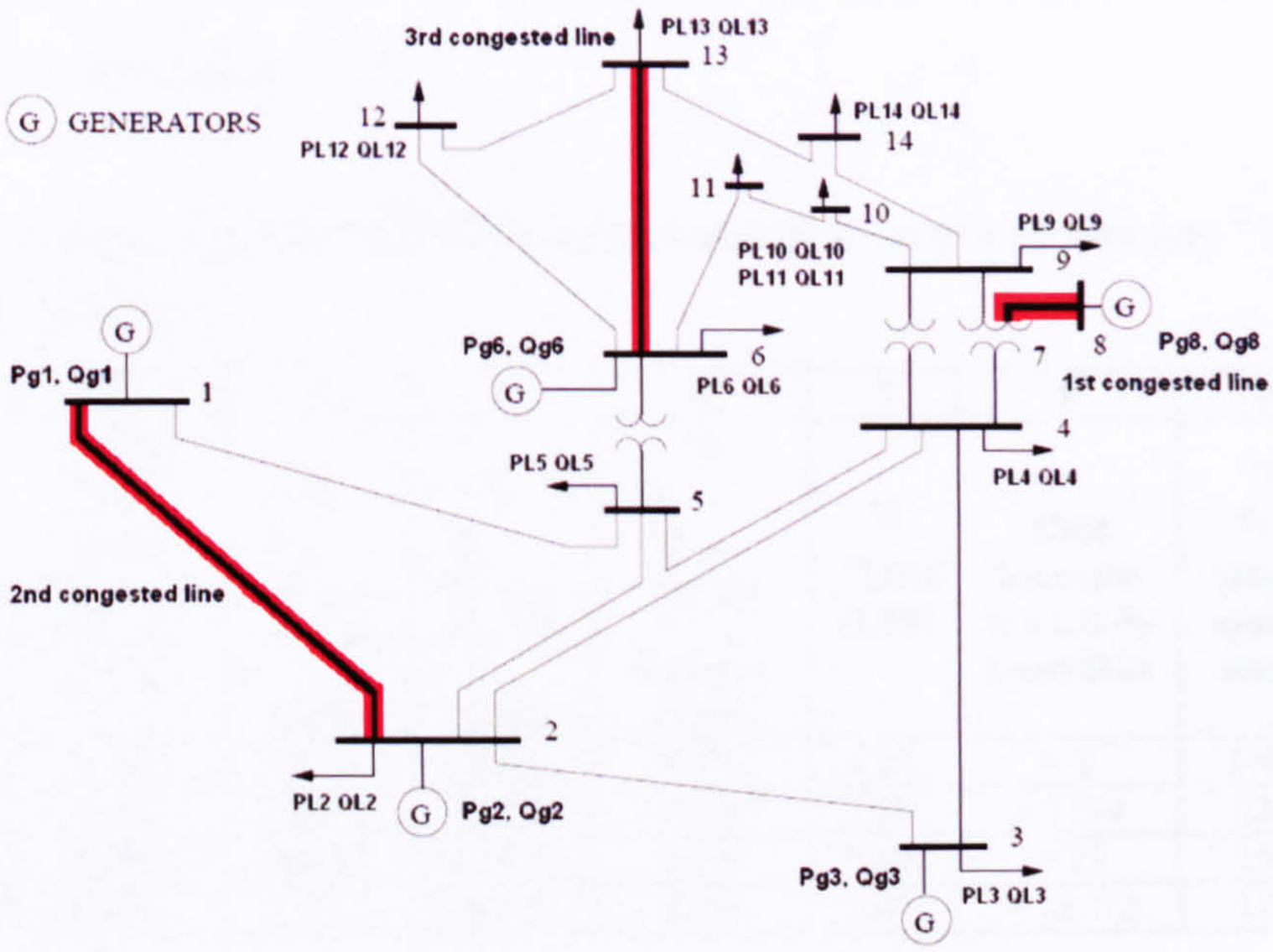

Figure 2.3(b): IEEE 14 bus system: highlighting the congested lines and showing the order in which the three lines become congested as % Load Rise is increased.

$$\%\sum_{i}^{N_g}\left[P_{g_i}^{+}\right]=\left(\sum_{i}^{N_g}\left[P_{g_i}^{+}\right]\Big/\sum_{i}^{N_g}\left[P_{g_i}^{0}\right]\right)\times 100 \tag{2.92}$$

$$\%\sum_{i}^{N_g}\left[P_{g_i}^{-}\right]=\left(\sum_{i}^{N_g}\left[P_{g_i}^{-}\right]\Big/\sum_{i}^{N_g}\left[P_{g_i}^{0}\right]\right)\times 100 \tag{2.93}$$

$$\%\sum_{i}^{N_g}\left[P_{g_i}\right]\text{Increase}=\left(\left(\sum_{i}^{N_g}\left[P_{g_i}\right]\Big/\sum_{i}^{N_g}\left[P_{g_i}^{0}\right]\right)-1\right)\times 100 \tag{2.94}$$

$$\%P_{LOSS}=\left(P_{LOSS}\Big/\sum_{i}^{N_g}\left[P_{g_i}^{0}\right]\right)\times 100 \tag{2.95}$$

The cost increase is measured with respect to the nominal case (0% Load Rise). The two right hand side columns show the percentage of system cost $f(x)$ due to system losses and congestion.

In Table 2-4 the % Load Rise values have been chosen to show cases with zero to three congested lines. With no congestion, the results follow the conditions set out in Table 2-1, where system cost $f(x)$ is due to system loss only. Congestion causes active power decrease

as well as increase and changes the relative percentage of the system cost. In the congested cases system losses average 16.3%.

Table 2-4: IEEE 14 bus system: System comparison with no congestion and "% Load Rise" of 30%, 50% and 70%.

1	2	3	4	5	6	7	8	9	10
% Load Rise	No. of cong-ested lines	Initial total (p.u.) $\sum_{i}^{N_g} P^0_{g_i}$	% $\sum_{i}^{N_g} P^+_{g_i}$ (2.92)	% $\sum_{i}^{N_g} P^-_{g_i}$ (2.93)	% $\sum_{i=1}^{N_g} P_{g_i}$ increase (2.94)	% P_{LOSS} (2.95)	Cost increase w.r.t. 0 % Load Rise	% $f(x)$ due to system losses	% $f(x)$ due to cong-estion
0	0	2.59	4.2%	0.0%	4.2%	4.2%	× 1	100%	0%
30	1	3.367	18.3%	13.0%	5.3%	5.3%	× 7 3/4	22%	78%
50	2	3.885	26.0%	20.4%	5.6%	5.6%	× 13	15%	85%
70	3	4.403	32.0%	26.6%	5.4%	5.4%	× 18 1/2	12%	88%

Table 2-5 shows the breakdown of generator changes for the system at 50% Load Rise. To overcome congestion at least cost, increase in active power is required from Pg_2 and Pg_3, and decrease in active power from Pg_1, there are no changes at Pg_6 and Pg_8. As in the 4 bus results, Tables 2-2 and 2-3 show that the objective function and model is behaving as expected. All of the IEEE 14 bus system test results converged in 20 iterations or fewer.

Table 2-5: IEEE 14 bus system: Changes at each generator at 50% Load Rise.

14 bus system at 50% Load Rise	Initial active power generation $P^0_{g_i}$ (p.u.)	Increase in active power $P^+_{g_i}$ (p.u.)	Decrease in active power $P^-_{g_i}$ (p.u.)	Change in active power generation $\left(P^+_{g_i} - P^-_{g_i}\right)$ (p.u.)	Active power output P_{g_i} (p.u.)
Pg_1	3.240	0	0.792	-0.792	2.448
Pg_2	0.600	0.900	0	0.900	1.500
Pg_3	0.015	0.108	0	0.108	0.123
Pg_6	0.015	0	0	0	0.015
Pg_8	0.015	0	0	0	0.015
System total $\sum_{i}^{N_g} P^0_{g_i}$ (p.u.)		% System change w.r.t. total initial active power generation			
3.885		26.0%	20.4%	5.4%	5.4%

2.7 Conclusions

In this Chapter, the linear bilateral market objective function has been implemented into a non-linear IP OPF method. Expected behaviour and characteristics of the model have then been described. Numerical examples using the 4 bus and IEEE 14 bus systems demonstrate that the expected characteristics are met, and two methods to cause system congestion are

presented. The results also show that the bilateral market object function shows similar iteration speed to previous quadratic objective functions applied to the IP OPF algorithm.

The following characteristics of the model were identified,

- Active power change from scheduled generation at each bus can increase, decrease or remain unchanged only;
- Active power system loss is the difference between the system scheduled active power and the active power demand;
- Increase in active power generation is the sum of real power system losses and real power required to overcome system congestion;
- Decrease in active power generation is the magnitude of the real power change in scheduled generation require to overcome system congestion only;
- When congestion exists the active power system generation increase is always greater than active power system generation decrease. This is due to real power system losses.

The next chapter integrates FACTS controller models into the IP OPF method with the bilateral market objective function.

Chapter 3

FACTS controllers and the interior point OPF method

3.1 Introduction

FACTS controllers are one possible solution to the congestion management problem. This chapter presents the voltage sourced converter (VSC) based FACTS controller models applied to the OPF analysis with the bilateral market model. Initial results show that FACTS controllers can relieve system congestion when installed at certain locations.

Section 3.2 gives an overview of the three main VSC based FACTS controllers. In Section 3.3 steady state modelling assumptions are stated, controller models presented by functional diagrams, and equivalent circuits with power flow equations. Section 3.4 highlights the changes made to the interior point (IP) OPF algorithm when each FACTS controller is included. Consequently, an adjustment of the system setup is necessary, as described in Section 3.5. The influence of the FACTS controller on the bilateral market model is included in Section 3.6 and the solution procedure in Section 3.7. Numerical results for systems with FACTS controllers are presented in Section 3.8 and finally conclusions drawn in Section 3.9.

3.2 Voltage sourced converter based FACTS controller models

The mathematical models employed in this chapter are suitable for OPF studies as presented by [Zhang et al. (2006)] and [Zhang and Handschin (2001a)]. An overview of the three main controllers namely the shunt controller (Static Compensator, STATCOM), the series controller (Static Synchronous Series Compensator, SSSC) and the combination shunt-series controller (Unified Power Flow Controller, UPFC) models are described by functional and steady state mathematical models. Table 3-1 gives an overview of possible controller steady state functions.

3.3 Steady state modelling assumptions and FACTS controller models

For ideal steady state analysis the following modelling assumptions are applied to gain the equivalent circuits of the FACTS controllers,

- active power exchange (PE) between,

  - the a.c. system and the STATCOM is neglected,
  - the a.c. system and the SSSC is neglected,
  - the shunt and series converter with the DC link of the UPFC is neglected,
- harmonics generated outside of the fundamental harmonic by the controllers are all neglected,
- the system and the controllers are three phase balanced at all times.

Table 3-1: Overview of voltage sourced converter based FACTS control functions.

FACTS controller	**Connection configuration**	**Possible local control functions** [Zhang et al. (2006)]
STATCOM	Shunt	• Voltage magnitude at local bus • Reactive power at local bus and reactive power flow • Impedance of STATCOM • Current magnitude of STATCOM • Voltage injection from STATCOM • Apparent power or current of a local or remote transmission line
SSSC	Series	• Active power flow of transmission line • Reactive power flow of transmission line • Bus voltage • Impedance of transmission line

UPFC	Shunt-Series	• Local bus voltage
		• Active power flow of transmission line
		• Reactive power flow of transmission line
		• Simultaneous control of local bus voltage and power flow of transmission line allows control of:
		  ○ Circuit impedance
		  ○ Bus voltage angle
		  ○ Transmission line power flow

3.3.1 STATCOM model

Shunt connected controllers are the most commonly used controller types and primarily operate as reactive power compensators to control transmission voltage. STATCOMs are usually composed of three components, a coupling transformer, an inverter and a capacitor connected to the DC input terminals of the inverter, [Schauder et al. (1996)]. As represented in the functional model, Figure 3.1(a).

The STATCOM can be represented by an equivalent circuit, Figure 3.1(b); composed of an impedance and a controllable fundamental frequency positive sequence voltage source. The voltage source is regulated to control the reactive power from the STATOM at the local bus.

As active power exchange is neglected, only reactive power exchange can occur between the STATCOM and the system, [Zhang et al. (2004)].

Power flow constraints of the STATCOM are based on the derivation in Appendix II:

$$P_{sh} = V_i^2 g_{sh} - V_i V_{sh}\left(g_{sh}\cos(\theta_i - \theta_{sh}) + b_{sh}\sin(\theta_i - \theta_{sh})\right) \tag{3.1}$$

$$Q_{sh} = -V_i^2 b_{sh} - V_i V_{sh}\left(g_{sh}\sin(\theta_i - \theta_{sh}) - b_{sh}\cos(\theta_i - \theta_{sh})\right) \tag{3.2}$$

where,

$\overline{V_{sh}} = V_{sh}\angle\theta_{sh}$ is the voltage source from the STATCOM,

$\overline{V_i} = V_i\angle\theta_i$ is the bus voltage at bus i,

$g_{sh} + jb_{sh} = 1/Z_{sh}$ is the STATCOM equivalent admittance,

g_{sh} is the STATCOM conductance,

b_{sh} is the STATCOM susceptance.

The operating constraint of the STATCOM is the active power exchange (PE) between the controller and the system via the DC link:

$$PE_{STATCOM} = \mathrm{Re}\left(V_{sh} I_{sh}^*\right) = 0 \tag{3.3}$$

where,

$$\mathrm{Re}\left(V_{sh} I_{sh}^*\right) = V_{sh}^2 g_{sh} - V_i V_{sh}\left(g_{sh}\cos(\theta_i - \theta_{sh}) - b_{sh}\sin(\theta_i - \theta_{sh})\right).$$

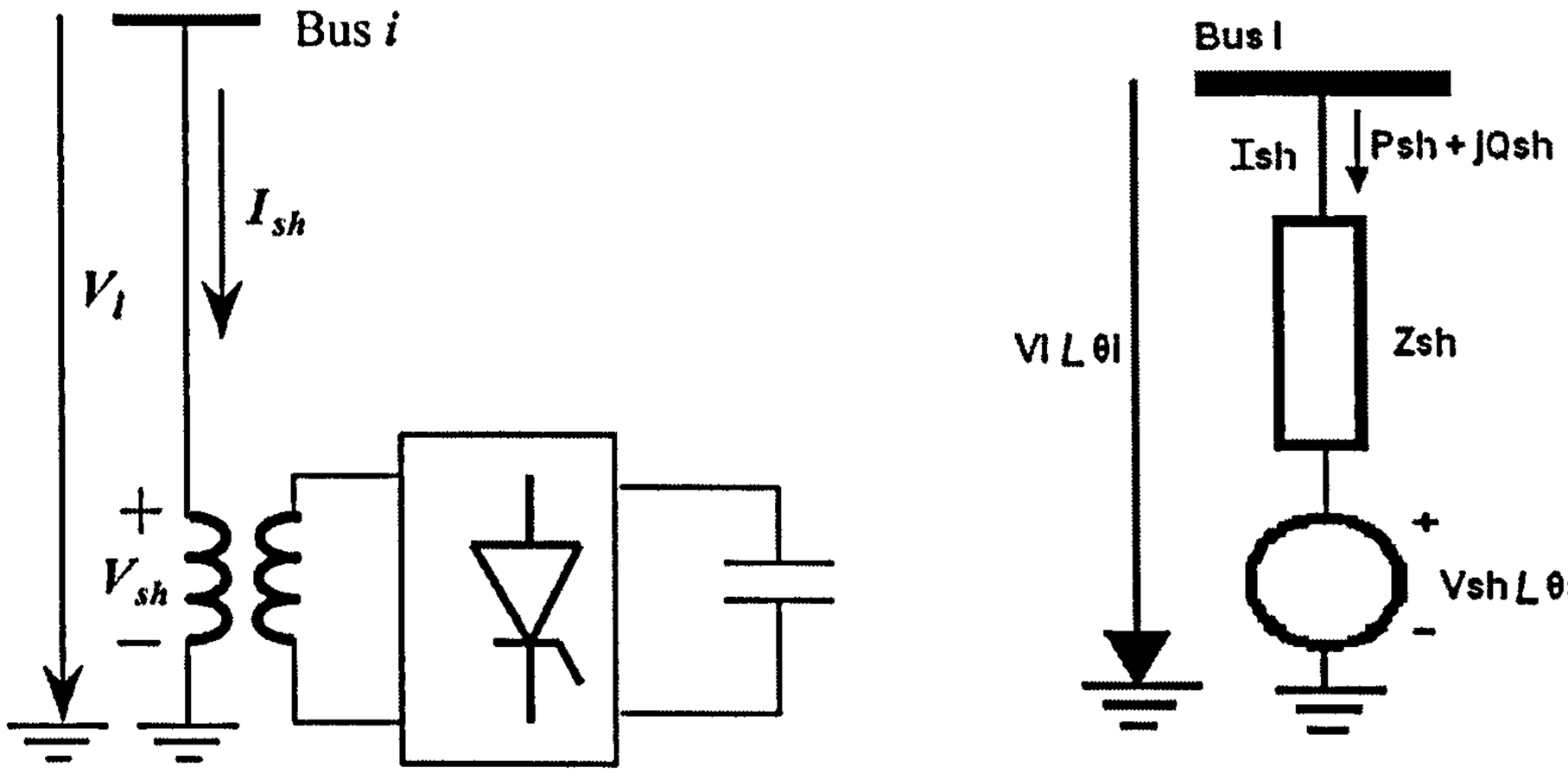

Figure 3.1: (a) Functional model of a STATCOM [Zhang et al. (2004)], (b) STATCOM equivalent circuit.

3.3.2 SSSC model

SSSCs can be connected at any convenient point along a line, and usually consist of three components, a coupling transformer, an inverter and a capacitor. The functional model, Figure 3.2(a) looks similar to that of the STATCOM however; the SSSC is a more complex device due to necessary platform mounting and thyristor or power electronics protection (especially when using insulated gate bipolar transistors (IGBT)). Therefore the increased complexity and required protection makes the SSSC a more expensive controller compared to the STATCOM. SSSCs for steady state operation are used to control any one of the following parameters,

- active power flow of the transmission line;
- reactive power flow of the transmission line;
- bus voltage;
- impedance of the transmission line.

Another popular series controller is the Thyristor Controlled Series Compensator (TCSC), which can provide similar control functions to those listed above. The TCSC is also be used to control dynamic problems in transmission systems such as providing an increase in damping and overcoming Subsynchronous Resonance (SSR).

The SSSC model equivalent circuit is represented in Figure 3.2(b). It consists of an impedance and a variable fundamental frequency positive sequence voltage source between two buses. Again, as active power exchange is neglected, only reactive power exchange can occur between the SSSC and the system. As the SSSC is series connected with a transmission line the active power flow of the SSSC branch *ij* is equal to the sending end active power flow of the transmission line. The same applies to the reactive power flow [Zhang (2003)].

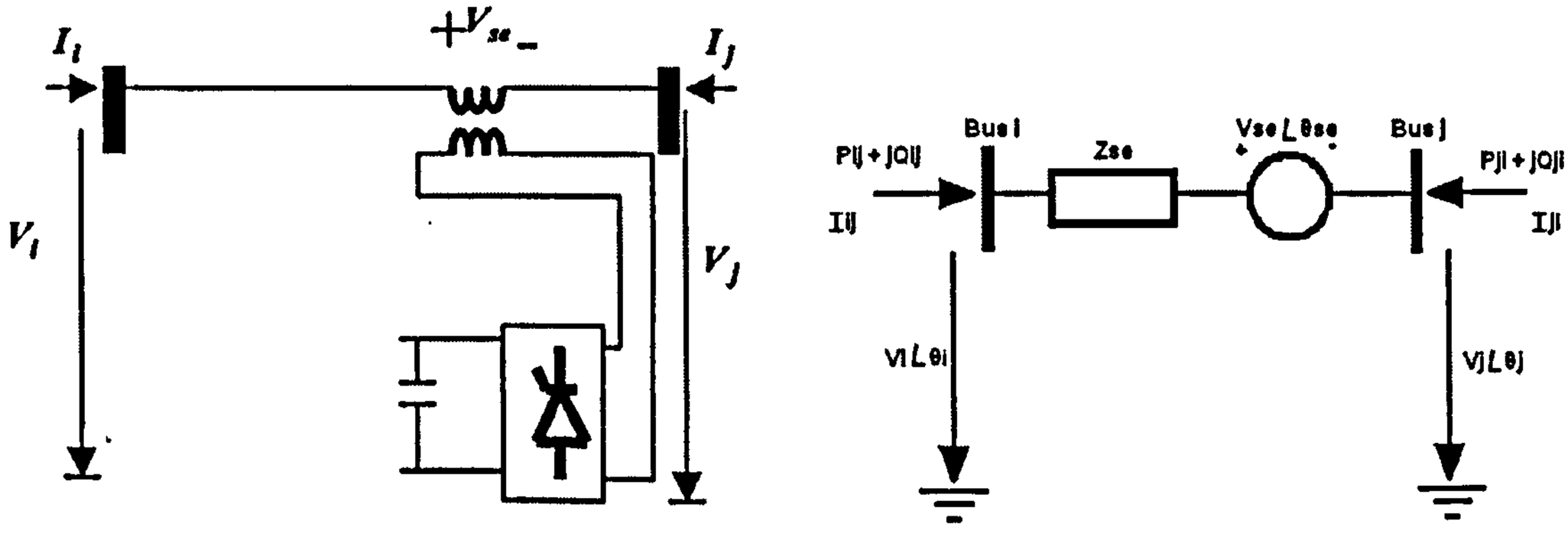

Figure 3.2: (a) Functional model of a SSSC [Zhang (2003)], (b) SSSC equivalent circuit.

The power flow constraints of the SSSC are based on the derivation in Appendix II:

$$P_{ij} = V_i^2 g_{ii} - V_i V_j \left(g_{ij}\cos(\theta_i - \theta_j) + b_{ij}\sin(\theta_i - \theta_j)\right) - V_i V_{se}\left(g_{ij}\cos(\theta_i - \theta_{se}) + b_{ij}\sin(\theta_i - \theta_{se})\right) \tag{3.4}$$

$$Q_{ij} = -V_i^2 b_{ii} - V_i V_j \left(g_{ij}\sin(\theta_i - \theta_j) - b_{ij}\cos(\theta_i - \theta_j)\right) - V_i V_{se}\left(g_{ij}\cos(\theta_i - \theta_{se}) - b_{ij}\sin(\theta_i - \theta_{se})\right) \tag{3.5}$$

$$P_{ji} = V_j^2 g_{jj} - V_i V_j \left(g_{ij}\cos(\theta_j - \theta_i) + b_{ij}\sin(\theta_j - \theta_i)\right) + V_j V_{se}\left(g_{ij}\cos(\theta_j - \theta_{se}) + b_{ij}\sin(\theta_j - \theta_{se})\right) \tag{3.6}$$

$$Q_{ji} = -V_j^2 b_{jj} - V_i V_j \left(g_{ij}\sin(\theta_j - \theta_i) - b_{ij}\cos(\theta_j - \theta_i)\right) - V_j V_{se}\left(g_{ij}\sin(\theta_j - \theta_{se}) - b_{ij}\cos(\theta_j - \theta_{se})\right) \tag{3.7}$$

where,

$\overline{V_{se}} = V_{se}\angle\theta_{se}$ is the voltage source from the SSSC,

$\overline{V_j} = V_j\angle\theta_j$ is the bus voltage at bus j,

$g_{ij} + jb_{ij} = 1/Z_{se}$ is the SSSC admittance,

$g_{ii} = g_{ij}$, $b_{ii} = b_{ij}$, $g_{jj} = g_{ij}$, $b_{jj} = b_{ij}$ are the bus conductances and susceptances.

The operating constraint of the SSSC is the active power exchange between the controller and the system via the DC link,

$$PE_{SSSC} = \mathrm{Re}\left(V_{se} I_{ji}^{*}\right) = 0 \tag{3.8}$$

where,

$$\mathrm{Re}\left(V_{se} I_{ji}^{*}\right) = -V_i V_{se}\left(g_{ij}\cos(\theta_i - \theta_{se}) - b_{ij}\sin(\theta_i - \theta_{se})\right) + V_j V_{se}\left(g_{ij}\cos(\theta_j - \theta_{se}) - b_{ij}\sin(\theta_j - \theta_{se})\right)$$

3.3.3 UPFC model

The UPFC consists of two switching converters, one shunt converter and one series converter. The converters are connected by a common DC link. The shunt converter is coupled by a shunt-connected transformer to a local bus *i*. The series converter is coupled via a series transformer to a transmission line, Figure 3.3(a). The shunt converter is able to generate or absorb reactive power, and it can provide active power exchange to the series converter for control requirements when necessary. For steady state operation, it is able to control the following,

- simultaneous control of a local bus voltage and power flows of a transmission line;
- circuit impedance;
- voltage angle;
- system power flows.

This equivalent circuit model can be seen as a STATCOM and an SSSC combined as each shunt and series branches are represented by an impedance and a voltage source respectively, Figure 3.3(b).

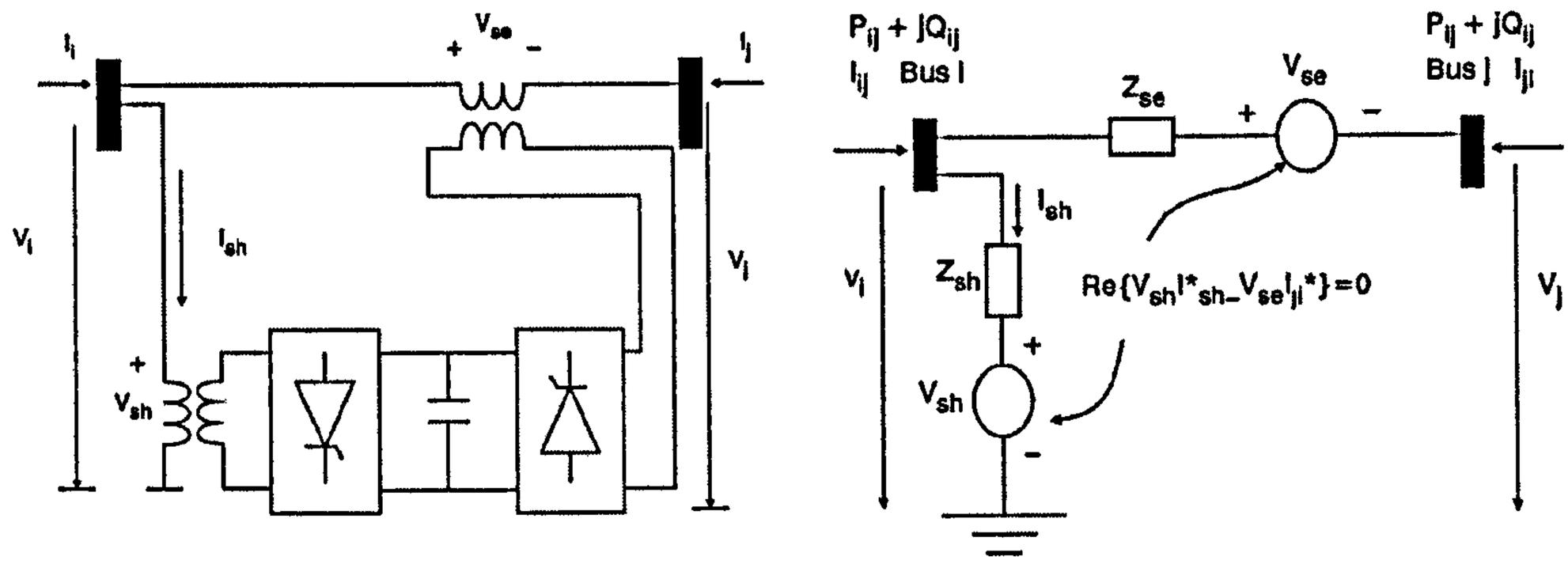

Figure 3.3: (a) Functional model of UPFC, (b) UPFC equivalent circuit [Zhang and Handschin (2001a) and Zhang (2003a)]

The power flow constraints for both shunt and series branches of the UPFC are based on the derivation in Appendix II:

$$P_{sh} = V_i^2 g_{sh} - V_i V_{sh}\left(g_{sh}\cos(\theta_i - \theta_{sh}) + b_{sh}\sin(\theta_i - \theta_{sh})\right) \tag{3.9}$$

$$Q_{sh} = -V_i^2 b_{sh} - V_i V_{sh}\left(g_{sh}\sin(\theta_i - \theta_{sh}) - b_{sh}\cos(\theta_i - \theta_{sh})\right) \tag{3.10}$$

$$\begin{aligned} P_{ij} = {} & V_i^2 g_{ij} - V_i V_j\left(g_{ij}\cos(\theta_i - \theta_j) + b_{ij}\sin(\theta_i - \theta_j)\right) \\ & - V_i V_{se}\left(g_{ij}\cos(\theta_i - \theta_{se}) + b_{ij}\sin(\theta_i - \theta_{se})\right) \end{aligned} \tag{3.11}$$

$$\begin{aligned} Q_{ij} = {} & -V_i^2 b_{ij} - V_i V_j\left(g_{ij}\sin(\theta_i - \theta_j) - b_{ij}\cos(\theta_i - \theta_j)\right) \\ & - V_i V_{se}\left(g_{ij}\cos(\theta_i - \theta_{se}) - b_{ij}\sin(\theta_i - \theta_{se})\right) \end{aligned} \tag{3.12}$$

$$\begin{aligned} P_{ji} = {} & V_j^2 g_{ij} - V_i V_j\left(g_{ij}\cos(\theta_j - \theta_i) + b_{ij}\sin(\theta_j - \theta_i)\right) \\ & + V_j V_{se}\left(g_{ij}\cos(\theta_j - \theta_{se}) + b_{ij}\sin(\theta_j - \theta_{se})\right) \end{aligned} \tag{3.13}$$

$$\begin{aligned} Q_{ji} = {} & -V_j^2 b_{ij} - V_i V_j\left(g_{ij}\sin(\theta_j - \theta_i) - b_{ij}\cos(\theta_j - \theta_i)\right) \\ & - V_j V_{se}\left(g_{ij}\sin(\theta_j - \theta_{se}) - b_{ij}\cos(\theta_j - \theta_{se})\right) \end{aligned} \tag{3.14}$$

where,

$\overline{V_{sh}} = V_{sh}\angle\theta_{sh}$ is the voltage source from the shunt branch,

$\overline{V_{se}} = V_{se}\angle\theta_{se}$ is the voltage source from the series branch,

$g_{sh} + jb_{sh} = 1/Z_{sh}$ is the admittance from the shunt branch,

$g_{ij} + jb_{ij} = 1/Z_{se}$ is the admittance from the series branch,

$g_{ij} = g_{ji}$ and $b_{ij} = b_{ji}$ are the branch conductances and susceptances.

The operating constraint of the UPFC is the active power balance between the two inverters via the common DC link,

$$PE_{UPFC} = PE_{sh} - PE_{se} = \mathrm{Re}\left(V_{sh}I_{sh}^{*} - V_{se}I_{ji}^{*}\right) = 0 \tag{3.15}$$

where, $PE_{sh} = \mathrm{Re}\left(V_{sh}I_{sh}^{*}\right) = 0$ and $PE_{se} = \mathrm{Re}\left(V_{se}I_{ji}^{*}\right) = 0$ are the active power exchanges of the shunt converter and the series converter to the DC link as expressed in equations (3.3) and (3.8) respectively.

Derivations of power mismatch equations for the three FACTS controllers are presented in Appendix IV.

3.3.4 Control modes of FACTS controller models

Each FACTS controller has a different set of control functions which can be activated. When there is a control target specified, the control is called local control (Table 3-1). When no explicit control target is specified for a FACTS controller the control is known as global control. The results presented in this work utilises the global control.

3.4 Integration of FACTS controller models into interior point OPF method

Inclusion of the FACTS controller increases the complexity of the simulation and dimension of the matrix of Newton equations. Table 3-2 summaries the additional system variables, equality constraints and inequality constraints required when each FACTS controller is utilised. For all case studies presented no power flow controls are specified, therefore only the equality constraint $PE = 0$ and the corresponding Lagrange multiplier, λ_{PE} are utilised.

The UPFC is the most complex model of the three controllers. This section gives a summary of the additional system variables, slack variables, dual variables, Lagrange multipliers and

equations required when a UPFC is utilised on a system. For the shunt connected STATCOM controller ignore all terms with the series subscript se, and for the series connected SSSC controller subtract all terms with the shunt subscript sh.

Table 3-2: Summary of additional elements modelled on system when FACTS controllers are included.

FACTS controller	**UPFC**	**SSSC**	**STATCOM**
System variables	θ_{se}, V_{se} θ_{sh}, V_{sh}	θ_{se}, V_{se}	θ_{sh}, V_{sh}
Inequality constraints	$h_{\theta_{se}}^{\min} \le \theta_{se} \le h_{\theta_{se}}^{\max}$, $h_{V_{se}}^{\min} \le V_{se} \le h_{V_{se}}^{\max}$, $h_{\theta_{sh}}^{\min} \le \theta_{sh} \le h_{\theta_{sh}}^{\max}$, $h_{V_{sh}}^{\min} \le V_{sh} \le h_{V_{sh}}^{\max}$.	$h_{\theta_{se}}^{\min} \le \theta_{se} \le h_{\theta_{se}}^{\max}$, $h_{V_{se}}^{\min} \le V_{se} \le h_{V_{se}}^{\max}$.	$h_{\theta_{sh}}^{\min} \le \theta_{sh} \le h_{\theta_{sh}}^{\max}$, $h_{V_{sh}}^{\min} \le V_{sh} \le h_{V_{sh}}^{\max}$.
Dual variables	$sl_{\theta_{se}}, \pi l_{\theta_{se}}, su_{\theta_{se}}, \pi u_{\theta_{se}}$, $sl_{V_{se}}, \pi l_{V_{se}}, su_{V_{se}}, \pi u_{V_{se}}$, $sl_{\theta_{sh}}, \pi l_{\theta_{sh}}, su_{\theta_{sh}}, \pi u_{\theta_{sh}}$, $sl_{V_{sh}}, \pi l_{V_{sh}}, su_{V_{sh}}, \pi u_{V_{sh}}$.	$sl_{\theta_{se}}, \pi l_{\theta_{se}}, su_{\theta_{se}}, \pi u_{\theta_{se}}$, $sl_{V_{se}}, \pi l_{V_{se}}, su_{V_{se}}, \pi u_{V_{se}}$.	$sl_{\theta_{sh}}, \pi l_{\theta_{sh}}, su_{\theta_{sh}}, \pi u_{\theta_{sh}}$, $sl_{V_{sh}}, \pi l_{V_{sh}}, su_{V_{sh}}, \pi u_{V_{sh}}$.
Equality constraint	$PE_{UPFC} = 0$	$PE_{SSSC} = 0$	$PE_{STATCOM} = 0$
Lagrange multiplier	λ_{PE}	λ_{PE}	λ_{PE}
Power flow control equality constraints, Lagrange multipliers	Active power flow control $PC = P_{ji} - P_{ji}^{Spec} = 0$ λ_{PC}	Active power flow control $PC = P_{ji} - P_{ji}^{Spec} = 0$ λ_{PC}	N/A
	Reactive power flow control $QC = Q_{ji} - Q_{ji}^{Spec} = 0$ λ_{QC}	Reactive power flow control $QC = Q_{ji} - Q_{ji}^{Spec} = 0$ λ_{QC}	N/A
	Active and reactive power flow control $PC = P_{ji} - P_{ji}^{Spec} = 0$ $QC = Q_{ji} - Q_{ji}^{Spec} = 0$ λ_{PC} and λ_{QC}	N/A	N/A

where the system variables are;

$$x = \left[\theta_{se}, V_{se}, \theta_{sh}, V_{sh}, t_i, \theta_i, V_i, \theta_j, V_j, Pg_i^+, Pg_i^-, Qg\right]^T,$$

N total number of system buses,

N_h total number of inequality constraints,

N_F total number of FACTS controller variables, dependent on the number of FACTS controllers on the system and control mode of operation,

$h(x)$ inequality constraints including those concerning $\theta_{se}, V_{se}, \theta_{sh}$ and V_{sh}.

3.4.1 Lagrange function for optimisation with equalities

Lagrange function with additional equalities due to a FACTS controller updated from equation (2.25),

$$\begin{aligned} L_\mu \doteq f(x) &- \mu\sum_{j=1}^{N_h}\ln(sl_j) - \mu\sum_{j=1}^{N_h}\ln(su_j) - \sum_{i=1}^{N}\lambda_{p_i}\Delta P_i - \sum_{i=1}^{N}\lambda_{q_i}\Delta Q_i \\ &- \sum_{i=1}^{N_F}\lambda_{PE_i}PE_i - \sum_{i=1}^{N_F}\lambda_{PC_i}PC_i - \sum_{i=1}^{N_F}\lambda_{QC_i}QC_i \\ &- \sum_{j=1}^{N_h}\pi l_j(h_j - sl_j - h_j^{\min}) - \sum_{j=1}^{N_h}\pi u_j(h_j + su_j - h_j^{\max}) \end{aligned} \tag{3.16}$$

3.4.2 First order KKT conditions

The first order KKT conditions (equations (2.26)-(2.32)) update to,

$$\begin{aligned} \nabla_{x_\alpha} L_\mu = \nabla_x f(x) &- \sum_{i=1}^{N}\nabla_x \Delta P_i \lambda_{p_i} - \sum_{i=1}^{N}\nabla_x \Delta Q_i \lambda_{q_i} \\ &- \sum_{i=1}^{N_F}\nabla_x PE_i \lambda_{PE_i} - \sum_{i=1}^{N_F}\nabla_x PC_i \lambda_{PC_i} - \sum_{i=1}^{N}\nabla_x QC_i \lambda_{QC_i} \\ &- \sum_{j=1}^{N_h}\nabla_x h_j \pi l_j - \sum_{j=1}^{N_h}\nabla_x h_j \pi u_j = 0 \end{aligned} \tag{3.17}$$

$$\nabla_{\lambda_{p_i}} L_\mu = -\Delta P_i = 0 \tag{3.18}$$

$$\nabla_{\lambda_{q_i}} L_\mu = -\Delta Q_i = 0 \tag{3.19}$$

$$\nabla_{\lambda_{PE_i}} L_\mu = -PE_i = 0 \tag{3.20}$$

$$\nabla_{\lambda_{PC_i}} L_\mu = -PC_i = 0 \tag{3.21}$$

$$\nabla_{\lambda_{QC_i}} L_\mu = -QC_i = 0 \tag{3.22}$$

$$\nabla_{\pi l_j} L_\mu = -\left(h_j - sl_j - h_j^{\min}\right) = 0 \tag{3.23}$$

$$\nabla_{\pi u_j} L_\mu = -\left(h_j + su_j - h_j^{\max}\right) = 0 \tag{3.24}$$

$$\nabla_{sl_j} L_\mu = \mu - sl_j \pi l_j = 0 \tag{3.25}$$

$$\nabla_{su_j} L_\mu = \mu + su_j \pi u_j = 0 \tag{3.26}$$

where,

$x_\alpha = \left[x, \lambda_{p_i}, \lambda_{q_i}, \lambda_{PE_i}, \lambda_{PC_i}, \lambda_{QC_i}, sl_j, su_j, \pi l_j, \pi u_j\right]$,

$\alpha = 1, 2, \ldots 2N + 3N_g + N_t + eN_F$,

e integer that depends upon the number of FACTS controllers.

First order KKT conditions (equations (3.17) – (3.36)) formulae are listed in Appendix III and a corresponding list of first and second order derivatives can be found in Appendix VI.

3.4.3 Newton's method for solving nonlinear equations

Equations (2.37)-(2.43) update to,

$$\begin{aligned}
-\nabla_{x_\alpha} L_\mu = \Bigg[& -\sum_{i=1}^{N} \nabla_x (\nabla_x \Delta P_i) \lambda_{p_i} - \sum_{i=1}^{N} \nabla_x (\nabla_x \Delta Q_i) \lambda_{q_i} - \sum_{i=1}^{N_F} \nabla_x (\nabla_x PE_i) \lambda_{PE_i} - \sum_{i=1}^{N_F} \nabla_x (\nabla_x PC_i) \lambda_{PC_i} \\
& - \sum_{i=1}^{N_F} \nabla_x (\nabla_x QC_i) \lambda_{QC_i} - \sum_{j=1}^{N_h} \nabla_x (\nabla_x h_j) \pi l_j - \sum_{j=1}^{N_h} \nabla_x (\nabla_x h_j) \pi u_j \Bigg] \Delta x \\
& - \sum_{i=1}^{N} \nabla_{x_\alpha} \Delta P_i \Delta \lambda_{p_i} - \sum_{i=1}^{N} \nabla_{x_\alpha} \Delta Q_i \Delta \lambda_{q_i} - \sum_{i=1}^{N_F} \nabla_{x_\alpha} PE_i \Delta \lambda_{PE_i} - \sum_{i=1}^{N_F} \nabla_{x_\alpha} PC_i \Delta \lambda_{PC_i} \\
& - \sum_{i=1}^{N_F} \nabla_{x_\alpha} QC_i \Delta \lambda_{QC_i} - \sum_{j=1}^{N_h} \nabla_{x_\alpha} h_j \Delta \pi l_j - \sum_{j=1}^{N_h} \nabla_{x_\alpha} h_j \Delta \pi u_j + \sum_{i=1}^{N_g} \nabla_x \nabla_x f(x) \Delta x
\end{aligned} \tag{3.27}$$

$$-\nabla_{\lambda_{p_i}} L_\mu = -\sum_{i=1}^{N} \nabla_x \Delta P_i \Delta x \tag{3.28}$$

$$-\nabla_{\lambda_{q_i}} L_\mu = -\sum_{i=1}^{N} \nabla_x \Delta Q_i \Delta x \tag{3.29}$$

$$-\nabla \lambda_{PE_i} L_\mu = -\sum_{i=1}^{N_F} \nabla_x PE_i \Delta x \tag{3.30}$$

$$-\nabla \lambda_{PC_i} L_\mu = -\sum_{i=1}^{N_F} \nabla_x PC_i \Delta x \tag{3.31}$$

$$-\nabla \lambda_{QC_i} L_\mu = -\sum_{i=1}^{N_F} \nabla_x QC_i \Delta x \tag{3.32}$$

$$-\nabla \pi l_j L_\mu = -\sum_{j=1}^{N_h} \nabla_x h_j \Delta x + \Delta s l_j \tag{3.33}$$

$$-\nabla \pi u_j L_\mu = -\sum_{j=1}^{N_h} \nabla_x h_j \Delta x - \Delta s u_j \tag{3.34}$$

$$-\nabla sl_j L_\mu = -sl_j \Delta \pi l_j - \pi l_j \Delta s l_j \tag{3.35}$$

$$-\nabla su_j L_\mu = -su_j \Delta \pi u_j - \pi u_j \Delta s u_j \tag{3.36}$$

The matrix of Newton equations (2.44) updates to,

$$\begin{bmatrix}
Sl^{-1}\Pi l & 0 & I & 0 & 0 & 0 & 0 & 0 & 0 & 0 \\
0 & -Sl^{-1}\Pi u & 0 & -I & 0 & 0 & 0 & 0 & 0 & 0 \\
I & 0 & 0 & 0 & -\nabla h & 0 & 0 & 0 & 0 & 0 \\
0 & -I & 0 & 0 & -\nabla h & 0 & 0 & 0 & 0 & 0 \\
0 & 0 & -\nabla h^T & -\nabla h^T & H & -Jp^T & -Jq^T & -J_{PE}{}^T & -J_{PC}{}^T & -J_{QC}{}^T \\
0 & 0 & 0 & 0 & -Jp & 0 & 0 & 0 & 0 & 0 \\
0 & 0 & 0 & 0 & -Jq & 0 & 0 & 0 & 0 & 0 \\
0 & 0 & 0 & 0 & -J_{PE} & 0 & 0 & 0 & 0 & 0 \\
0 & 0 & 0 & 0 & -J_{PC} & 0 & 0 & 0 & 0 & 0 \\
0 & 0 & 0 & 0 & -J_{QC} & 0 & 0 & 0 & 0 & 0
\end{bmatrix} \times$$

$$\begin{bmatrix} \Delta sl \\ \Delta su \\ \Delta \pi l \\ \Delta \pi u \\ \Delta x \\ \Delta \lambda_p \\ \Delta \lambda_q \\ \Delta \lambda_{PE} \\ \Delta \lambda_{PC} \\ \Delta \lambda_{QC} \end{bmatrix} = \begin{bmatrix} Sl^{-1}\nabla_{sl}L_\mu \\ Su^{-1}\nabla_{su}L_\mu \\ -\nabla_{\pi l}L_\mu \\ -\nabla_{\pi u}L_\mu \\ -\nabla_x L_\mu \\ -\nabla_{\lambda p}L_\mu \\ -\nabla_{\lambda q}L_\mu \\ -\nabla_{\lambda_{PE}}L_\mu \\ -\nabla_{\lambda_{PC}}L_\mu \\ -\nabla_{\lambda_{QC}}L_\mu \end{bmatrix} \tag{3.37}$$

where,

H equation (2.45) updates to,

$$\begin{aligned} H\left(x,\lambda_p,\lambda_q,\lambda_{PE},\lambda_{PC},\lambda_{QC},\pi l,\pi u\right) = {} & \nabla_x\nabla_x f(x) - \sum_{i=1}^{N}\nabla_x\left(\nabla_x\Delta P_i\right)\lambda_{pi} - \sum_{i=1}^{N}\nabla_x\left(\nabla_x\Delta Q_i\right)\lambda_{qi} \\ & - \sum_{i=1}^{N_F}\nabla_x\left(\nabla_x PE_i\right)\lambda_{PE_i} - \sum_{i=1}^{N_F}\nabla_x\left(\nabla_x PC_i\right)\lambda_{PC_i} \\ & - \sum_{i=1}^{N_F}\nabla_x\left(\nabla_x QC_i\right)\lambda_{QC_i} - \sum_{j=1}^{N_h}\nabla_x\left(\nabla_x h_j\right)\pi l_j \\ & - \sum_{j=1}^{N_h}\nabla_x\left(\nabla_x h_j\right)\pi u_j \end{aligned} \tag{3.38}$$

J_{PE}, J_{PC} and J_{QC} are the Jacobian matrices of first order partial derivatives,

$$J_{PE_i}(x) = \left[\frac{\partial PE_i(x)}{\partial x}\right] = \nabla_x PE_i$$

$$J_{PC_i}(x) = \left[\frac{\partial PC_i(x)}{\partial x}\right] = \nabla_x PC_i$$

$$J_{QC_i}(x) = \left[\frac{\partial QC_i(x)}{\partial x}\right] = \nabla_x QC_i$$

The Hessian matrix, H is updated from equation (2.52),

$$\begin{bmatrix}
H_{t_i t_i} & 0 & 0 & 0 & H_{t_i\theta_i} & H_{t_i V_i} & H_{t_i\theta_{se}} & H_{t_i V_{se}} & H_{t_i\theta_{sh}} & H_{t_i V_{sh}} \\
0 & H_{P_{g_i}^+ P_{g_i}^+} & 0 & 0 & 0 & 0 & 0 & 0 & 0 & 0 \\
0 & 0 & H_{P_{g_i}^- P_{g_i}^-} & 0 & 0 & 0 & 0 & 0 & 0 & 0 \\
0 & 0 & 0 & H_{Q_{g_i} Q_{g_i}} & 0 & 0 & 0 & 0 & 0 & 0 \\
H_{t_i\theta_i} & 0 & 0 & 0 & H_{\theta_i\theta_i} & H_{\theta_i V_i} & H_{\theta_i\theta_{se}} & H_{\theta_i V_{se}} & H_{\theta_i\theta_{sh}} & H_{\theta_i V_{sh}} \\
H_{t_i V_i} & 0 & 0 & 0 & H_{\theta_i V_i} & H_{V_i V_i} & H_{V_i\theta_{se}} & H_{V_i V_{se}} & H_{V_i\theta_{sh}} & H_{V_i V_{sh}} \\
H_{t_i\theta_{se}} & 0 & 0 & 0 & H_{\theta_i\theta_{se}} & H_{V_i\theta_{se}} & H_{\theta_{se}\theta_{se}} & H_{\theta_{se} V_{se}} & H_{\theta_{se}\theta_{sh}} & H_{\theta_{se} V_{sh}} \\
H_{t_i V_{se}} & 0 & 0 & 0 & H_{\theta_i V_{se}} & H_{V_i V_{se}} & H_{\theta_{se} V_{se}} & H_{V_{se} V_{se}} & H_{V_{se}\theta_{sh}} & H_{V_{se} V_{sh}} \\
H_{t_i\theta_{sh}} & 0 & 0 & 0 & H_{\theta_i\theta_{sh}} & H_{V_i\theta_{sh}} & H_{\theta_{se}\theta_{sh}} & H_{V_{se}\theta_{sh}} & H_{\theta_{sh}\theta_{sh}} & H_{\theta_{sh} V_{sh}} \\
H_{t_i V_{sh}} & 0 & 0 & 0 & H_{\theta_i V_{sh}} & H_{V_i V_{sh}} & H_{\theta_{se} V_{sh}} & H_{V_{se} V_{sh}} & H_{\theta_{sh} V_{sh}} & H_{V_{sh} V_{sh}}
\end{bmatrix} \times$$

$$\begin{bmatrix}
\Delta t_i \\ \Delta P_{g_i}^+ \\ \Delta P_{g_i}^- \\ \Delta Q_{g_i} \\ \Delta\theta_i \\ \Delta V_i \\ \Delta\theta_{se} \\ \Delta V_{se} \\ \Delta\theta_{sh} \\ \Delta V_{sh}
\end{bmatrix} = \begin{bmatrix}
-\nabla_{t_i} L_\mu \\ -\nabla_{\Delta P_{g_i}^+} L_\mu \\ -\nabla_{\Delta P_{g_i}^-} L_\mu \\ -\nabla_{\Delta Q_{g_i}} L_\mu \\ -\nabla_{\theta_i} L_\mu \\ -\nabla_{V_i} L_\mu \\ -\nabla_{\theta_{se}} L_\mu \\ -\nabla_{V_{se}} L_\mu \\ -\nabla_{\theta_{sh}} L_\mu \\ -\nabla_{V_{sh}} L_\mu
\end{bmatrix} \tag{3.39}$$

where,

$$x = \left[t_i, P_{g_i}^+, P_{g_i}^-, Q_{g_i}, \theta_i, V_i, \theta_{se}, V_{se}, \theta_{sh}, V_{sh} \right]$$

3.4.4 Reduced Newton equations

The elimination of slack variables refers to the slack variables of the inequality constraints only, the general form presented in equations (2.55) to (2.63) are still valid. There is the necessary addition of equations (3.30)-(3.32) where the matrix of (2.64) updates to,

$$\begin{bmatrix} \Pi l^{-1} Sl & 0 & -\nabla h & 0 & 0 & 0 & 0 & 0 \\ 0 & \Pi u^{-1} Su & -\nabla h & 0 & 0 & 0 & 0 & 0 \\ -\nabla h^T & -\nabla h^T & H & -Jp^T & -Jq^T & -J_{PE}{}^T & -J_{PC}{}^T & -J_{QC}{}^T \\ 0 & 0 & -Jp & 0 & 0 & 0 & 0 & 0 \\ 0 & 0 & -Jq & 0 & 0 & 0 & 0 & 0 \\ 0 & 0 & -J_{PE} & 0 & 0 & 0 & 0 & 0 \\ 0 & 0 & -J_{PC} & 0 & 0 & 0 & 0 & 0 \\ 0 & 0 & -J_{QC} & 0 & 0 & 0 & 0 & 0 \end{bmatrix} \times$$

$$\begin{bmatrix} \Delta\pi l \\ \Delta\pi u \\ \Delta x \\ \Delta\lambda p \\ \Delta\lambda q \\ \Delta\lambda_{PE} \\ \Delta\lambda_{PC} \\ \Delta\lambda_{QC} \end{bmatrix} = \begin{bmatrix} -\nabla_{\pi l_j} L_\mu - \Pi l_j^{-1} \nabla_{sl_j} L_\mu \\ -\nabla_{\pi u_j} L_\mu - \Pi u_j^{-1} \nabla_{su_j} L_\mu \\ -\nabla_x L_\mu \\ -\nabla_{\lambda p} L_\mu \\ -\nabla_{\lambda q} L_\mu \\ -\nabla_{\lambda_{PE}} L_\mu \\ -\nabla_{\lambda_{PC}} L_\mu \\ -\nabla_{\lambda_{QC}} L_\mu \end{bmatrix} \tag{3.40}$$

where,

$$H = \nabla_x \nabla_x f(x) - \sum_{i=1}^{N} \nabla_x \left(J_{p_i}(x) \right) \lambda p_i - \sum_{i=1}^{N} \nabla_x \left(J_{q_i}(x) \right) \lambda q_i - \sum_{i=1}^{N_F} \nabla_x \left(J_{PE_i}(x) \right) \lambda_{PE_i}$$
$$- \sum_{i=1}^{N_F} \nabla_x \left(J_{PC_i}(x) \right) \lambda_{PC_i} - \sum_{i=1}^{N_F} \nabla_x \left(J_{QC_i}(x) \right) \lambda_{QC_i} - \sum_{j=1}^{N_h} \nabla_x \left(\nabla_x h_j \right) \pi l_j - \sum_{j=1}^{N_h} \nabla_x \left(\nabla_x h_j \right) \pi u_j \tag{3.41}$$

During the process of elimination of dual variables $\Delta\pi l_j$ and $\Delta\pi u_j$, equations (2.67), (2.68), (2.70), (2.71) and (2.73) remain the same. In equation (2.69), $-\nabla^*_{x_\alpha} L_\mu$ is updated to,

$$-\nabla^*_{x_\alpha} L_\mu = H\Delta x + \sum_{i=1}^{N_g} \nabla_x \nabla_x f(x) \Delta x - \sum_{i=1}^{N} \nabla_{x_\alpha} \Delta P_i \Delta\lambda_{p_i} - \sum_{i=1}^{N} \nabla_{x_\alpha} \Delta Q_i \Delta\lambda_{q_i}$$
$$- \sum_{i=1}^{N_F} \nabla_{x_\alpha} PE_i \Delta\lambda_{PE_i} - \sum_{i=1}^{N_F} \nabla_{x_\alpha} PC_i \Delta\lambda_{PC_i} - \sum_{i=1}^{N_F} \nabla_{x_\alpha} QC_i \Delta\lambda_{QC_i} \tag{3.42}$$
$$+ \pi l_j s l_j^{-1} \sum_{j=1}^{N_h} \nabla_x h_j \nabla_x h_j \Delta x - \pi u_j s u_j^{-1} \sum_{j=1}^{N_h} \nabla_x h_j \nabla_x h_j \Delta x$$

where, equation (2.72) is updated to,

$$H=\left[-\sum_{i=1}^{N}\nabla_x(\nabla_x\Delta P_i)\lambda_{p_i}-\sum_{i=1}^{N}\nabla_x(\nabla_x\Delta Q_i)\lambda_{q_i}-\sum_{i=1}^{N_F}\nabla_x(\nabla_x PE_i)\lambda_{PE_i}-\sum_{i=1}^{N_F}\nabla_x(\nabla_x PC_i)\lambda_{PC_i}\right.$$
$$\left.-\sum_{i=1}^{N_F}\nabla_x(\nabla_x QC_i)\lambda_{QC_i}-\sum_{j=1}^{N_h}\nabla_x(\nabla_x h_j)\pi l_j-\sum_{j=1}^{N_h}\nabla_x(\nabla_x h_j)\pi u_j\right] \tag{3.43}$$

The compact form is at maximum dimension when both P and Q control are specified for the UPFC,

$$\begin{bmatrix} H* & -Jp^T & -Jq^T & -J_{PE}{}^T & -J_{PC}{}^T & -J_{QC}{}^T \\ -Jp & 0 & 0 & 0 & 0 & 0 \\ -Jq & 0 & 0 & 0 & 0 & 0 \\ -J_{PE} & 0 & 0 & 0 & 0 & 0 \\ -J_{PC} & 0 & 0 & 0 & 0 & 0 \\ -J_{QC} & 0 & 0 & 0 & 0 & 0 \end{bmatrix}\begin{bmatrix} \Delta x \\ \Delta\lambda p \\ \Delta\lambda q \\ \Delta\lambda PE \\ \Delta\lambda PC \\ \Delta\lambda QC \end{bmatrix}=\begin{bmatrix} -\nabla^*_x L_\mu \\ -\nabla\lambda p L_\mu \\ -\nabla\lambda q L_\mu \\ -\nabla\lambda_{PE} L_\mu \\ -\nabla\lambda_{PC} L_\mu \\ -\nabla\lambda_{QC} L_\mu \end{bmatrix} \tag{3.44}$$

where,

$$H^*=H+\sum_{i=1}^{N_g}\nabla_x\nabla_x f(x)+\sum_{j=1}^{N_h}\nabla_x h_j\nabla_x h_j\left(\pi l_j sl_j^{-1}-\pi u_j su_j^{-1}\right) \tag{3.45}$$

N_g is the number of generator buses and H is as defined in equation (3.43).

$-\nabla^*_{x_\alpha} L_\mu$ is initially defined in equation (2.73), with the inclusion of the FACTS controller it is updated to equation (3.46).

The right hand side terms are updated to,

$$-\nabla^*_{x_\alpha} L_\mu=-\nabla_{x_\alpha} L_\mu+sl_j^{-1}\sum_{j=1}^{N_h}\nabla_x h_j^T\left(\pi l_j\nabla\pi l_j L_\mu+\nabla sl_j L_\mu\right)$$
$$-su_j^{-1}\sum_{j=1}^{N_h}\nabla_x h_j^T\left(\pi u_j\nabla\pi u_j L_\mu+\nabla su_j L_\mu\right) \tag{3.46}$$

where,

$$\nabla_{x_\alpha} L_\mu=\sum_{i=1}^{N_g}\nabla_x f(x)-\sum_{i=1}^{N}\nabla_{x_\alpha}\Delta P_i\lambda_{p_i}-\sum_{i=1}^{N}\nabla_{x_\alpha}\Delta Q_i\lambda_{q_i}-\sum_{i=1}^{N_F}\nabla_{x_\alpha} PE_i\lambda_{PE_i}-\sum_{i=1}^{N_F}\nabla_{x_\alpha} PC_i\lambda_{PC_i}$$
$$-\sum_{i=1}^{N_F}\nabla_{x_\alpha} QC_i\lambda_{QC_i}-\sum_{j=1}^{N_h}\nabla_x h_j\pi l_j-\sum_{j=1}^{N_h}\nabla_x h_j\,\pi u_j \tag{3.47}$$

$$\nabla_{\pi l_j} L_\mu=-\left(h_j-sl_j-h_j^{\min}\right) \tag{3.48}$$

$$\nabla_{\pi u_j} L_\mu = -\left(h_j + su_j - h_j^{\max}\right) \tag{3.49}$$

$$\nabla_{sl_j} L_\mu = \mu - sl_j \pi l_j \tag{3.50}$$

$$\nabla_{su_j} L_\mu = \mu + su_j \pi u_j \tag{3.51}$$

$$\nabla_{\lambda_{p_i}} L_\mu = -\Delta P_i \tag{3.52}$$

$$\nabla_{\lambda_{q_i}} L_\mu = -\Delta Q_i \tag{3.53}$$

$$\nabla_{\lambda_{PE_i}} L_\mu = -PE_i = -\left(PE_i^{sh} - PE_i^{se}\right) \tag{3.54}$$

$$\nabla_{\lambda_{PC_i}} L_\mu = -PC_i \tag{3.55}$$

$$\nabla_{\lambda_{QC_i}} L_\mu = -QC_i \tag{3.56}$$

The expanded form of the compact matrix of Newton equations, showing all the system variable differentials related to bus i and FACTS controllers is shown analytically in equation (3.57).

3.4.5 Initialisation of FACTS controller variables

Initial conditions must still satisfy the slack and dual variable properties; $sl_j > 0$, $su_j > 0$, $\pi l_j > 0$ and $\pi u_j < 0$. For UPFC controller with non-specified control the system variables are initialised as follows,

1. series and shunt voltage angles, $\theta_{se}^0 = \theta_{sh}^0 = 0.001$
2. series voltage magnitude, $V_{se}^0 = 0.5\left(V_{se}^{\max} + V_{se}^{\min}\right)$
3. shunt voltage magnitude, $V_{sh}^0 = 0.5\left(V_{sh}^{\max} + V_{sh}^{\min}\right)$
4. all series and shunt slack variables sl_j are set to $h_j - h_h^{\min}$ and dual variables πl_j are set to μ / sl_j;
5. all series and shunt slack variables su_j are set to $h_h^{\max} - h_j$ and dual variables πu_j are set to $-\mu / su_j$;
6. dual variables $\lambda_{PE_i} = \lambda_{PC_i} = \lambda_{QC_i} = 0$.

The update of the solution remains the same as previously explained in Chapter 2, equations (2.78) to (2.91).

$$
\begin{bmatrix}
H^{*}_{tt} & 0 & 0 & 0 & H^{*}_{t\theta_i} & H^{*}_{tV_i} & H^{*}_{t\theta_{se}} & H^{*}_{tV_{se}} & H^{*}_{t\theta_{sh}} & H^{*}_{tV_{sh}} & -J_{p_i,t} & -J_{q_i,t} & -J_{PE_i,t} & -J_{PC_i,t} & -J_{QC_i,t} \\
0 & H^{*}_{\Delta P_g^+} & 0 & 0 & 0 & 0 & 0 & 0 & 0 & 0 & -J_{p_i,\Delta P_{g_i}^+} & 0 & 0 & 0 & 0 \\
0 & 0 & H^{*}_{\Delta P_g^-} & 0 & 0 & 0 & 0 & 0 & 0 & 0 & -J_{p_i,\Delta P_{g_i}^-} & 0 & 0 & 0 & 0 \\
0 & 0 & 0 & H^{*}_{Q_g} & 0 & 0 & 0 & 0 & 0 & 0 & 0 & -J_{p_i,Q_{g_i}} & 0 & 0 & 0 \\
H^{*}_{t\theta_i} & 0 & 0 & 0 & H^{*}_{\theta_i\theta_i} & H^{*}_{\theta_iV_i} & H^{*}_{\theta_i\theta_{se}} & H^{*}_{\theta_iV_{se}} & H^{*}_{\theta_i\theta_{sh}} & H^{*}_{\theta_iV_{sh}} & -J_{p_i,\theta_i} & -J_{q_i,\theta_i} & -J_{PE_i,\theta_i} & -J_{PC_i,\theta_i} & -J_{QC_i,\theta_i} \\
H^{*}_{tV_i} & 0 & 0 & 0 & H^{*}_{\theta_iV_i} & H^{*}_{V_iV_i} & H^{*}_{V_i\theta_{se}} & H^{*}_{V_iV_{se}} & H^{*}_{V_i\theta_{sh}} & H^{*}_{V_iV_{sh}} & -J_{p_i,V_i} & -J_{q_i,V_i} & -J_{PE_i,V_i} & -J_{PC_i,V_i} & -J_{QC_i,V_i} \\
H^{*}_{t\theta_{se}} & 0 & 0 & 0 & H^{*}_{\theta_i\theta_{se}} & H^{*}_{V_i\theta_{se}} & H^{*}_{\theta_{se}\theta_{se}} & H^{*}_{\theta_{se}V_{se}} & H^{*}_{\theta_{se}\theta_{sh}} & H^{*}_{\theta_{se}V_{sh}} & -J_{p_i,\theta_{se}} & -J_{q_i,\theta_{se}} & -J_{PE_i,\theta_{se}} & -J_{PC_i,\theta_{se}} & -J_{QC_i,\theta_{se}} \\
H^{*}_{tV_{se}} & 0 & 0 & 0 & H^{*}_{\theta_iV_{se}} & H^{*}_{V_iV_{se}} & H^{*}_{\theta_{se}V_{se}} & H^{*}_{V_{se}V_{se}} & H^{*}_{V_{se}\theta_{sh}} & H^{*}_{V_{se}V_{sh}} & -J_{p_i,V_{se}} & -J_{q_i,V_{se}} & -J_{PE_i,V_{se}} & -J_{PC_i,V_{se}} & -J_{QC_i,V_{se}} \\
H^{*}_{t\theta_{sh}} & 0 & 0 & 0 & H^{*}_{\theta_i\theta_{sh}} & H^{*}_{V_i\theta_{sh}} & H^{*}_{\theta_{se}\theta_{sh}} & H^{*}_{V_{se}\theta_{sh}} & H^{*}_{\theta_{sh}\theta_{sh}} & H^{*}_{V_{sh}\theta_{sh}} & -J_{p_i,\theta_{sh}} & -J_{q_i,\theta_{sh}} & -J_{PE_i,\theta_{sh}} & -J_{PC_i,\theta_{sh}} & -J_{QC_i,\theta_{sh}} \\
H^{*}_{tV_{sh}} & 0 & 0 & 0 & H^{*}_{\theta_iV_{sh}} & H^{*}_{V_iV_{sh}} & H^{*}_{\theta_{se}V_{sh}} & H^{*}_{V_{se}V_{sh}} & H^{*}_{V_{sh}\theta_{sh}} & H^{*}_{V_{sh}V_{sh}} & -J_{p_i,V_{sh}} & -J_{q_i,V_{sh}} & -J_{PE_i,V_{sh}} & -J_{PC_i,V_{sh}} & -J_{QC_i,V_{sh}} \\
-J_{p_i,t} & -J_{p_i,\Delta P_{g_i}^+} & -J_{p_i,\Delta P_{g_i}^-} & 0 & -J_{p_i,\theta_i} & -J_{p_i,V_i} & -J_{p_i,\theta_{se}} & -J_{p_i,V_{se}} & -J_{p_i,\theta_{sh}} & -J_{p_i,V_{sh}} & 0 & 0 & 0 & 0 & 0 \\
-J_{q_i,t} & 0 & 0 & -J_{p_i,Q_{g_i}} & -J_{q_i,\theta_i} & -J_{q_i,V_i} & -J_{q_i,\theta_{se}} & -J_{q_i,V_{se}} & -J_{q_i,\theta_{sh}} & -J_{q_i,V_{sh}} & 0 & 0 & 0 & 0 & 0 \\
-J_{PE_i,t} & 0 & 0 & 0 & -J_{PE_i,\theta_i} & -J_{PE_i,V_i} & -J_{PE_i,\theta_{se}} & -J_{PE_i,V_{se}} & -J_{PE_i,\theta_{sh}} & -J_{PE_i,V_{sh}} & 0 & 0 & 0 & 0 & 0 \\
-J_{PC_i,t} & 0 & 0 & 0 & -J_{PC_i,\theta_i} & -J_{PC_i,V_i} & -J_{PC_i,\theta_{se}} & -J_{PC_i,V_{se}} & -J_{PC_i,\theta_{sh}} & -J_{PC_i,V_{sh}} & 0 & 0 & 0 & 0 & 0 \\
-J_{QC_i,t} & 0 & 0 & 0 & -J_{QC_i,\theta_i} & -J_{QC_i,V_i} & -J_{QC_i,\theta_{se}} & -J_{QC_i,V_{se}} & -J_{QC_i,\theta_{sh}} & -J_{QC_i,V_{sh}} & 0 & 0 & 0 & 0 & 0
\end{bmatrix}
\begin{bmatrix}
\Delta t \\ \Delta P_{g_i}^+ \\ \Delta P_{g_i}^- \\ \Delta Q_{g_i} \\ \Delta\theta_i \\ \Delta V_i \\ \Delta\theta_{se} \\ \Delta V_{se} \\ \Delta\theta_{sh} \\ \Delta V_{sh} \\ \Delta\lambda_{p_i} \\ \Delta\lambda_{q_i} \\ \Delta\lambda_{PE_i} \\ \Delta\lambda_{PC_i} \\ \Delta\lambda_{QC_i}
\end{bmatrix}
=
\begin{bmatrix}
-\nabla^{*}_{t} L_\mu \\ -\nabla^{*}_{\Delta P_{g_i}^+} L_\mu \\ -\nabla^{*}_{\Delta P_{g_i}^-} L_\mu \\ -\nabla^{*}_{Q_{g_i}} L_\mu \\ -\nabla^{*}_{\theta_i} L_\mu \\ -\nabla^{*}_{V_i} L_\mu \\ -\nabla^{*}_{\theta_{se}} L_\mu \\ -\nabla^{*}_{V_{se}} L_\mu \\ -\nabla^{*}_{\theta_{sh}} L_\mu \\ -\nabla^{*}_{V_{sh}} L_\mu \\ -\nabla_{\lambda_{p_i}} L_\mu \\ -\nabla_{\lambda_{q_i}} L_\mu \\ -\nabla_{\lambda_{PE_i}} L_\mu \\ -\nabla_{\lambda_{PC_i}} L_\mu \\ -\nabla_{\lambda_{QC_i}} L_\mu
\end{bmatrix}
\tag{3.57}
$$

3.5 Setup of scheduled active power generation for system initial conditions

To measure how FACTS controllers can change the optimal solution to the power flow problem around a system, all the initial conditions excluding the variables concerning the FACTS controller must be the same. The bilateral market objective function is concerned with changes in real power at the generator buses. The following procedure describes how the initial real power generation levels are setup for the base case (System II) and the cases with a FACTS controller installed (System III) from the original system (System I). For all Systems I, II and III, the vector of initial per unit MW demand from each load bus, $\left[P_{d_i}\right]$, is constant.

3.5.1 System I

System I is the original system input file at a nominal loading level with no congestion and no FACTS controller installed. The input vector of per unit MW demand is, $\left[P_{d_i}\right]$ and remains constant for all three systems. The input vector of initial per unit MW generation is $\begin{bmatrix} P_{g_i}^{0_{SysI}} \end{bmatrix}$.

After the optimal solution is found, the following information can be obtained,

- active power system losses, P_{LOSS}^{SysI};
- vector of per unit MW generation output, $\left[P_{g_i OUT}^{SysI}\right]$;
- system per unit MW generation output, $\sum_{i}^{N_g} P_{g_i OUT}^{SysI}$, which is equal to the system per unit MW demand and system losses, $\sum_{i}^{N_g} P_{g_i OUT}^{SysI} = \sum_{i}^{N_d}\left[P_{d_i}\right] + P_{LOSS}^{SysI}$;
- system cost $f(x)^{SysI}$ is purely due to system losses.

3.5.2 System II

System II is the base case system, set at the congested situation without a FACTS controller installed. For an individual congested line, the maximum complex power constraint, $S_{ij}^{2\max}$ of specified line is reduced and for observation of daily demand fluctuations, the % Load

Rise factor is increased. The input vector of initial per unit MW demand remains unchanged, $\left[P_{d_i}\right]$.The input vector of initial per unit MW generation for System II is equal to the vector of per unit MW generation output of System I, $\left[P_{g_i}^{0\,SysII}\right]=\left[P_{g_iOUT}^{SysI}\right]$. This allows a system generation level that covers nominal system losses and allows the algorithm to start near a known optimal solution (output of System I). As congestion is caused in System II, it is anticipated that $P_{LOSS}^{SysII} > P_{LOSS}^{SysI}$ and congestion $P_C > 0$.

The optimal solution output from System II returns information on,

- active power system losses, P_{LOSS}^{SysII};
- system per unit MW generation output, $\sum_{i}^{N_g} P_{g_iOUT}^{SysII} = \sum_{i}^{N_d}\left[P_{d_i}\right] + P_{LOSS}^{SysII} + P_C^{SysII}$;
- system cost $f(x)^{SysII}$ due to system losses and congestion.

3.5.3 System III

System III is the same as the base case of System II with a FACTS controller installed at a specified location. The input vector of initial per unit MW generation for System III is equal to the vector of System II, $\left[P_{g_i}^{0\,SysIII}\right]=\left[P_{g_i}^{0\,SysII}\right]$. This keeps all initial variables the same as System II except from the variables concerning the FACTS controller.

The optimal solution output from System III returns information on,

- active power system losses, P_{LOSS}^{SysIII};
- system per unit MW generation output, $\sum_{i}^{N_g} P_{g_iOUT}^{SysIII} = \sum_{i}^{N_d}\left[P_{d_i}\right] + P_{LOSS}^{SysIII} + P_C^{SysIII}$;
- system cost $f(x)^{SysIII}$ due to system losses and congestion.

Due to the influence of the installed FACTS controller it is possible for losses in System III to be less than the losses from System II, $P_{LOSS}^{SysIII} < P_{LOSS}^{SysII}$. Therefore, excess system

generation may exist. Where "per unit MWh generation excess" for individual systems is defined as,

$$P_{EXCESS} = \sum_{i}^{N_g}\left[P_{g_i}^{0}\right] - \sum_{i}^{N_d}\left[P_{d_i}\right],\ P_{EXCESS} > 0, \tag{3.58}$$

and loss, as defined in equation (2.11),

$$P_{LOSS} = \sum_{i}^{N_g}\left[P_{g_i}\right] - \sum_{i}^{N_d}\left[P_{d_i}\right],\ P_{LOSS} > 0 \tag{3.59}$$

The existence of P_{EXCESS} is dependent upon the relative sizes of losses from System III and System II. Table 3-3 summaries the three result types, Types A and C have no system congestion and result Type B can have system congestion.

Table 3-3: Summary of result types from System III, with a FACTS controller installed.

Result Type	Result properties	Behaviour without congestion	Behaviour with congestion
A(i)	• $P_{LOSS}^{SysIII} = P_{LOSS}^{SysII}$ • $P_{EXCESS} > 0$	No change in generation $\left[P_{g_iOUT}^{SysIII}\right] = \left[P_{g_i}^{0\,SysIII}\right]$	N/A
A(ii)	• $P_{LOSS}^{SysIII} < P_{LOSS}^{SysII}$ • $P_{EXCESS} > 0$	Decrease in generation due to P_{EXCESS} $\sum_{i}^{N_g} P_{g_iOUT}^{SysIII} < \sum_{i}^{N_g} P_{g_i}^{0\,SysIII}$	N/A
B(i)	• $P_{LOSS}^{SysIII} > P_{LOSS}^{SysII}$ • $P_{LOSS}^{SysIII} > P_{EXCESS}$	Increase in generation due to P_{LOSS} increase $\sum_{i}^{N_g} P_{g_iOUT}^{SysIII} > \sum_{i}^{N_g} P_{g_i}^{0\,SysIII}$	Increase in generation due to P_{LOSS} and congestion P_C increase $\sum_{i}^{N_g} P_{g_iOUT}^{SysIII} > \sum_{i}^{N_g} P_{g_i}^{0\,SysIII}$
B(ii)	• $P_{LOSS}^{SysIII} < P_{LOSS}^{SysII}$ • $P_{LOSS}^{SysIII} > P_{EXCESS}$	Increase in generation due to P_{LOSS} increase $\sum_{i}^{N_g} P_{g_iOUT}^{SysIII} > \sum_{i}^{N_g} P_{g_i}^{0\,SysIII}$	Increase in generation due to P_{LOSS} and congestion P_C reduction $\sum_{i}^{N_g} P_{g_iOUT}^{SysIII} > \sum_{i}^{N_g} P_{g_i}^{0\,SysIII}$
C	• $P_{LOSS}^{SysIII} = P_{LOSS}^{SysII}$ • $P_{LOSS}^{SysIII} = P_{EXCESS}$	No change in generation $\left[P_{g_iOUT}^{SysIII}\right] = \left[P_{g_i}^{0\,SysIII}\right]$	N/A

3.6 Influence of FACTS controllers on the bilateral electricity market model

There are two possible situations for the system with no FACTS controller, (as described Chapter 2, Table 2-1); a system without or with congestion. The installation of a FACTS

controller and the "setup of scheduled active power generation for system initial conditions" (Section 3.5) produce three possible conditions when there is no congestion. Table 3-4 summaries the conditions which are defined by the relationship between P_{EXCESS} to system congestion, system cost, system loss, and generation changes.

Table 3-4: Summary of bilateral market behaviour with P_{EXCESS} and a FACTS controller.

	Condition	System cost $f(x)$	Generation excess P_{EXCESS}	Generation change	Cause of generation change	Result Type (Table 3-3)
No congestion	1a	0	$P_{LOSS} < P_{EXCESS}$ $P_{EXCESS} > 0$	$\sum_i^{N_g}\left[P_{g_i}^+\right]=0,\ \sum_i^{N_g}\left[P_{g_i}^-\right]=0$	No change	A(i)
			$P_{LOSS} = P_{EXCESS}$ $P_{EXCESS} > 0$			C
	1b	>0	$P_{LOSS} < P_{EXCESS}$ $P_{EXCESS} > 0$	$\sum_i^{N_g}\left[P_{g_i}^+\right]=0,\ \sum_i^{N_g}\left[P_{g_i}^-\right]>0$	P_{EXCESS}	A(ii)
	1c	>0	$P_{EXCESS} < P_{LOSS}$ $P_{EXCESS} > 0$	$\sum_i^{N_g}\left[P_{g_i}^+\right]>0,\ \sum_i^{N_g}\left[P_{g_i}^-\right]=0$	P_{LOSS}	A(i)
Congestion	2	>0	$P_{EXCESS} < P_{LOSS}$ $P_{EXCESS} > 0$	$\sum_i^{N_g}\left[P_{g_i}^+\right]>0,\ \sum_i^{N_g}\left[P_{g_i}^-\right]>0$	$P_{LOSS} + P_C$	B(ii)
	3	>0	$P_{LOSS} < P_{EXCESS}$ $P_{EXCESS} > 0$	$\sum_i^{N_g}\left[P_{g_i}^+\right]>0,\ \sum_i^{N_g}\left[P_{g_i}^-\right]>0$	$P_{LOSS} + P_C$	B(ii)

3.7 Solution procedure: General two-step method for finding optimal location and rating of a FACTS controller in a bilateral market

Three physical constraints limit the possible locations of any FACTS controller location [Fang and Ngan (1999):

1. No more than one FACTS controller is required to be installed in one branch or at one bus;
2. A series FACTS controller is not required if the transmission line impedance is relatively small (i.e. a physically short line);
3. A shunt FACTS controller is not required at any bus that can be conveniently controlled by means of generator of synchronous compensator.

Figure 3.4 shows the general two-step method to find the optimal location and rating of a FACTS controller at a specified transmission line. In Step 1, the congestion management problem is solved without a FACTS controller by the IP OPF algorithm and the congested transmission lines are identified (System II). The solution is expected to have a high system cost due to system losses and congestion. In Step 2, the congestion management problem is solved with the incorporation of a FACTS controller at a specified location (System III). This solution determines the optimal controller rating that minimises the objective function.

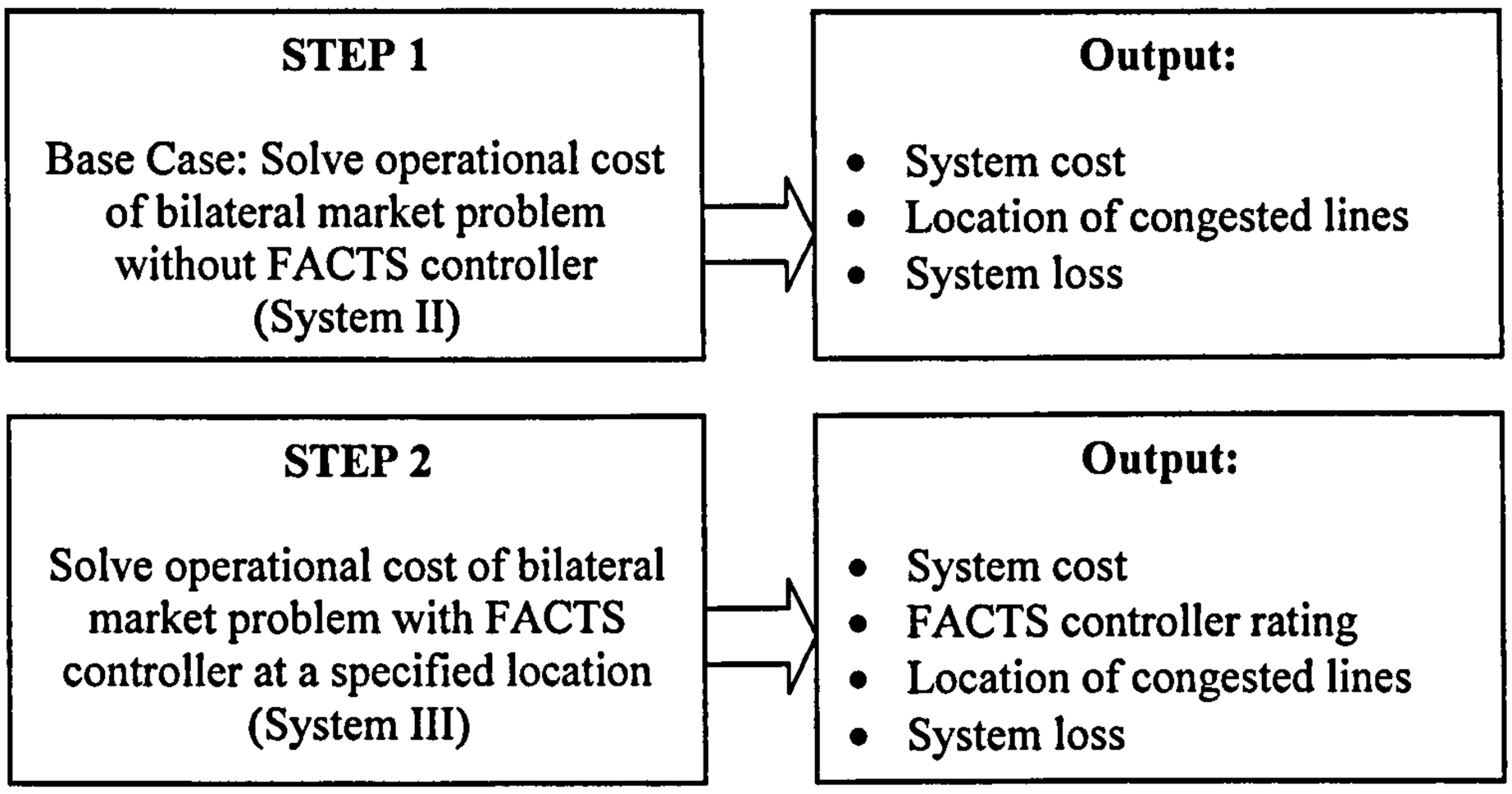

Figure 3.4: Overview of general two-step method to find optimal location and rating of FACTS controller.

This general method will be utilised in the proceeding test cases, where the specified locations are limited by the physical constraints and testing at the congested lines.

3.8 Numerical results: Initial test systems with FACTS controllers

The initial test cases for the bilateral market model with FACTS controllers are,

- STATCOM on 4 bus system with a single congested line,
- STATCOM on IEEE 14 bus system with daily demand fluctuations,
- UPFC on IEEE 14 bus system with daily demand fluctuations.

3.8.1 STATCOM on 4 bus system

The 4 bus system is the same as introduced in Chapter 2, Section 2.6, where line 1-2 is congested by the transmission line power capacity, $S_{12}^{2\max}$ is reduced by 60% to 2 p.u. from

5 p.u. The two generators have cost coefficient values of $C_{g_i}^{+} = 20$ \$/MWh and $C_{g_i}^{-} = 10$ \$/MWh. Constraint 3, from Section 3.2, eliminates generator buses 1 and 2. Figures 3.5(a) and 3.5(b) show the 4 bus system with the STATCOM connected at bus 2 and 4 respectively. Table 3-5 shows system comparison of the generator output values, active power losses, congestion, system cost and breakdown of costs due to system losses and congestion.

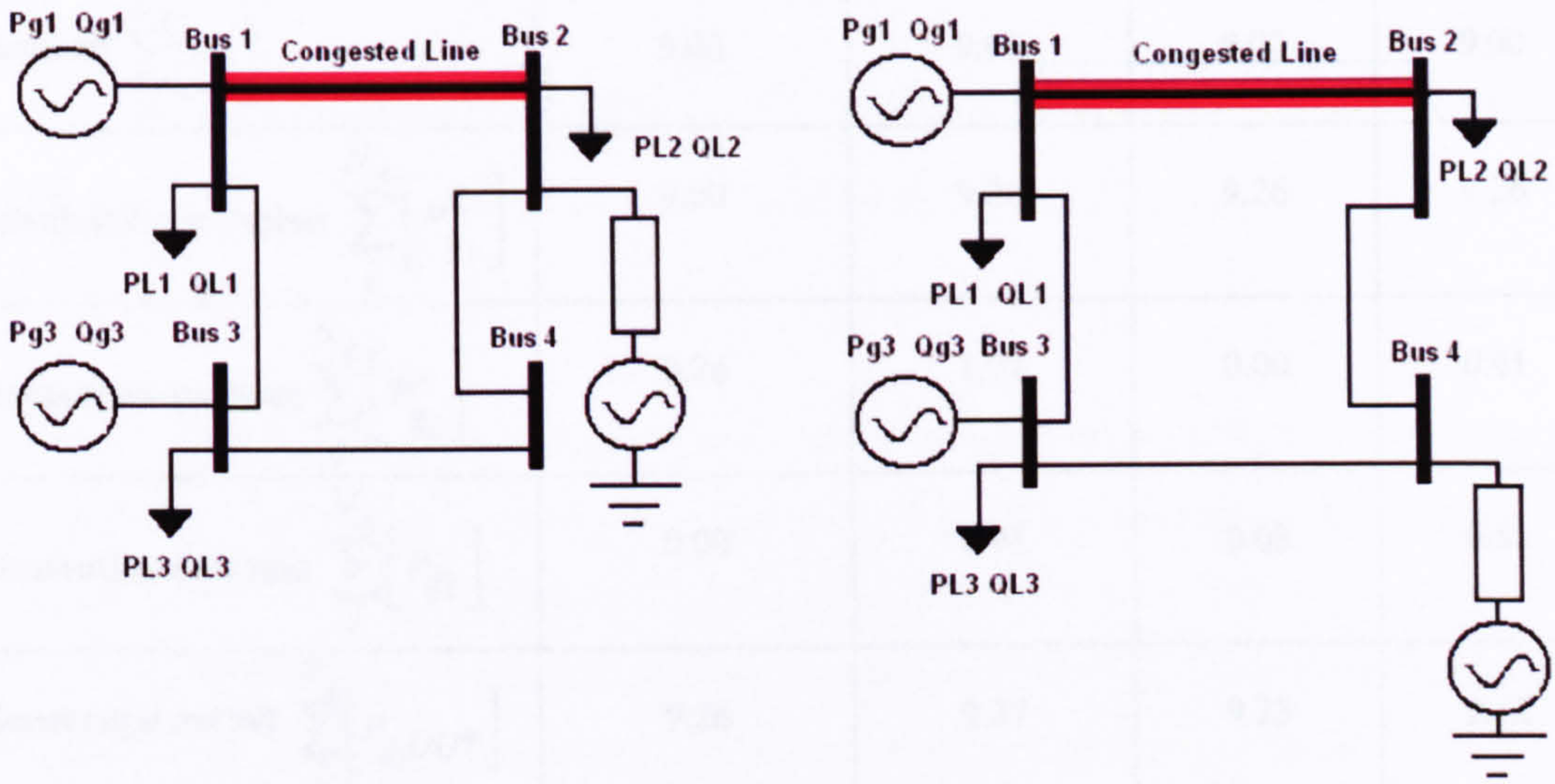

Figure 3.5: System III 4 bus system with STATCOM connected at (a) bus 2 (b) bus 4.

System I, the original system with no congestion is used to find the optimal initial generation levels and to observe the system power losses. There is only increase in power generation therefore the system cost is purely due to losses. System II, where congestion is caused at line 1-2 by decreasing the maximum complex power capacity constraint by 60% and the system scheduled generation level is adjusted for the system losses; the congestion causes an increase in system losses because $P_{LOSS}^{SysII} > P_{EXCESS}^{SysII}$ and system cost is 7% due to losses and 93% due to congestion.

The installation of the STATCOM at either bus can reduce the system cost considerably; refer to Table 3-5. In System IIIa the STATCOM is installed at bus 2. A 99% reduction in system cost (RSC) is achieved because system losses are lower than that of System II and $P_{LOSS} < P_{EXCESS}$. The required STATCOM rating for this solution is 117MVA. In System

IIIb the STATCOM is installed at bus 4 and the same initial conditions of System II are applied. A 40% RSC is achieved using a STATCOM with a rating of 201MVA. The result is of Type A(ii) and Condition 1b (Tables 3-3 and 3-4) because system loss has decreased with respect to System II ($P_{EXCESS} < P_{LOSS}$) and congestion is present.

Table 3-5: 4 bus, System I, II and III comparison with STATCOM at buses 2 and 4.

System number	I	II	IIIa	IIIb
System description (across) / Total system values (down) (units: p.u.)	No congestion $S_{12}^{max} = 5$	Congested line $S_{12}^{max} = 2$	STATCOM at bus 2	STATCOM at bus 4
Demand $\sum_{i}^{N_d}\left[P_{d_i}\right]$	9.00	9.00	9.00	9.00
Scheduled generation $\sum_{i}^{N_g}\left[P_{g_i}^{0}\right]$	9.00	9.26	9.26	9.26
Generation increase $\sum_{i}^{N_g}\left[P_{g_i}^{+}\right]$	0.26	1.02	0.00	0.61
Generation decrease $\sum_{i}^{N_g}\left[P_{g_i}^{-}\right]$	0.00	0.91	0.03	0.55
Generation output $\sum_{i}^{N_g}\left[P_{g_iOUT}\right]$	9.26	9.37	9.23	9.32
Loss P_{LOSS}	0.26	0.37	0.23	0.32
% Ploss w.r.t. $\sum_{i}^{N_g}\left[P_{g_i}^{0}\right]$	2.9 %	4.0 %	2.5 %	3.5 %
P_g^0 Excess P_{EXCESS}	0.00	0.26	0.26	0.26
Result Type/Condition (Table. 3-3 and Table 3-4)	N/A	N/A	A(ii)/1b	B(ii)/2
System cost $f(x)$ \$/MWh	5.2	29.6	0.26	17.8
% RSC wrt System II	N/A	N/A	99 %	40 %
% Cost due to P_{LOSS}	100%	7%	$P_{LOSS} < P_{EXCESS}$	7 %
% Cost due to congestion	0 %	93 %	1 %	93 %
% Cost due to P_{EXCESS}	0 %	0 %	99 %	0 %
Congested lines	None	1-2	1-2	1-2
STATCOM rating (MVA)	N/A	N/A	117	201

When the STATCOM is located at bus 2 there is reduction in congestion and system losses, therefore, this is the preferred location for STATCOM installation. The result is of Type B(ii) and Condition 2, the system cost is due to decrease in MW generation only due to excess

scheduled MW generation. This result is an example of a case where the potential global minimum (zero system cost) is not achieved; most likely due to the system equality constraints. Instead the result converged to a minimum where there is only decrease in system generation to balance initial generation with final generation.

3.8.2 IEEE 14 bus system with daily demand fluctuations

The 14 bus system is the same as introduced in Chapter 2, Section 2.6, where a maximum of three lines are congested by a linear increase in system demand and generation levels up to 70% Load Rise. All generators have equal generator cost coefficient values of $C_{gi}^{+} = 20$ \$/MWh and $C_{gi}^{-} = 10$ \$/MWh. Table 3-6 shows the initial system setup results with 70% Load Rise and FACTS controller test results with STATCOM at bus 4 and UPFC at congested line 1-2.

System I, the system at nominal loading and with no congestion is used to find optimal initial generation levels for each generator. The change in scheduled generation is solely to overcome system losses. In System II, congestion is caused by a 70% Load Rise and the system generation level accounts for losses incurred in System I. Congestion has increased losses and the extra demand has increased system cost, now 3% due to losses and 97% due to congestion. System III[a]; with STATCOM rated at 205MVA installed at bus 2 has reduced congestion cost by 10%. System III[b]; with UPFC rated at 15MVA installed at line 1-2 has reduced congestion cost by 41%, a significant saving. Both systems with a FACTS controller installed are able to reduce congestion costs by the redirecting the power flow to minimise change from scheduled generation.

3.8.3 STATCOM on IEEE 14 bus system

Physical constraints limit the location of STATCOM controllers to buses with no generators or synchronous compensators. Table 3-7 examines buses 4, 5 and 7 and limits the solution to a single installed controller. When the STATCOM is simulated at buses 9 to 14 the % RSC is less than 2%.

Table 3-6: IEEE 14 bus system at 70% Load Rise, Systems I, II and III comparison with STATCOM and UPFC.

System number	**I**	**II**	**III[a]**	**III[b]**
System description (across) / **Total system values (down) (units: p.u.)**	**No congestion**	**Congestion no FACTS**	**STATCOM at bus 4**	**UPFC at line 1-2**
Demand $\sum_{i}^{N_d}\left[P_{d_i}\right]$	2.59	4.40	4.40	4.40
Scheduled generation $\sum_{i}^{N_g}\left[P_{g_i}^{0}\right]$	2.59	4.59	4.59	4.59
Generation increase $\sum_{i}^{N_g}\left[P_{g_i}^{+}\right]$	0.11	1.22	1.11	0.74
Generation decrease $\sum_{i}^{N_g}\left[P_{g_i}^{-}\right]$	0.00	1.17	1.03	0.67
Generation output $\sum_{i}^{N_g}\left[P_{g_i OUT}\right]$	2.70	4.64	4.67	4.66
Loss P_{LOSS}	0.11	0.24	0.26	0.25
% Ploss w.r.t. $\sum_{i}^{N_g}\left[P_{g_i}^{0}\right]$	4.2%	5.2%	5.7%	5.5%
P_g^0 **Excess** P_{EXCESS}	0.00	0.19	0.19	0.19
Result Type /Condition (Table. 3-3 and Table 3-4)	N/A	N/A	B(ii)/2	B(ii)/2
System cost $f(x)$ **\$/h**	2.20	36.2	32.6	21.4
% RSC wrt System II	N/A	N/A	10 %	41 %
% Cost due to P_{LOSS}	100 %	3 %	5 %	3 %
% Cost due to congestion	0 %	97 %	95 %	97 %
% Cost due to P_{EXCESS}	None	N/A $P_{EXCESS} < P_{LOSS}$	N/A $P_{EXCESS} < P_{LOSS}$	N/A $P_{EXCESS} < P_{LOSS}$
Congested lines	None	1-2, 7-8, 6-13	1-2, 2-5, 6-13	1-2, 1-5, 7-8, 6-13
FACTS controller rating (MVA)	N/A	N/A	205	15

The largest % RSCs are found when the STATCOM is installed at bus 5 (13% RSC) and secondly at bus 4 (10% RSC). At buses 7 and 9 to 14 (because bus 8 is a generator bus) the % RSC is 2% or below. The relative percentage of system cost due to losses and congestion are similar in all cases. The required STATCOM ratings to reduce system cost by 10% or more are reasonable at 205MVA and 347MVA. The congestion is not mitigated completely as there are still some congested lines at the optimal solution. The STATCOM has shown that it

is able to help congestion by a small percentage, but this controller is more commonly used for voltage control.

Table 3-7: IEEE 14 bus system with STATCOM installed at buses 4, 5 and 7.

70% Load Rise	**Base case**	**STATCOM at bus 4**	**STATCOM at bus 5**	**STATCOM at bus 7**
System cost $f(x)$ \$/h	36.2	32.6	31.4	35.5
% RSC w.r.t. Base Case	N/A	10 %	13 %	2 %
STATCOM rating MVA	N/A	205 MVA	347 MVA	102 MVA
% Cost due to P_{LOSS}	3 %	5 %	8 %	9 %
% Cost due to congestion	97 %	95 %	92 %	97 %
% Ploss w.r.t. $\sum_{i}^{N_g}\left[P_{g_i}^{0}\right]$	5.2 %	5.7 %	4.6 %	5.1 %
Congested lines	1-2, 7-8, 6-13	1-2, 2-5, 6-13	1-2, 4-5, 7-8, 6-13	1-2, 7-9, 6-13

3.8.4 UPFC on IEEE 14 bus system

For this set of test results, the UPFC is installed on the congested transmission lines. At 30% Load Rise this was line 7-8 only, at 50% Load Rise they were 7-8 and 1-2 and at 70% Load Rise, 7-8, 1-2 and 6-13 (Chapter 2, Section 2.6.3). Tables 3-8 to 3-10 show the results at each location. When located at lines 7-8 and 6-13 there is no significant % RSCs. When located at line 1-2 there is significant reduction at 50% and 70% Load Rise.

Table 3-8: IEEE 14 bus system at 30% Load Rise with UPFC installed at congested line 7-8.

30% Load Rise	**Base case**	**UPFC at line 7-8**
System cost $f(x)$ \$/h	14.1	13.7
% RSC w.r.t. base case	N/A	3 %
UPFC rating (MVA)	N/A	99 MVA
% Cost due to P_{LOSS}	100 %	4 %
% Cost due to congestion	0 %	96 %
% P_{LOSS} w.r.t. $\sum_{i}^{N_g}\left[P_{g_i}^{0}\right]$	4.7 %	4.7 %
Congested lines	1-2	1-2

At 50% Load Rise the RSCs has been reduced by 70% when the UPFC is installed at congested line 1-2. At line 7-8 the % RSC is only 2%. At 70% Load Rise the RSC has been reduced to 41% when the UPFC is installed at congested line 1-2. At lines 7-8 and 6-13 % RSC is 3%. The required UPFC rating for each solution is the smallest when installed at line 1-2 for both % Load Rise levels. Therefore, UPFC installation at line 1-2 is the optimal location as it saves money by reducing congestion and has minimal installation cost due to

the low UPFC rating required. The system losses are similar for all cases and congestion is not mitigated completely as there are still some congested lines at the optimal solutions. System input data for 4 and IEEE 14 bus systems is presented in Appendix VIII.

Table 3-9: IEEE 14 bus system at 50% Load Rise with UPFC installed at congested lines 7-8 and 1-2.

50% Load Rise	**Base case**	**UPFC at line 7-8**	**UPFC at line 1-2**
System cost $f(x)$ \$/h	24.9	24.3	7.5
% RSC w.r.t. base case	N/A	2 %	70 %
UPFC rating (MVA)	N/A	35 MVA	13 MVA
% Cost due to P_{LOSS}	4 %	18 %	4 %
% Cost due to congestion	96 %	82 %	96 %
% P_{LOSS} w.r.t. $\sum_{i}^{N_g}\left[P_{g_i}^{0}\right]$	5.2 %	5.1 %	5.7 %
Congested lines	1-2, 7-8	1-2, 7-9	1-2, 7-8, 1-5

Table 3-10: IEEE 14 bus system at 70% Load Rise with UPFC installed at congested lines 7-8, 1-2 and 6-13.

70% Load Rise	**Base case**	**UPFC at line 7-8**	**UPFC at line 1-2**	**UPFC at line 6-13**
System cost $f(x)$ \$/h	36.2	35.5	21.4	35.1
% RSC w.r.t. base case	N/A	2 %	41 %	3 %
UPFC rating (MVA)	N/A	118 MVA	15 MVA	157 MVA
% Cost due to P_{LOSS}	9 %	7 %	3 %	3 %
% Cost due to congestion	97 %	93 %	97 %	97 %
% P_{LOSS} w.r.t. $\sum_{i}^{N_g}\left[P_{g_i}^{0}\right]$	5.2 %	5.1 %	5.5 %	5.3 %
Congested lines	1-2, 7-8, 6-13	1-2, 7-9, 6-13	1-2, 1-5, 7-8, 6-13	1-2, 7-8, 13-15, 10-11

3.9 Conclusions

In this Chapter, the VSC based STATCOM, SSSC and UPFC FACTS controller models are presented and implemented into the IP OPF method. The additional equipment on the system increases the complexity of the IP OPF solution but is able to provide greater power flow control when STATCOM and UPFC FACTS controllers are applied.

Numerical tests on the 4 bus systems have demonstrated that the STATCOM is the only controller that is able to reduce congestion considerably. Simulations on the IEEE 14 bus systems show that the STATCOM is able to improve RSC by approximately 10% but with the addition of series control by installing the UPFC; it is able to reduce system costs much

further, to approximately 40%. System losses are similar with and without FACTS controller installations; therefore it is congestion and not losses that has the greater effect on the system cost. The efficiency of RSC is dependent upon location of installation and amount of system congestion. Both these factors are further investigated in the proceeding chapters.

Chapter 4

Daily demand and annual cost savings using FACTS controllers

4.1 Introduction

In Chapter 3, the test case results for the IEEE 14 bus systems concentrate on 30%, 50% and 70% Load Rises resulting with one, two or three congested lines respectively. In practice to maximise the financial benefits of the controller it is vital to assess the capability of the controller at different levels of demand and during a range of situations. For example, the change in MW load demand over a typical 24 hour day in summer and winter in Britain are significantly different. In this chapter the average cost savings made over the summer and winter demand profiles are examined and the results are used to determine average annual system costs. This gives a quantitative measure of the STATCOM and UPFC performances.

The daily demand profile of Britain in 2004/5 presented in Section 4.2 is used as the base case. Section 4.3 includes the methods used to map the base case for simulation and for interpretation of the results. Sections 4.4 and 4.5 detail the base cases for the IEEE 14 bus and IEEE 30 bus systems respectively. Section 4.6 is the first of two case studies investigating the effect of the FACTS controllers on the 14 bus and 30 bus systems. The STATCOM is investigated in Section 4.6 and the UPFC in Section 4.7 (the second of the two case studies), where the location and installation orientation of the controllers are considered. Conclusions and references are given in Sections 4.8 and 4.9 respectively.

4.2 Daily demand profile of Britain

The wholesale electricity market structure used in Britain (Chapter 1, Section 1.5) has a single system operator, the National Grid plc. that coordinates the continuous flow of electricity and electricity trade surrounding usage of the transmission grid. Forward and futures contracts and the short term bilateral market are active until Gate Closure, one hour before point of delivery or real-time. Between Gate Closure and point of delivery the balancing mechanism ensures all demand is met and is used to balance supply and demand in each half-hour trading period of every day [Elexon (2005) and National Grid plc. (2007a)].

Figure 4.1 shows four average demand profiles on Britain's system recorded during 2004/5. The coloured lines running from bottom to top are as follows; red was the Summer Minimum, green was a Typical Summer day, blue was Typical Winter day and black was the Winter Maximum. The results are plotted over a 24 hour day with 48 half-hour intervals.

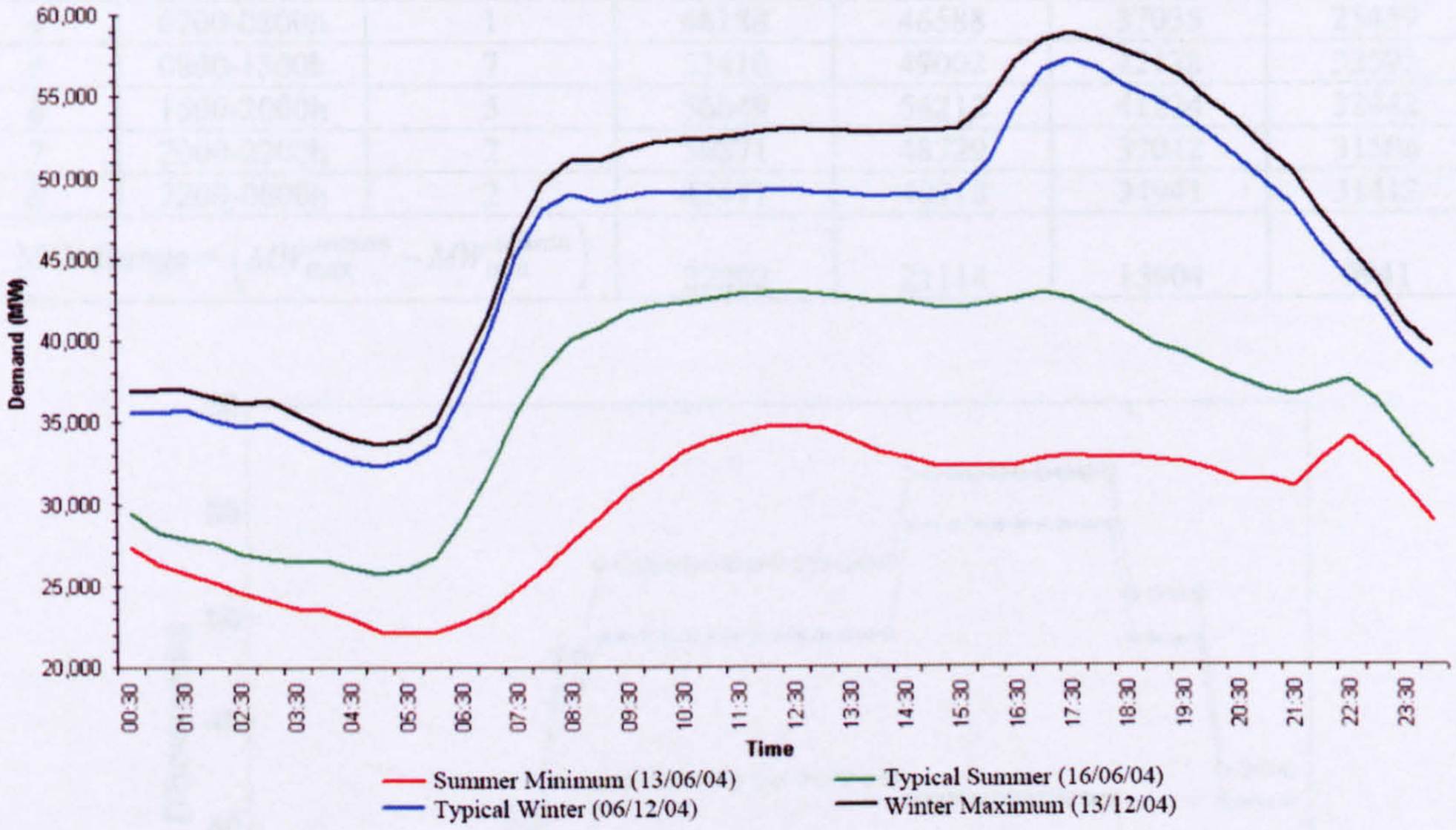

Figure 4.1: National Grid record of Britain's summer and winter daily demand profiles for 2004/5 [National Grid plc. (2006a)].

For simplification, the load curve has been divided into eight sections and the average MW demand is taken over each. Table 4-1 details the section number, section start and end times, duration and average MW demand at each of the four seasonal categories. Figure 4.2 shows the approximated MW demand profiles. For a conservative annual approximation, a 365 day year is assumed to be 182.5 days at Typical Summer demand and 182.5 days at Winter Maximum demand.

4.3 General mechanism for assessing the behaviour of FACTS controllers

The following case studies presented in this chapter aim to show the behaviour of FACTS controllers over different load levels that represent normal daily and seasonal changes in demand profile. All simulation results give a comparison of system behaviour relative to the fraction of MW demand change over the full MW demand range as expressed in equations (4.1) and (4.2), and do not aim to represent the absolute MW demand levels of Britain's system.

Table 4-1: Average MW eight section approximation of National Grid record of Britain's summer and winter daily demand profiles for 2004/5.

Section Number *k*	**Time**	**Duration (hours)**	**Average MW**			
			Winter Maximum	**Typical Winter**	**Typical Summer**	**Summer Minimum**
1	0000-0300h	3	36643	35294	27812	25443
2	0300-0600h	3	34447	33098	26275	22651
3	0600-0700h	1	40047	38682	30682	23059
4	0700-0800h	1	48188	46588	37035	25459
5	0800-1500h	7	52410	49002	42178	32592
6	1500-2000h	5	56649	54212	41224	32442
7	2000-2200h	2	50871	48729	37012	31506
8	2200-0000h	2	42471	40918	34941	31412
MW Range $= \left(MW_{\max}^{season} - MW_{\min}^{season} \right)$			22202	21114	15904	9941

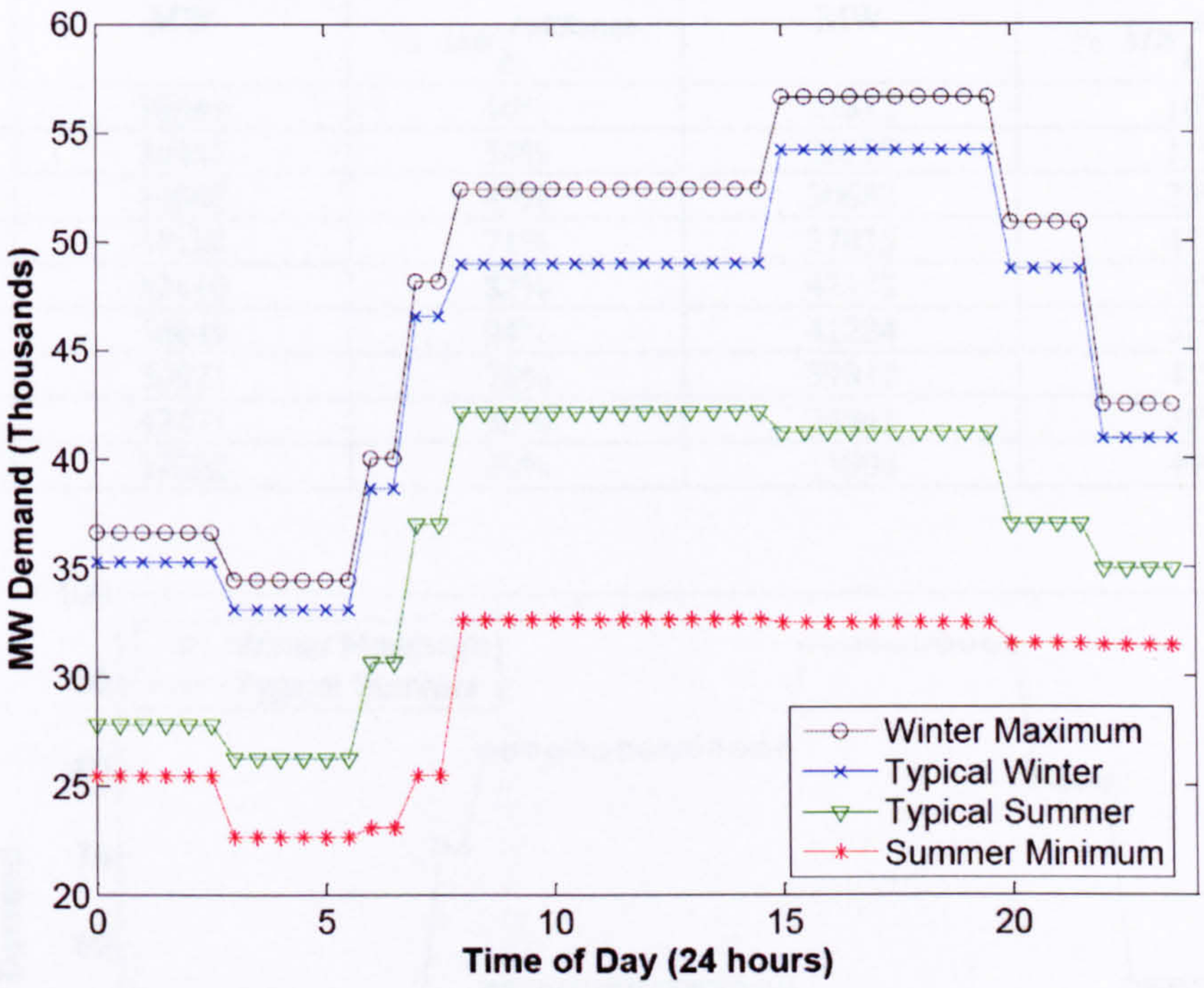

Figure 4.2: Average MW eight section approximation of National Grid record of Britain's summer and winter daily demand profiles for 2004/5.

Percent change in MW demand is measured relative to the full MW demand range over an entire year and is calculated as follows,

$$\%\ MW_k^{FullRange} = \left\{ (MW_k - MW_{\min}) / MW_{FullRange} \right\} \times 100 \qquad (4.1)$$

where,

MW_k is the MW demand at section number k, $k = 1, 2, \ldots 8$.

$MW_{\min}$ = 22071 MW, occurs during Summer Minimum between 0430 and 0630 hours,

$MW_{\max}$ = 58871 MW, occurs during Winter Maximum between 1700 and 1730 hours,

$$MW_{FullRange} = MW_{\max} - MW_{\min} \quad (4.2)$$

$$= 36800 \text{ MW}$$

Table 4-2 shows the percent increase of MW demand relative to the MW full range for Winter Maximum and Typical Summer demand profiles.

Table 4-2: % $MW_k^{FullRange}$ approximation of Britain's Winter Maximum and Typical Summer daily demand profiles 2004/5.

Section Number *k*	**Winter Maximum**		**Typical Summer**	
	MW	% $MW_k^{FullRange}$	MW	% $MW_k^{FullRange}$
1	36643	40%	27812	16%
2	34447	34%	26275	11%
3	40047	49%	30682	23%
4	48188	71%	37035	41%
5	52410	82%	42178	55%
6	56649	94%	41224	52%
7	50871	78%	37012	41%
8	42471	55%	34941	35%
Range	22202	60%	15904	44%

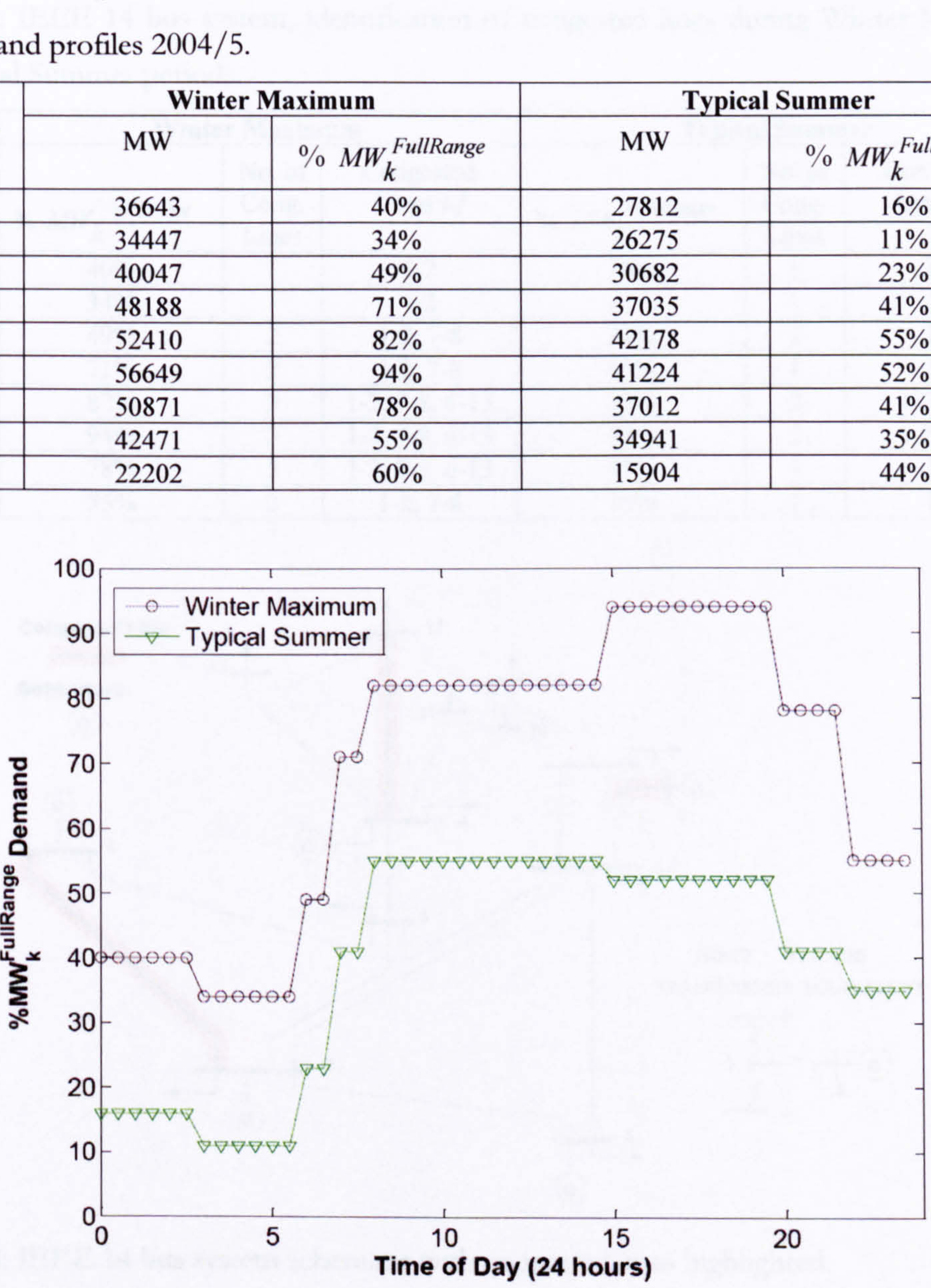

Figure 4.3: % $MW_k^{FullRange}$ approximation of Britain's Winter Maximum and Typical Summer from daily demand profiles 2004/5.

4.4 IEEE 14 bus system daily demand base case

The maximum number of congested lines is three, at $78\%MW_7^{FullRange}$, $82\%MW_5^{FullRange}$ and $94\%MW_6^{FullRange}$ during the Winter Maximum period. Table 4-3 lists the number and the location of congested lines over the eight sections during Winter Maximum and Typical Summer. Figure 4.4 highlights the locations of all congested lines, where the definition of a congested line is a line being utilised at its maximum S_{ij}^{2Max} thermal limit.

Table 4-3: IEEE 14 bus system, identification of congested lines during Winter Maximum and Typical Summer periods.

14 Bus	**Winter Maximum**			**Typical Summer**		
Section Number *k*	$\%\ MW_k^{FullRange}$	No. of Cong. Lines	Congested Lines *i-j*	$\%\ MW_k^{FullRange}$	No. of Cong. Lines	Congested Lines *i-j*
1	40%	1	1-2	16%	1	1-2
2	34%	1	1-2	11%	1	1-2
3	49%	2	1-2, 7-8	23%	1	1-2
4	71%	2	1-2, 7-8	41%	1	1-2
5	82%	3	1-2, 7-8, 6-13	55%	2	1-2, 7-8
6	94%	3	1-2, 7-8, 6-13	52%	2	1-2, 7-8
7	78%	3	1-2, 7-8, 6-13	41%	1	1-2
8	55%	2	1-2, 7-8	35%	1	1-2

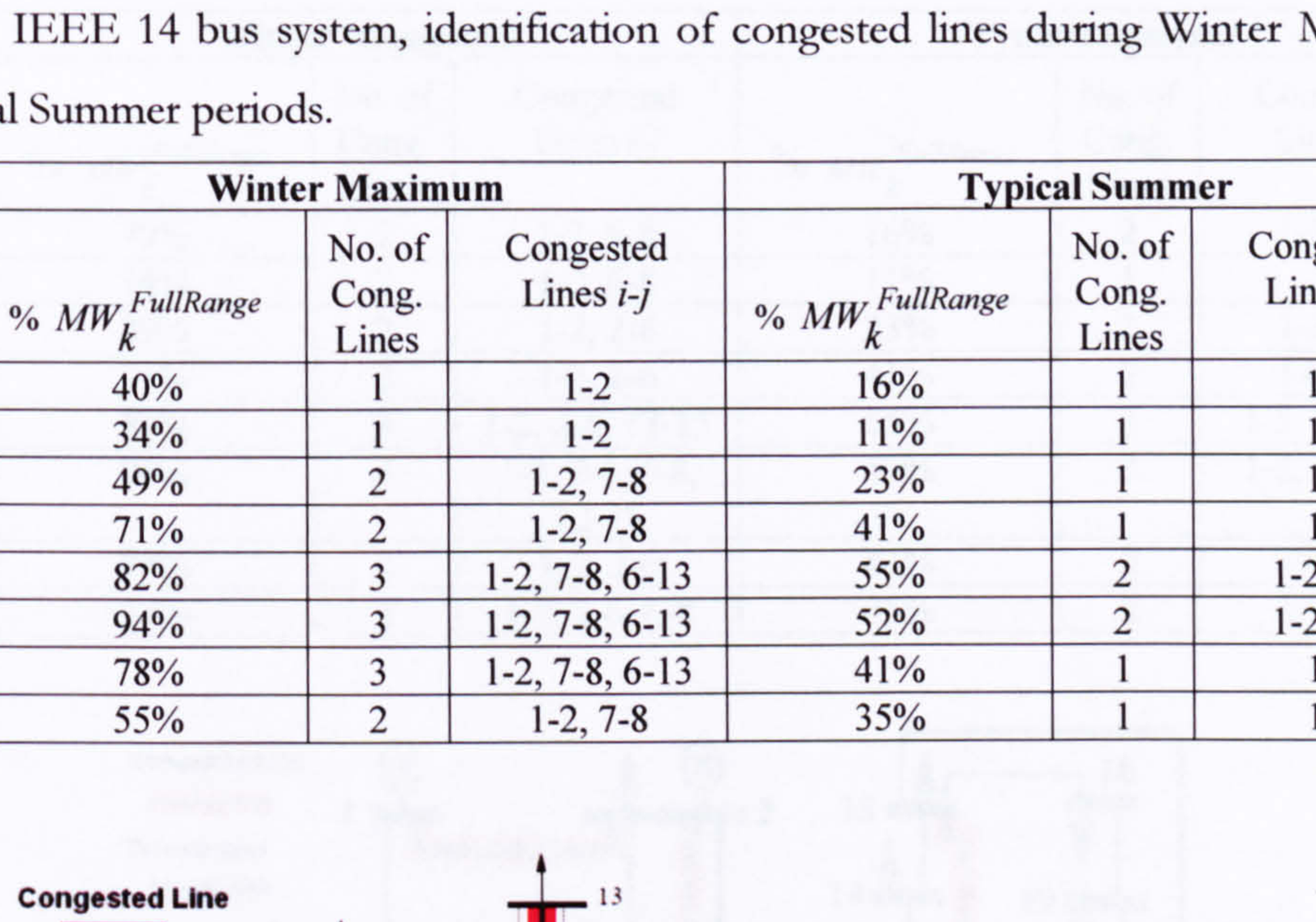

Figure 4.4: IEEE 14 bus system schematic with congested lines highlighted.

4.5 IEEE 30 bus system daily demand base case

The maximum number of congested lines is four at 94% $MW_6^{FullRange}$ during the Winter Maximum period. Table 4-4 lists the number and the location of congested lines over the eight sections during the two seasons. Figure 4.5 highlights the locations of all congested lines.

Table 4-4: IEEE 30 bus system, identification of congested lines during Winter Maximum and Typical Summer periods.

30 bus	**Winter Maximum**			**Typical Summer**		
Section Number *k*	% $MW_k^{FullRange}$	No. of Cong. Lines	Congested Lines *i-j*	% $MW_k^{FullRange}$	No. of Cong. Lines	Congested Lines *i-j*
1	40%	2	1-2, 6-8	16%	2	1-2, 6-8
2	34%	2	1-2, 6-8	11%	1	1-2
3	49%	2	1-2, 2-6	23%	2	1-2, 6-8
4	71%	2	1-2, 2-6	41%	2	1-2, 6-8
5	82%	3	1-2, 2-6, 12-15	55%	3	1-2, 2-6, 6-8
6	94%	4	1-2, 2-6, 6-8, 12-15	52%	3	1-2, 2-6, 6-8
7	78%	2	1-2, 2-6	41%	2	1-2, 6-8
8	55%	3	1-2, 2-6, 6-8	35%	2	1-2, 6-8

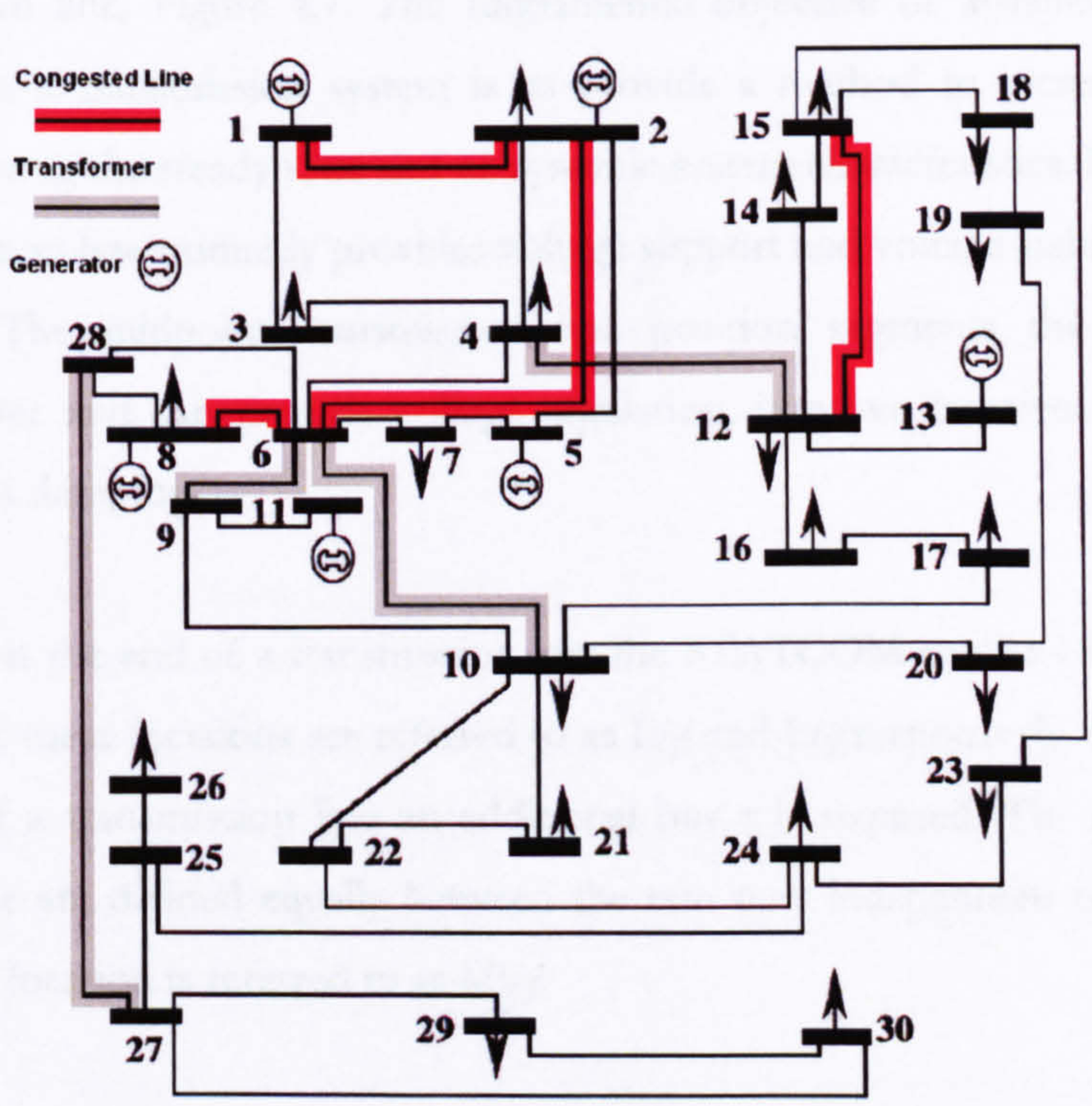

Figure 4.5: IEEE 30 bus system schematic with congested lines highlighted.

The general mechanism applied in this chapter is the extension of the general two-step method as presented in Chapter 3, Section 3.7. The IEEE 14 bus and 30 bus systems are used for the following case studies.

4.6 Case study 1: Daily demand profiles and locating the STATCOM to manage congestion

The STATCOM is tested at all physically viable transmission line locations. The results of particular interest are (i) the ability of the controller to reduce the system cost, (ii) the location of the controller, (iii) the change of system real power loss in comparison to the base case, and (iv) the rating of the FACTS controller required to achieve the corresponding system cost reduction. The system cost is so called as it measures the system congestion costs and transmission line real power losses and does not take into account losses from any generation unit, load or FACTS controller.

4.6.1 STATCOM location and position

The STATCOM is, in general installed in one of two positions with respect to the transmission line; at either end of a transmission line, Figure 4.6(a) and (b) or at the midpoint of a transmission line, Figure 4.7. The fundamental objective of installing reactive shunt compensation in a transmission system is to provide a method to increase transmittable power by improving the steady state and or dynamic system characteristics. Positioning at the end of transmission line primarily provides voltage support and voltage stability for loads at a specified bus. The midpoint transmission line position segments the line, making it electrically shorter and can provide voltage regulation, improve transient stability and aid power oscillation damping.

For installation at the end of a transmission line the STATCOM can be connected in shunt to bus i or bus j, these locations are referred to as I:i-j and J:i-j respectively. For installation at the midpoint of a transmission line an additional bus κ is required. The properties of the transmission line are divided equally between the two new independent transmission lines, $i\kappa$ and κj, this location is referred to as M:i-j.

4.6.2 IEEE 14 bus system cases with STATCOM

In Chapter 3, it has been shown that with a STATCOM on the 14 bus system, the system cost can be reduced to 10% and 13% when installed at buses 4 and 5 at 70% Load Rise

(Table 3-7), where system cost includes the costs incurred due to congestion and system transmission losses only. This section assesses the behaviour of the STATCOM at all possible locations over a Typical Summer and Winter Maximum for an average year. Table 4-5 lists percentage Reduction in System Costs (RSC) for all locations and three positions, where the annual % RSC is compared to the system base case.

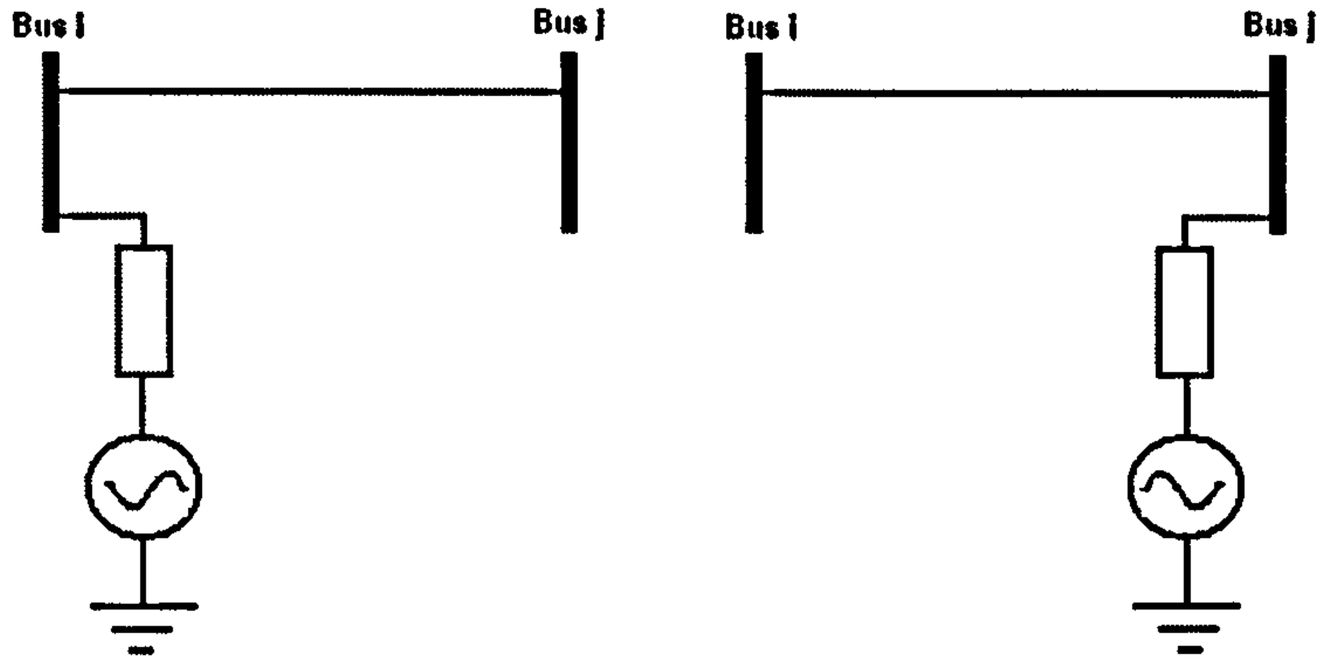

Figure 4.6: Two positions for STATCOM at each end of transmission line *ij*, (a) connected at bus *i*, I:*i-j*, (b) connected at bus *j*, J:*i-j*.

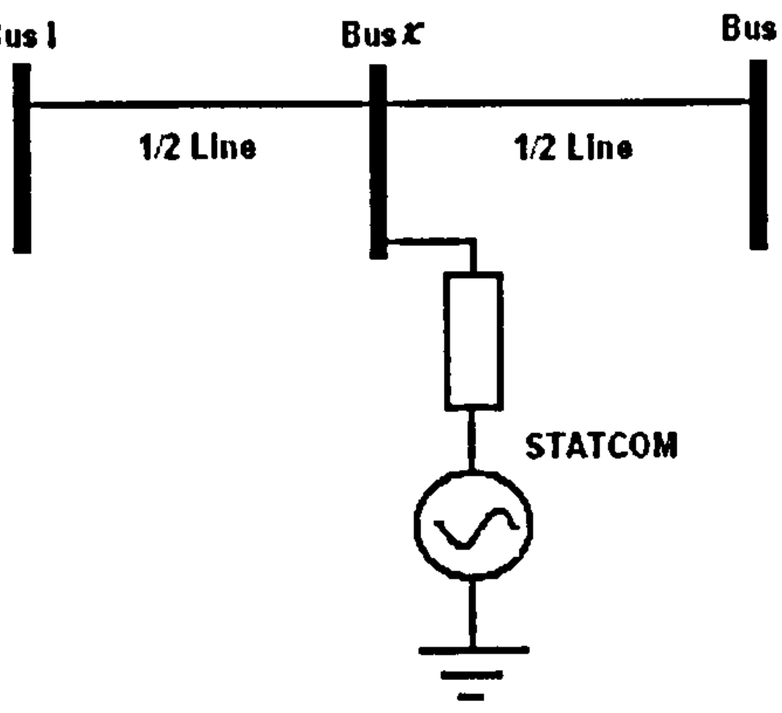

Figure 4.7: STATCOM installed at midpoint of transmission line *ij*, M:*i-j*.

Installation of a STATCOM at the ends of transmission lines can equally apply to transformers between buses *ij*; transformer locations have been tested in addition to all transmission line locations. Therefore, excluding generator buses (buses 1, 2, 3, 6 and 8) and utilising both ends of every transmission line and transformer, there are 27 potential locations for installation. Midpoint installation of STATCOM only applies to transmission lines; therefore, there are 17 potential locations for installation (line numbers 8-10 in Table 4-5 are transformers). In total, there are 44 potential locations for STATCOM installation on the 14 bus system.

Table 4-5: IEEE 14 bus system, all STATCOM locations and positions I:*i-j*, J:*i-j* and M:*i-j*.

Line no.	Line *i-j*	Annual % Reduction in System Cost w.r.t. base case		
		I:*i-j* (At bus *i*)	J:*i-j* (At bus *j*)	M:*i-j* (At midpoint)
1	**1-2 Congested**	Generator Bus	Generator Bus	**61%**
2	**1-5**	Generator Bus	-25%	-25%
3	**2-3**	Generator Bus	Generator Bus	6%
4	**2-4**	Generator Bus	**14%**	**11%**
5	**2-5**	Generator Bus	**19%**	**12%**
6	**3-4**	Generator Bus	3%	0%
7	**4-5**	-5%	-7%	-7%
8	**4-7 Transformer**	5%	3%	Transformer
9	**4-9 Transformer**	5%	3%	Transformer
10	**5-6 Transformer**	8%	Generator Bus	Transformer
11	**6-11**	Generator Bus	1%	2%
12	**6-12**	Generator Bus	2%	2%
13	**6-13 Congested**	Generator Bus	2%	2%
14	**7-8 Congested**	3%	Generator Bus	0%
15	**7-9**	3%	3%	3%
16	**9-10**	3%	1%	1%
17	**9-14**	3%	2%	2%
18	**10-11**	1%	2%	1%
19	**12-13**	2%	2%	1%
20	**13-14**	2%	2%	1%

Six positions; I:5-6, J:2-4, J:2-5, M:2-3, M:2-4 and M:2-5 produced annual RSC greater than 5%. Five positions, I:4-5, J:1-5, J:4-5, M:1-5 and M:4-5 produce an increase in system cost and made the system congestion worse than the base case. The remaining 36 locations achieve RSCs of 5% or less. RSCs above 10% are highlighted in bold.

A. STATCOM installed at ends of transmission lines

Figures 4.8 and 4.9 show the system cost profiles for the Typical Summer and Winter Maximum periods over 24 hours for J:2-4, J:2-5 and I:5-6 respectively. In both seasons STATCOM location J:2-5 provides the largest RSCs.

B. STATCOM installed at midpoint of transmission lines

Figures 4.10 and 4.11 show the system cost profiles for the Typical Summer and Winter Maximum periods over 24 hour period for M:1-2, M:2-4 and M:2-5 respectively. In both seasons M:1-2 provides the largest savings.

Tables 4-5, 4-6 and 4-7 show that over a single year installing a STATCOM at specific line locations can achieve RSCs up to 61%. Any value over 10% RSC is considered a significant saving.

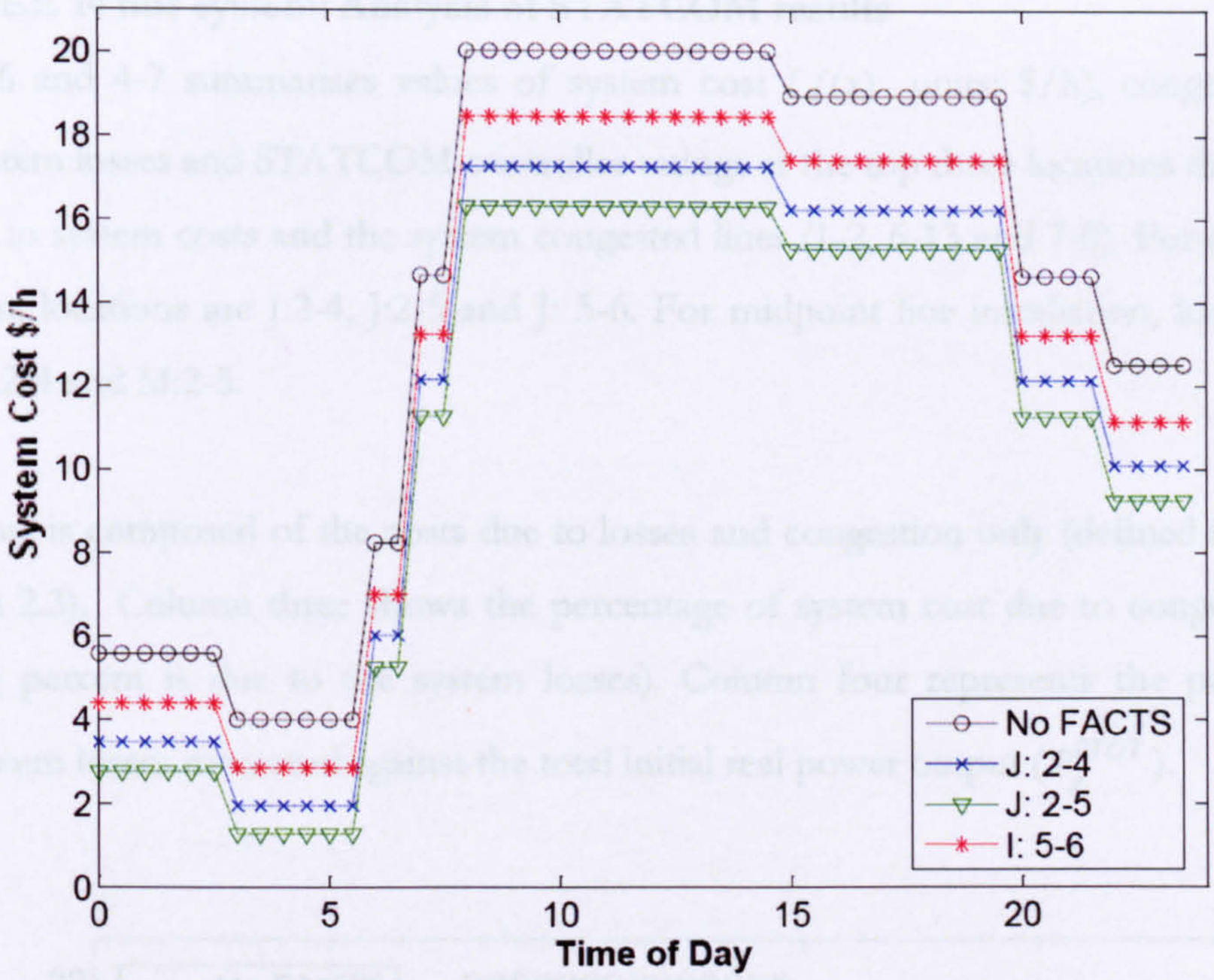

Figure 4.8: IEEE 14 bus system Typical Summer system cost profile with STATCOM located at ends of transmission lines, J:2-4, J:2-5 and I:5-6 (half hour time intervals).

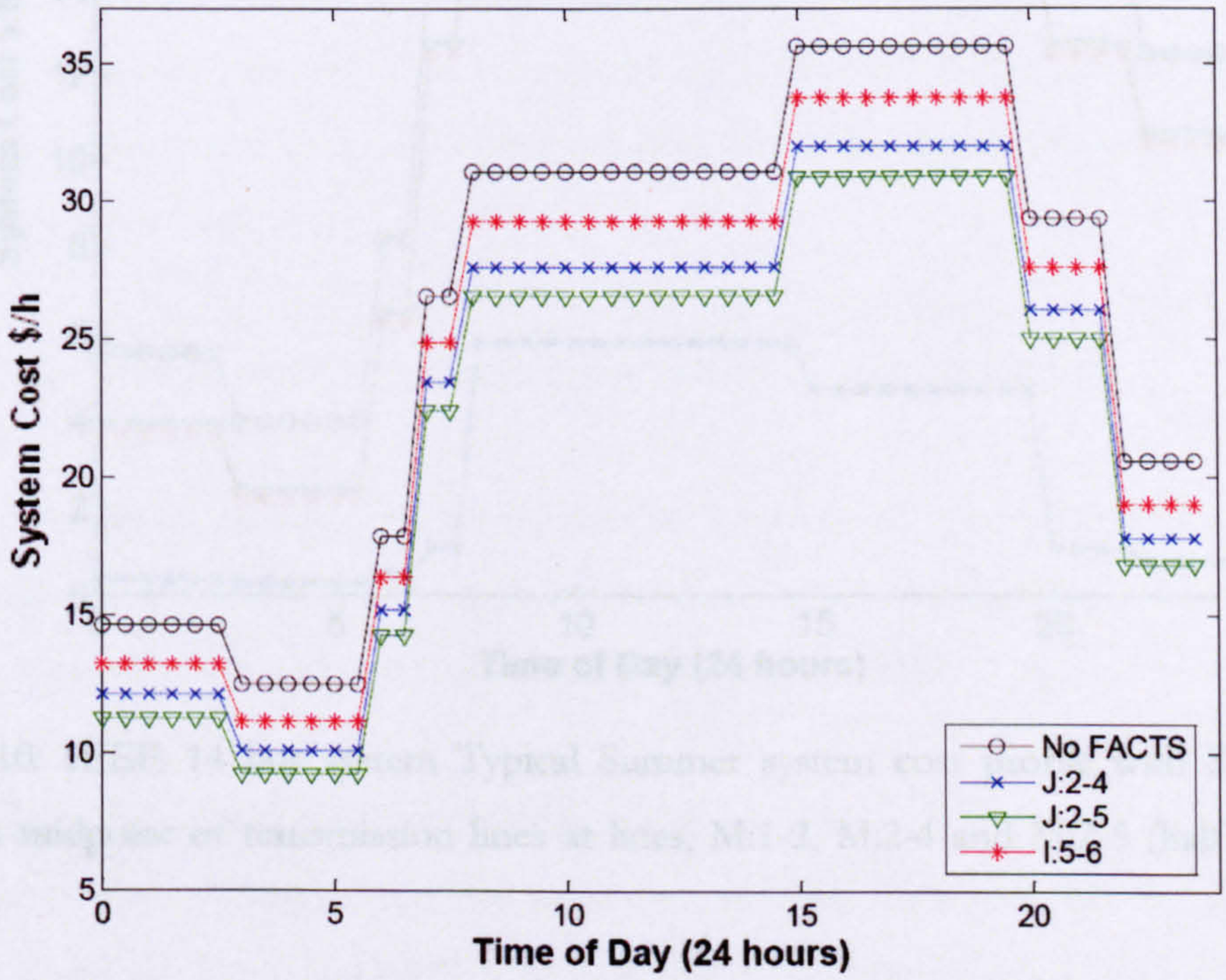

Figure 4.9: IEEE 14 bus system Winter Maximum system cost profile with STATCOM located at ends of transmission lines, J:2-4, J:2-5 and I:5-6 (half hour time intervals).

4.6.3 IEEE 14 bus system: Analysis of STATCOM results

Tables 4-6 and 4-7 summarises values of system cost ($f(x)$, units: \$/h), congestion, real power system losses and STATCOM controller ratings at the top three locations that provide reduction in system costs and the system congested lines (1-2, 6-13 and 7-8). For end of line installation, locations are J:2-4, J:2-5 and J: 5-6. For midpoint line installation, locations are M:1-2, M:2-4 and M:2-5.

System cost is composed of the costs due to losses and congestion only (defined in Chapter 2, Section 2.3). Column three shows the percentage of system cost due to congestion (the remaining percent is due to the system losses). Column four represents the percent real power system losses measured against the total initial real power output ($P_{g_i}^{0TOT}$).

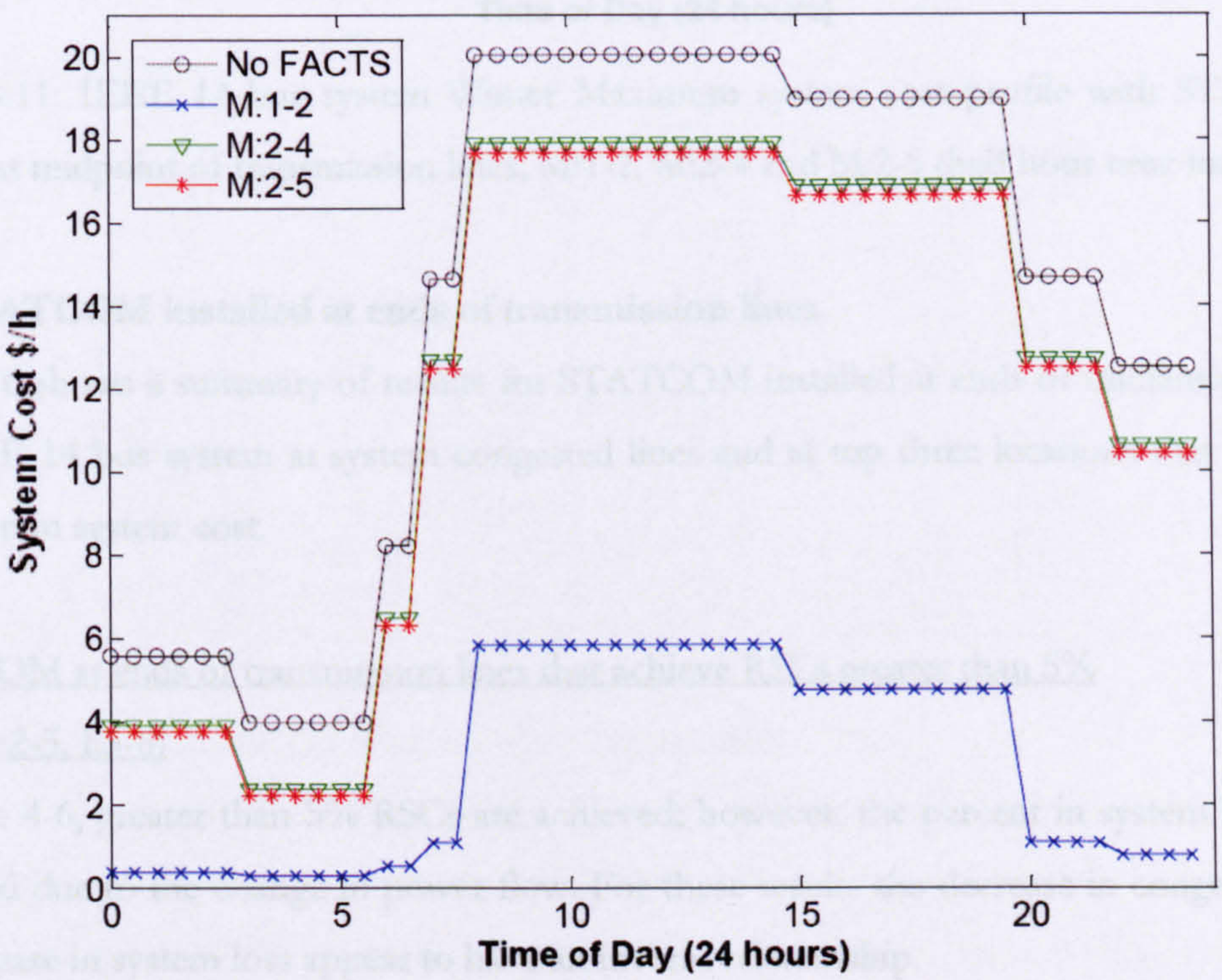

Figure 4.10: IEEE 14 bus system Typical Summer system cost profile with STATCOM located at midpoint of transmission lines at lines, M:1-2, M:2-4 and M:2-5 (half hour time intervals).

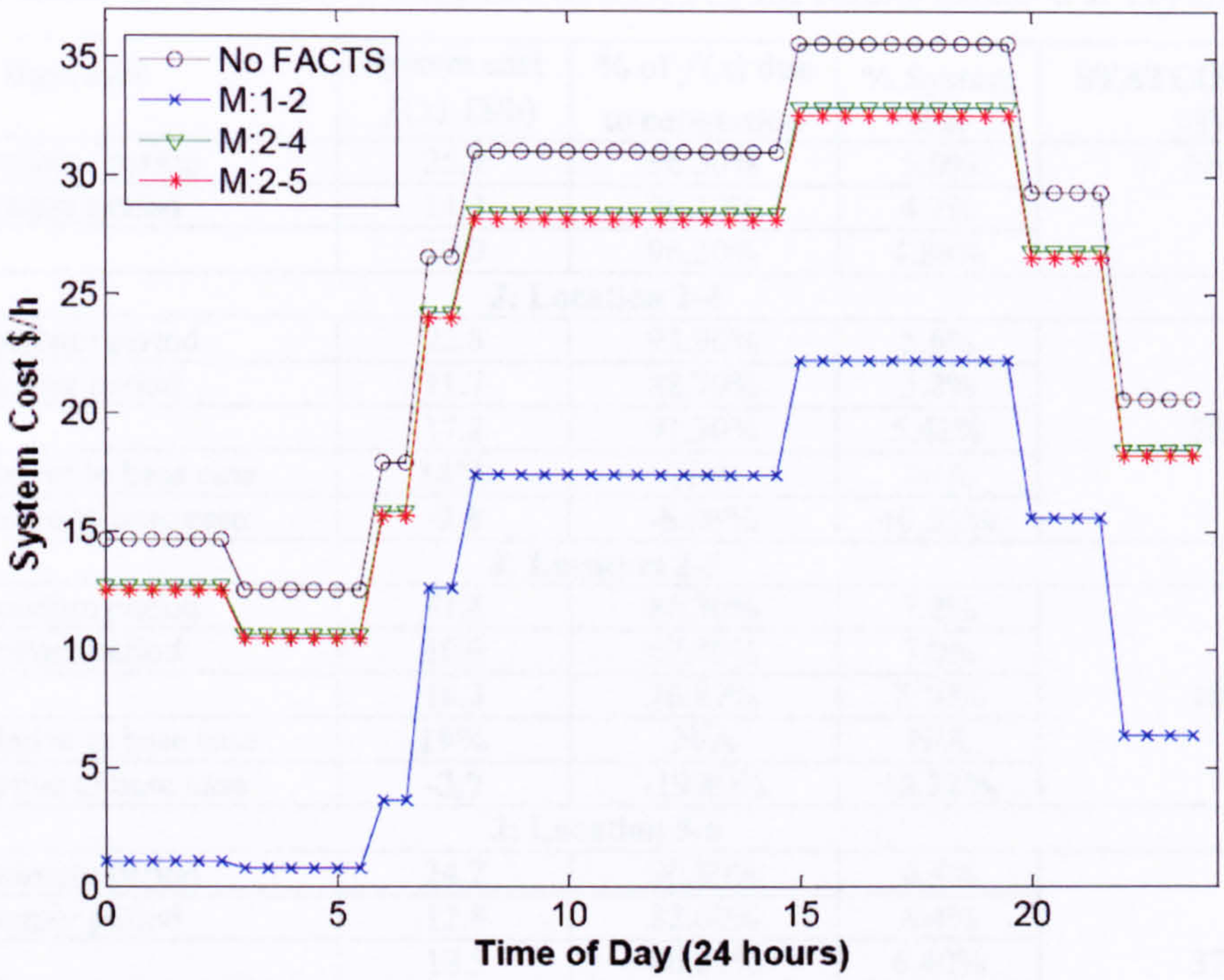

Figure 4.11: IEEE 14 bus system Winter Maximum system cost profile with STATCOM located at midpoint of transmission lines, M:1-2, M:2-4 and M:2-5 (half hour time intervals).

A. STATCOM installed at ends of transmission lines

Table 4-6 shows a summary of results for STATCOM installed at ends of transmission lines for IEEE 14 bus system at system congested lines and at top three locations that provided reduction in system cost.

STATCOM at ends of transmission lines that achieve RSCs greater than 5% (J:2-4, J:2-5, I:5-6)

In Table 4-6, greater than 5% RSCs are achieved; however, the percent in system losses are increased due to the change in power flow. For these results the decrease in congestion and the increase in system loss appear to have an inverse relationship.

STATCOM installed at ends of congested lines (J:6-13, I:7-8)

There are three congested lines but only two possible locations for the STATCOM controller, positions J:6-13 and I:7-8, as four buses are generator buses. RSCs are 2% and 3% respectively and change to system losses minimal. The performance of the system to deal with congestion when a STATCOM is used is not significantly improved. Similar results are obtained when the STATCOM is located at all other locations.

Table 4-6: IEEE 14 bus system, summary of STATCOM results installed at I:*i-j* and J:*i-j*.

Base case	System cost $f(x)$ ($/h)	% of $f(x)$ due to congestion	% System loss	STATCOM rating MVA
Winter Maximum period	25.9	96.50%	5.0%	N/A
Typical Summer period	14.2	96.10%	4.7%	
Annual	20.0	96.30%	4.89%	
J: Location 2-4				
Winter Maximum period	22.8	93.90%	5.6%	227
Typical Summer period	11.7	88.70%	5.2%	
Annual	17.2	91.30%	5.42%	
% RSCs relative to base case	**14%**	N/A	N/A	
Change relative to base case	**-2.8**	**-5.00%**	**+0.53%**	
J: Location 2-5				
Winter Maximum period	21.8	86.30%	7.2%	404
Typical Summer period	10.9	67.40%	7.0%	
Annual	16.3	76.87%	7.10%	
% RSCs relative to base case	**19%**	N/A	N/A	
Change relative to base case	**-3.7**	**-19.40%**	**+2.22%**	
J: Location 5-6				
Winter Maximum period	24.2	90.80%	6.4%	373
Typical Summer period	12.8	82.60%	6.4%	
Annual	18.5	86.69%	6.40%	
% RSCs relative to base case	8%	N/A	N/A	
Change relative to base case	**-1.5**	-9.60%	**+1.52%**	
J: Location 6-13 Congested line				
Winter Maximum period	25.4	96.00%	5.2%	59
Typical Summer period	13.8	94.10%	5.0%	
Annual	19.6	95.00%	5.06%	
% RSCs relative to base case	2%	N/A	N/A	
Change relative to base case	-0.4	**-1.30%**	**+0.17%**	
I: Location 7-8 Congested line				
Winter Maximum period	25.3	96.60%	5.0%	116
Typical Summer period	13.8	96.00%	4.7%	
Annual	19.5	96.29%	4.86%	
% RSCs relative to base case	3%	N/A	N/A	
Change relative to base case	-0.5	**-0.01%**	-0.03%	

<u>STATCOM ratings when installed at ends of transmission lines</u>

The results shown in Table 4-6 suggest that to achieve RSCs over 5% requires relatively high STATCOM ratings in comparison to the congested line locations. Location J:2-5 provides the largest RSC but at the same time requires 404MVA rating, the highest of all locations. At congested line locations and the remaining locations listed in Table 4-5 with savings of 5% or less, the STATCOM controller rating requirements range from 27.5MVA to 350MVA.

B. STATCOM installed at midpoint of transmission lines

Table 4-7 is a summary of midpoint STATCOM results for the IEEE 14 bus system at system congested lines and at the top three locations that provided reduction in system cost.

Table 4-7: IEEE 14 bus system, summary of STATCOM results installed at M:*i-j*.

Base case	**System cost $f(x)$ ($/h)**	**% of $f(x)$ due to congestion**	**% System loss**	**STATCOM rating MVA**
Winter Maximum period	25.9	96.50%	5.0%	N/A
Typical Summer period	14.2	96.10%	4.7%	
Annual	20.0	96.30%	4.89%	
M: Location 1-2 Congested line				
Winter Maximum period	12.5	65.44%	5.7%	68
Typical Summer period	3.0	33.43%	5.6%	
Annual	7.7	49.44%	5.64%	
% RSCs relative to base case	**61%**	N/A	N/A	
Change relative to base case	**-12.3**	**-46.86%**	**+0.75%**	
M: Location 2-4				
Winter Maximum period	23.5	95.51%	5.3%	68
Typical Summer period	12.3	93.43%	4.9%	
Annual	17.9	94.47%	5.09%	
% RSCs relative to base case	**11%**	N/A	N/A	
Change relative to base case	**-2.1**	**-1.83%**	**+0.2%**	
M: Location 2-5				
Winter Maximum period	23.2	94.66%	5.5%	90
Typical Summer period	12.1	92.23%	5.0%	
Annual	17.7	93.45%	5.23%	
% RSCs relative to base case	**12%**	N/A	N/A	
Change relative to base case	**-2.3**	**-2.85%**	**+0.34%**	
M: Location 6-13 Congested line				
Winter Maximum period	25.4	96.23%	5.1%	48
Typical Summer period	13.8	95.08%	4.8%	
Annual	19.6	95.66%	4.97%	
% RSCs relative to base case	**2%**	N/A	N/A	
Change relative to base case	**-0.4**	**-0.64%**	**+0.08%**	
M: Location 7-8 Congested line				
Winter Maximum period	25.9	96.59%	5.04%	39
Typical Summer period	14.2	96.19%	4.71%	
Annual	20.0	96.40%	4.90%	
% RSCs relative to base case	**0%**	N/A	N/A	
Change relative to base case	**0.0**	**+0.1%**	**+0.01%**	

<u>STATCOM at midpoint location of transmission lines that achieve RSCs greater than 10% (M:1-2, M:2-4, M:2-5)</u>

61% RSC is achieved at congested line M:1-2 and 11% and 12% at locations M:2-4 and M:2-5 respectively, on average these are greater than the RSCs made when installed at the ends of the transmission lines. Similar to results in Table 4-6, the results show decrease in congestion and simultaneous increase in system loss.

STATCOM installed at midpoint of congested transmission lines (M:6-13, M:7-8)

Installation at congested line locations M:6-13 and M:7-8 achieved 2% and 0% RSC respectively and increased system losses. Similar results are obtained when the STATCOM is located at the midpoint of all other transmission lines, as listed in Table 4-5.

STATCOM ratings when installed a midpoint of transmission lines

Results shown in Table 4-7 suggest that to achieve RSCs over 10% requires relatively high STATCOM ratings in comparison to congested line locations M:6-13 and M:7-8. Congested line location M:1-2 provides the largest RSC and requires a STATCOM of 69MVA. In comparison to results given in Table 4-6, the required ratings are an order of magnitude lower, tens of MVA instead of hundreds of MVA. At all other locations, RSCs are 5% or less and the STATCOM controller rating requirements range from 3MVA to 270MVA.

Based on annual RSCs, midpoint position at location M:1-2 is the best location for the STATCOM on the 14 bus system.

4.6.4 IEEE 30 bus system cases with STATCOM

For installation of STATCOM at the ends of transmission lines and transformer locations, (excluding generator buses 1, 2, 5, 8, 11 and 13) there are 71 potential locations for the STATCOM. For midpoint transmission line installation of STATCOM there are 37 potential locations as line numbers 11, 12, 15 and 36 are transformers. In total, there are 108 potential locations for STATCOM installation on the IEEE 30 bus system. The first 20 are detailed in Table 4-8, it lists all STATCOM locations using both ends and midpoint of transmission lines, where the annual % RSC is compared to the system base case and line numbers 21 to 41 inclusive show no significant RSC (≤ 1%). System setup and setup results for the IEEE 30 bus system can be found in Appendix VII, similar to that presented for IEEE 14 bus system in Chapter 3.

Four locations (J:2-4, J:2-6, M:1-2 and M:2-6) produced annual RSCs equal or greater than 10%, two locations produced RSCs between 1% and 9%, 18 locations produced an increase in system cost, making the system congestion worse, the remaining 84 locations achieve annual % RSCs between 0% and 1%.

Table 4-8: IEEE 30 bus system, all STATCOM locations and positions I:*i-j*, J:*i-j* and M:*i-j*.

Line no.	Line *i-j*	Annual % Reduction in System Cost w.r.t. base case		
		I:*i-j* (At bus *i*)	J:*i-j* (At bus *j*)	M:*i-j* (At midpoint)
1	1-2 Congested	Generator Bus	Generator Bus	**70%**
2	1-3	Generator Bus	% Increase	% Increase
3	2-4	Generator Bus	**10%**	7%
4	3-4	% Increase	% Increase	% Increase
5	2-5	Generator Bus	Generator Bus	2%
6	2-6 Congested	Generator Bus	**14%**	**13%**
7	4-6	% Increase	% Increase	% Increase
8	5-7	Generator Bus	% Increase	% Increase
9	6-7	% Increase	% Increase	% Increase
10	6-8 Congested	< 1%	Generator Bus	< 1%
11	6-9 Transformer	< 1%	< 1%	Transformer
12	6-10 Transformer	< 1%	< 1%	Transformer
13	9-11	< 1%	Generator Bus	% Increase
14	9-10	< 1%	< 1%	< 1%
15	4-12 Transformer	< 1%	% Increase	Transformer
16	12-13	< 1%	Generator Bus	% Increase
17	12-14	< 1%	% Increase	< 1%
18	12-15 Congested	< 1%	% Increase	< 1%
19	12-16	< 1%	0%	< 1%
20	14-15	< 1%	1%	< 1%
21 - 41	Includes buses 16 to 30	≤ 1%	≤ 1%	0% < and < 1%

A. STATCOM installed at ends of transmission lines

Figures 4.12 and 4.13 show the profiles for the Typical Summer and Winter Maximum periods over 24 hours for J:2-4 and J:2-6 respectively. In both seasons STATCOM location J:2-4 provides the largest RSC.

B. STATCOM installed at midpoint of transmission lines

Figures 4.14 and 4.15 show the system cost profiles for the Typical Summer and Winter Maximum periods over 24 hour period for M:1-2 and M:2-4 respectively. In both seasons M:1-2 provides the largest RSCs.

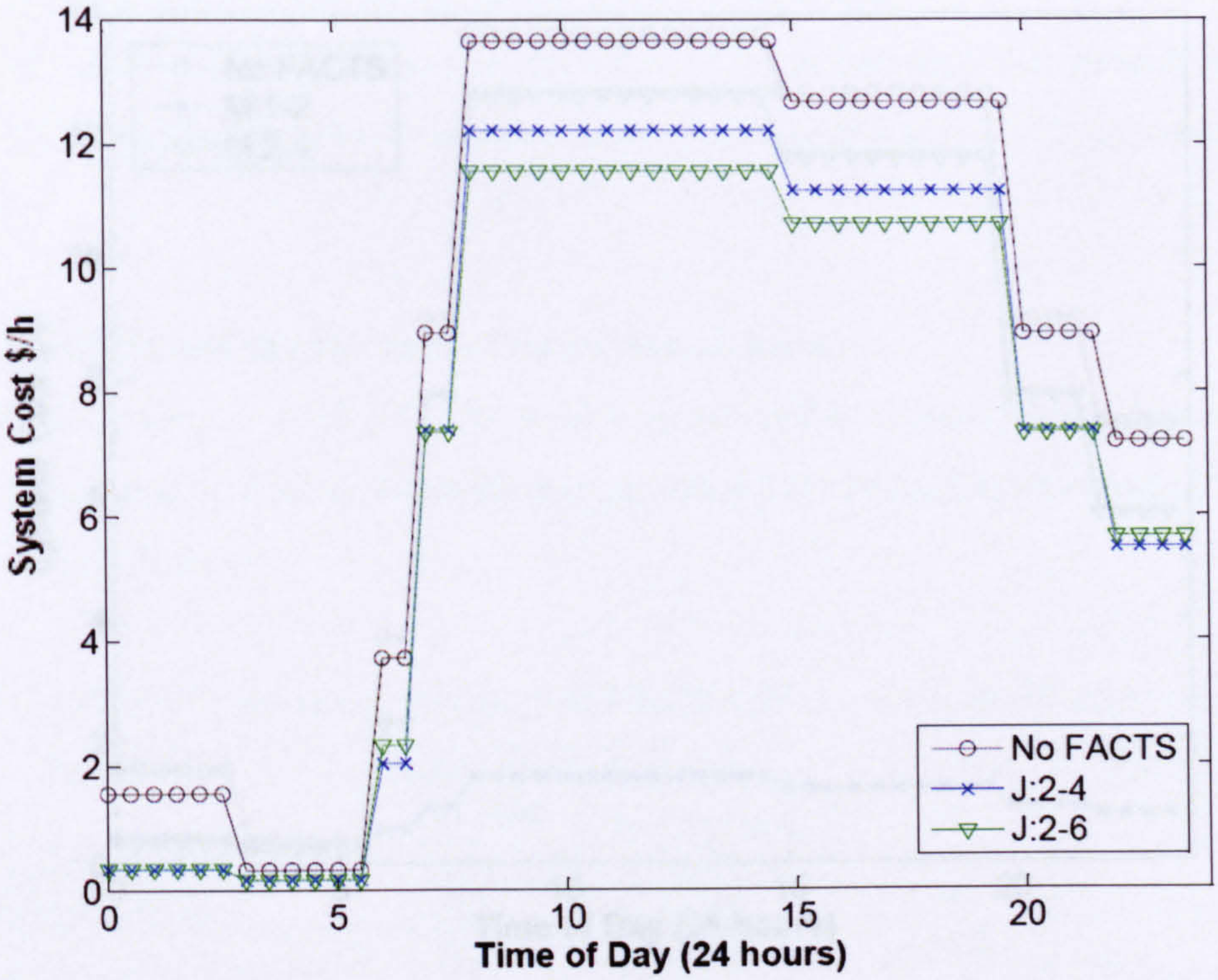

Figure 4.12: IEEE 30 bus system Typical Summer system cost profile with STATCOM located at ends of transmission lines, J:2-4 and J:2-6 (half hour time intervals).

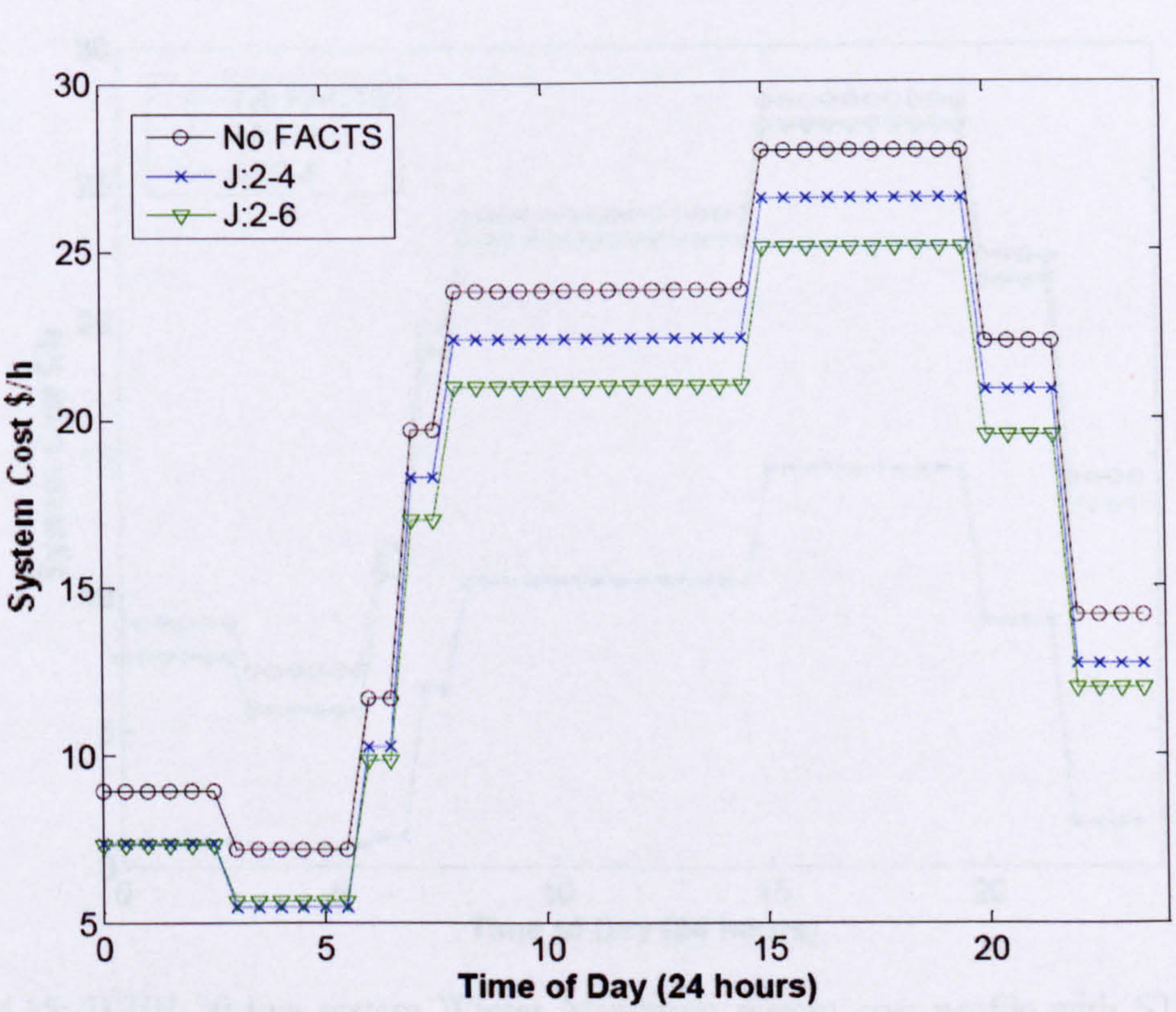

Figure 4.13: IEEE 30 bus system Winter Maximum system cost profile with STATCOM located at ends of transmission lines, J:2-4 and J:2-6 (half hour time intervals).

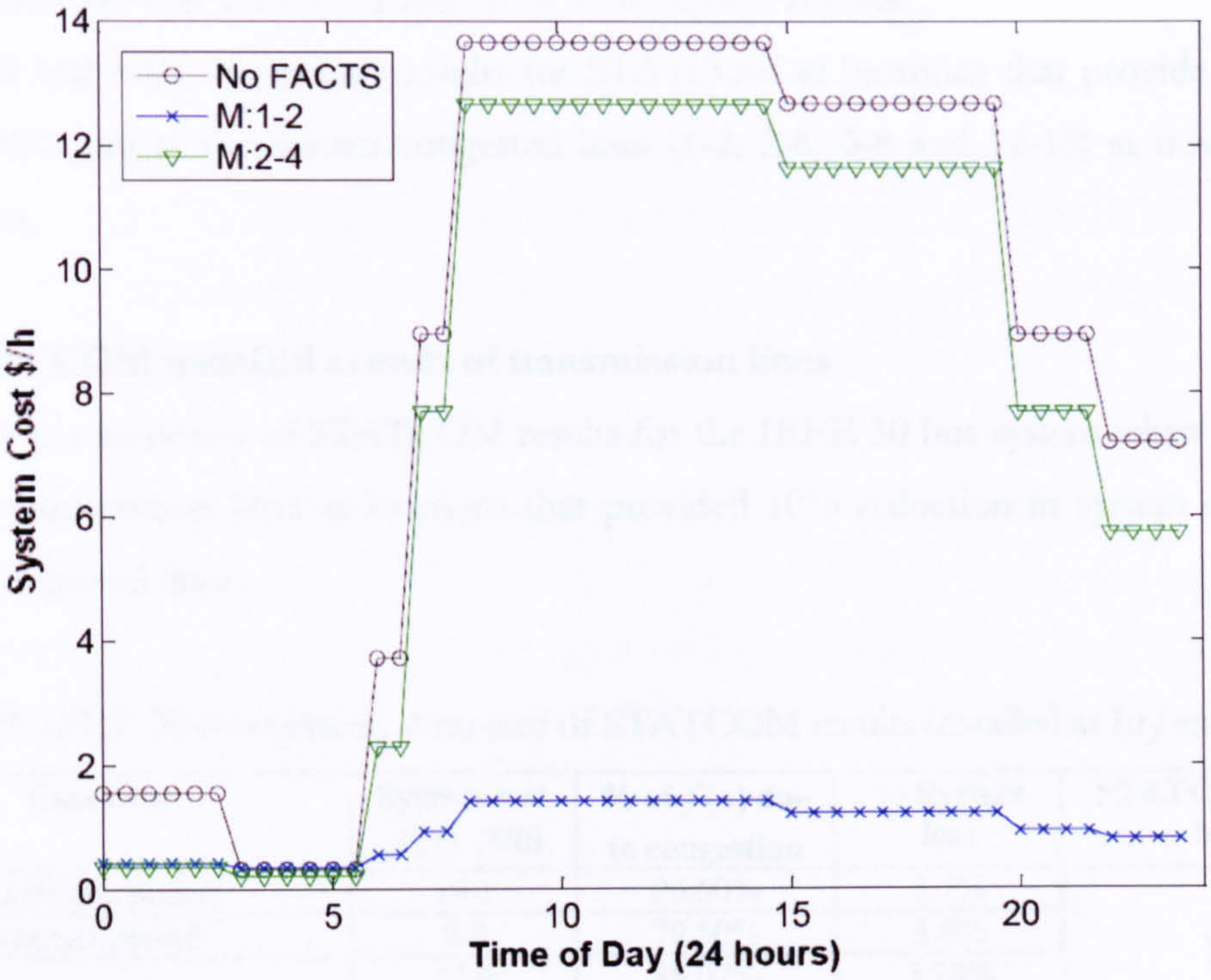

Figure 4.14: IEEE 30 bus system Typical Summer system cost profile with STATCOM located at midpoint of transmission lines, M:1-2 and M:2-4 (half hour time intervals).

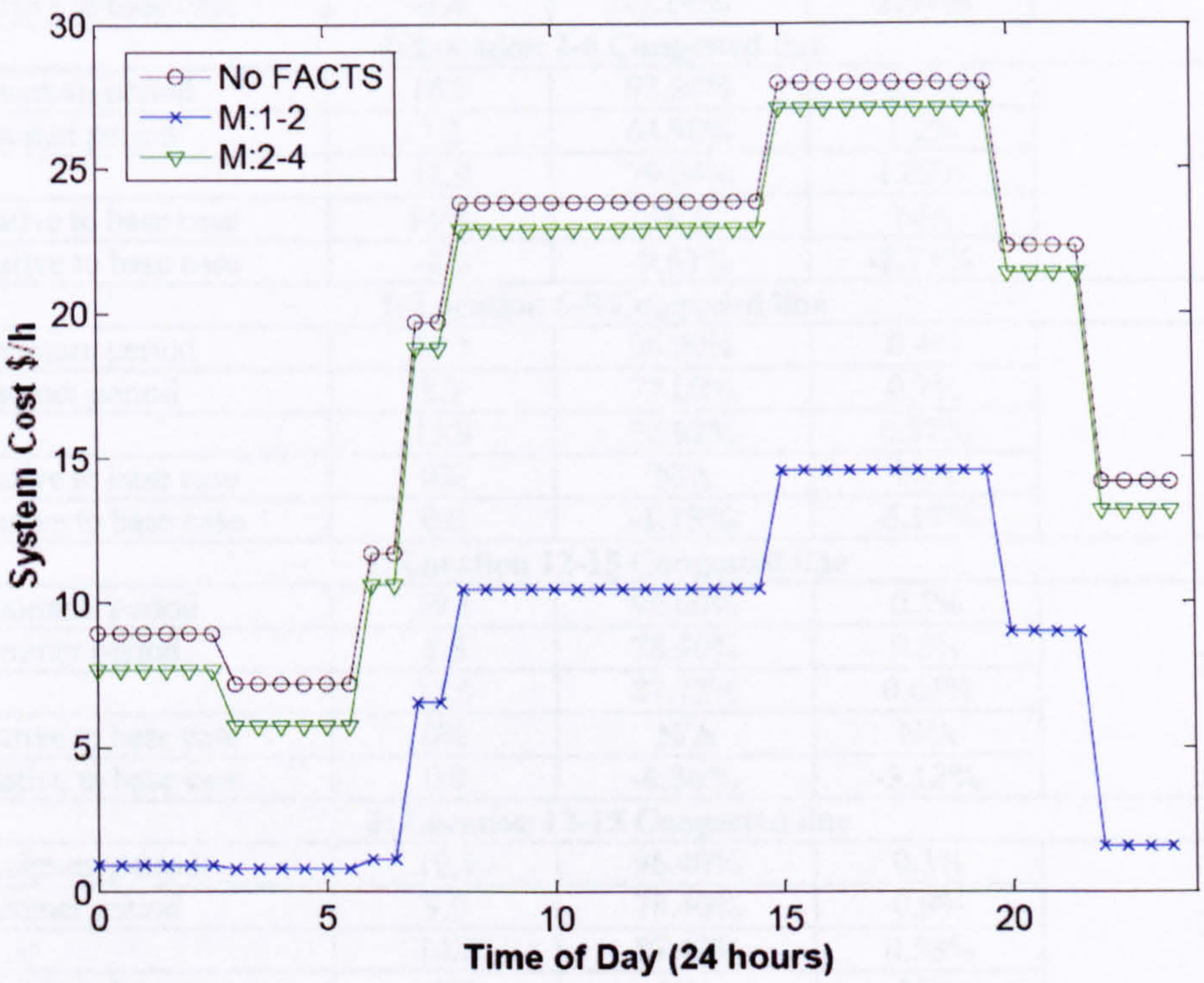

Figure 4.15: IEEE 30 bus system Winter Maximum system cost profile with STATCOM located at midpoint of transmission lines M:1-2 and M:2-4 (half hour time intervals).

4.6.5 IEEE 30 bus system: Analysis of STATCOM results

Table 4-9 and 4-10 summarises results for STATCOM at locations that provide significant annual RSC and at the system congested lines (1-2, 2-6, 6-8 and 12-15) at buses without generators.

A. STATCOM installed at ends of transmission lines

Table 4-9 is a summary of STATCOM results for the IEEE 30 bus system when installed at ends of transmission lines at locations that provided 10% reduction in system cost and at system congested lines.

Table 4-9: IEEE 30 bus system, summary of STATCOM results installed at I:*i-j* and J:*i-j*.

Base case	System cost $f(x)$ ($/h)	% of $f(x)$ due to congestion	% System loss	STATCOM rating MVA
Winter Maximum period	19.1	96.60%	3.7%	N/A
Typical Summer period	8.7	79.50%	3.8%	
Annual	13.9	88.07%	3.74%	
J: Location 2-4				
Winter Maximum period	17.6	94.70%	0.6%	191
Typical Summer period	7.4	67.10%	0.8%	
Annual	12.5	80.89%	0.70%	
% RSC relative to base case	**10%**	N/A	N/A	
Change relative to base case	**-1.4**	**-7.19%**	**-3.04%**	
J: Location 2-6 Congested line				
Winter Maximum period	16.7	93.20%	0.9%	132
Typical Summer period	7.2	64.90%	1.2%	
Annual	11.9	79.04%	1.02%	
% RSC relative to base case	**14%**	N/A	N/A	
Change relative to base case	**-2.0**	**-9.03%**	**-2.73%**	
I: Location 6-8 Congested line				
Winter Maximum period	19.1	96.90%	0.4%	111
Typical Summer period	8.7	77.00%	0.7%	
Annual	13.9	86.92%	0.57%	
% RSC relative to base case	0%	N/A	N/A	
Change relative to base case	0.0	**-1.15%**	**-3.17%**	
I: Location 12-15 Congested line				
Winter Maximum period	19.1	96.60%	0.5%	76
Typical Summer period	8.8	78.90%	0.8%	
Annual	13.9	87.72%	0.63%	
% RSC relative to base case	0%	N/A	N/A	
Change relative to base case	0.0	**-0.36%**	**-3.12%**	
J: Location 12-15 Congested line				
Winter Maximum period	19.4	96.40%	0.3%	33
Typical Summer period	9.0	78.40%	0.9%	
Annual	14.2	87.42%	0.58%	
% RSC relative to base case	-2%	N/A	N/A	
Change relative to base case	+0.3	**-0.66%**	**-3.16%**	

STATCOM installed at ends of transmission lines that achieve RSCs of 10% or greater (J:2-4 and J:2-6)

Total annual cost is reduced at the two locations due to decreases in both system losses and congestion. Approximately 2% higher RSCs are made at J:2-4 than J:2-6. The results reinforce that congestion is more significant to the contribution of annual system cost than system losses.

STATCOM installed at ends of congested lines (I: 6-8, I:12-15 and J:12-15)

0% annual RSCs are made at I:6-8 and I:12-15 and at J:12-15 an increase in annual system cost occurs. All locations reduce system losses by approximately 3%. A similar trend is seen when the STATCOM is located at other system locations, as listed in Table 4-8.

STATCOM ratings when installed at ends of transmission lines

Similar to results shown in Table 4-6, results in Table 4-9 suggest that a relatively higher STATCOM rating is required to achieve RSCs of 10% or greater. Unlike results from Table 4-6 the largest STATCOM rating does not coincide with the greatest RSC.

B. STATCOM installed at midpoint of transmission lines

Table 4-10 is a summary of midpoint STATCOM results at locations that provided reduction in system cost and at system congested lines for IEEE 30 bus system.

STATCOM at midpoint location of transmission lines that achieve RSCs greater than 10% (M:1-2, M:2-4, M:2-6)

Significant annual RSCs are achieved at two locations, 70% at M:1-2, and 13% at M:2-6, where both locations experience increase in system loss. Similar to results seen in the 14 bus system, on average the RSCs are greater than when installed at the ends of transmission lines.

STATCOM at midpoint locations with less than 10% RSC (M:2-4, M:2-6, M:6-8, M:12-15)

0% annual RSCs are made at locations M:6-8 and M: 12-15. All locations give increase in system losses of less than 1%. At all other locations listed in Table 4-8 RSCs are less than 1% and a similar trend is seen in system losses.

STATCOM ratings when installed a midpoint of transmission line

In Table 4-10, the required STATCOM ratings are varied, the highest rating is 37MVA at M:12-15 where there is 0% RSC and the lowest rating is 13MVA at M:2-6 where there is 13% RSC.

Table 4-10: IEEE 30 bus system, summary of STATCOM results installed at M:*i-j*.

Base case	**System cost $f(x)$ ($/h)**	**% of $f(x)$ due to congestion**	**% System loss**	**STATCOM rating MVA**
Winter Maximum period	19.1	96.60%	3.7%	N/A
Typical Summer period	8.7	79.50%	3.8%	
Annual	13.9	88.07%	3.74%	
M: Location 1-2				
Winter Maximum period	7.5	51.50%	4.9%	26
Typical Summer period	1.0	0.00%	4.4%	
Annual	4.2	25.75%	4.63%	
% RSC relative to base case	**70%**	N/A	N/A	
Change relative to base case	**-9.7**	**-62.32%**	**+0.89%**	
M: Location 2-4				
Winter Maximum period	18.1	96.89%	3.52%	33
Typical Summer period	7.7	70.61%	3.64%	
Annual	12.9	83.75%	3.58%	
% RSC relative to base case	**7%**	N/A	N/A	
Change relative to base case	**-1.0**	**-4.32%**	**+0.16%**	
M: Location 2-6 Congested line				
Winter Maximum period	16.8	93.97%	3.98%	13
Typical Summer period	7.5	67.25%	4.09%	
Annual	12.1	80.61%	4.04%	
% RSC relative to base case	**13%**	N/A	N/A	
Change relative to base case	**-1.8**	**-7.46%**	**+0.3%**	
M: Location 6-8 Congested line				
Winter Maximum period	19.1	96.55%	3.65%	35
Typical Summer period	8.7	78.98%	3.85%	
Annual	13.9	87.77%	3.75%	
% RSC relative to base case	**0%**	N/A	N/A	
Change relative to base case	**0.0**	**-0.3%**	**+0.01%**	
M: Location 12-15 Congested line				
Winter Maximum period	19.1	96.66%	3.66%	37
Typical Summer period	8.7	78.33%	3.90%	
Annual	13.9	87.49%	3.78%	
% RSC elative to base case	**0%**	N/A	N/A	
Change relative to base case	**0.0**	**-0.58%**	**+0.04%**	

Based on annual RSCs midpoint position at location M:1-2 is the best location for the STATCOM on the IEEE 30 bus system.

4.6.6 Summary of case study 1 results

Tables 4-6, 4-7 and 4-9, 4-10 show that congestion is a higher contribution to system cost compared to system loss. Therefore, to reduce overall costs it is logical find the FACTS

controller location that minimises system congestion, and not system losses as suggested in Singh and David (2000) and Preedavichit and Srivastava (1998).

Comparing results in Table 4-6 to 4-7 and Table 4-9 to 4-10 shows that positioning the STATCOM at the midpoint of transmission lines gives higher RSCs compared to positioning at the ends of transmission lines. In addition STATCOM ratings when installed at midpoint require relatively smaller ratings than positioning at the end of transmission lines.

Installing the STATCOM on congested lines was only effective at M:1-2 for both the IEEE 14 and 30 bus systems. At other congested lines RSCs were less than 10%.

At both positions there is no direct relationship between RSC and required STATCOM rating. It indicates that the nonlinearity of the problem results in a nonlinear relationship between system cost and STATCOM controller rating.

4.7 Case study 2: Daily demand profiles and locating the UPFC to manage congestion

It is well known that the UPFC along with other FACTS controllers are likely to continue to be useful tools to mitigate congestion and provide effective expansion of future power systems [Sood (2004), Hingorani et al. (2000) and Zhang et al. (2005)]. The following case studies carried out on the IEEE 14 bus and 30 bus systems show how the UPFC performs when it is installed at all possible locations (including congested lines) during normal daily demand changes. The primary interest is in the system cost savings due to congestion. The system losses are also observed to compare the changes made due to FACTS controller installation and the proportion of real system loss to the scheduled output power. The general two-step solution procedure as described in Chapter 3, Section 3.7 is applied.

4.7.1 UPFC orientations

The UPFC has a shunt and a series branch and can be placed at different orientations on transmission lines *i-j*. Figures 4.6(a) to (d) shows the four orientations used for these case studies;

Orientation 1 – Shunt branch of UPFC attached to bus *i*, series branch to bus κ,

Orientation 2 – Shunt branch of UPFC attached to bus *j*, series branch to bus κ,

Orientation 3 – Series branch of UPFC attached to bus *i*, shunt branch to bus κ,

Orientation 4 – Series branch of UPFC attached to bus *j*, shunt branch to bus κ.

A review of literature reveals that Orientation 1 is the most common orientation for schematic of the UPFC, that is, the shunt branch connected to the left hand bus *i* and the series branch connected to the additional intermediate bus κ [Nabavi-Niaki (1996), Fuerte-Esquivel et al. (1997) and Zhang et al. (2006)].

The orientation of the UPFC in any practical installation is dependent upon the individual system problem and the desired outcome. For example the first UPFC installation was commissioned in Kentucky, USA to increase power transfer capability and provide voltage support due to the low population density and rural nature of the area [Schauder et al. (1998)] and the Converter Static Compensator (CSC) was installed at a New York Power Authority substation to increase the power flow transfer limit and provide greater control precision during contingency situations [Edris et al. (2002)]. In each example static and dynamic attributes were taken into account to decide the orientation of the controller.

The objective of exploring the different orientations in this chapter is to observe if there are any major differences in the reduction of congestion and system costs.

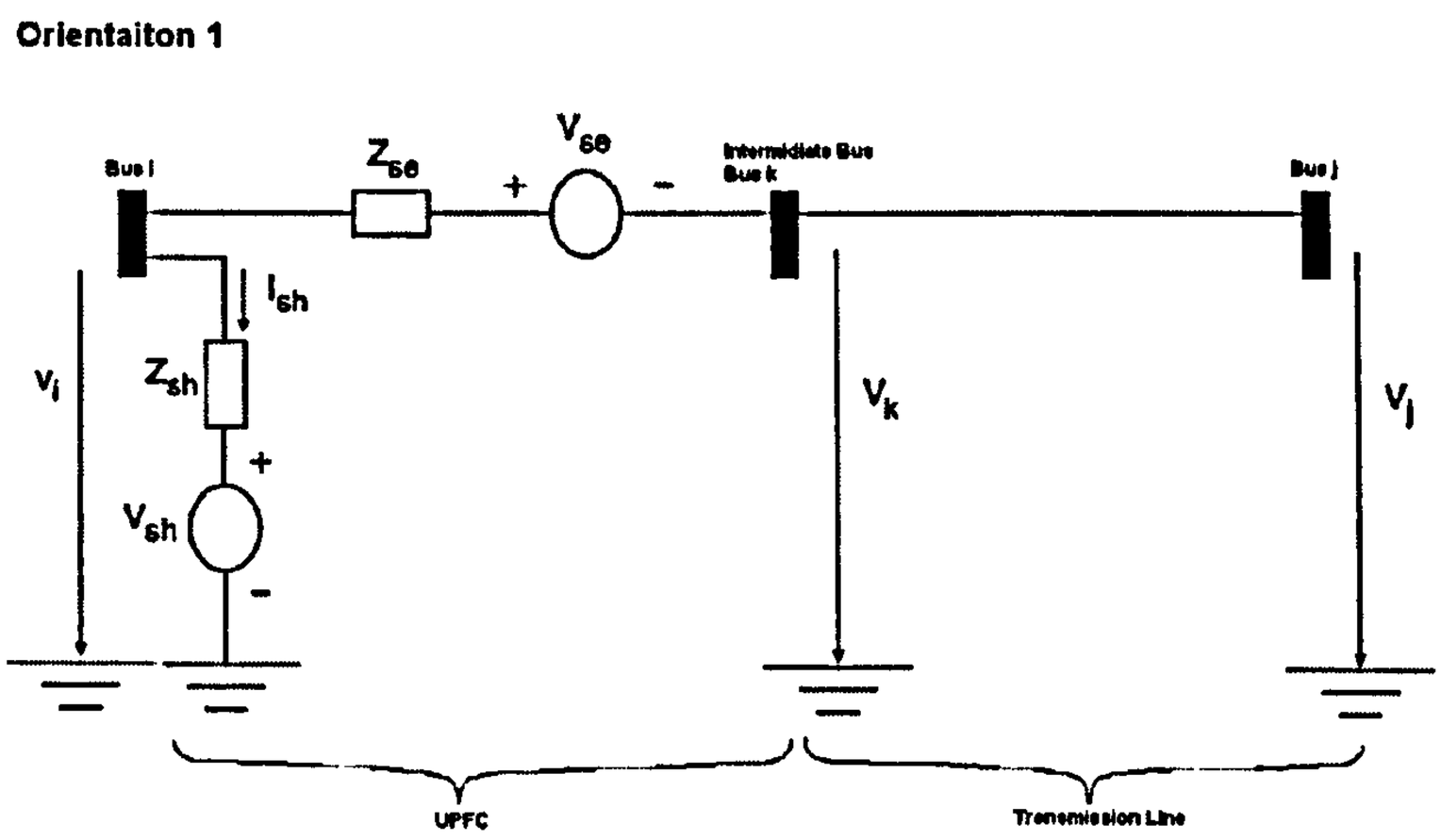

Figure 4.16(a): Four UPFC Orientations: Orientation 1 (O1).

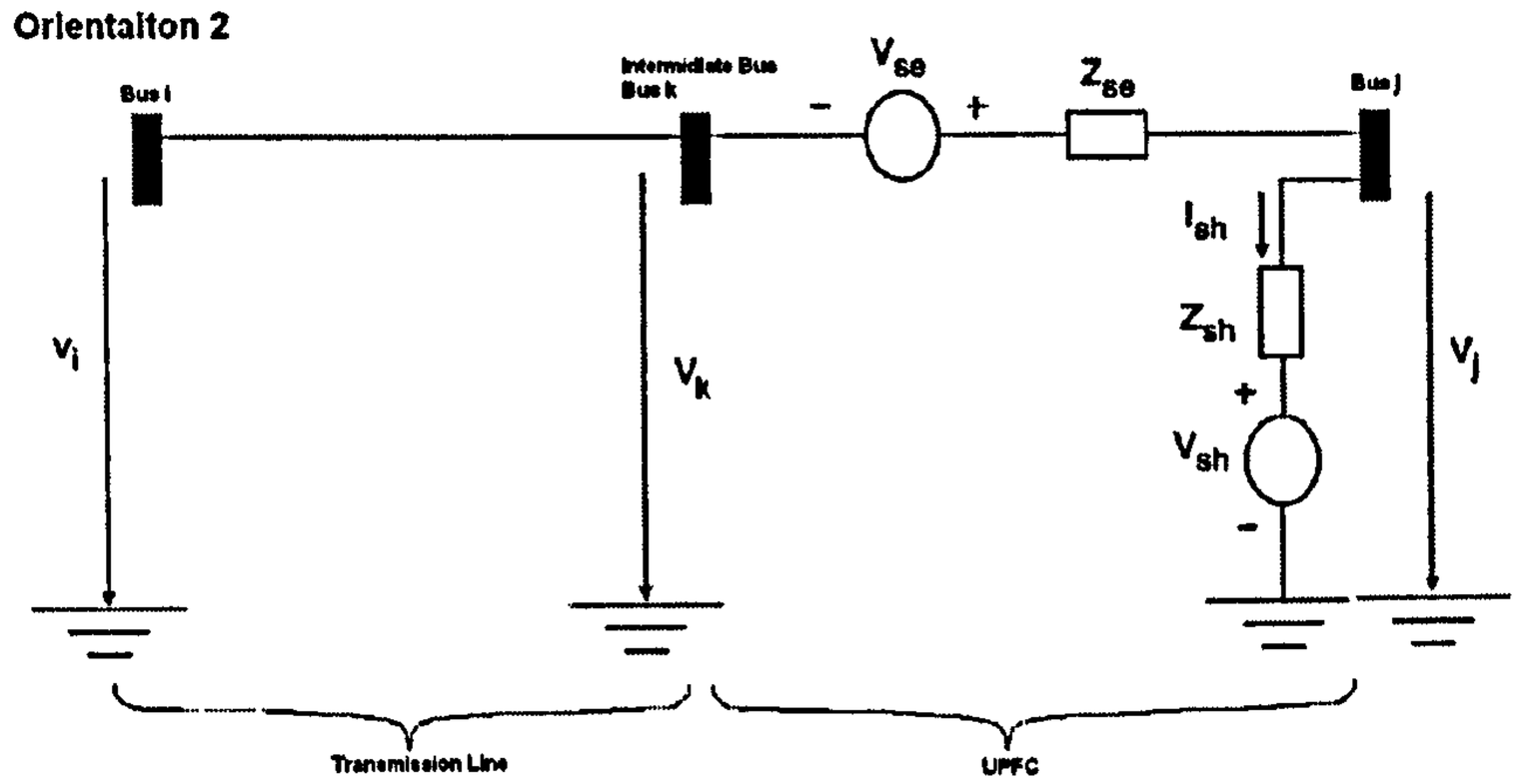

Figure 4.16(b): Four UPFC Orientations: Orientation 2 (O2).

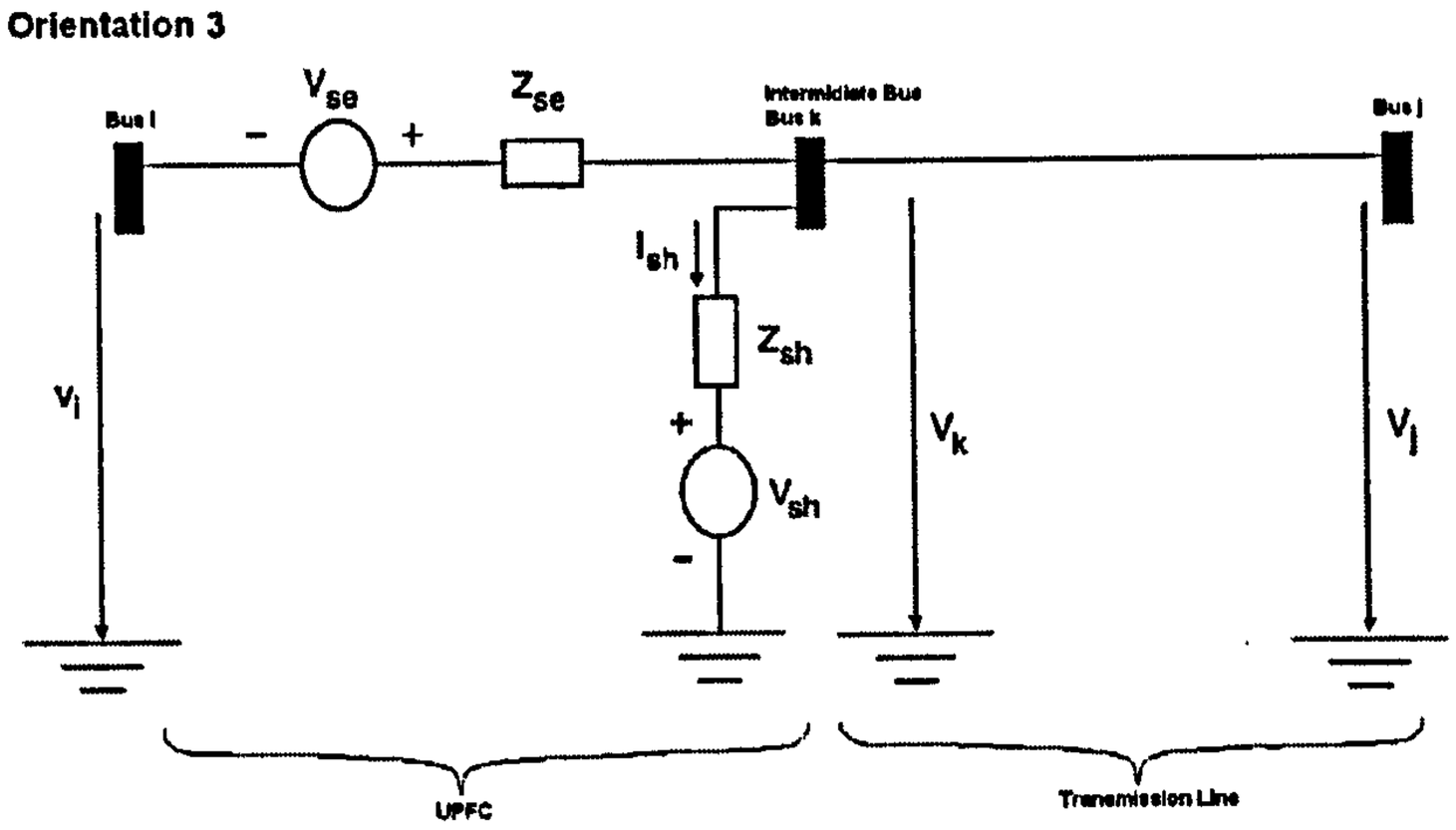

Figure 4.16(c): Four UPFC Orientations: Orientation 3 (O3).

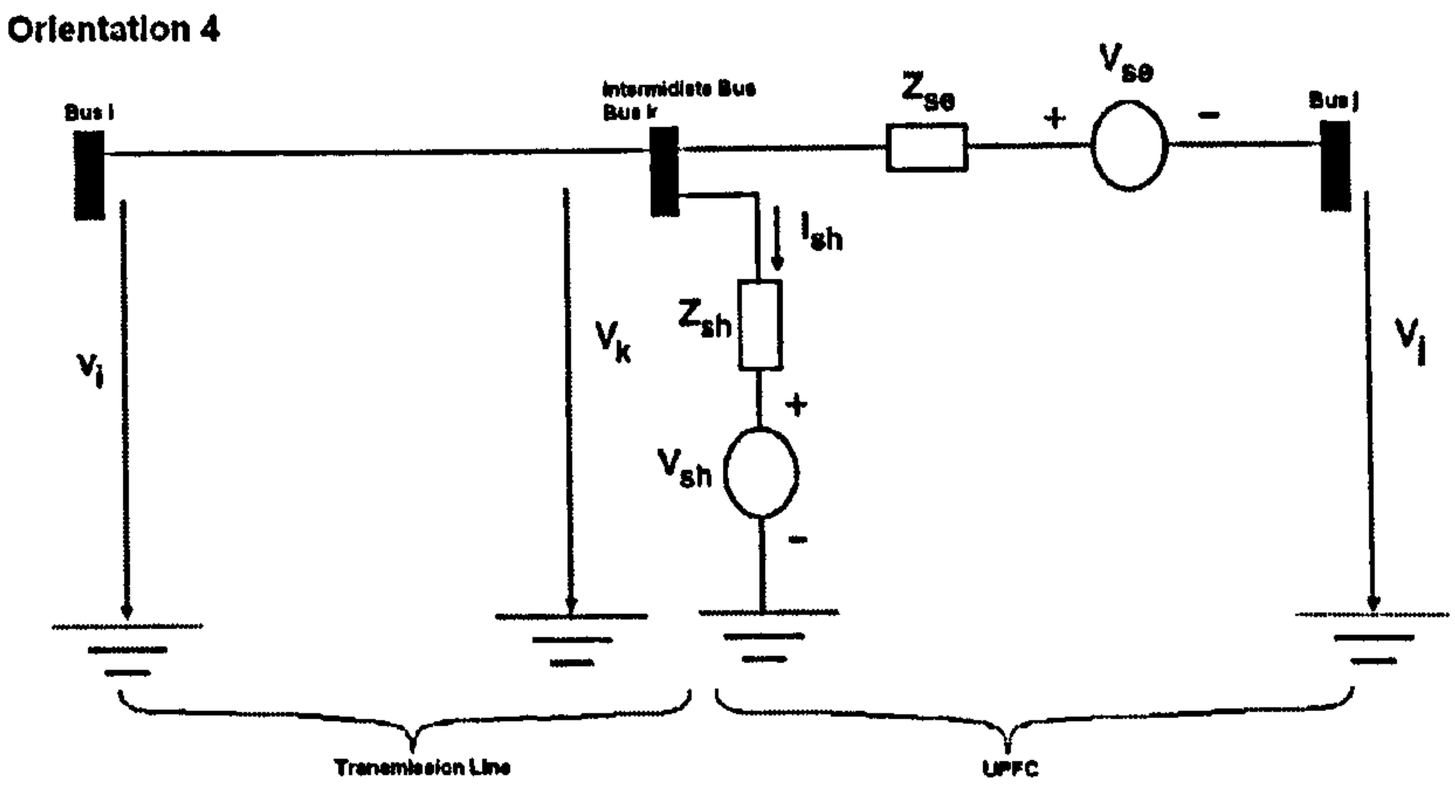

Figure 4.16(d): Four UPFC Orientations: Orientation 4 (O4).

4.7.2 IEEE 14 bus system case with UPFC

The IEEE 14 bus system was first introduced in Chapter 2, Section 2.6. All generation cost coefficients are equal and set to $C_{gi}^{+} = 20$ \$/MWh and $C_{gi}^{-} = 10$ \$/MWh. All lines are simulated with a single UPFC at the four possible orientations. For the 14 bus system there are 17 transmission lines and 3 transformers, making 20 potential locations for the UPFC. Five lines (1-2, 1-5, 2-4, 2-5 and 4-5) at all four orientations show RSCs over 10%. Only when located at congested line 1-2 does the UPFC show large RSC, and this is also the location that shows the best results overall. Table 4-11 lists the annual % RSC due the addition of a UPFC at each combination of line and orientation compared to the base case system. Percentages above 10% RSCs are highlighted in bold.

Table 4-11: IEEE 14 bus system listing all UPFC locations and four orientations.

Line no.	Line *i-j*	Annual % Reduction in System cost w.r.t. base case			
		O1	O2	O3	O4
1	1-2 Congested	**71%**	**68%**	**70%**	**66%**
2	1-5	**61%**	**32%**	**57%**	**27%**
3	2-3	7%	**12%**	**13%**	6%
4	2-4	**15%**	**31%**	**27%**	**24%**
5	2-5	**38%**	**58%**	**18%**	**51%**
6	3-4	**11%**	9%	7%	9%
7	4-5	**14%**	**31%**	**26%**	**16%**
8	4-7 Transformer	3%	4%	5%	4%
9	4-9 Transformer	5%	4%	5%	4%
10	5-6 Transformer	7%	6%	9%	5%
11	6-11	7%	3%	5%	2%
12	6-12	2%	2%	5%	2%
13	6-13 Congested	5%	2%	4%	2%
14	7-8 Congested	3%	0%	3%	0%
15	7-9	4%	4%	4%	4%
16	9-10	4%	2%	3%	2%
17	9-14	3%	2%	3%	2%
18	10-11	2%	2%	2%	2%
19	12-13	2%	2%	2%	1%
20	13-14	2%	2%	2%	2%

Figures 4.17(a) and (b) shows the results for the UPFC in Orientation 1 at lines 1-2, 1-5, 2-3, 2-4, 2-5, 3-4 and 5-6 during Typical Summer and Figures 4.18(a) and (b) at Winter Maximum period. The performance of the UPFC during the summer period is better compared to the winter, because the level of congestion experienced during the winter is more severe.

The orientation of the UPFC does have some effect on the system performance to minimise congestion costs. For example, line number 5 indicates that if installed using Orientation 1, there would be an annual RSC 40% higher than Orientation 3. The results have highlighted

that this is another important factor that should have been given more consideration in published literature to date. For steady state analysis presented from here on Orientation 1 is examined to indicate common trends.

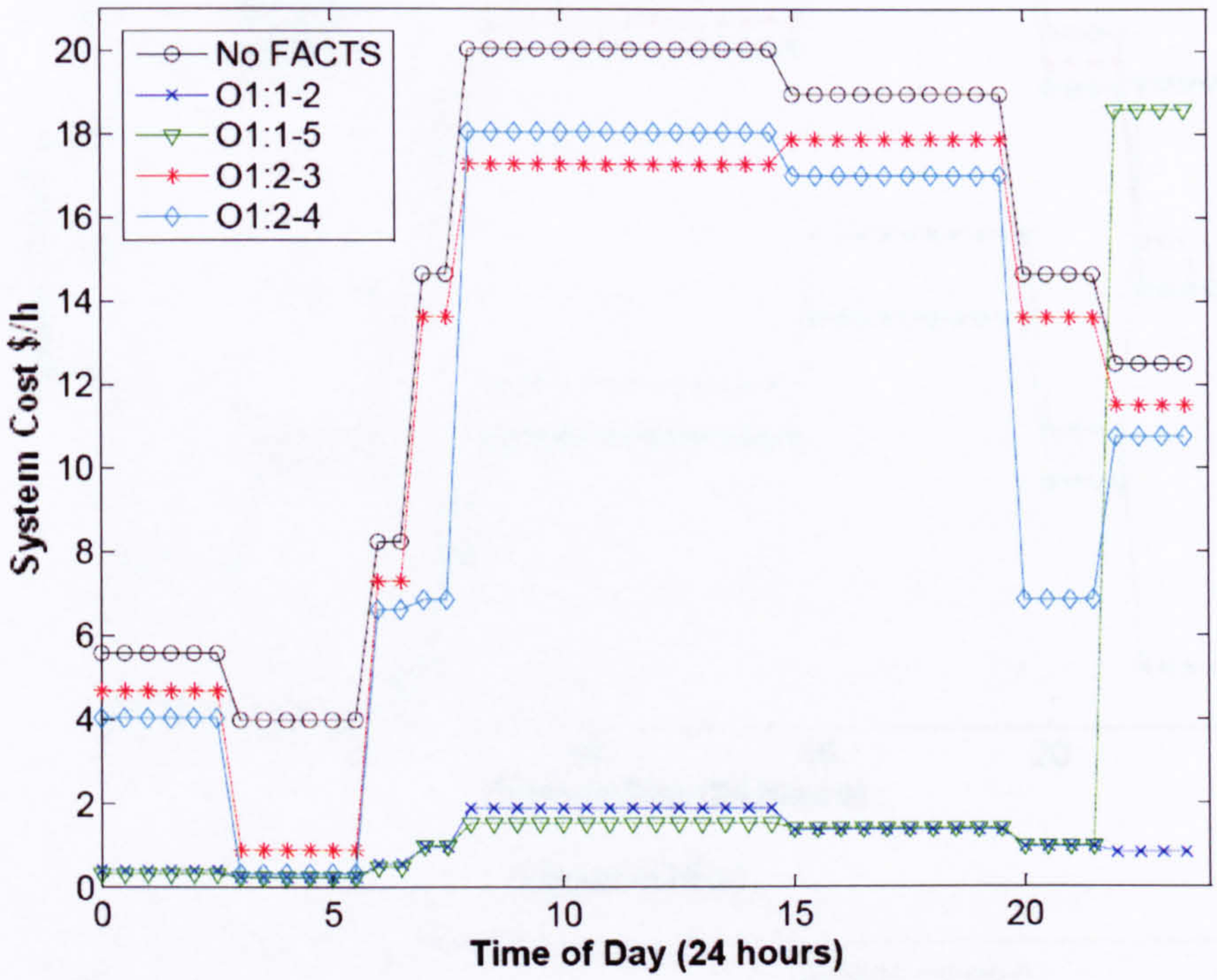

Figure 4.17(a)

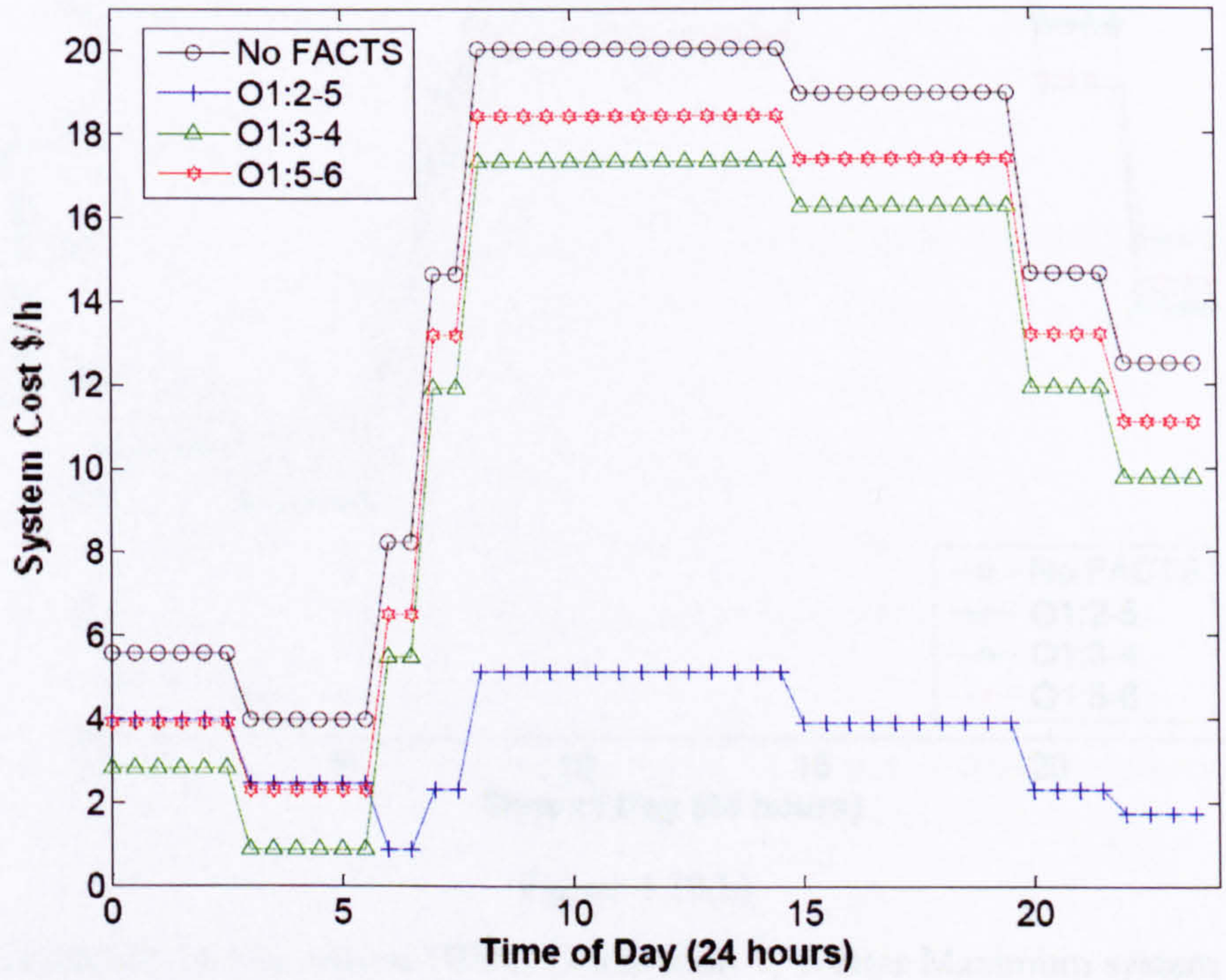

Figure 4.17(b)

Figure 4.17: IEEE 14 bus system UPFC Orientation 1, Typical Summer system cost profile at: (a) locations 1-2, 1-5, 2-3 and 2-4 (b) locations 2-5, 3-4 and 5-6 (half hour time intervals).

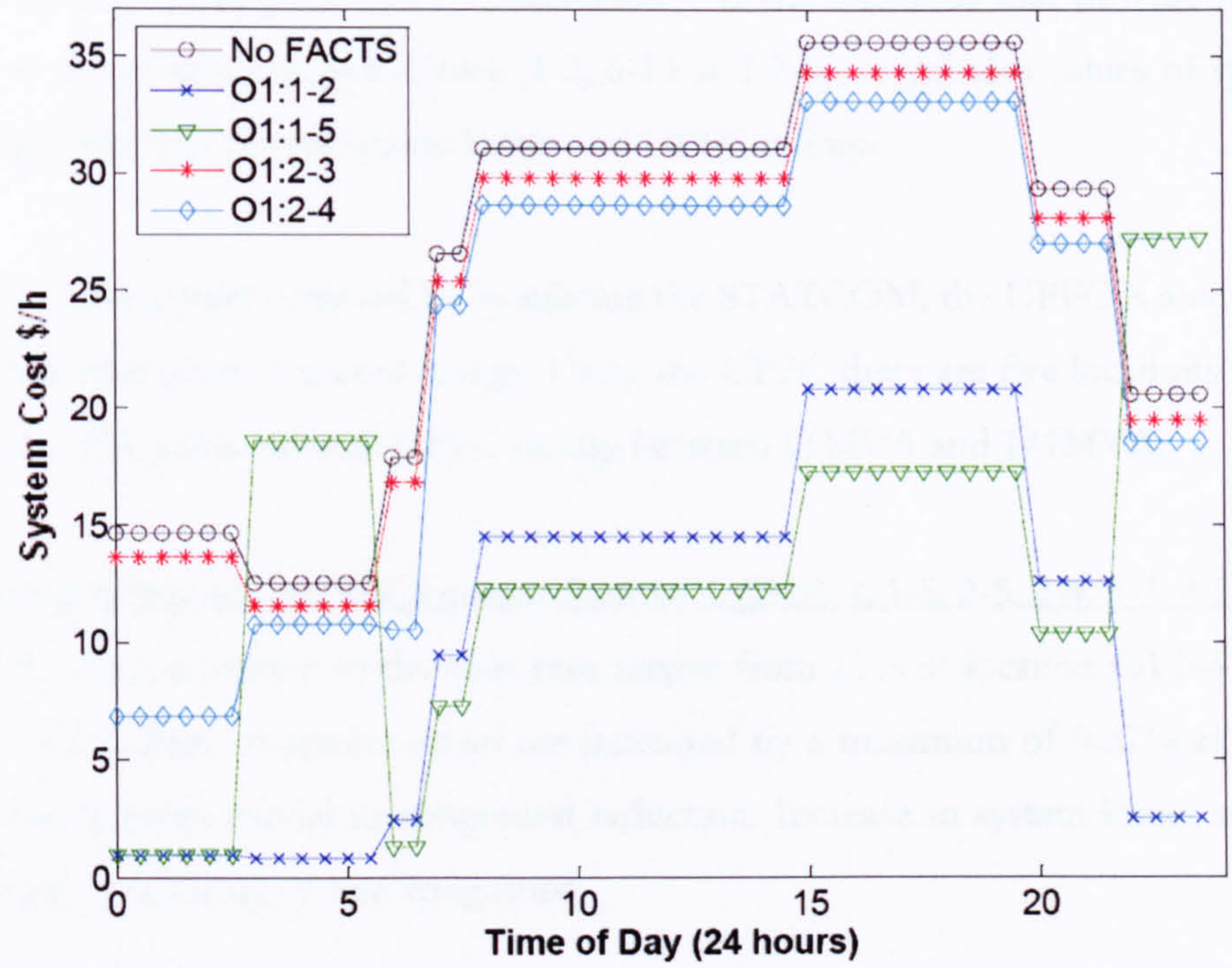

Figure 4.18(a)

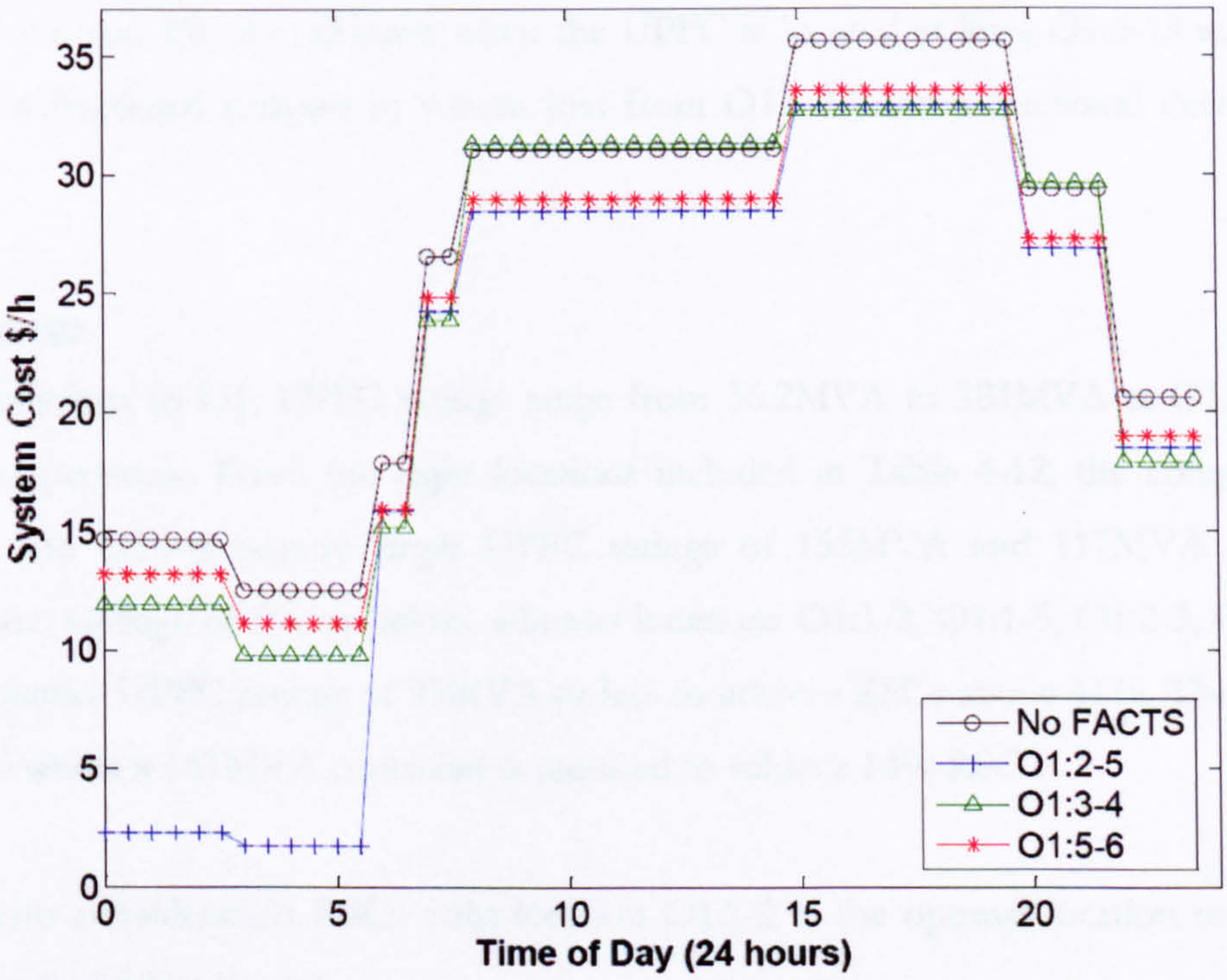

Figure 4.18(b)

Figure 4.18: IEEE 14 bus system UPFC Orientation 1, Winter Maximum system cost profile at: (a) locations 1-2, 1-5, 2-3 and 2-4, (b) locations 2-5, 3-4 and 5-6 (half hour time intervals).

IEEE 14 bus system: Analysis of UPFC results

Table 4-12 shows results for UPFC Orientation 1 at the locations that provide RSC above 10% and at the system congested lines (1-2, 6-13 and 7-8). It includes values of system cost $f(x)$, congestion, real power system losses and UPFC ratings.

Compared to the results achieved by simulating the STATCOM, the UPFC is able to achieve greater RSCs with lower required ratings. Using the UPFC there are five locations with RSCs greater than 10%, achieved with UPFC ratings between 66MVA and 141MVA.

UPFC locations that achieve RSCs greater than 10% (O1:1-2, 1-5, 2-5, 2-4, 3-4, 4-5)

The % RSC change relative to the base case ranges from 11% at location O1:3-4 to 71% at location O1:1-2. Percent system losses are increased by a maximum of 0.82% at O:2-5 and are not directly proportional to congestion reduction. Increase in system losses are a minor consequence of reducing system congestion.

UPFC locations at congested lines and with RSCs equal to 5% or less (O1:6-13, 7-8)

RSCs of 5% and 3% are achieved when the UPFC is located at lines O1:6-13 and O1:7-8. There is a fractional increase in system loss from O1:6-13 and a fractional decrease from O1:7-8.

UPFC ratings

For all locations in O1, UPFC ratings range from 36.2MVA to 381MVA at O1:10-11 and O1:5-6 respectively. From the eight locations included in Table 4-12, the congested lines O1:6-13 and O1:7-8 require larger UPFC ratings of 155MVA and 117MVA to achieve system cost savings of 5% or below, whereas locations O1:1-2, O1:1-5, O1:2-5, O1:2-4 and O1:3-4 require UPFC ratings of 93MVA or less to achieve RSCs above 11%. The exception is O1:4-5 where a 141MVA controller is required to achieve 14% RSC.

Taking into consideration RSCs only; location O1:1-2 is the optimal location to install the UPFC on the 14 bus system.

Table 4-12: IEEE 14 bus system, summary of UPFC Orientation 1 results.

Base case	System cost $f(x)$ ($/h)	% of $f(x)$ due to congestion	% System loss	UPFC rating MVA
Winter Maximum period	25.9	96.50%	5.10%	N/A
Typical Summer period	14.2	96.40%	4.90%	
Annual	20.0	96.44%	4.98%	
O1: Location 1-2 Congested line				
Winter Maximum period	1.1	5.10%	5.40%	70
Typical Summer period	10.5	61.90%	5.50%	
Annual	5.8	33.49%	5.48%	
% RSC relative to base case	**71%**	N/A	N/A	
Change relative to base case	-14.2	**-63.95%**	**+0.50%**	
O1: Location 1-5				
Winter Maximum period	13.1	74.00%	5.6%	92
Typical Summer period	2.5	8.20%	5.3%	
Annual	7.8	41.08%	5.49%	
% RSC relative to base case	**61%**	N/A	N/A	
Change relative to base case	-12.2	**-55.36%**	**+0.52%**	
O1: Location 2-5				
Winter Maximum period	21.1	71.50%	5.80%	93
Typical Summer period	3.6	38.30%	7.10%	
Annual	12.4	54.87%	6.46%	
% RSC relative to base case	**38%**	N/A	N/A	
Change relative to base case	-7.7	**-41.57%**	**+0.82%**	
O1: Location 2-4				
Winter Maximum period	22.7	92.50%	5.50%	66
Typical Summer period	11.4	80.70%	5.10%	
Annual	17.0	86.60%	5.30%	
% RSC relative to base case	**15%**	N/A	N/A	
Change relative to base case	-3.0	**-9.85%**	**+0.52%**	
O1: Location 3-4				
Winter Maximum period	24.2	92.60%	5.70%	39
Typical Summer period	11.4	78.30%	5.70%	
Annual	17.8	85.46%	5.70%	
% RSC relative to base case	**11%**	N/A	N/A	
Change relative to base case	-2.2	**-10.98%**	**+0.72%**	
O1: Location 4-5				
Winter Maximum period	20.3	94.50%	4.80%	141
Typical Summer period	14.2	90.90%	5.40%	
Annual	17.2	92.71%	5.11%	
% RSC relative to base case	**14%**	N/A	N/A	
Change relative to base case	-2.8	**-3.73%**	**+0.13%**	
O1: Location 6-13 Congested line				
Winter Maximum period	24.9	95.70%	5.3%	155
Typical Summer period	13.3	93.70%	5.0%	
Annual	19.1	94.65%	5.12%	
% RSC relative to base case	**5%**	N/A	N/A	
Change relative to base case	-0.9	**-1.79%**	**+0.14%**	
O1: Location 7-8 Congested line				
Winter Maximum period	25.3	96.60%	5.00%	117
Typical Summer period	13.7	96.00%	4.70%	
Annual	19.5	96.29%	4.86%	
% RSC relative to base case	**3%**	N/A	N/A	
Change relative to base case	-0.6	**-0.16%**	**-0.12%**	

4.7.3 IEEE 30 bus system case with UPFC

A similar analysis has been carried out on the IEEE 30 bus system. All generation cost coefficients are equal and set to $C_{gi}^{+} = 20$ \$/MWh and $C_{gi}^{-} = 10$ \$/MWh All lines are simulated with a single UPFC at all four possible orientations, for the 30 bus system there are 37 transmission lines and four transformers, that equals 41 potential locations for the UPFC, making 164 locations. Appendix IV details of IEEE 30 bus systems setup, similar to that shown for the IEEE 14 bus system in Chapter 3. Table 4-13 shows the first 20 transmission lines and transformers and lists each UPFC location, the % RSC is compared to the IEEE 30 bus base case system, line numbers 21-41 inclusive show no significant RSC ≤ 1% and RSCs greater than 10% are highlighted in bold.

Figures 4.19 and 4.20 shows system cost profiles of the 30 bus system with UPFC Orientation 1 during Typical Summer and Winter Maximum respectively. Locations 1-2, 1-3, 2-4 and 3-4 are shown in 19(a) and 20(a) and locations 2-4, 4-6 and 6-7 in 19(b) and 20(b).

Table 4-13: IEEE 30 bus system, all UPFC orientations and corresponding % RSC.

Line no.	Line *i-j*	Annual % Reduction in System Cost w.r.t. base case			
		O1	O2	O3	O4
1	1-2 Congested	70%	73%	73%	72%
2	1-3	75%	29%	76%	60%
3	2-4	10%	14%	11%	10%
4	3-4	52%	63%	72%	71%
5	2-5	2%	3%	2%	2%
6	2-6 Congested	14%	19%	21%	15%
7	4-6	16%	9%	21%	17%
8	5-7	1%	2%	2%	0%
9	6-7	10%	% Increase	0%	1%
10	6-8 Congested	0%	0%	0%	0%
11	6-9 Transformer	1%	1%	2%	1%
12	6-10 Transformer	1%	1%	2%	1%
13	9-11	0%	1%	0%	0%
14	9-10	1%	2%	1%	1%
15	4-12 Transformer	3%	1%	5%	1%
16	12-13	0%	% Increase	0%	% Increase
17	12-14	0%	0%	0%	0%
18	12-15 Congested	1%	1%	1%	1%
19	12-16	1%	1%	1%	1%
20	14-15	0%	1%	0%	1%
21 - 41	Includes buses 16 to 30	≤1%	≤1%	≤1%	≤1%

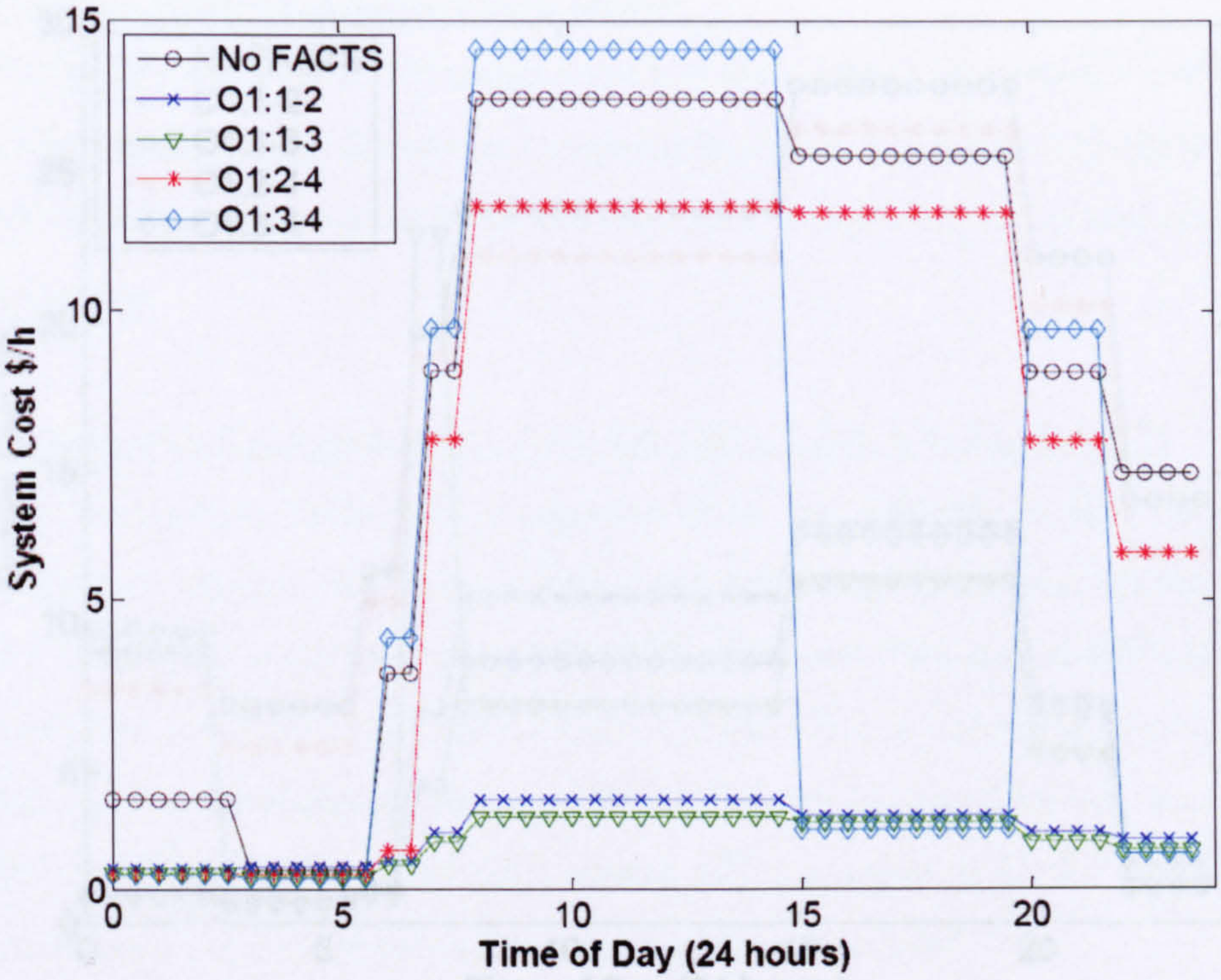

Figure 4.19(a)

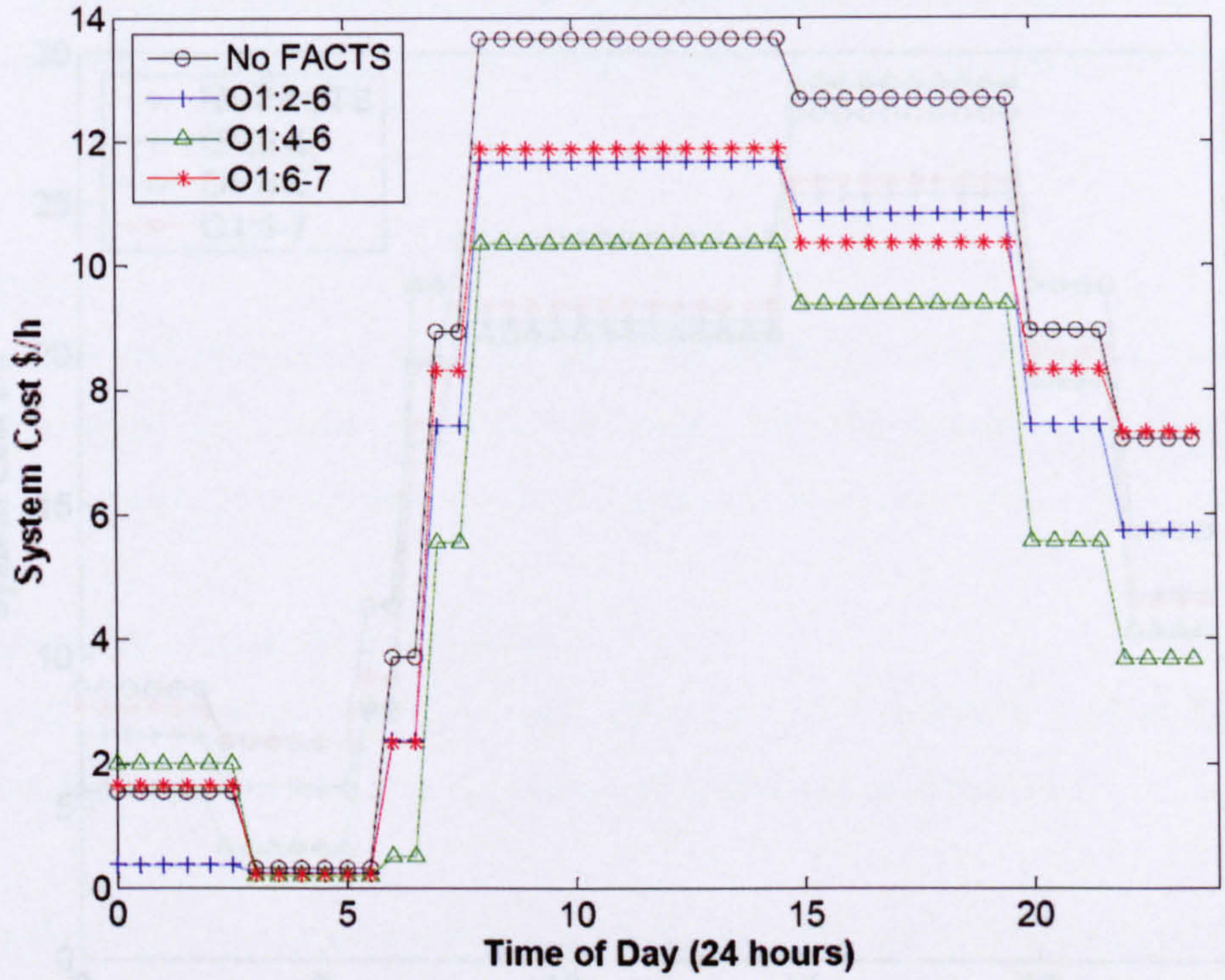

Figure 4.19(b)

Figure 4.19: IEEE 30 bus system UPFC Orientation 1, Typical Summer system cost profile at: (a) locations 1-2, 1-3, 2-4 and 3-4, (b) locations 2-6, 4-6 and 6-7 (half hour time intervals).

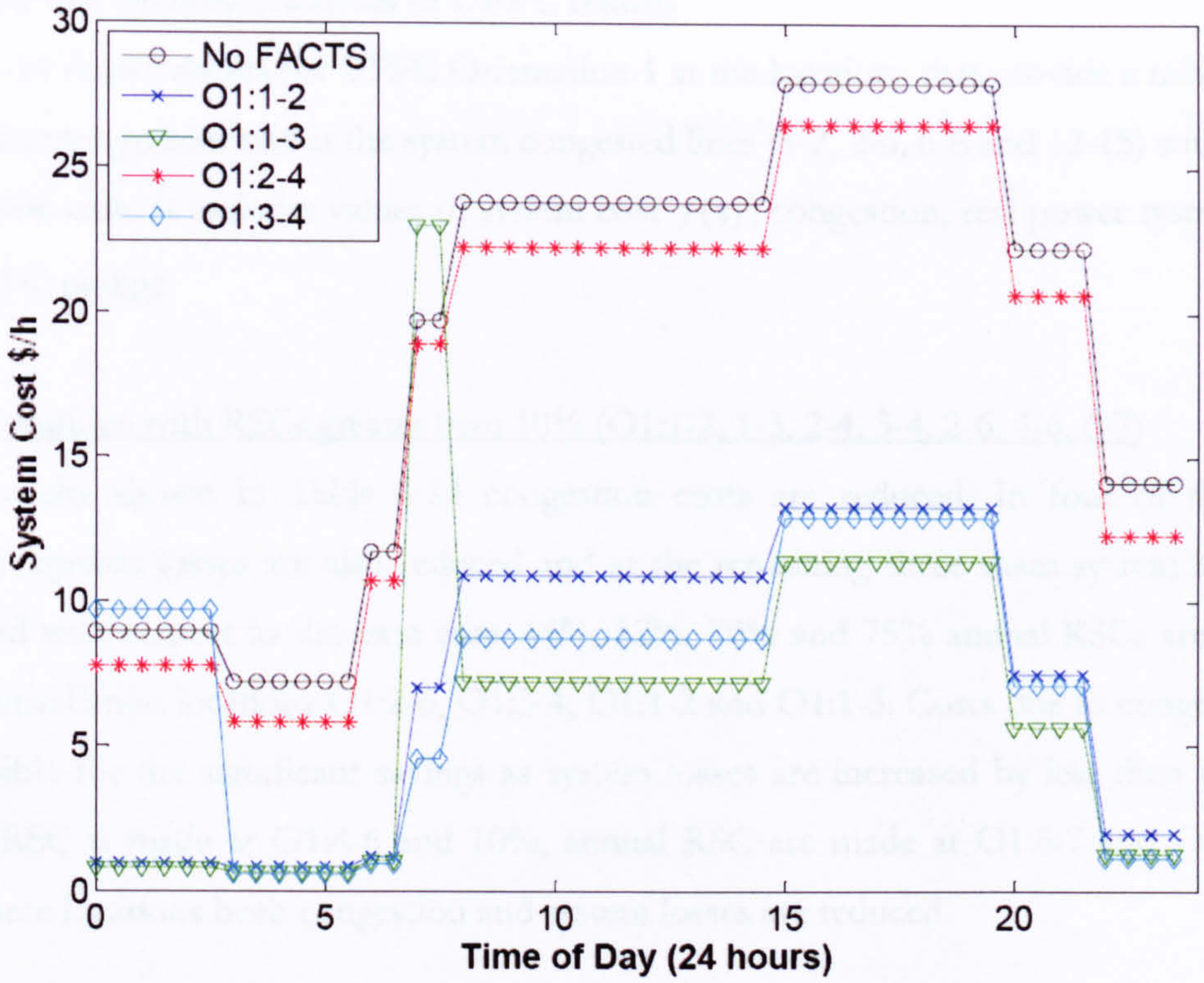

Figure 4.20(a)

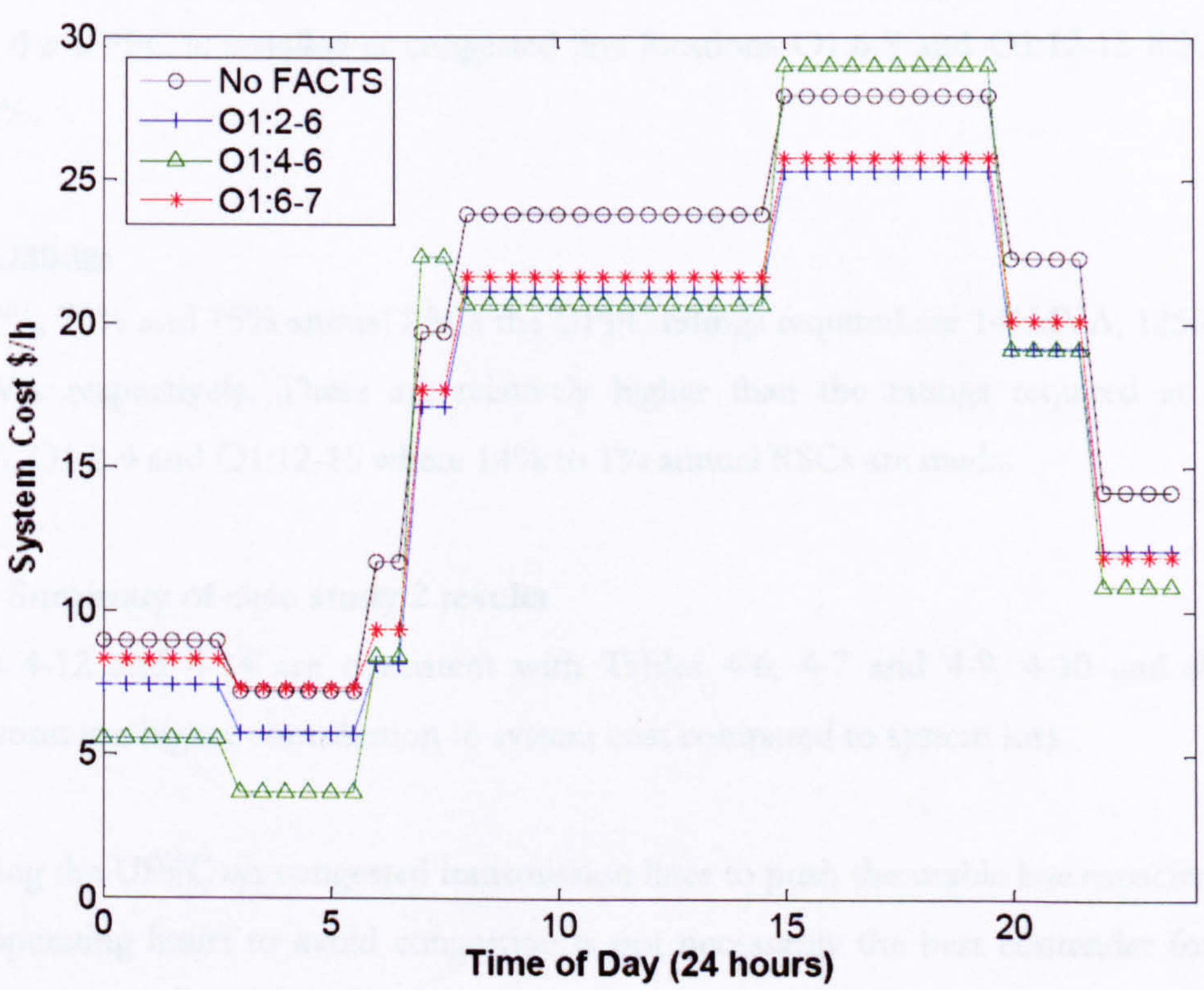

Figure 4.20(b)

Figure 4.20: IEEE 30 bus system UPFC Orientation 1, Winter Maximum system cost profile at: (a) locations 1-2, 1-3, 2-4 and 3-4, (b) locations 2-6, 4-6 and 6-7 (half hour time intervals).

IEEE 30 bus system: Analysis of UPFC results

Table 4-14 shows results for UPFC Orientation 1 at the locations that provide a minimum of 10% reduction in cost and at the system congested lines (1-2, 2-6, 6-8 and 12-15) with respect to the base case. It includes values of system cost $f(x)$, congestion, real power system losses and UPFC ratings.

UPFC locations with RSCs greater than 10% (O1:1-2, 1-3, 2-4, 3-4, 2-6, 4-6, 6-7)

In all results shown in Table 4-14 congestion costs are reduced. In four of the seven locations system losses are also reduced and at the remaining three cases system losses are increased with respect to the base case. 14%, 52%, 70% and 75% annual RSCs are made at UPFC installation locations O1:2-6, O1:3-4, O1:1-2 and O1:1-3. Costs due to congestion are responsible for the significant savings as system losses are increased by less than 1%. 17% annual RSC is made at O1:4-6 and 10%, annual RSC are made at O1:6-7 and O1:2-4. At these three locations both congestion and system losses are reduced.

UPFC locations at congested lines and with RSC of less than 10% (O1:6-8, 12-15)

When the UPFC is installed at congested line locations O1:6-8 and O1:12-15 RSC are less than 2%.

UPFC ratings

For 52%, 70% and 75% annual RSCs the UPFC ratings required are 141MVA, 125MVA and 169MVA respectively. These are relatively higher than the ratings required at locations O1:2-6, O1:2-4 and O1:12-15 where 14% to 1% annual RSCs are made.

4.7.4 Summary of case study 2 results

Tables 4-12 and 4-14 are consistent with Tables 4-6, 4-7 and 4-9, 4-10 and show that congestion is a higher contribution to system cost compared to system loss.

Installing the UPFC on congested transmission lines to push the usable line capacity closer to their operating limits to avoid congestion is not necessarily the best contender for FACTS controller installation, similarly to the conclusions in [De Oliveira et al. (2000)]. This was only successful for O1:1-2 on both the 14 and 30 bus systems.

Table 4-14: IEEE 30 bus system, summary of UPFC Orientation 1 results.

Base case	System cost $f(x)$ ($/h)	% of $f(x)$ due to congestion	% System loss	UPFC rating MVA
Winter Maximum period	19.1	96.6%	3.6%	N/A
Typical Summer period	8.7	79.5%	3.8%	
Annual	13.9	88.07%	3.74%	
O1: Location 1-2 Congested line				
Winter Maximum period	7.3	54.0%	4.8%	125
Typical Summer period	1.0	0.0%	4.4%	
Annual	4.2	27.02%	4.60%	
% RSC relative to base case	**70%**	N/A	N/A	
Change relative to base case	9.8	**-61.10%**	**+0.86%**	
O1: Location 1-3				
Winter Maximum period	6.3	47.68%	4.80%	169
Typical Summer period	0.8	0.00%	4.20%	
Annual	3.6	23.84%	4.50%	
% RSC relative to base case	**75%**	N/A	N/A	
Change relative to base case	10.4	**-64.23%**	**+0.76%**	
O1: Location 2-4				
Winter Maximum period	17.7	96.56%	3.59%	49
Typical Summer period	7.4	67.81%	3.68%	
Annual	12.6	82.19%	3.64%	
% RSC relative to base case	**10%**	N/A	N/A	
Change relative to base case	1.4	**-5.89%**	**-0.11%**	
O1: Location 3-4				
Winter Maximum period	7.4	59.73%	4.44%	141
Typical Summer period	5.9	39.78%	4.37%	
Annual	6.7	49.76%	4.41%	
% RSC relative to base case	**52%**	N/A	N/A	
Change relative to base case	**7.2**	**-38.32%**	**+0.67%**	
O1: Location 2-6 Congested line				
Winter Maximum period	16.73121	94.13%	3.96%	44
Typical Summer period	7.25	67.24%	4.08%	
Annual	11.99	80.69%	4.02%	
% RSC relative to base case	**14%**	N/A	N/A	
Change relative to base case	1.9	**-7.39%**	**+0.28%**	
O1: Location 4-6				
Winter Maximum period	17.0	93.21%	0.00%	117
Typical Summer period	6.3	69.44%	0.43%	
Annual	11.6	81.33%	0.22%	
% RSC relative to base case	**17%**	N/A	N/A	
Change relative to base case	**2.3**	**-6.75%**	**-3.53%**	
O1: Location 6-7				
Winter Maximum period	17.4	96.34%	< 0.01%	106
Typical Summer period	7.6	74.27%	< 0.01%	
Annual	12.5	85.31%	< 0.01%	
% RSC relative to base case	**10%**	N/A	N/A	
Change relative to base case	1.4	**-2.77%**	**-3.74%**	

Table 4-14 continued overleaf.

Table 4-14 continued: IEEE 30 bus system, summary of UPFC Orientation 1 results.

Base case	System cost $f(x)$ ($/h)	% of $f(x)$ due to congestion	% System loss	UPFC rating MVA
O 1: Location 6-8 Congested line				
Winter Maximum period	19.1	96.41%	< 0.01%	110
Typical Summer period	8.7	76.12%	< 0.01%	
Annual	13.9	86.27%	< 0.01%	
% RSC relative to base case	**1%**	N/A	N/A	
Change relative to base case	0.1	**-1.81%**	**-3.74%**	
O1: Location 12-15 Congested line				
Winter Maximum period	19.0	96.06%	< 0.01%	76
Typical Summer period	8.7	77.61%	< 0.01%	
Annual	13.9	86.84%	< 0.01%	
% RSC relative to base case	**1%**	N/A	N/A	
Change relative to base case	0.1	**-1.23%**	**-3.74%**	

4.8 Conclusions

Results from the IEEE 14 bus system show that both the STATCOM and UPFC can substantially improve the annual RSC due to congestion if located correctly. For the STATCOM there are five out of the possible 44 locations, with a maximum of 61% RSC at M:1-2 but for the UPFC there are five or six from each orientation that achieve RSC of over 10%.

Results from the IEEE 30 bus system also show that both the STATCOM and UPFC can substantially improve the annual RSC if located correctly. For the STATCOM there are only four out of a possible 110 locations giving a RSC greater than 10%, with a maximum of 70% RSC at M:1-2. For the UPFC there are five to seven locations within each orientation that are able to provide 10% to 75% RSCs.

A one-by-one method to find the optimal location of both the STATCOM and UPFC has been used in this chapter. The next chapter investigates methods of sensitivity analysis to reduce the number of simulations required to find the optimal locations identified so far.

Results shown indicate that FACTS controller ratings are not directly proportional to the % RSCs; the cost minimisation and rating are both dependent upon the location. The decision to utilise a FACTS controller is not only dependent upon its performance but it can be in conflict with the financial constraints. One of the most important of these is the installation cost, which amongst other things is directly dependent upon the rating of the controller. In Chapter 6 the conflict between minimisation of congestion and controller rating cost problem is investigated.

Chapter 5

Sensitivity based three-step method for locating FACTS controllers

5.1 Introduction

Although the technology required for the fast switching action for the STATCOM and UPFC has been available for approximately two decades, they are still considered high priced equipment [Schauder et al. (1998) and Mehraban et al. (1998)]. Therefore, finding the appropriate site for installation to provide maximum system benefits is key to maximizing the assets of these controllers. Chapter 4 presented results from daily and annual congestion cost savings for the STATCOM and UPFC using the IEEE 14 and 30 bus systems. However, for real electricity transmission networks, the size of the network, number of buses and number of lines are far greater than that of these small test systems. The simple trial and error method applied in Chapters 3 and 4 may not be efficient for large scale system analysis. Therefore, it is desirable to develop a method for finding the optimal locations for FACTS controller installations, which is suitable for large scale power systems.

This chapter is organised as follows; a literature review of sensitivity-based indicators, methods applied to seek optimal FACTS controller locations and the type of controllers applied is discussed in Section 5.2. Section 5.3 presents the aims of this chapter. The theory and derivation of the proposed sensitivity indicators are shown in Section 5.4; first for the shunt branch and then for the series branch. Section 5.5 describes the sensitivity-based three-step method for application in large scale systems as an extension of the general two-step method presented in Chapter 3. Numerical results are then presented in Section 5.6. In Section 5.7, Scenario 1 tests the ability of sensitivity to indicate the individual locations and in Section 5.8, Scenario 2 tests the ability of averaged area sensitivity to identify the best area to install FACTS controllers. Finally in Section 5.9 conclusions are drawn.

5.2 Overview of literature

There are many publications relating sensitivity techniques to OPF algorithms and sensitivity-based methods with and without the consideration of FACTS controllers. This section aims

to give the reader an overview of techniques most similar to the work carried out in this chapter.

5.2.1 Sensitivity-based indicator methods

Sensitivity-based indicator methods have been commonly used within the steady state time domain to find the best location to improve the overall performance of a power system for some time [Gribik et al. (1990) and Belati et al. (2005)]. These include analyses on both d.c. load flow models [Lie and Deng (1997)] and more commonly on a.c. load flow models, where the latter is more complex as it takes into account the influence of reactive power on the economic dispatch or OPF model of interest.

Frequently, sensitivity indicators are first order differentials or elements in the Jacobian matrix. There has been a variety of applications of sensitivity analysis. For example, Zhang et al. (2006a) finds the optimal location of a SSSC and TCSC (Thyristor Controlled Series Compensator) for maximising the transfer capacity over interconnected transmission systems while in Ramirez and Oliva (2005) an inspection of voltage level, line losses and generation costs is made with respect to the system's objective function. In addition in An et al. (2007) inspection of voltage magnitude, phase shift angle and shunt susceptance for deciphering appropriate FACTS controller settings is achieved, while reactive power capability is measured in Yao and Strbac (1999).

In publications by Singh and David [(2001), (2001a) and (2000)], a measure called the real power flow performance index (PI) is used as a guide to sensitivity. PI is a measure of severity of the line overloads, which is compared to the parameters of the TCSC and the TCPAR (Thyristor-Controlled Phase Angle Regulator) controllers to give sensitivity values in a predominant pool based market. The same PI measure has also been applied to find best location for UPFCs but without clear reference to the market structure [Verma et al. (2001)].

Loss sensitivity approaches were used in Verma et al. (2001), Singh and David (2000) and Preedavichit and Srivastava (1998) to find the optimal FACTS location. An et al. (2007) and Gotham and Heydt (1998) suggest that it is best to install FACTS controllers onto heavily congested lines to provide enhanced economic operation. However, neither of these trails of thought is appropriate or correct for the minimisation of congestion in a pure bilateral market; as seen in Chapter 4 the system loss is insignificant relative to the cost incurred by

system congestion and heavily congested lines are not always the best locations for the reduction of congestion costs.

The research group headed by T. W. Gedra developed first and second order sensitivity factors for various uses such as; locating phase shifters [Gedra and Damrongkulkamjorn (1995) and (1994)] and estimation of control settings for UPFC by inserting on all transmission lines [An and Gedra (2002)]. Furthermore, a second order sensitivity approach, is able to provide an estimate on the incremental value of the phase shifter (or other resource) without resolving the complete OPF algorithm lines [An and Gedra (2002)].

5.2.2 Methods used to find optimal FACTS controller locations

The one-by-one approach presented in Chapter 3 has also been applied by Singh and David (2001a) for series FACTS controllers, the TCSC and TCPAR.

Genetic algorithms (GA) have also been a popular choice for tackling the location and number of FACTS controllers to install on a system [Gerbex et al. (2001), Ramirez and Oliva (2005) and Ippolito et al. (2006)]. GA methods are usually more computationally extensive, for example in Cai et al. (2004) the algorithm simultaneously attempts to solve congestion by finding the optimal type of FACTS controller as well as the location and rating of the device.

Nevertheless, the OPF based method by linear and non-linear programming is by far the most common approach. Use of sensitivity-based methods fall into four broad categories of objective function;

(i) minimising active power system losses only, as presented in Verma et al. (2001) and Preedavichit and Srivastava (1998);

(ii) minimisation of generation costs, (linear and quadratic representation);

(iii) minimising congestion costs as presented in this work, and in Singh and David (2001) for both pool and bilateral market models and;

(iv) minimising FACTS installation cost together with active power system losses [Lie and Deng (1997), Fang and Ngan (1999) and Singh and David (2001a)].

5.2.3 FACTS controller types applied

Shunt, series and combination (shunt-series) FACTS controller steady state models have been applied to various objective functions including; minimisation of generation costs, minimisation of system real power losses, minimisation of FACTS controller installation costs, and minimisation of congestion costs measured on the pool and bilateral markets in the literature.

The series FACTS controllers, TCSC and the TCPAR are used in Singh and David (2000) and Farahani et al. (2006) within bilateral market models with the aim of providing congestion management and reducing load curtailments respectively. However, the sensitivity indices relate to real power transmission line losses, total system losses, and not congestion. A similar sensitivity measure is used with the UPFC in Verma et al. (2001) in which an additional sensitivity factor associated with the level of congestion on each line is measured. As seen from previous results, the reduction in system congestion bears a greater proportion of total system cost therefore it is logical to seek a sensitivity factor that reflects this finding.

An alternative steady state UPFC model is applied in An et al. (2007) where sensitivity values are derived from the change in generation cost with respect to UPFC variables to provide a first scan of the potential controller locations. The method applied is similar to that applied in this chapter as first-order sensitivity is measured by running the OPF problem a single time only. In addition for the alleviation of congestion on bilateral based markets in Singh and David (2001), sensitivity is not directly linked to congestion cost performance. The work presented in this chapter aims to fill that gap.

5.3 Aims

Computationally, the general two-step method implemented in Chapter 3, Section 3.7 can become time consuming for real large-scale power systems with thousands of buses. To save time and expenditure, a sensitivity-based analysis is applied to reduce the number of potential buses and transmission lines for testing FACTS controller performance for alleviating congestion.

The following list highlights the features of the sensitivity-based method applied to the STATCOM and UPFC presented in this chapter:

- Sensitivity is related to the control variable of interest of the specified FACTS controller;

- The steady state FACTS models applied are widely accepted for static time domain studies;
- Sensitivity analysis aims to substantially reduce the number of potential locations for controller installation;
- In the averaged area approach, sensitivity analysis aims to indicate the most suitable area for FACTS controller installation.

5.4 Theory and sensitivity derivations

Sensitivity analysis applied to nonlinear models is more complex than that applied to linear models [Saltelli (2005)]. In this case, the equations defining the transmission system, transmission line, transformers and FACTS controllers are nonlinear.

The derivation for both the shunt and series branch sensitivity measures start with the Lagrange equation for transmission line between buses i and j, first stated in Chapter 2, equation (2.25). The Lagrange equation encapsulates the objective function $f(x)$ equation (2.1) and all equality and inequality constraints of the OPF problem; the inclusion of a FACTS controller introduces additional variables and constraints. The Lagrange equation in (5.1) includes system buses i and j without reference to the additional FACTS controller variables.

$$\begin{aligned} L(x) = f(x) &- \mu\left(\ln(sl_i) + \ln(sl_j)\right) - \mu\left(\ln(su_i) + \ln(su_j)\right) \\ &- \lambda_{p_i}\Delta P_i(x) - \lambda_{q_i}\Delta Q_i(x) - \lambda_{p_j}\Delta P_j(x) - \lambda_{q_j}\Delta Q_j(x) \\ &- \pi l_i\left(h_i - sl_i - h_i^{\min}\right) - \pi u_i\left(h_i - su_i - h_i^{\max}\right) \\ &- \pi l_j\left(h_j - sl_j - h_j^{\min}\right) - \pi u_j\left(h_j - su_j - h_j^{\max}\right) \end{aligned} \tag{5.1}$$

where the objective function is equal to,

$$f(x) = \sum_{i}^{N_g}\left[C_{g_i}^{+} P_{g_i}^{+}\right] + \sum_{i}^{N_g}\left[C_{g_i}^{-} P_{g_i}^{-}\right]$$

and all other variables are as defined in Chapter 2. Derivations of power mismatch equations for the shunt, series and combination controllers can be found in Appendix IV.

5.4.1 Shunt bus sensitivity

The shunt controller or STATCOM is able to inject or absorb reactive power at the local bus. The control variable of interest is the reactive power Q_i at the local bus *i*. The derivative of the Lagrange equation (5.1) with respect to Q_i is,

$$\frac{\partial L(x)}{\partial Q_i} = -\lambda_{q_i} \frac{\partial \Delta Q_i(x)}{\partial Q_i} \tag{5.2}$$

where, $\Delta Q_i(x)$ is the reactive power mismatch given by,

$$\Delta Q_i(x) = Q_{g_i} - Q_{d_i} - Q_i \tag{5.3}$$

Thus $$\frac{\partial \Delta Q_i(x)}{\partial Q_i} = -1 \tag{5.4}$$

and $$\frac{\partial L(x)}{\partial Q_i} = \lambda_{q_i} \tag{5.5}$$

The control variable Q_i is an implicit variable of the objective function $f(x)$ through the Lagrange equation (5.1). Sensitivity S_i^{sh} is represented as in Zhang et al. (2007),

$$\frac{\partial L(x)}{\partial Q_i} = S_i^{sh} \tag{5.6}$$

$$S_i^{sh} = \lambda_{q_i} \tag{5.7}$$

5.4.2 Series branch sensitivity

The UPFC is a combination controller, composed of a shunt and a series branch. The series component of the UPFC is able to influence the transmission line impedance, variable X_{ij} between buses *i* and *j*. The lumped π-equivalent circuit shown in Figure 5.1 is assumed for the model of the transmission line. Derivation of power mismatch equations for transmission lines and transformers can be found in Appendix II.

Bus and line conductance (g_{ii} and g_{ij} respectively) and susceptance (b_{ii} and b_{ij} respectively) are dependent upon the transmission line properties, resistance R_{ij}, reactance X_{ij} and shunt susceptance B_c by the following relationships,

$$g_{ii} = g_{jj} = g_{ij} = \frac{R_{ij}}{R_{ij}^2 + X_{ij}^2} \tag{5.8}$$

$$b_{ii} = b_{jj} = b_{ij} + \frac{B_c}{2} \tag{5.9}$$

$$b_{ij} = \frac{-X_{ij}}{R_{ij}^2 + X_{ij}^2} \tag{5.10}$$

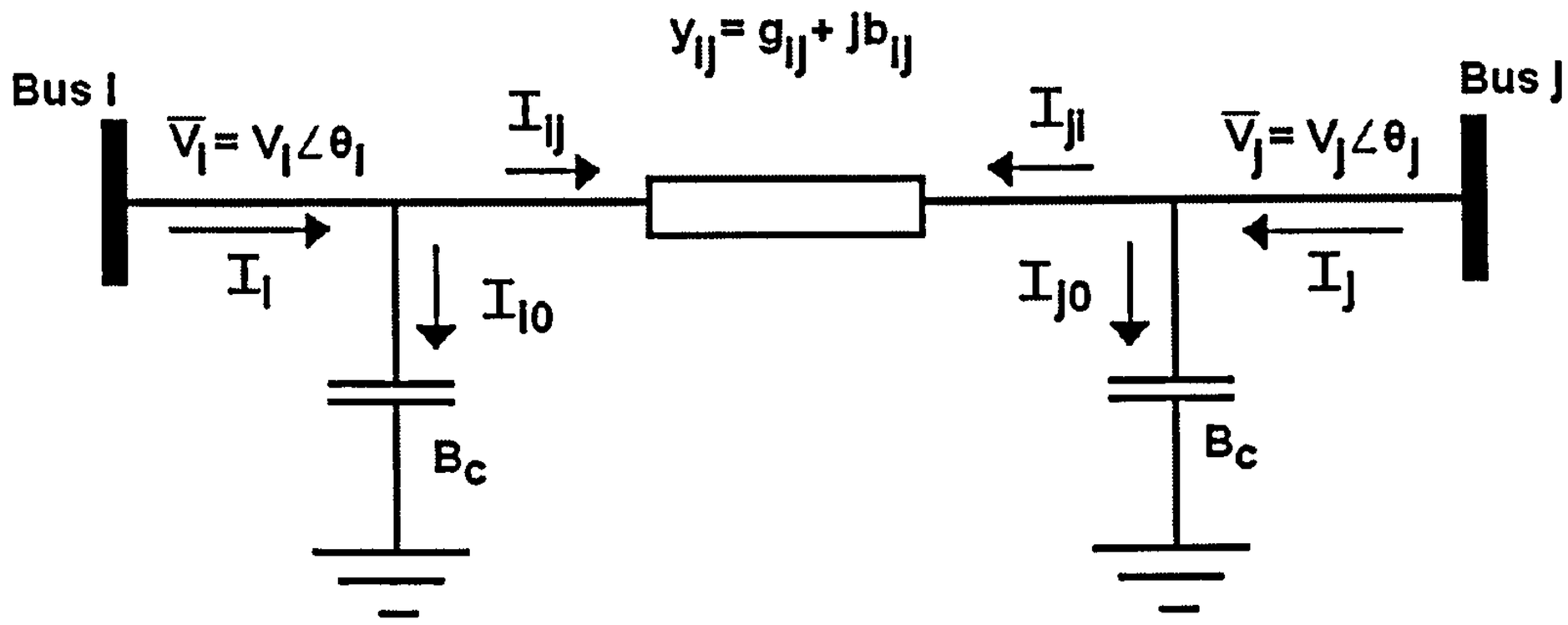

Figure 5.1: Transmission line π-equivalent circuit model.

The transmission line reactance X_{ij} is an implicit variable of the objective function $f(x)$ through the Lagrange equation (5.1). Sensitivity with respect to X_{ij} is calculated by,

$$\frac{\partial L(x)}{\partial X_{ij}} = S_{ij} \tag{5.11}$$

where,

$$\begin{aligned} S_{ij} = &-\lambda_{p_i}\left\{\left[-V_i^2 + V_iV_j\cos\left(\theta_i-\theta_j\right)\right]\frac{\partial g_{ii}}{\partial X_{ij}} + \left[V_iV_j\sin\left(\theta_i-\theta_j\right)\right]\frac{\partial b_{ij}}{\partial X_{ij}}\right\} \\ &-\lambda_{q_i}\left\{\left[V_iV_j\sin\left(\theta_i-\theta_j\right)\right]\frac{\partial g_{ij}}{\partial X_{ij}} + \left[V_i^2 - V_iV_j\cos\left(\theta_i-\theta_j\right)\right]\frac{\partial b_{ii}}{\partial X_{ij}}\right\} \\ &-\lambda_{p_j}\left\{\left[-V_j^2 + V_iV_j\cos\left(\theta_j-\theta_i\right)\right]\frac{\partial g_{jj}}{\partial X_{ij}} + \left[V_iV_j\sin\left(\theta_j-\theta_i\right)\right]\frac{\partial b_{ij}}{\partial X_{ij}}\right\} \\ &-\lambda_{q_j}\left\{\left[V_iV_j\sin\left(\theta_j-\theta_i\right)\right]\frac{\partial g_{ij}}{\partial X_{ij}} + \left[V_i^2 - V_iV_j\cos\left(\theta_j-\theta_i\right)\right]\frac{\partial b_{jj}}{\partial X_{ij}}\right\} \end{aligned} \tag{5.12}$$

A similar sensitivity analysis for the SSSC can be found in Zhang et al. (2006a). Derivation of both sensitivity equations can be found in Appendix VII.

5.5 Sensitivity based three-step method

A general sensitivity based three-step method for finding the optimal location and rating of a FACTS controller is presented. Step 1 is similar to that presented in the two-step method (Chapter 3, Section 3.7). Step 2 utilises sensitivity analysis. The input variable of interest is dependent upon the type of FACTS controller applied to the system. The output from Step 2 will identify the most sensitive locations and congested lines. At Step 3, the simulation is run with the controller at the locations with the largest sensitivity values only.

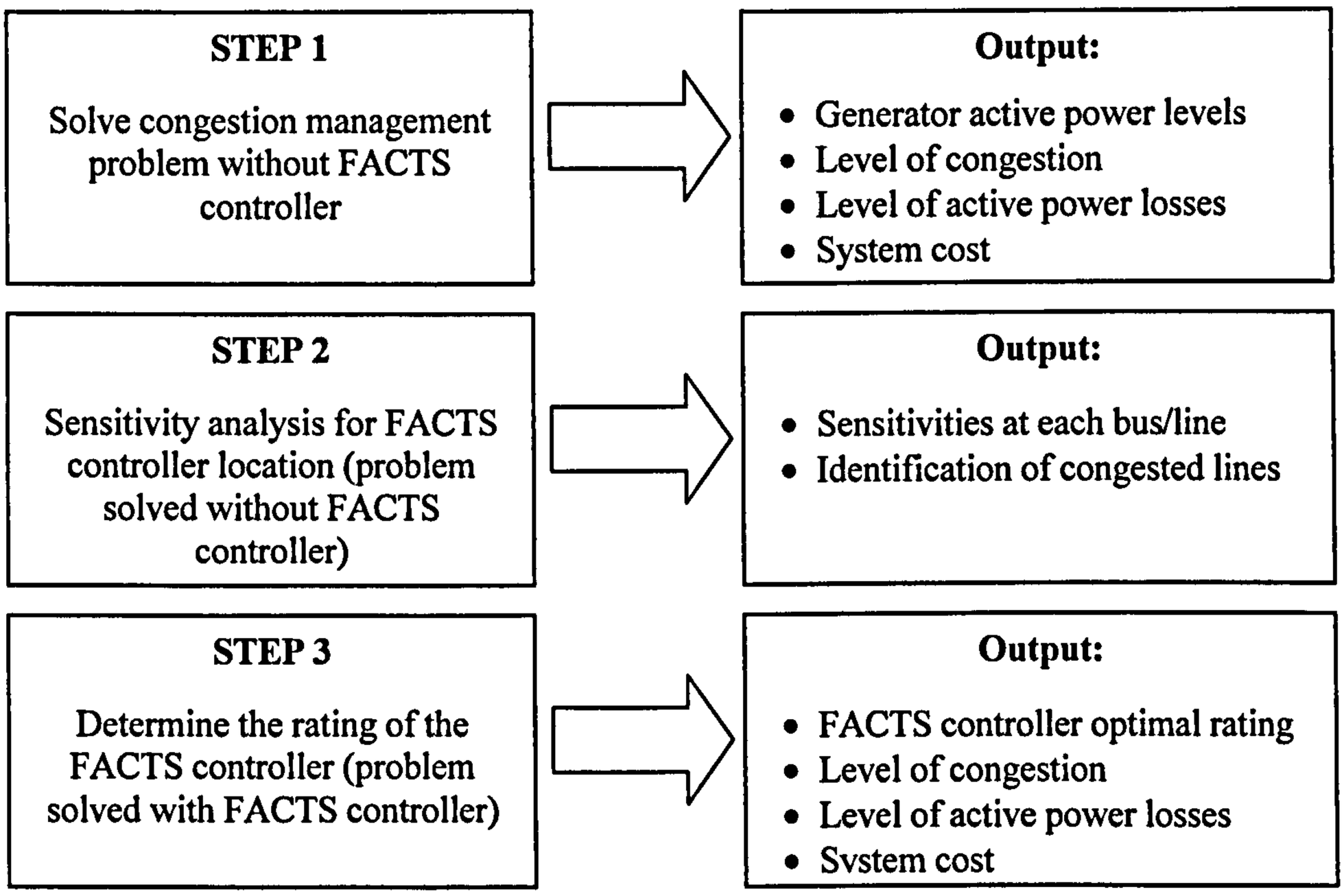

Figure 5.2: Overview of sensitivity-based three-step method.

5.6 Numerical results

The IEEE 14 bus and 30 bus system models used in previous chapters combined with STATCOM and UPFC models provide the numerical results presented in this chapter. The sensitivity method has been tested using two scenarios,

- Scenario 1: ability of sensitivity factor to identify individual buses or lines as the optimal location;
- Scenario 2: ability of averaged area sensitivity factor to identify the optimal area.

Under each scenario the shunt bus sensitivity results are assessed against the STATCOM simulation results and then the series line sensitivity results are assessed against the UPFC simulation results at specified locations. The three key points of interest are,

1. the rank of the sensitivity measures;
2. the performance of the controller at specified locations;
3. the correlation between the locations identified by sensitivity analysis and the performance of the controller at those locations.

For Scenario 2, the IEEE 14 and 30 bus systems are divided into four and five areas respectively.

5.7 Scenario 1: Sensitivity for identifying individual buses or lines for FACTS controller optimal location

First the shunt bus sensitivity, S_i^{sh} and the results gathered from simulating the STATCOM installed at the ends of the transmission lines on the 14 and the 30 bus systems are presented. Secondly, the series line sensitivity, S_{ij} and results gathered using the UPFC on the same systems are shown.

5.7.1 Shunt bus sensitivity for STATCOM

As shunt bus sensitivity is measured at bus *i*, results in this section only refer to a STATCOM installed at the ends of the transmission lines.

Tables 5-1 and 5-2 are to be read in two sections with Column 1 common to both. Columns 2 to 4 show the bus numbers with the highest sensitivities as gathered from Step 2 of the general sensitivity based three-step method. Columns 5 to 10 show the locations (and positions) and corresponding % reduction in system cost (RSC), results from Step 3 of the proposed method. Table 5-1 and 5-2 show results for the STATCOM locations that achieve the greatest % RSC for the 14 bus and the 30 bus systems respectively.

<u>Sensitivity measures (results from Step 2)</u>

14 bus system results show the same three bus numbers are consistently the most sensitive, 12, 13 and 14. 30 bus results show two out of three bus numbers are consistently the most sensitive, 3 and 26.

Performance of STATCOM (results from Step 3)

For both systems, during system operation at 16 % $MW_k^{FullRange}$, i.e. no congestion, the STATCOM is able to provide significant RSCs, the most varied seen from 30 bus system results, ranging from 16% to 78% RSC. As the level of system congestion increases, the STATCOM is less able to reduce system costs.

Table 5-1: IEEE 14 bus system, top three shunt sensitivity and % RSC when STATCOM installed at I:*i-j* and J:*i-j*.

1	2	3	4	5	6	7	8	9	10
% $MW_k^{FullRange}$	Bus numbers with highest sensitivity			Locations *i-j* and corresponding % reduction in system cost					
	1st	2nd	3rd	1st		2nd		3rd	
16%	13	12	14	J:2-5	50%	J:2-4	38%	I:5-6	21%
55%	13	14	12	J:2-5	19%	J:2-4	10%	I:5-6	8%
94%	13	14	12	J:2-5	13%	J:2-4	10%	I:5-6	5%

Table 5-2: IEEE 30 bus system, top three shunt sensitivity and % RSC when STATCOM installed at I:*i-j* and J:*i-j*.

1	2	3	4	5	6	7	8	9	10
% $MW_k^{FullRange}$	Bus numbers with highest sensitivity			Locations *i-j* and corresponding % reductions in system cost					
	1st	2nd	3rd	1st		2nd		3rd	
16%	3	26	30	J:2-4	78%	I:2-6	77%	I:4-12	16%
55%	26	3	24	J:2-4	10%	I:2-6	15%	N/A	< 1%
94%	26	3	23	I:2-6	10%	J:2-4	5%	I:4-12	1%

Correlation between sensitivity and STATCOM performance

There is no correlation between the shunt bus sensitivity and the % RSC results for either the 14 or the 30 bus system with STATCOM, because no common bus numbers are listed. Although results from Step 2 and Step 3 individually show consistent results at the three different levels of congestion (16, 55 and 94 % $MW_k^{FullRange}$), the results show this method is not successful at detecting the optimal position for minimising congestion costs.

A possible reason for this result is the fact that STATCOMs are only able to inject and absorb Q_i at the local bus, and therefore mainly affect the local bus voltages. Congestion however is predominantly related to active power flows and in this situation, in this case the STATCOM does not appear to be effective for congestion management. The transmission line limits, together with the power flow constraints restrict the amount of Q_i that can be injected and absorbed, and therefore limit the feasible solution space; although the

STATCOM may be able to inject greater Q_i. For completeness, Appendix VII shows tables of the top three STATCOM locations using midpoint installation for each system, there is also no correlation in these results with bus sensitivity.

5.7.2 Series line sensitivity for UPFC

Table 5-3 and 5-4 show results for the UPFC locations using Orientation 1 that achieve the greatest % RSC for the 14 bus and the 30 bus systems respectively. The structure of the tables is the same as that described previously for Tables 5-1 and 5-2.

Table 5-3: IEEE 14 bus system, top three series sensitivity and % RSC using UPFC for Scenario 1.

1	2	3	4	5	6	7	8	9	10
% $MW_k^{FullRange}$	Lines with highest sensitivity			Locations and corresponding % reductions in system cost					
	1st	2nd	3rd	1st		2nd		3rd	
16%	1-2	1-5	4-5	1-5	95%	1-2	93%	3-4	50%
55%	1-2	1-5	4-5	1-5	92%	1-2	91%	2-5	74%
94%	1-2	1-5	4-5	1-5	51%	1-2	42%	4-5	14%

Table 5-4: IEEE 30 bus system, top three series sensitivity and % RSC using UPFC cost for Scenario 1.

1	2	3	4	5	6	7	8	9	10
% $MW_k^{FullRange}$	Lines with highest sensitivity			Locations and corresponding % reductions in system cost					
	1st	2nd	3rd	1st		2nd		3rd	
16%	1-2	1-3	3-4	3-4	83%	2-4	82%	1-3	81%
55%	1-2	1-3	3-4	1-3	91%	1-2	89%	4-6	24%
94%	1-2	1-3	3-4	1-3	57%	3-4	54%	1-2	52%

Sensitivity measures (results from Step 2)

Both the 14 and 30 bus systems show consistent line locations for the top three sensitivities and at all congestion levels (% $MW_k^{FullRange}$).

Performance of UPFC (results from Step 3)

Within both systems significant RSCs are made; at all locations listed and at all congestion levels, and a clear fall in % RSC is made at the highest level of congestion, 95% $MW_k^{FullRange}$. For the 14 bus system the top two locations are consistent at all congestion levels. The third highest % RSC differs and is dependent upon the level of congestion. For the 30 bus system there is more variability in the locations that provide the highest % RSC.

Line 1-3 is common for all load levels, lines 1-2, 3-4 are common for two load levels and; lines 2-4, 4-6 occur once at different load levels.

Correlation between sensitivity and UPFC performance

14 bus system results at 16% and 55% $MW_k^{FullRange}$ levels list two out of three locations (1-2 and 1-5) high in sensitivity and ability to produce significant % RSC. At 95% $MW_k^{FullRange}$ all three locations with highest sensitivity can also produce significant % RSC.

30 bus system results at 16% and 55% $MW_k^{FullRange}$ levels list two out of three top sensitivity locations (1-3 and 3-4, and 1-2 and 1-3 respectively) that also provide the highest % RSC. At 94% $MW_k^{FullRange}$ the locations identified by sensitivity are also the locations that provide the greatest % RSC.

The order of sensitivity and locations that provide % RSC are not exactly matched. However, results from both systems show that the series sensitivity method presented is able to give some indication to the lines that provide good % RSCs.

Figures 5.3 show the % RSC when the UPFC is installed at all lines of the 14 bus system and Figure 5.4 for lines 1-20 of the 30 bus system at 55% and 94% $MW_k^{FullRange}$. The top three or four locations at each % $MW_k^{FullRange}$ level can be easily identified by the bar graphs, after which the remaining line locations produce similar levels of reduction, mostly under 10% for the 14 bus system and under 5% for the 30 bus system. Note that in a minority of cases there is a negative reduction in system cost.

In general, the location of generators on both systems is within the lower bus numbers or left hand half of the graphs. Refer to Figures 5.5 and 5.6 to identify the exact locations of generators.

The series sensitivity measured on the individual lines is unable to identify the exact location that will provide the greatest % RSC for the UPFC. However, the results have shown

successful identification of locations that do provide significant reductions in system costs. Due to this, in Scenario 2 each system is divided into distinct areas for investigation.

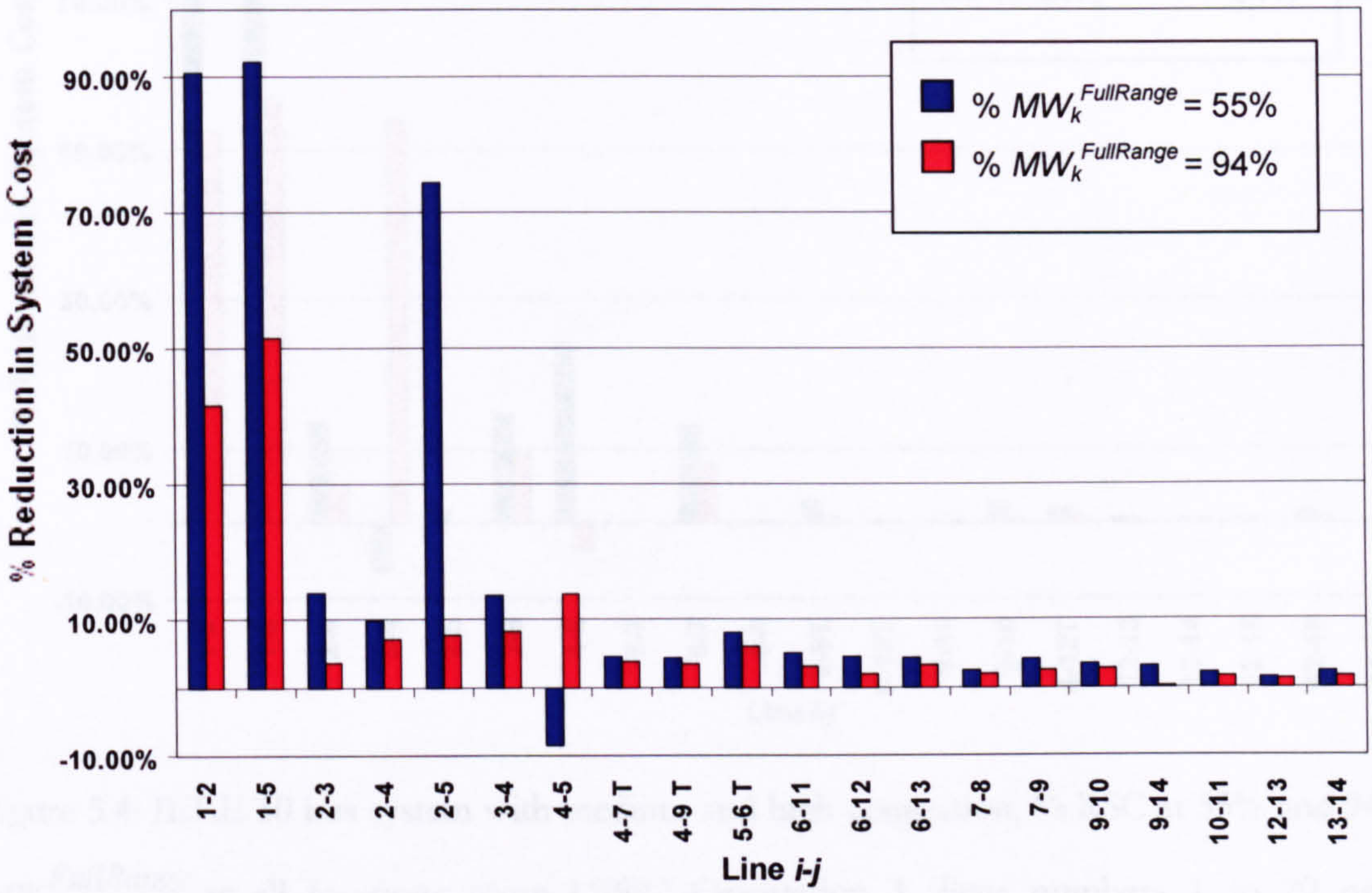

Figure 5.3: IEEE 14 bus system with medium and high congestion, % RSC at 55% and 94% $MW_k^{FullRange}$ at all locations using UPFC Orientation 1.

5.8 Scenario 2: Averaged area sensitivity analysis

Scenario 1 showed that shunt sensitivity and series sensitivity are unable to indicate the single bus or line that is able to give the greatest % RSC. However, series sensitivity and UPFC results showed some positive correlation. Scenario 2 employs averaged sensitivity information on distinct areas of the system. It aims to measure the ability to indicate the area with the most promising locations for UPFC installation.

The 14 bus system has been divided into four areas and the 30 bus system into five areas as detailed in Section 5.8.1. The averaged area sensitivity measurement is first applied to shunt sensitivity and STATCOM; Section 5.8.2. Secondly, series sensitivity and its investigation with UPFC results are presented; Section 5.8.3.

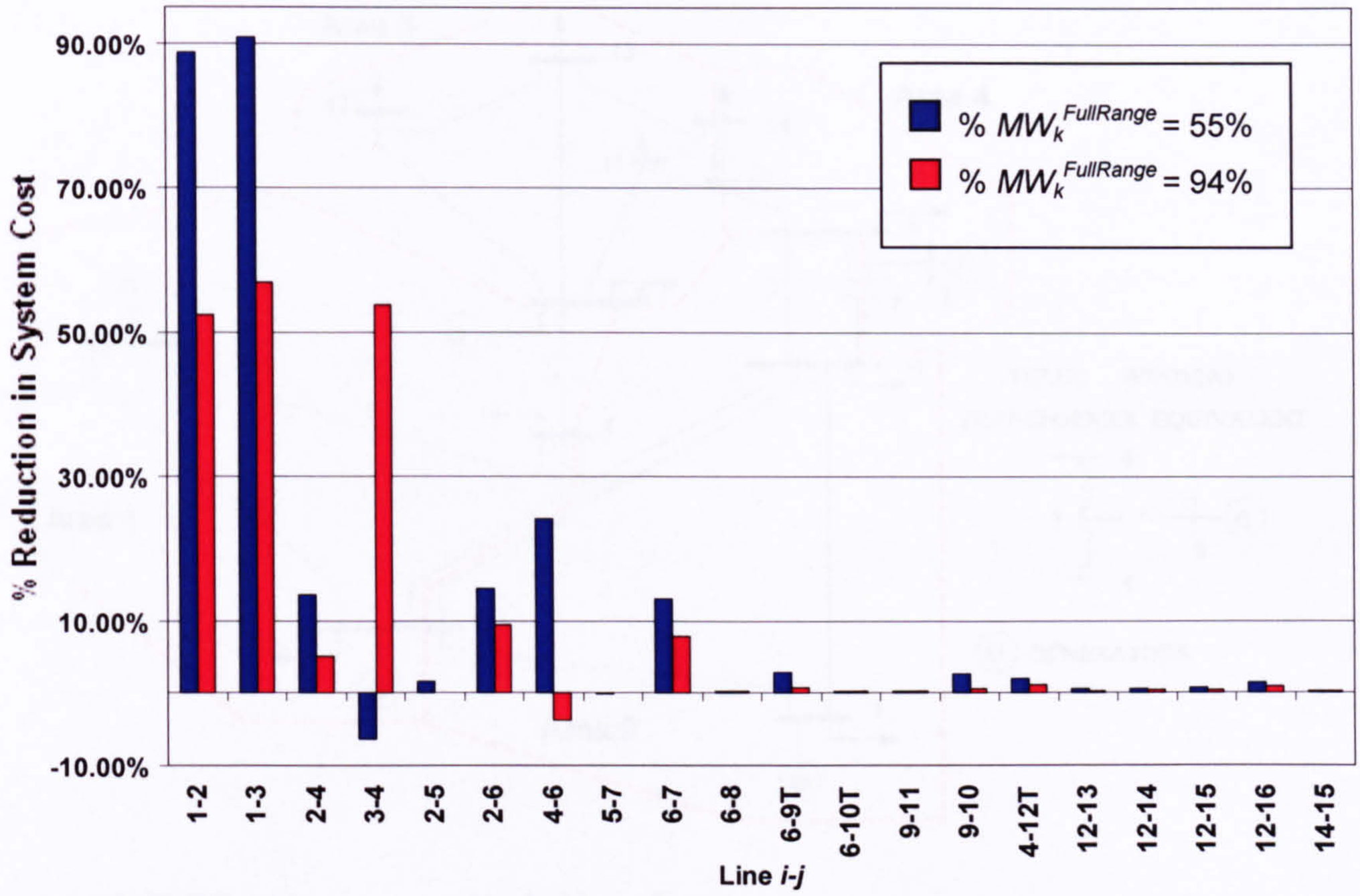

Figure 5.4: IEEE 30 bus system with medium and high congestion, % RSC at 55% and 94% $MW_k^{FullRange}$ at all locations using UPFC Orientation 1, lines numbers 1 to 20 only.

5.8.1 Area division

The IEEE 14 and 30 bus systems have been divided into four and five separate areas respectively. The number of buses in each area of the 14 bus system ranges from four to six and for the 30 bus system from five to nine, where some buses are included in more than one area. Figures 5.5 and 5.6 show the division lines marking the boundaries of each area. Tables 5-5 and 5-6 list the lines and transformers within each area on each of the systems respectively, where T next to the latter bus number denotes a transformer.

Table 5-5: 14 bus system transmission lines and transformers within the four areas.

Area no. β	**Lines and transformers *i-j***	**No. of lines**	**No. of transformers**
1	1-2, 1-5, 2-5, 5-6T	3	1
2	2-3, 2-4, 3-4, 4-5, 4-7T, 4-9T	4	2
3	6-11, 6-12, 6-13, 10-11, 12-13, 13-14	6	0
4	7-8, 7-9, 9-10, 9-14	4	0
Total number of lines and transformers = 20		17	3

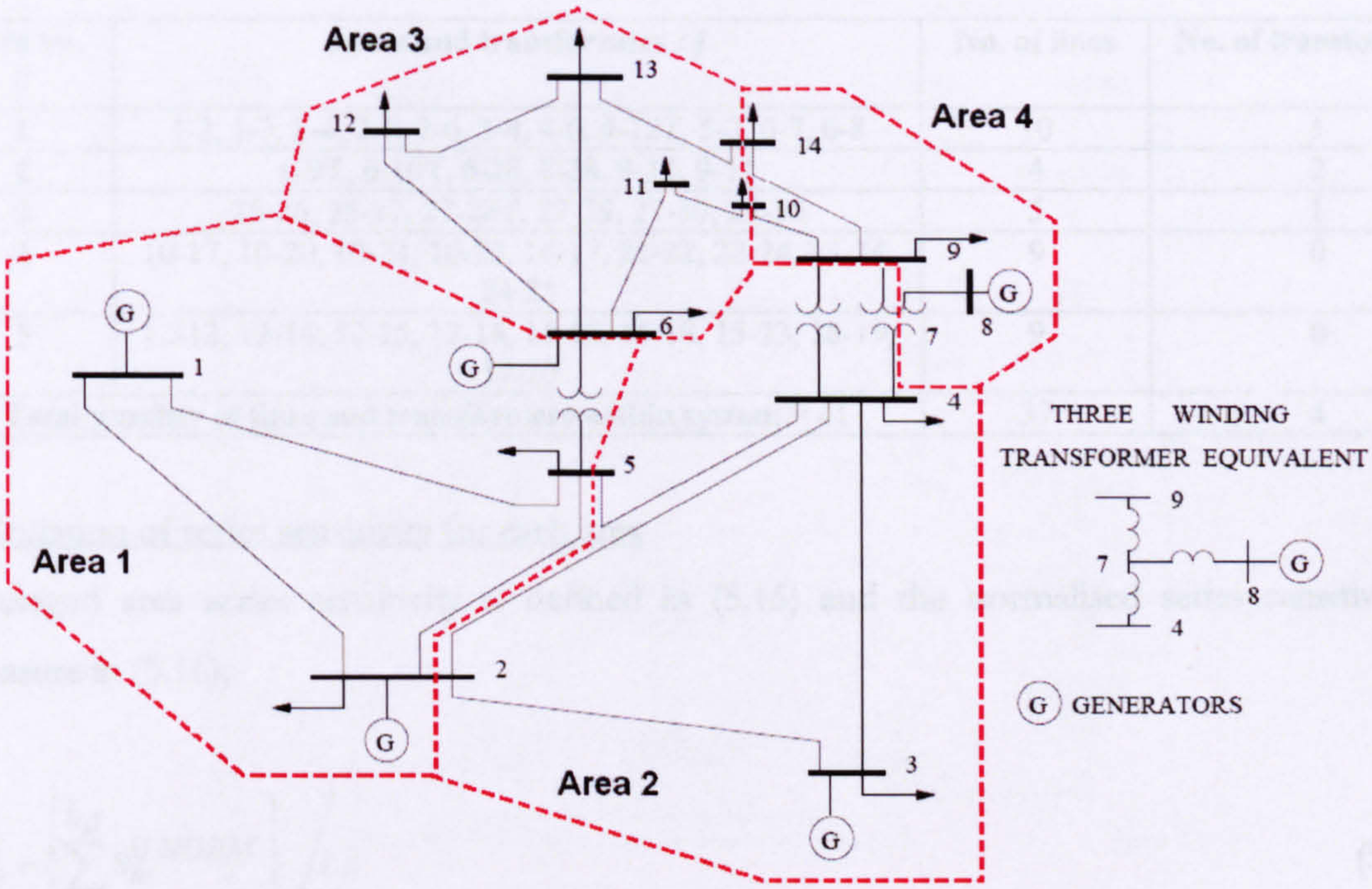

Figure 5.5: IEEE 14 bus system divided into four areas.

Calculation of shunt sensitivity for each area

Averaged area shunt sensitivity is defined in (5.13) and the normalised shunt sensitivity measure in (5.14),

$$A_{\beta}^{sh} = \left\{ \sum_{i}^{N_{\beta}-N_{g\beta}} S_i^{shNORM} \right\} \Big/ N_{\beta} - N_{g_{\beta}} \tag{5.13}$$

$$S_i^{shNORM} = S_i^{sh} \Big/ S^{shMAX} \tag{5.14}$$

where,

β area number, $\beta = 1, 2, \ldots K$,

K total number of areas in system,

N_{β} total number of buses in area β,

$N_{g_{\beta}}$ total number of generator buses in area β,

S_i^{sh} shunt sensitivity at bus i,

S^{shMAX} largest system bus sensitivity value.

Table 5-6: IEEE 30 bus system transmission lines and transformers within the five areas.

Area no. β	Lines and transformers *i-j*	No. of lines	No. of transformers
1	1-2, 1-3, 2-4, 2-5, 2-6, 3-4, 4-6, 4-12T, 5-7, 6-7, 6-8	10	1
2	6-9T, 6-10T, 6-28, 8-28, 9-10, 9-11	4	2
3	25-26, 25-27, 27-28T, 27-29, 27-30, 29-30	5	1
4	10-17, 10-20, 10-21, 10-22, 16-17, 21-22, 22-24, 23-24, 24-25	9	0
5	12-13, 12-14, 12-15, 12-16, 14-15, 15-18, 15-23, 18-19, 19-20	9	0
Total number of lines and transformers within system = 41		37	4

Calculation of series sensitivity for each area

Averaged area series sensitivity is defined in (5.15) and the normalised series sensitivity measure in (5.16),

$$A_{\beta}^{ij} = \left\{ \sum_{m}^{L_\beta} S_m^{ij\,NORM} \right\} \Big/ L_\beta \tag{5.15}$$

$$S_m^{ijNORM} = S_m^{ij} \Big/ S^{ijMAX} \tag{5.16}$$

where,

β area number, $\beta = 1, 2, \ldots K$,

K total number of areas in system,

m line number, $m = 1, 2, \ldots L_\beta$,

L_β total number of lines in area β,

S_m^{ij} series sensitivity at line m,

S^{ijMAX} largest system line sensitivity value.

5.8.2 Shunt bus area sensitivity for STATCOM

Results from the previous section of this chapter show that the STATCOM is only able to produce a few significant % RSCs in comparison to the UPFC. In addition, in some cases the % RSC is negative compared to the base.

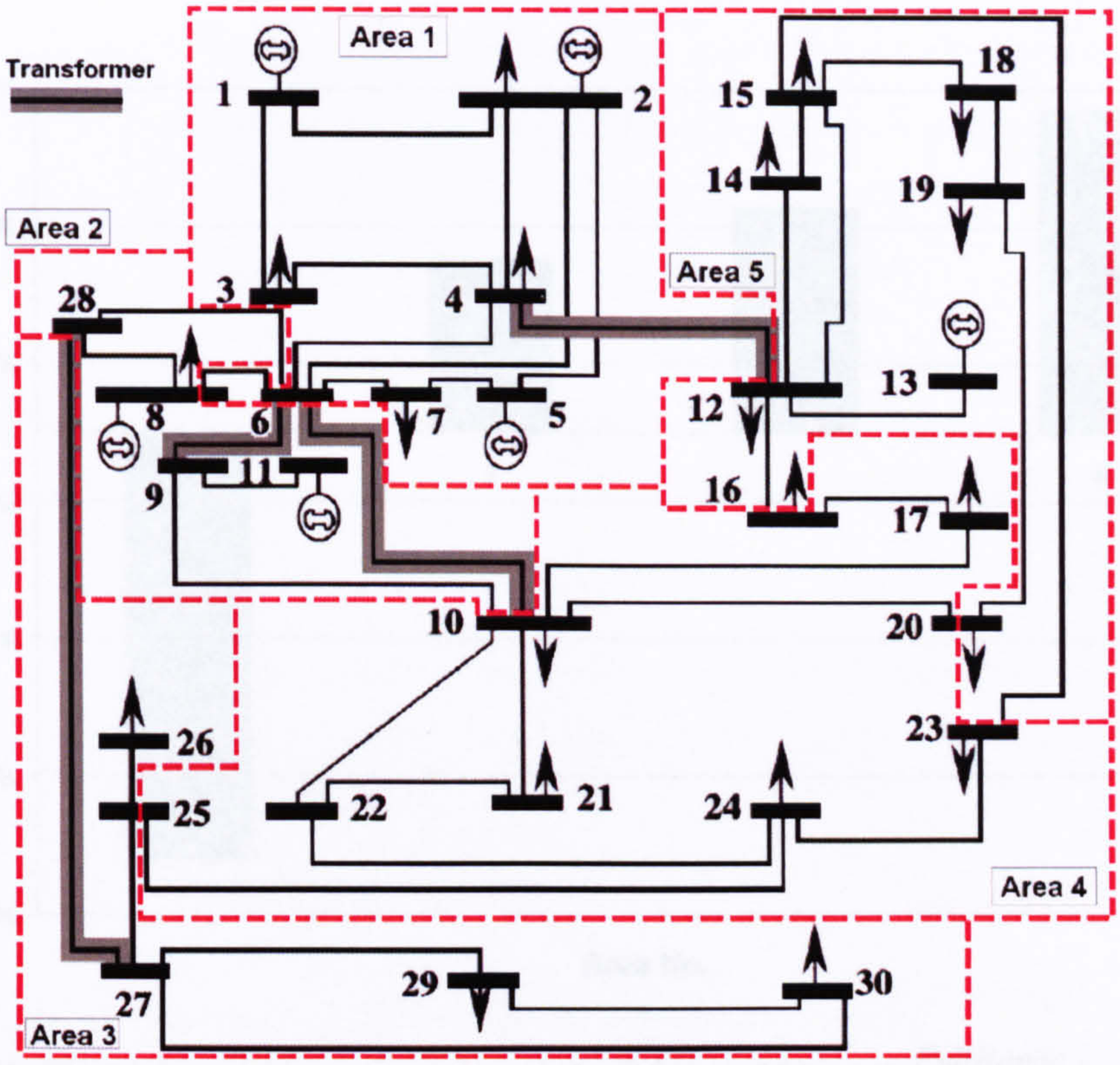

Figure 5.6: IEEE 30 bus system divided into five areas.

A. IEEE 14 bus system: Divided into 4 areas

Table 5-7 shows the rank in which the averaged area sensitivity method indicates for each area. Figure 5.7 shows the average area % RSCs.

Table 5-7: IEEE 14 bus system, shunt sensitivity at different % $MW_k^{FullRange}$.

% $MW_k^{FullRange}$	Sensitivity Ranking			
	Area 1	**Area 2**	**Area 3**	**Area 4**
16%	4th	3rd	1st	2nd
55%	4th	3rd	1st	2nd
94%	4th	3rd	1st	2nd

There is no correlation between the order of the sensitivities and averaged area % RSC. The most sensitive areas are Areas 3 and 4 respectively but the areas which provide the highest % RSC is Areas 4 then Area 3. The method has managed to reduce the number of potential areas in half. Figure 5.7 shows the % RSCs for 55 % $MW_k^{FullRange}$, a similar trend is found with 16% and 94% $MW_k^{FullRange}$. Note the very limited % RSC; all less than 2.5% in Areas 2 to 4 and negative for Area 1, approximately -3%.

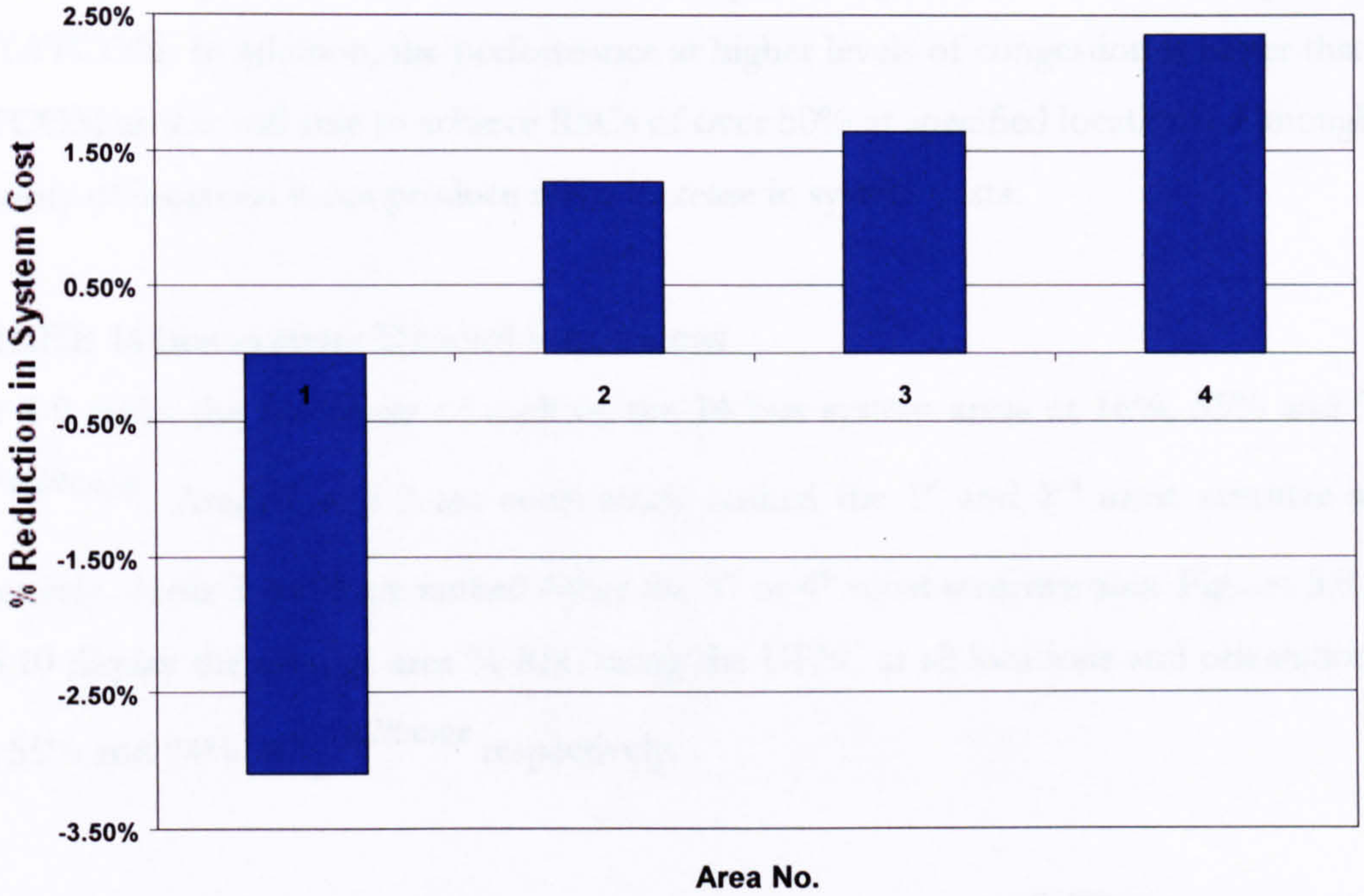

Figure 5.7: IEEE 14 bus system average area % RSC at 55% $MW_k^{FullRange}$ for STATCOM installed at ends of transmission lines, I:*i-j* and J:*i-j*, installed at all feasible locations.

B. IEEE 30 bus system: Divided into 5 areas

Table 5-8 shows the rank in which the averaged area sensitivity method indicated for each area. A similar trend has been displayed in the 14 bys system in Figure 5.7. Within the 30 bus system the STATCOM is only able to provide significant % RSC (above 10%) at a limited number of locations. In most cases the STATCOM does not manage to achieve any RSC.

Shunt bus sensitivity analysis is unable to provide accurate indication for effective STATCOM installation to minimise congestion costs. In addition, the STATCOM is able to provide some congestion relief at a very limited number of locations. The STATCOM has not provided a sufficient level of improvement to the reduction in congestion.

Table 5-8: IEEE 30 bus system, shunt sensitivity at different % $MW_k^{FullRange}$.

% $MW_k^{FullRange}$	Sensitivity Ranking				
	Area 1	**Area 2**	**Area 3**	**Area 4**	**Area 5**
16%	4th	5th	1st	2nd	3rd
55%	4th	5th	1st	2nd	3rd
94%	4th	5th	2nd	1st	3rd

5.8.3 Series bus area sensitivity for UPFC

Results from Chapter 4 show that the UPFC can produce greater % RSCs in comparison to the STATCOM. In addition, the performance at higher levels of congestion is better that the STATCOM as it is still able to achieve RSCs of over 50% at specified locations. Although, in a minority of locations it can produce some increase in system costs.

A. IEEE 14 bus system: Divided into 4 areas

Table 5-9 ranks the sensitivity of each of the 14 bus system areas at 16%, 55% and 94% $MW_k^{FullRange}$. Areas 1 and 2 are consistently ranked the 1st and 2nd most sensitive areas respectively. Areas 3 and 4 are ranked either the 3rd or 4th most sensitive area. Figures 5.8, 5.9, and 5.10 display the average area % RSC using the UPFC at all locations and orientations at 16%, 55% and 94% $MW_k^{FullRange}$ respectively.

Table 5-9: IEEE 14 bus system, series sensitivity at different % $MW_k^{FullRange}$.

% $MW_k^{FullRange}$	Sensitivity Ranking			
	Area 1	**Area 2**	**Area 3**	**Area 4**
16%	1st	2nd	4th	3rd
55%	1st	2nd	4th	3rd
94%	1st	2nd	3rd	4th

Sensitivity measures (results from Step 2)

Table 5-9 shows that Areas 1 and 2 are consistently the most sensitive. Only at 94% $MW_k^{FullRange}$ does that sensitivity of Area 3 become greater than that of Area 4.

Performance of UPFC (results from Step 3)

From Figures 5.8, 5.9 and 5.10, the greatest and second greatest % RSC take place when the UPFC is installed in Areas 1 and 2 respectively. This occurs at all four orientations of the UPFC except at 16% $MW_k^{FullRange}$, where results from Orientation 3 show that Area 2 produces on average the greatest RSC, then Area 1. Therefore, for the 14 bus system the applied sensitivity analysis method is able to indicate the optimum area to install a UPFC when considering the minimisation of system cost $f(x)$.

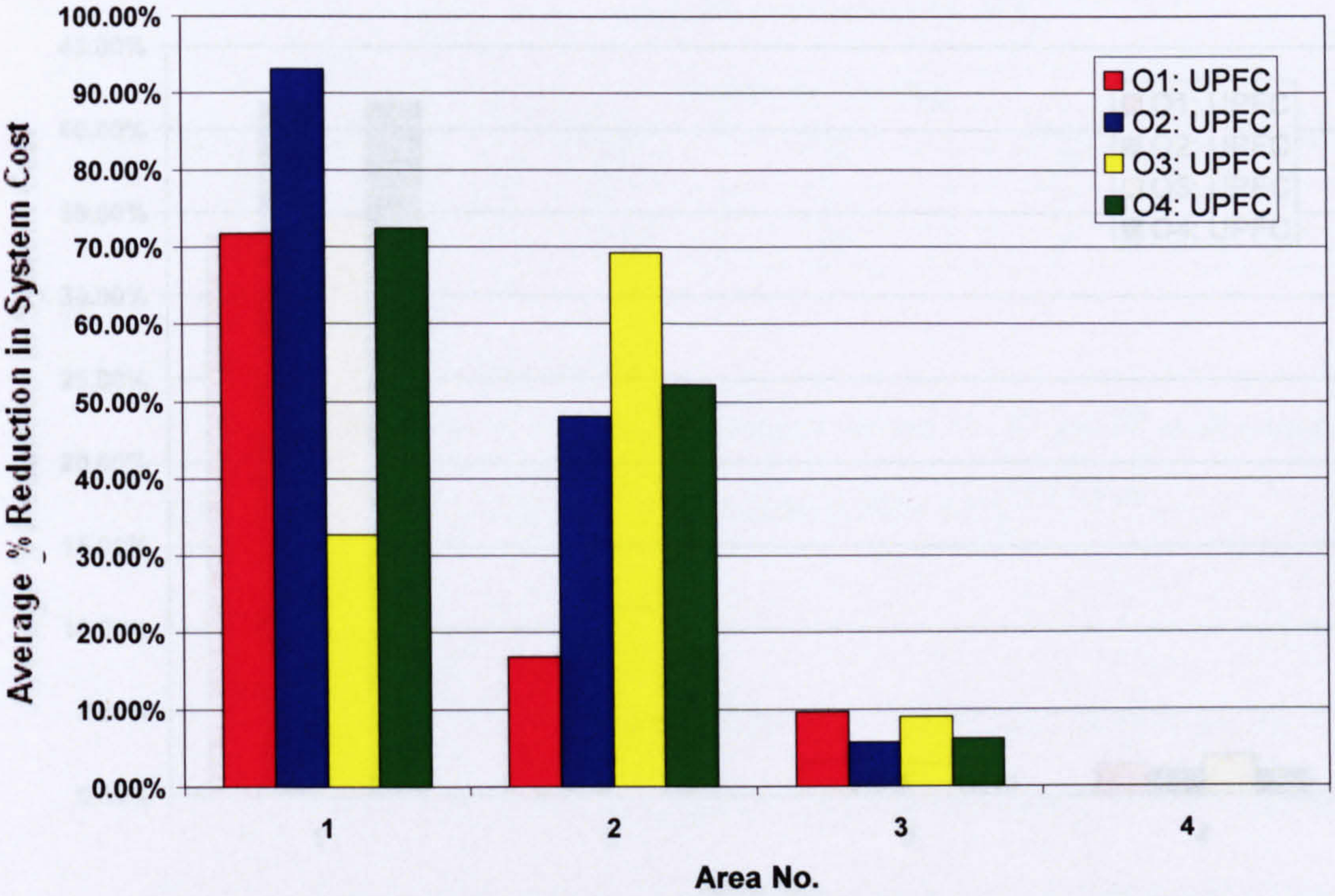

Figure 5.8: IEEE 14 bus system average area % RSC with UPFC (all orientations) at 16% $MW_k^{FullRange}$.

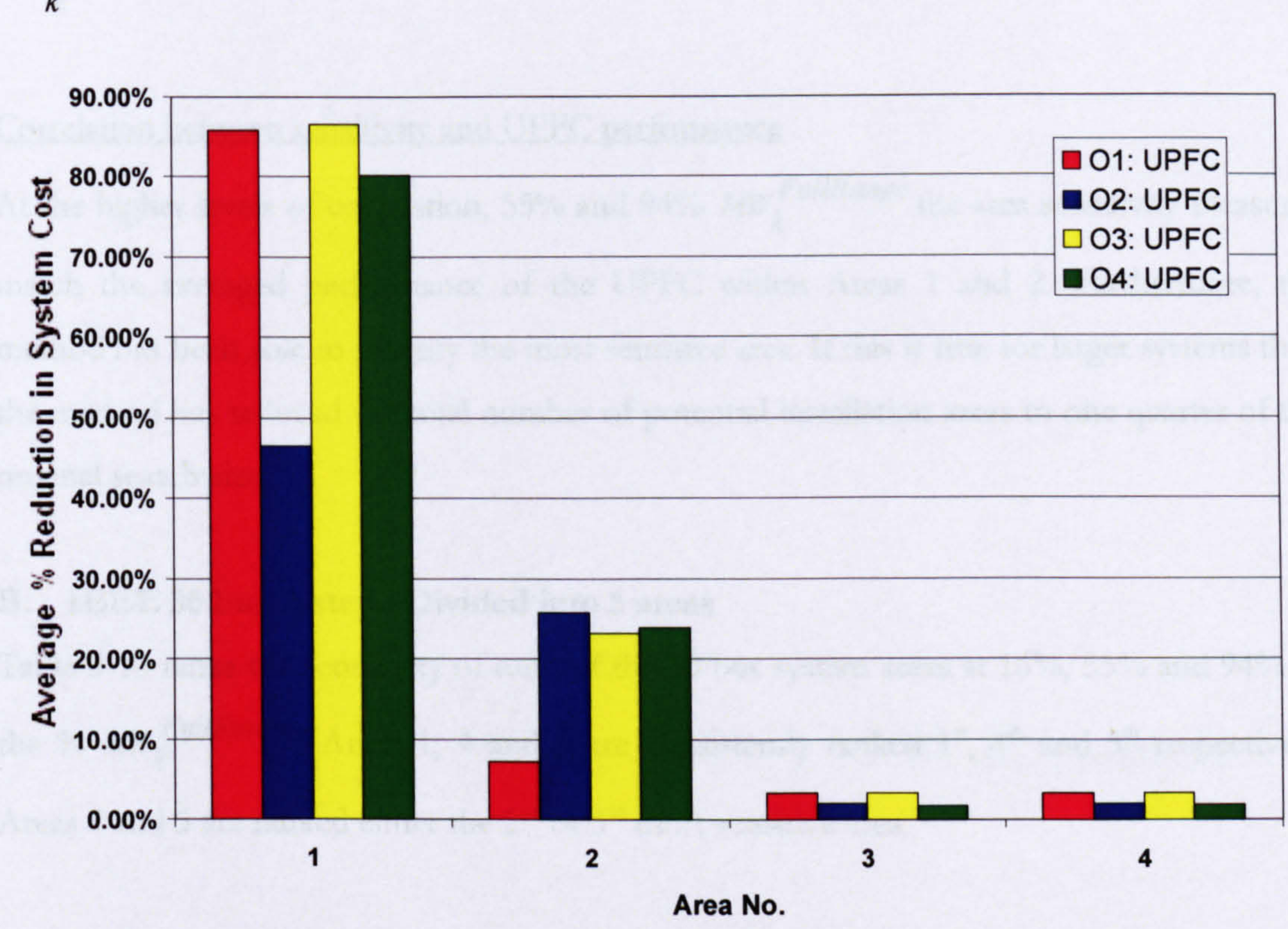

Figure 5.9: IEEE 14 bus system average area % RSC with UPFC (all orientations) at 55% $MW_k^{FullRange}$.

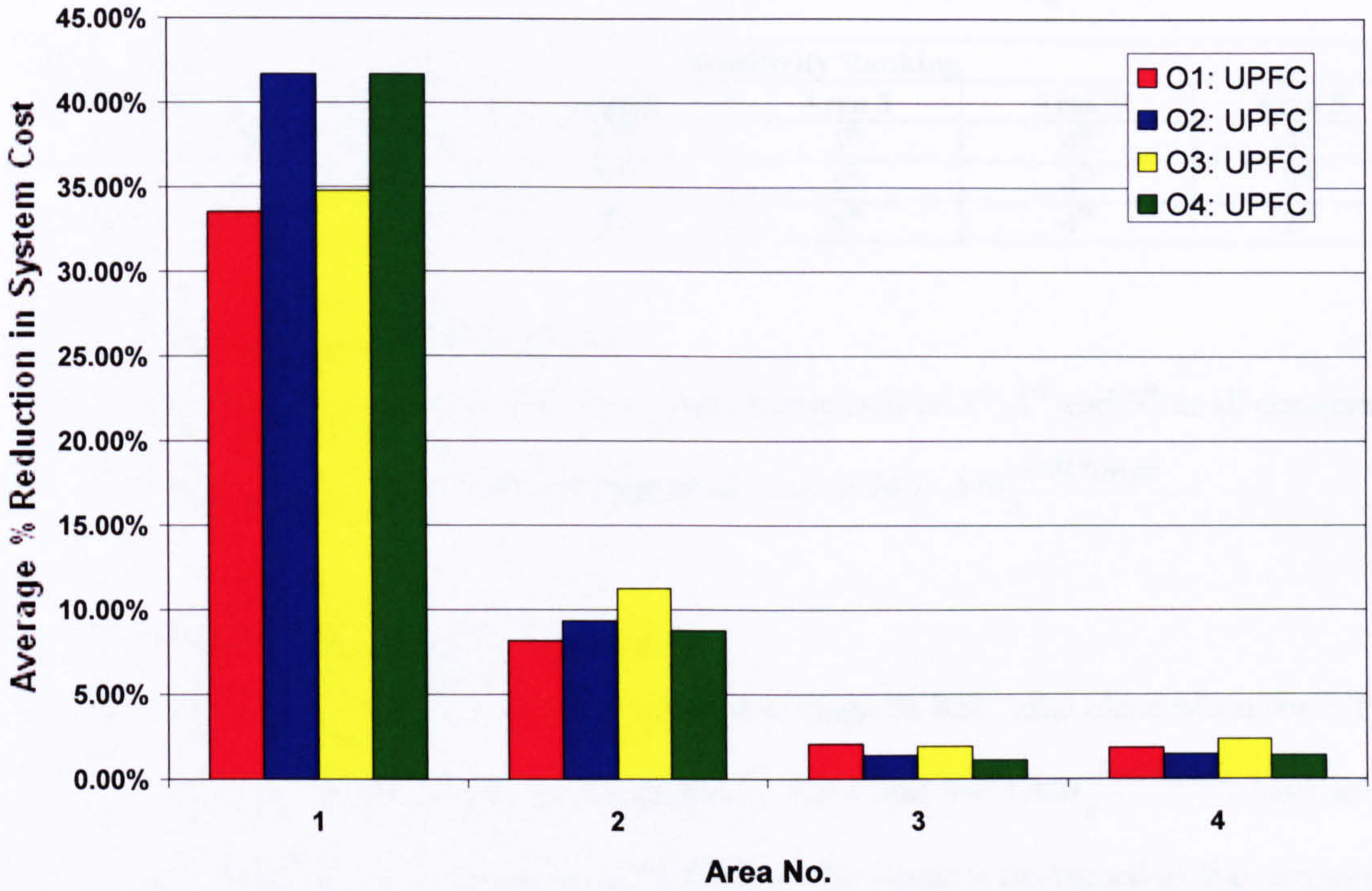

Figure 5.10: IEEE 14 bus system average area % RSC with UPFC (all orientations) at 94% $MW_k^{FullRange}$.

Correlation between sensitivity and UPFC performance

At the higher levels of congestion, 55% and 94% $MW_k^{FullRange}$ the area sensitivity measures match the averaged performance of the UPFC within Areas 1 and 2. Furthermore, the method has been able to identify the most sensitive area. If this is true for larger systems then the method has reduced the total number of potential installation areas to one quarter of the original search size.

B. IEEE 30 bus system: Divided into 5 areas

Table 5-10 ranks the sensitivity of each of the 30 bus system areas at 16%, 55% and 94% of the % $MW_k^{FullRange}$. Areas 1, 4 and 3 are consistently ranked 1st, 4th and 5th respectively. Areas 2 and 5 are ranked either the 2nd or 3rd most sensitive area.

Figures 5.11, 5.12 and 5.13 display the average area % RSC for each area using the UPFC at all locations and orientation at 16%, 55% and 94% $MW_k^{FullRange}$ respectively.

Table 5-10: IEEE 30 bus system, series sensitivity at different % $MW_k^{FullRange}$.

% $MW_k^{FullRange}$	Sensitivity Ranking				
	Area 1	**Area 2**	**Area 3**	**Area 4**	**Area 5**
16%	1st	2nd	5th	4th	3rd
55%	1st	2nd	5th	4th	3rd
94%	1st	3rd	5th	4th	2nd

Sensitivity measures (results from Step 2)

Table 5-10 shows that Areas 1, 4 and 3 are consistently ranked 1st, 4th and 5th at all congestion levels, whereas in Areas 2 and 5 interchange their rank at 94% $MW_k^{FullRange}$.

Performance of UPFC (results from Step 3)

Figures 5.11, 5.12 and 5.13 show that the greatest average % RSC take place when the UPFC is installed in Area 1. This distinction is clearer at 55% and 94% $MW_k^{FullRange}$ load levels. Note there is a decrease in the quantity of % RSC on the y-axis is decreased as the congestion increases in from Figure 5.11 to 5.13. In addition, there is still a small number of cases where the reduction has a negative value.

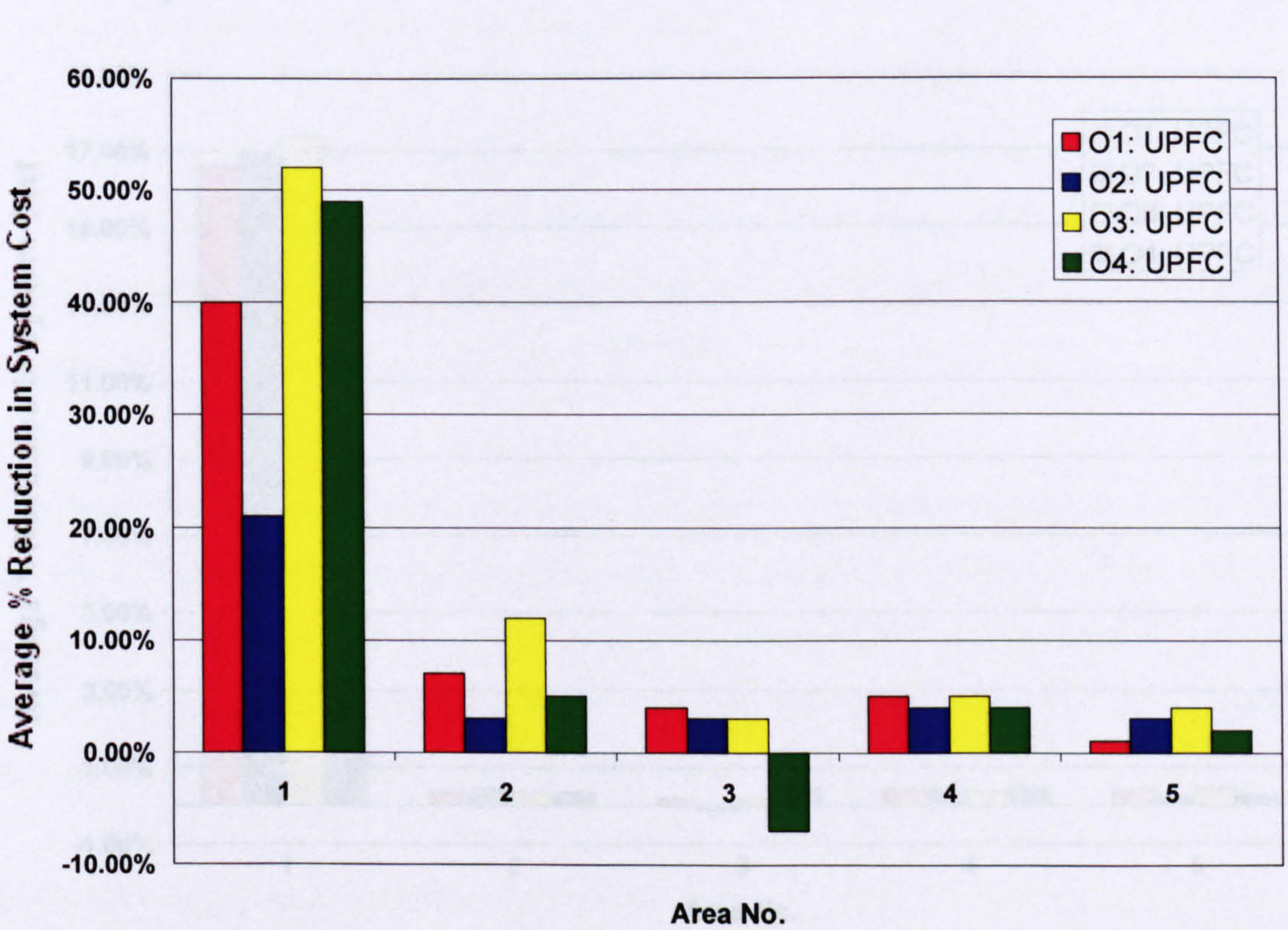

Figure 5.11: IEEE 30 bus system average area % RSC with UPFC installed (all orientations) at 16 % $MW_k^{FullRange}$.

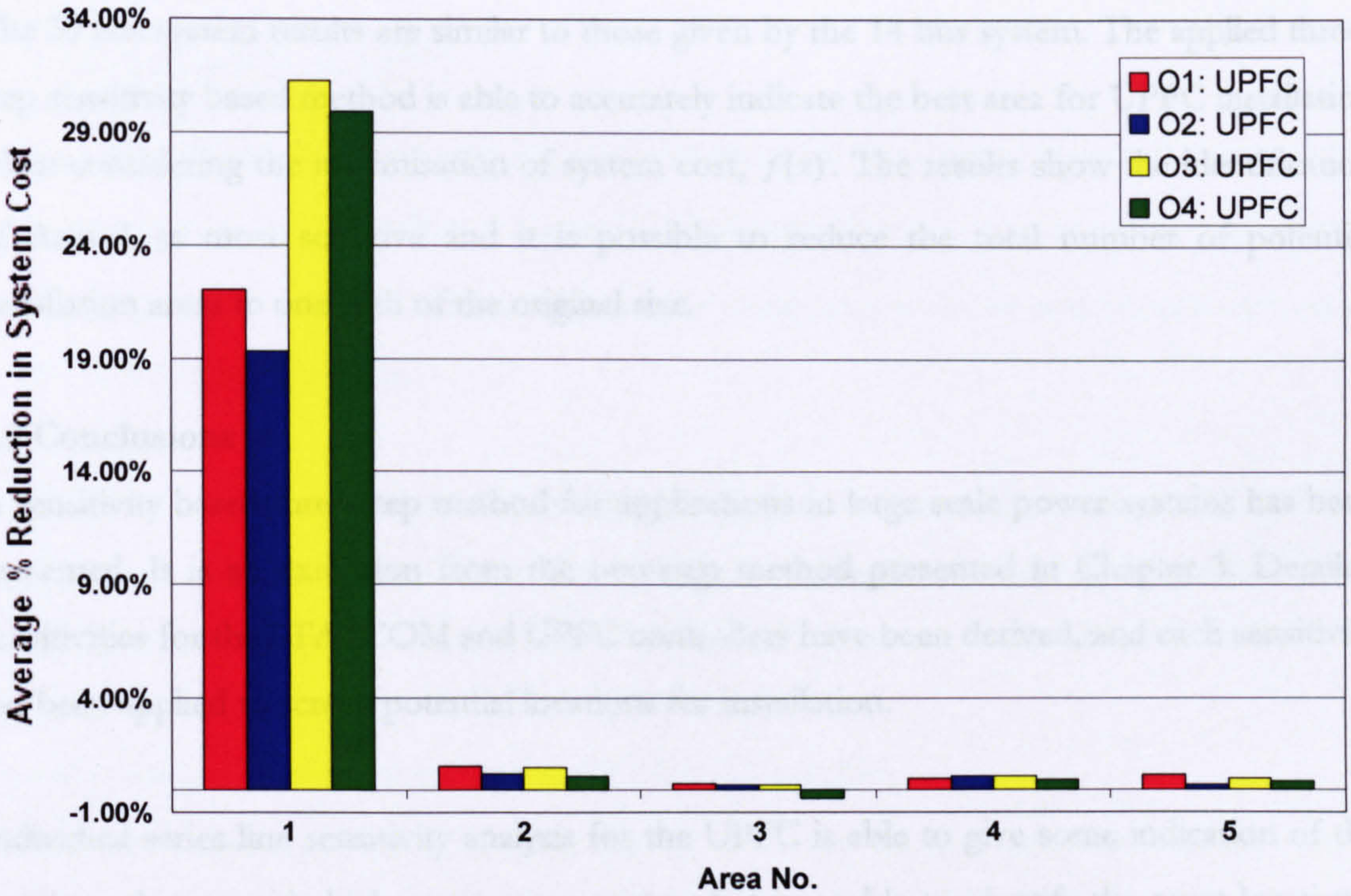

Figure 5.12: IEEE 30 bus system average area % RSC with UPFC installed (all orientations) at 55% $MW_k^{FullRange}$.

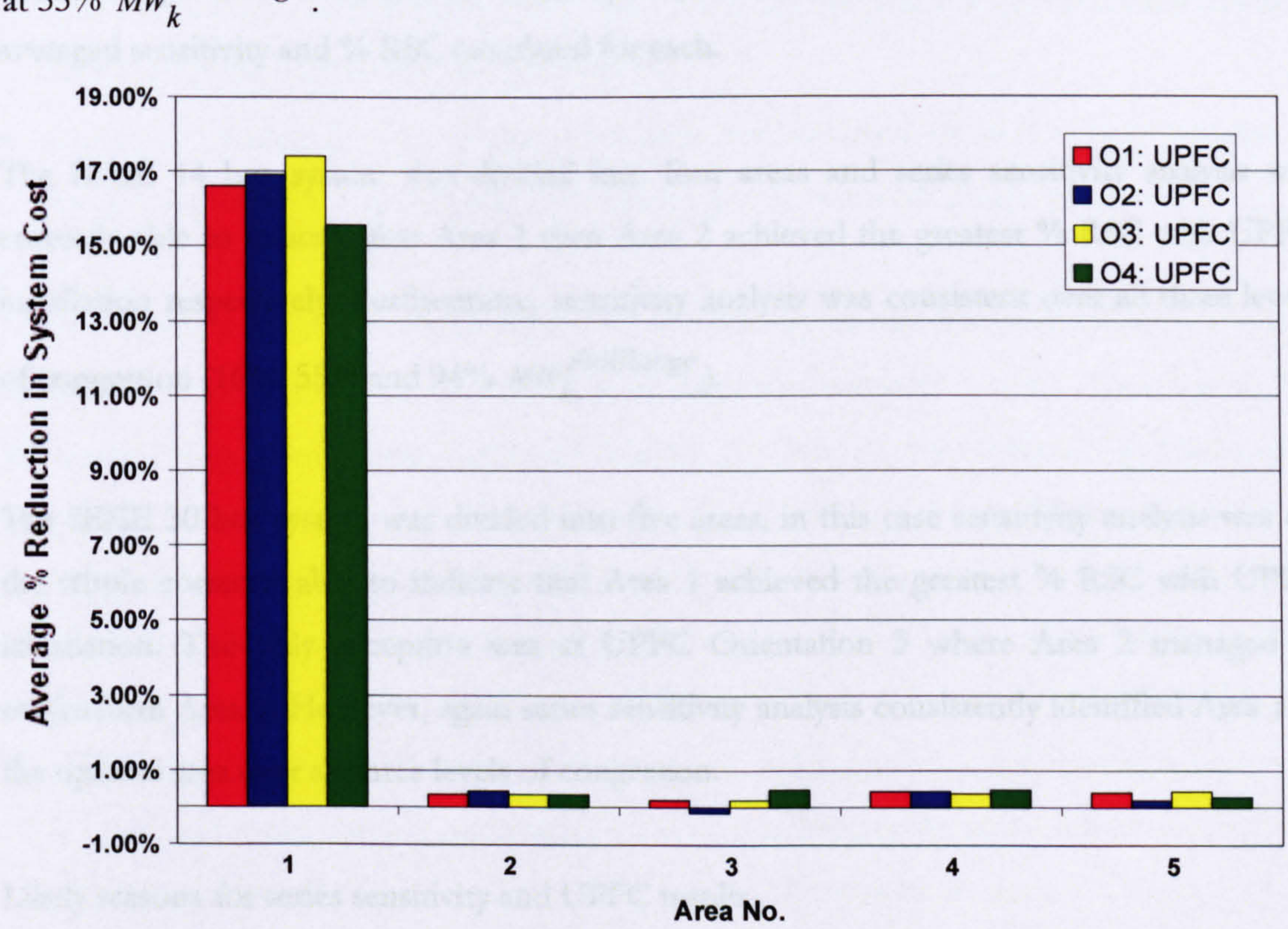

Figure 5.13: IEEE 30 bus system average area % RSC with UPFC installed (all orientations) at 94% $MW_k^{FullRange}$.

Correlation between sensitivity and UPFC performance

The 30 bus system results are similar to those given by the 14 bus system. The applied three-step sensitivity based method is able to accurately indicate the best area for UPFC installation when considering the minimisation of system cost, $f(x)$. The results show the identification of Area 1 as most sensitive and it is possible to reduce the total number of potential installation areas to one fifth of the original size.

5.9 Conclusions

A sensitivity based three-step method for applications in large scale power systems has been presented. It is an extension from the two-step method presented in Chapter 3. Detailed sensitivities for the STATCOM and UPFC controllers have been derived, and each sensitivity has been applied to screen potential locations for installation.

Individual series line sensitivity analysis for the UPFC is able to give some indication of the locations that provide high system cost savings but is unable to identify the exact locations. Results gathered from the 14 and 30 bus systems were consistent. These results motivated the investigation of Scenario 2, where systems were divided into distinct areas and an averaged sensitivity and % RSC calculated for each.

The IEEE 14 bus system was divided into four areas and series sensitivity analysis was correctly able to indicate that Area 1 then Area 2 achieved the greatest % RSC with UPFC installation respectively. Furthermore, sensitivity analysis was consistent over all three levels of congestion (16%, 55% and 94% $MW_k^{FullRange}$).

The IEEE 30 bus system was divided into five areas, in this case sensitivity analysis was on the whole correctly able to indicate that Area 1 achieved the greatest % RSC with UPFC installation. The only exception was at UPFC Orientation 3 where Area 2 managed to outperform Area 1. However, again series sensitivity analysis consistently identified Area 1 as the optimal area over all three levels of congestion.

Likely reasons for series sensitivity and UPFC results,

- the control of transmission line reactance X_{ij} has greater influence on system power flows, reliving congestion and hence on total system costs;

- change of X_{ij} has a larger feasible solution space where the primary parameter limiter is the thermal line limit, S_{ij}^{max};
- the UPFC is able to inject reactive power at the local bus Q_i and influence transmission line reactance, X_{ij}; therefore the possibility of converging to a minima for total system cost is greater and can be achieved through a combination of the two control options of the shunt-series controller.

Individual shunt bus sensitivity and averaged area shunt bus sensitivity for the STATCOM has proven to be unsuccessful at predicting best locations for minimising congestion costs. Results gathered using the IEEE 14 and 30 bus systems show similar results.

Possible reasons for shunt sensitivity and STATCOM results,

- reactive power injection at a local bus Q_i has very limited influence on the system congestion costs, as seen in Sections 5.8.2.1 and 5.8.2.2, where the averaged are reduction in system cost is at best approximately 2.5%;
- transmission line reactive power limits have been reached and the STATCOM is not able to influence the reactive power flow further;
- too large a change in reactive power increases the likelihood of an infeasible solution to the system, therefore feasible solutions cannot greatly influence congestion costs.

Series sensitivity analysis has been successful at reducing the number of simulations required to find the optimal location for the UPFC to minimise congestion costs. This chapter has shown that at the second step of the applied three-step method the number of potential areas and therefore individual locations is reduced by approximately $4/5^{th}$ in the case of the 30 bus system and $3/4^{th}$ in the 14 bus system. The method is an improvement from the one-by-one approach described in the previous chapter. The sensitivity-based method is efficient because sensitivity analysis only requires a single OPF simulation and does not explicitly require the FACTS controller model. Therefore, it is extremely helpful as an initial screening technique before further detailed studies are applied. Chapter 6 will utilise the identified locations of the UPFC to investigate the conflict of controller rating and installation cost.

Chapter 6

Economic analysis of FACTS controller investment costs for congestion management

6.1 Introduction

In Chapter 4, four case studies identified optimal locations for the STATCOM and UPFC controllers when installed on the IEEE 14 bus and 30 bus systems in turn with the objective to minimise total annual costs. The decision for optimal location was determined by the largest annual % reduction in system costs (RSCs). For any transmission system operator (TSO), economic constraints are necessary considerations. This chapter begins with a short literature review, Section 6.2, which includes the three most regularly cited references for FACTS controller cost estimates. In two of these, investment cost is broken down into two components, the equipment costs and the infrastructure costs. Equipment cost is predominantly dependent upon FACTS controller rating; an averaged linear function is applied for estimates within this chapter. In Section 6.3, the optimal locations for the FACTS controllers identified in Chapter 4 are re-evaluated in a general economic analysis framework using the "Return Index" (RI), which aims to relate the system cost savings made by FACTS controllers at specific locations to the cost required to install the controller. Lastly, conclusions are drawn and references listed in Sections 6.5 and 6.6 respectively.

6.2 Investment cost estimates

A literature review of FACTS controller price and cost information reveals only two main sources of free and widely published information. A shortage of adequate information on FACTS controller investment costs limits the accuracy of economic estimates for justifying their use [CIGRE JWG (2001)]. Consideration of inflation has been given, therefore cost estimates published before 1996 are not referenced here; although some cost estimates published before 1996 are cited in CIGRE JWG (2001) and Adapa (2000). The first source is from 1996 published by the IEEE Power Engineering Society, is referenced in Hauth et al. (1997) and Mathur and Varma (2002), and the latter from Siemens AG Database for a World Bank publication by Habur and O'Leary. Cost information from Siemens AG Database has been used in a variety of publications including Cai et al. (2004), TEN-E (2005), L'Abbate et al. (2007) and most recently by Vaijayakumar et al. (2007). A range of "investment costs" are

given; the lower estimate limit representing the "equipment costs" and the upper estimate limit includes equipment and "infrastructure costs".

A third source of UPFC costing information is considered in this analysis, a consultation report published by the California Energy Commission in 1999 [California Energy Commission (1999)]. The report compares five possible solutions for locating a UPFC with the objective of increasing import capability to the San Diego Gas & Electric (SDG&E) system and delay transmission system expansion. Simulation studies estimated the required equipment (UPFC capacity ratings), transmission reinforcements and substation costs.

Within this chapter the term "equipment costs" will primarily refer to the costs associated with the FACTS controller capacity rating; "infrastructure costs" refer to any necessary modifications required of existing transmission system assets, including upgrading of substations and extension of communication systems; the final total is the "investment cost" and is related by expression (6.1).

$$C_{FACTS} = C^{E}_{FACTS} + C^{I}_{FACTS} \tag{6.1}$$

where,

C_{FACTS} investment cost, $

C^{E}_{FACTS} equipment cost, $

C^{I}_{FACTS} infrastructure cost, $

Sections 6.2.1 to 6.2.6 summarise estimates given by the three references, then compares the proportion of equipment and infrastructure cost estimates given by Siemens AG Database (SAGD) and California Energy Commission (CEC) reports. The IEEE PES publication cannot be included in this comparison because it does not consider infrastructure costs.

6.2.1 IEEE PES report: cost estimates

The IEEE PES report only gives an estimate on equipment price as 'price per capacity rating' for a range of controllers including the conventional thyristor based controllers. The STATCOM estimate is $50/kVAR ($50 000/MVAR) and the UPFC estimate is $50/kW

($50 000/MW) for the series portion and $50/kVAR ($50 000/MVAR) for the shunt portion. References that cite these report price estimates are Hauth et al. (1997) and Mathur and Varma (2002).

6.2.2 Siemens AG Database infrastructure cost estimates

The estimates provided by the SAGD publication give lower and upper curves for price limits, where the lower bound indicates equipment prices and the upper bound indicates installation prices in $/kVAR. Table 6-1 gives estimates of equipment cost, investment cost and percent equipment cost relative to the installation costs for the STATCOM and UPFC for a range of capacity ratings. For guideline purposes, it is assumed that the $/kW for the real power capacity rating equals the reactive power capacity rating. Note that as the UPFC requires two branch controllers, it has a higher percentage equipment cost relative to the STATCOM.

Table 6-1: Estimation of STATCOM and UPFC equipment and infrastructure cost from Siemens AG Database.

Rating MVA	STATCOM equipment cost C^E_{FACTS} $ million	STATCOM installation cost C_{FACTS} $ million	% Equipment cost C^E_{FACTS}	UPFC equipment cost C^E_{FACTS} $ million	UPFC installation cost C_{FACTS} $ million	% Equipment cost C^E_{FACTS}
100	8.7	12.7	67%	12.4	16.9	73%
200	15.5	23.4	66%	21.4	30.0	71%
300	20.3	32.1	63%	26.8	39.3	68%
350	21.9	35.7	60%	28.3	42.5	67%
-	Ave. % equipment cost		64%	Ave. % equipment cost		70%

6.2.3 California Energy Commission infrastructure cost estimates

The estimates provided by CEC report give a different breakdown of costs compared to the other references. They include UPFC series and shunt branch costs, transmission reinforcements and substation costs. Five alternatives are explored with the aim to increase the San Diego Gas & Electric's import capability and to determine if FACTS controllers were capable to increase the usable capacity of the existing South-of-San Onofre Nuclear Generating Station transmission system. A short description of the five alternatives are listed,

- Alternative 1 – UPFC for control of flow on San Onofre – Talega 230 kV line
- Alternative 2 – UPFC for control of flow on San Onofre – Enchina 230 kV line
- Alternative 3 – UPFC for control of flow on San Onofre – Mission 230 kV line

- Alternative 4 – UPFC for control of flow on San Onofre/San Luis Rey Tap – Mission 230 kV line
- Alternative 5 – two UPFCs for control of flow on San Onofre – Mission and San Onofre – Talega 230 kV lines

In Table 6-2 the equipment cost is equivalent to the UPFC series and shunt branch costs and the infrastructure cost is equivalent to the transmission reinforcement and substation costs.

Table 6-2: Estimation of equipment, infrastructure and installation cost from CEC report.

Alternative	UPFC cquipment cost C^{E}_{FACTS} $ million	UPFC infrastructure cost C^{I}_{FACTS} $ million	UPFC installation cost C_{FACTS} $ million	% Equipment cost C^{E}_{FACTS}
1	6.8	18.6	25.4	27%
2	18.8	38.6	57.4	33%
3	10.3	30.6	40.9	25%
4	4.5	36.6	41.1	11%
5*	9.0	20.3	29.3	31%
Average	**9.9**	**28.9**	**38.8**	**25.4%**

*Alternative 5 has two UPFCs installed, the averaged cost of installing a single UPFC at this location has been considered for fair comparison.

Table 6-3 shows, the CEC report equipment price estimates. The average is rounded to $40/kVA or $40 000/MVA (to two significant figures).

Table 6-3: Estimation of price $/MVA from CEC report (1999).

Alternative	UPFC rating MVA	UPFC equipment cost C^{E}_{FACTS} $ millions	Estimate price $/MVA
1, 2, 3, 4, 5	85	3.4	40 000
2	385	15.4	40 000
3, 5	174	6.9	39 600
4	28	1.1	39 300
		Average	39 700

6.2.4 Relative size of equipment costs compared to infrastructure costs

The average quantities of equipment costs relative to the investment costs is summarised in Table 6-4, where the IEEE PES estimate cannot be included as only equipment costs are considered. The fact that the average equipment cost percentage is 70% from the SAGD publication and 30% from the CEC report shows how varied the published estimate prices and costs are. Although a discrepancy has been found, a reasonable and consistent cost estimation can still be a valuable aid for the decision making process.

Table 6-4: Comparison of % equipment and % infrastructure cost proportions from two estimates.

Installation Cost Components	Siemens AG Database	California Energy Commission
% Equipment cost C^{E}_{FACTS}	70%	30%
% Infrastructure cost C^{I}_{FACTS}	30%	70%

6.2.5 Applied equipment cost estimation

Due to the above observations, a simple FACTS controller price estimation is used for analysis in this chapter. It is only necessary to provide basic cost guidelines for comparison for two main reasons,

1. the standard IEEE 14 and 30 bus system models used cannot provide information about necessary infrastructure costs therefore, only equipment costs, as a function of the FACTS controller capacity can be quantified easily;
2. only the real power costs due to congestion and system losses are examined.

Justification of a more detailed explanation of installation costs with infrastructure costs requires further simulations of other quantifiable benefits, which are outside the scope of this work.

Reductions in costs due to congestion and system real power losses are only two of many benefits a FACTS controller could bring to the system. Therefore, the highest equipment price estimate presented in SAGD has been ignored and the remaining analysis uses the averaged equipment cost published in the IEEE PES and CED reports. That is, \$45/kVA or \$45 000/MVA ({\$50 000 + \$40 000}/2). A summary is given in Table 6-5 and Figure 6.1 shows the cost relationship applied. The same price is assumed for series and shunt branches of the FACTS controllers weather installed at system bus or at midpoint of transmission lines.

Table 6-5: Summary of averaged equipment cost estimates.

Reference Source	Estimated Equipment Prices \$/MVA
IEEE PES report	50 000
Siemens AG Database	67 000
California Energy Commission report	40 000

6.2.6 Other FACTS controller benefits

In addition to the specific control function benefits gained from the use of voltage source converter (VSC) based FACTS controllers, as listed in Table 3-1 of Chapter 3 there are also

overall system benefits, listed in Table 6-6. The benefits listed in both tables are often difficult to quantify in monetary terms but can improve the system in some way, locally and/or as a whole.

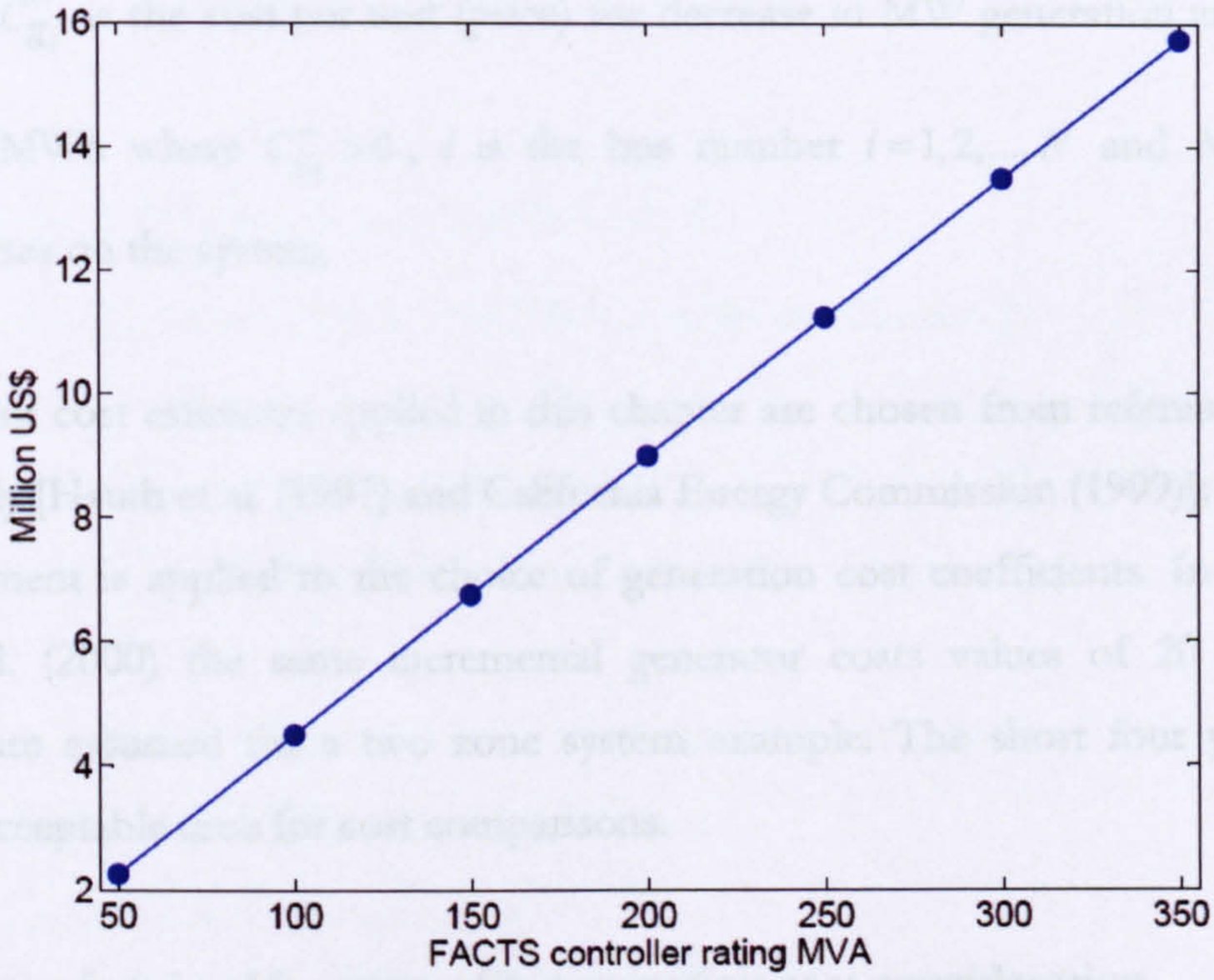

Figure 6.1: FACTS controller capacity-equipment cost relationship applied.

Table 6-6: Summary of possible benefits from installing VSC based FACTS controllers [Acharya et al. (2005) and Zhang et al. (2005)].

System Benefits	Steady State Applications	Dynamic Applications
• Increased system efficiency; • Better utilisation of existing assets on transmission system; • Increased reliability and availability, giving increased control during contingencies; • Increased dynamic and transient grid stability; • Increased quality of supply (required by specific industries); • Installing FACTS controllers can be more environmentally friendly than other solution methods.	• Increased voltage limits; • Increased thermal limits; • Increased control of loop flows; • Increased short circuit levels; • Increased control during subsynchronous resonances.	• Increased control of transient stability problems; • Increased damping ability; • Increased control of voltage during post contingencies; • Increased control for voltage stability.

Quantifying the benefits listed above is outside the scope of this work. More simulation studies in dynamic and static time domains are necessary.

6.3 Generation cost coefficients

The generation cost coefficients were introduced in Chapter 2, Section 2.3. $C_{g_i}^{+}$ is the cost per unit (price) for increase in MW generation and is equal to $C_{g_i}^{+} = 20$ \$/MWh where $C_{g_i}^{+} > 0$, and $C_{g_i}^{-}$ is the cost per unit (price) for decrease in MW generation and is equal to $C_{g_i}^{-} = 10$ \$/MWh where $C_{g_i}^{-} > 0$, i is the bus number $i = 1,2,...,N$ and N is the total number of buses on the system.

The investment cost estimates applied in this chapter are chosen from references published after 1996 only [Hauth et al. (1997) and California Energy Commission (1999)]; therefore, the same requirement is applied to the choice of generation cost coefficients. In the paper by Christie et al. (2000) the same incremental generator costs values of 20 \$/MWh and 10 \$/MWh are assumed for a two zone system example. The short four year period is assumed an acceptable time for cost comparisons.

6.4 Evaluation of optimal location with congestion cost consideration

To aid evaluation of the cost benefits from installing FACTS controllers at a particular location, a measure called the Return Index (RI) is utilised. The aim of the index is to relate the specific equipment cost to the annual system cost savings made at each controller location. Therefore, the RI can directly compare results within each case study and identify which has the highest rate of return. The system case studies used are the same as those presented in Chapter 4.

- IEEE 14 bus system case with STATCOM;
- IEEE 30 bus system case with STATCOM;
- IEEE 14 bus system case with UPFC;
- IEEE 30 bus system case with UPFC.

6.4.1 Return Index (RI)

The RI aims to identify the solution that has the relative greater rate of return from the FACTS controller installation. It is assumed that 25 years is a reasonable period expected for payback of transmission system equipment [California Energy Commission (1999)]. The RI

compares the relative equipment cost, C^E_{FACTS} which is a function of the equipment rating, S_{FACTS} (MVA) to the system cost savings made over 25 years. The RI is defined as,

$$RI = \frac{C^E_{FACTS}}{25 * A_S}, \text{RI} > 0 \qquad (6.2)$$

where,

C^E_{FACTS} is the FACTS controller equipment cost, $,

A_S annual cost savings made due to FACTS controller installation, $.

The smaller the RI value the higher the rate of return. For the RI to decrease either the equipment cost must be reduced or the annual cost savings increased.

The relationship between RI and payback period can be summarised as follows,

- RI > 1, payback period is longer than 25 years;
- RI = 1, payback period is 25 years;
- RI < 1, payback period is less than 25 years.

6.5 Results

The case studies presented in Chapter 4 are extended to investigate the viability of FACTS controller installations by applying the RI. This enables relative comparisons to identify the return rates at each location. For each case the smaller the RI the higher the rate of return and, therefore the faster the equipment cost will be recovered.

6.5.1 IEEE 14 bus system case with STATCOM

Five locations with the STATCOM on the 14 bus system managed an annual % RSC above 10%. For installation at ends of transmission lines, locations J:2-4 and J:2-5 and for installation at midpoint, locations M:1-2, M:2-4 and M:2-5. Table 6-7 summarises the system cost, savings, equipment rating and cost required at these locations and corresponding RIs. The base case system cost is 20.0 $/h, the generation cost coefficients remain a previously stated as $C^+_{g_i}$= 20 $/MWh and $C^-_{g_i}$ = 10 $/MWh, and the overall largest annual savings and the lowest equipment costs are highlighted in bold.

Table 6-7: IEEE 14 bus STATCOM: Summary of system costs, annual savings, equipment costs and return index.

STATCOM location *i-j* and position	System cost $f(x)$ \$/h	Savings w.r.t. base case \$/h	Annual savings \$	STATCOM rating MVA	Equipment cost C_{FACTS}^{E} \$ million	Return Index
J:2-4	17.2	2.8	24 528	227	10.22	16.7
J:2-5	16.3	3.7	32 412	404	18.18	22.4
M:1-2	7.7	**12.3**	**107 748**	68	**3.06**	1.1
M: 2-4	17.9	2.1	18 396	68	**3.06**	6.7
M: 2-5	17.7	2.3	20 148	90	4.05	8.0

For installation at ends of transmission lines J:2-5 has higher annual savings bus also requires a larger STATCOM rating. In Chapter 4 equipment costs were not considered and location J:2-5 was identified as the optimal location. In this analysis, restrictions on investment costs are also considered and the RI has indicated that location J:2-4 is now the optimal choice for locating the STATCOM.

For installation at the midpoint of transmission lines, location M:1-2 has the highest savings and lowest equipment cost with required rating of 68MVA. Therefore, it has the lowest RI of 1.1 and payback period of 27.5 years. The result given in Chapter 4 based on savings was also M:1-2.

Overall, M:1-2 is the optimal location based on savings, relative equipment cost required and position of STATCOM on transmission line.

6.5.2 IEEE 30 bus system case with STATCOM

Five locations with the STATCOM on the 30 bus system managed annual % RSCs above 10%. For installation at ends of transmission lines, locations J:2-4 and J:2-6 and for installation at midpoint, locations M:1-2, M:2-4 and M:2-6. Table 6-8 summarises the savings, equipment costs required at these locations and calculated RI. The base case system cost is 13.9 \$/h, the generation cost coefficients remain a previously stated as $C_{g_i}^{+}=$ 20 \$/MWh and $C_{g_i}^{-}$ = 10 \$/MWh, and the overall largest annual savings and lowest equipment costs are highlighted in bold.

For installation at ends of transmission lines J:2-6 has higher annual savings and requires a smaller controller rating. For installation at midpoint of transmission lines, location M:1-2 has

the highest cost savings and location M:2:6 has the lowest equipment rating and cost. The lowest RI of 0.6 is achieved by M:1-2, with payback period of 15 years.

Table 6-8: IEEE 30 bus system STATCOM: Summary of system costs, annual savings, equipment costs and return index.

STATCOM location *i-j* and position	**System cost $f(x)$ \$/h**	**Savings w.r.t. base case \$/h**	**Annual savings \$**	**STATCOM rating MVA**	**Equipment cost C_{FACTS}^{E} \$ million**	**Return Index**
J:2-4	12.5	1.4	12 264	191	8.60	28.0
J:2-6	11.9	2.0	17 520	132	5.94	13.6
M:1-2	4.2	**9.7**	**84 972**	26	1.17	**0.6**
M:2-4	12.9	1.0	8 760	33	1.49	6.8
M:2-6	12.1	1.8	15 768	13	**0.59**	1.5

The conclusions drawn in Chapter 4 both remain unchanged because location J:2-6 and M:1-2 have the lower RI values. Overall, M:1-2 is the optimal location based on savings and relative equipment cost required.

6.5.3 IEEE 14 bus system case with UPFC

Six UPFC locations using Orientation 1 on the 14 bus system managed annual % RSCs greater than 10%; these are locations 1-2, 1-5, 2-5, 2-4, 3-4 and 4-5. Table 6-9 summarises the savings and equipment costs required at these locations, the base case system cost is 20.0 \$/h, the generation cost coefficients remain a previously stated as $C_{g_i}^{+}=$ 20 \$/MWh and $C_{g_i}^{-}$ = 10 \$/MWh, and the largest annual savings and smallest equipment costs are highlighted in bold. Figure 6.2 shows the RIs for each location.

Table 6-9: IEEE 14 bus system UPFC: Summary of system costs, annual savings and equipment costs.

UPFC location *i-j* and orientation	**System cost $f(x)$ \$/h**	**Savings w.r.t. base case \$/h**	**Annual savings \$**	**UPFC rating MVA**	**Equipment cost C_{FACTS}^{E} \$ million**
O1:1-2	5.8	14.2	**124 392**	70	3.15
O1:1-5	7.8	12.2	106 872	92	4.14
O1:2-5	12.4	7.6	66 576	93	4.19
O1:2-4	17.0	3.0	26 280	66	2.97
O1:3-4	17.8	2.2	19 272	39	**1.76**
O1:4-5	17.2	2.8	24 528	141	6.35

In this case study UPFC location O1:1-2 has highest annual savings and requires one of the smaller controller ratings. Therefore, the conclusion drawn in Chapter 4 remains unchanged because location O1:1-2 also has the lowest RI. The payback period for the UPFC at location O1:1-2 is approximately 25 years because the RI is approximately unity.

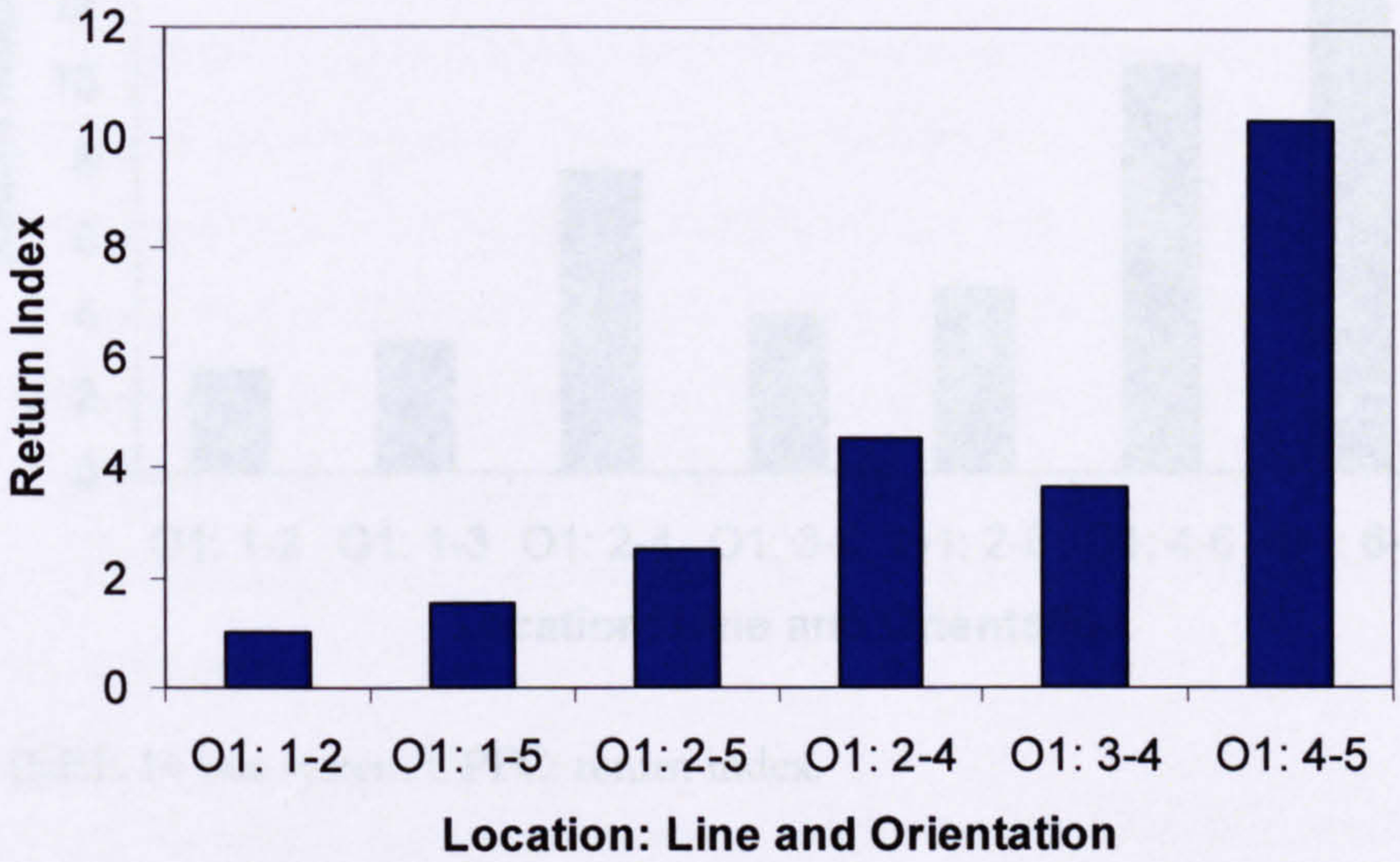

Figure 6.2: IEEE 14 bus system case study with UPFC: return index.

6.5.4 IEEE 30 bus system case with UPFC

Seven UPFC locations using Orientation 1 on the 30 bus system managed annual % RSCs greater than 10%, locations 1-2, 1-3, 2-4, 3-4, 2-6, 4-6 and 6-7. Table 6-10 summaries the savings and equipment costs required at these locations, the base case system cost is 13.9 \$/h, the generation cost coefficients remain as previously stated as $C_{g_i}^{+}$ = 20 \$/MWh and $C_{g_i}^{-}$ = 10 \$/MWh, and the greatest annual savings and smallest equipment costs are highlighted in bold and, Figure 6.3 shows the corresponding RIs.

Table 6-10: IEEE 14 bus system UPFC: Summary of system costs, annual savings and equipment costs.

UPFC location *i-j* and orientation	**System cost $f(x)$ \$/h**	**Savings w.r.t. base case \$/h**	**Annual savings \$**	**UPFC rating MVA**	**Equipment cost C_{FACTS}^{E} \$ million**
O1:1-2	4.2	15.8	84 972	125	5.63
O1:1-3	3.6	**16.4**	**90 228**	169	7.61
O1:2-4	12.6	7.4	11 388	49	2.21
O1:3-4	6.7	13.3	63 072	141	6.35
O1:2-6	12.0	8.0	16 644	44	**1.98**
O1:4-6	11.6	8.4	20 148	117	5.27
O1:6-7	12.5	7.5	12 264	106	4.78

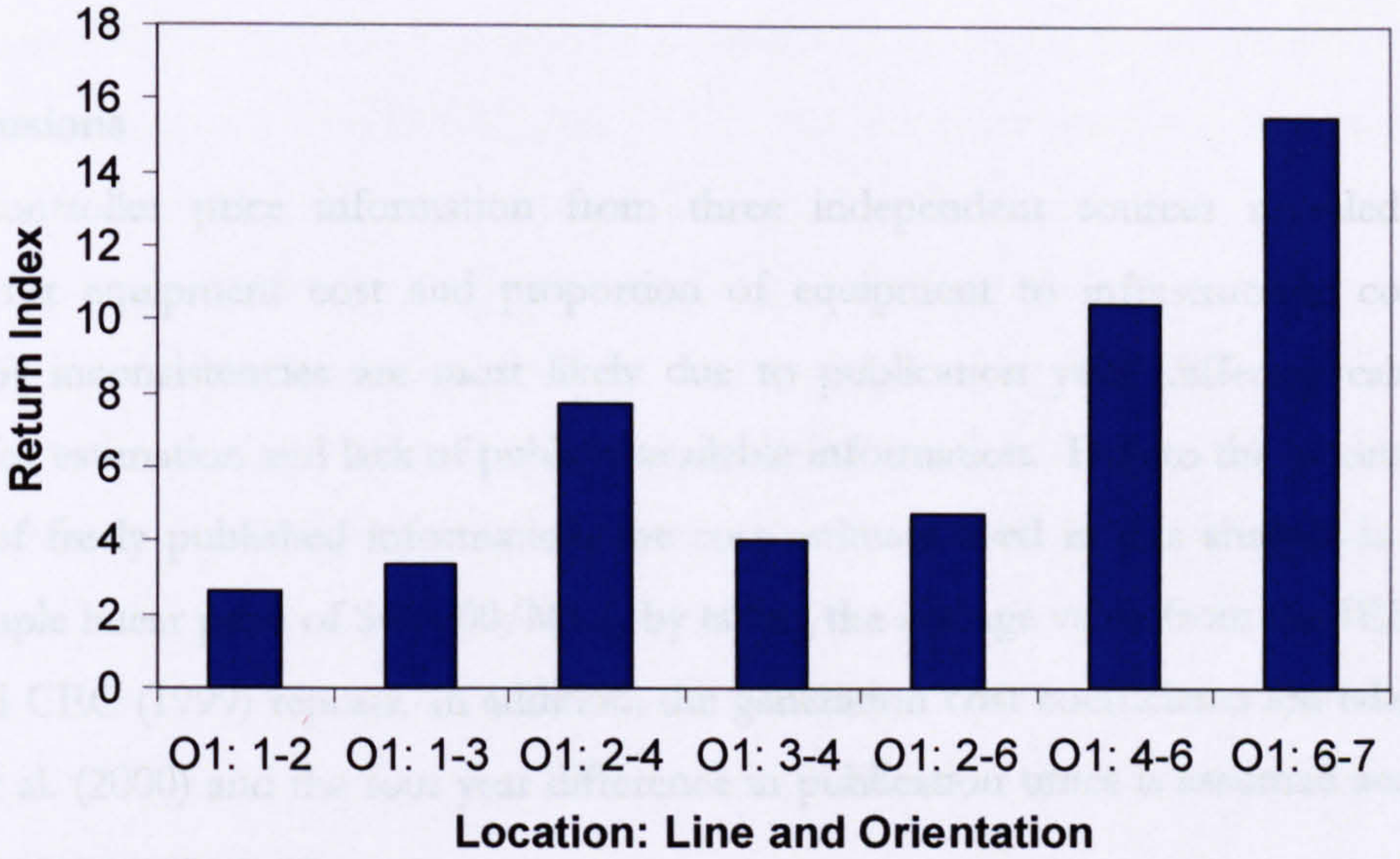

Figure 6.3: IEEE 14 bus system UPFC: return index.

On the 30 bus system, the highest annual RSC is made when UPFC is installed at location O1:3-4 and the location with the smallest required UPFC rating is at location O1:2-6. The RI is lowest at location O1:1-2; and is the optimal location for UPFC installation as its rate of return is the fastest. However, as the RI is 2.6, payback period is 65 years (2.6*25 years); this is an unacceptable duration for payback.

6.5.5 Results summary

Chapter 4 showed that the STATCOM and UPFC can reduce congestion and system losses and achieve annual % RSCs above 10% if located correctly on both the IEEE 14 and 30 bus systems. For the STATCOM, on each of the 14 and 30 bus systems, there were five possible locations with RSCs above 10%. Overall, in both system cases the RI reinforced the choice of optimal location as decided in Chapter 4, that is location M:1-2 for both the 14 and 30 bus systems.

For the UPFC, on the 14 bus system there were six locations that produced RSCs greater than 10% and the RI indicated that O1:1-2 was the optimal location, the same result as concluded in Chapter 4. For the UPFC on the 30 bus system there were seven locations that produced RSCs greater than 10%, in Chapter 4 O1:1-3 was identified as the optimal location because it had the greatest % RSC. However, as location O1:1-3 has the largest annual saving

but also the largest UPFC rating the RI indicated that location O1:1-2 was the optimal location.

6.6 Conclusions

FACTS controller price information from three independent sources revealed varied estimates for equipment cost and proportion of equipment to infrastructure cost. The reasons for inconsistencies are most likely due to publication year, differing calculation methods for estimation and lack of publicly available information. Due to the inconsistency, and lack of freely published information, the cost estimate used in this analysis is derived from a simple linear price of $45 000/MVA by taking the average value from the IEEE PES (1996) and CEC (1999) reports. In addition, the generation cost coefficients are taken from Christie et al. (2000) and the four year difference in publication times is assumed acceptable period for cost comparison.

The RI indicator considers the relative savings made by the FACTS controller to the equipment cost required for installation, and gives a measure similar to the rate of return for investments. The RI measure has been useful to the decision making process for the STATCOM at ends of transmission lines on 14 bus system and UPFC on the 30 bus system case study. For the former, the location identified in Chapter 4, J:2-5 had the lower system cost savings but required almost twice the rating of J:2-4; the RI has indicated that J:2-4 is actually the better location as the payback period is relatively shorter. For the latter, the location identified in Chapter 4, O1:1-3 also required the largest controller rating; by assessing the relative magnitudes in annual savings and equipment cost the RI identified location O1:1-2 as having the fastest rate of return and is able to achieve a payback period of approximately 25 years. Table 6-11 shows a summary of the optimal FACTS controller locations given in Chapter 4 and Chapter 6.

Table 6-11: Summary of optimal FACTS controller locations for all case studies

Case studies IEEE systems		Result change from Chapter 4	Overall optimal location given in	
Controller	Bus system size		Chapter 4	Chapter 6
STATCOM at ends of lines	14	Yes	J:2-5	J:2-4
	30	No	J:2-6	
STATCOM at midpoint of lines	14	No	M:1-2	
	30	No	M:1-2	
UPFC orientation 1	14	No	O1:1-2	
	30	Yes	O1:1-3	O1:1-2

As the results presented are restricted to the quantitative benefits of congestion and real power system losses, it is not possible to justify a complete FACTS controller installation cost. However, the RI has been shown to be a useful tool to aid the decision-making process for optimal location of STATCOM and UPFC FACTS controllers for minimisation of system congestion and real power losses. The results show that there is potential for application to larger existing transmission systems; however in the estimates presented the cost savings gained do not take into account any discount rate and FACTS controller power losses are also neglected. Therefore, although a conservative estimate is taken for annual demand levels the quantitative value of the FACTS controllers presented are likely to be over-estimated. Any increase in the rate of installation of FACTS controllers in the future depends upon; either a reduction in the overall installation cost and/or a change in system limitations, making a situation where FACTS controllers are one of a minority of solutions to solve electricity system problems.

Chapter 7

Conclusions

7.1 Concluding remarks

The contributions of this thesis are divided into two key areas. The first is related to the formulation of the bilateral market model using the interior point OPF algorithm with the modelling of FACTS controllers. The general formulation allows easy examination of system generation, demand, losses and congestions levels. The second area assesses the use of voltage source converter (VSC) based FACTS controllers as a suitable solution to the congestion management problem.

The first area, covered in Chapters 2 and 3 formed the basis of the results gathered in the thesis; it involved the implementation of the linear bilateral market model into interior point optimisation OPF algorithm together with FACTS controller models using hybrid parameter representation. Here, a setup procedure was proposed for fair and easy comparisons of test cases against relevant base cases, and the generalised two-step method was conceived.

In the second area, Chapters 4 to 6 presented results that assessed the performance of FACTS controllers for congestion minimisation. Comparison over daily and annual demand levels provided greater detail than single steady state instants in time. An extension was made to the generalised method for increased efficiency by the addition of a screening technique; this formed the sensitivity based three-step method. Consideration was also given to the economic benefits of FACTS controller installations.

7.1.1 Evaluation of results

The bilateral market model reflected the market structure used in Britain. The model included rational generators with predefined bids for change from scheduled generation which simulated the balancing mechanism. Congestion was imposed on the simulations by changes in the daily demand requirements. In all cases, when congestion was in existence the system active power generation increase was greater than the system active power generation decrease, due to the real power system losses. Consistently it was found that the contribution

of scheduled generation changes from congestion was much greater than the contribution from real power system losses and, the quantity of system losses were similar with and without the application of FACTS controllers. Therefore, to minimise system costs, the minimisation of congestion was more important than real power system losses.

Numerical results with the VSC based FACTS controllers, the STATCOM and UPFC showed that they were able to provide power flow control for congestion management. The bus or line installation location was the most important factor as it affects the quantity of reduction in system cost (RSC) and the corresponding required capacity of the FACTS controller. The orientation of the controller was not as important as the location of the controller. These aspects were especially true for the UPFC, as it achieved on average greater RSCs compared to STATCOM.

The area sensitivity method was able to identify the system area with the greatest average RSC for the UPFC consistently and across a range of demand levels. This area identification method was efficient because it required only a single simulation of the base case system. At the individual line level, the line sensitivity indicator was unable to identify the correct location for the UPFC. For the STATCOM, the area and individual bus sensitivity methods were not able to indicate best locations correctly.

Investment cost is often the limiting factor within the industrial decision-making processes. Application of the Return Index (RI) measure eased the final location decision by quantifying the equipment cost and corresponding system cost savings, giving an indicator similar to the economic rate of return.

Congestion management is an increasingly important issue for the entire electrical utility industry. The integration of new technologies such as FACTS controllers appears inevitable as the technical capability, statutory requirements and socially acceptable solutions available to the transmission system operators (TSO) are progressively becoming more demanding. Steady state modelling is an important first step to the decision making process for any transmission system upgrade. The results from the IEEE systems showed that with an appropriate choice of location, the installation of a UPFC is able to provide a solution to the congestion management problem with realistic equipment based investment payback periods.

7.1.2 Main contributions of this work

The major contributions of this thesis are summarised as follows:

a) Implementation of the non-linear interior point OPF algorithm for the calculation of power system congestion and power system losses in a pure bilateral market, using an a.c. power flow network model and reduced matrix of Newton equations.
b) Determination of the impact of FACTS controllers such as the STATCOM and UPFC on the power system congestion and power system losses in a pure bilateral electricity market during daily demand load profiles in (i) a Winter Maximum period, (ii) a typical Summer period, and (iii) an average 365 day year.
c) Proposal of a general two-step method for finding optimal FACTS controller location and rating for minimisation of congestion and real power system loss costs.
d) Formulation of an area sensitivity-based three-step screening technique to aid identification of optimal location for UPFC installation and rating, for minimising congestion and real power system loss costs to reduce the number of required simulations.
e) Determination of the impact of FACTS controller equipment costs on the decision making process of optimal location for solving the congestion management problem.

The a.c. power flow network representation implemented to determine the use of FACTS controllers for congestion management is able to investigate the implications of a wide range of network features and constraints that cannot be examined by approximate modelling techniques such as the d.c. power flow model.

Steady state analysis over a range of load levels has provided more information about long-term system performance with FACTS controllers for congestion management. The proposed screening technique method may be of interest to TSOs to aid first-step decision making by rapidly eliminating the majority of FACTS controller installation locations.

7.2 Further work

The interior point OPF algorithm for the calculation of congestion cost can be extended to investigate different features of dealing with congestion management with FACTS controllers. Some suggestions for future research work is presented below.

Bilateral electricity trading is most concerned with the delivery and consumption of real power; however, the amount of reactive power within the system can affect the quality and efficiency of power delivered. Extending the linear bilateral market objective function to include penalty charges for changes to scheduled reactive power can indicate how much congestion is affected by reactive power as well as active power. In addition, the FACTS controller models are able to influence the real and reactive power flow. Inclusion of reactive power in the objective function may further utilise this control feature.

FACTS controllers are examined for single installation; however, as their use becomes more widespread and installation costs reduced, the use of multiple FACTS controllers in large-scale systems is likely to become increasingly common. The interior point OPF algorithm already has the ability to deal with systems larger than 30 buses and for multiple FACTS installations, so that it is possible to investigate the impact of multiple FACTS controllers on congestion management.

The major case studies presented in this thesis were concerned with normal demand profiles. Planned and unplanned system outages are times where the system is highly stressed and serious congestion is most likely to occur. By setting up a variety of case studies with one or more transmission lines with reduced or with zero capacity, a test of FACTS controllers can be conducted to find the optimal type, rating and location.

The equipment cost for FACTS controller installation was considered after installation locations were identified. It may be possible to investigate the impact of the equipment cost on the rating of the FACTS controller by extension of the objective function to include equipment cost. The equipment cost curve and the bilateral market relationship are conflicting requirements, as they are linear functions with gradients of opposite sign. In this case, each installation location would simultaneously be tested for reduction in congestion and at low equipment cost and therefore smallest controller rating.

Other topics that could be examined concern the implementation of the algorithm and its performance with different objective function and equipment combinations. Increased efficiency was found using rectangular coordinate representation and the highly reduced matrix of Newton equations as used in [Zhang et al. (2005)]. If applied to the congestion management problem it could reduce the complexity of the matrix of Newton equations and therefore the time required to find a solution, particularly for large scale power system applications.

APPENDIX I

Formulation for interior point OPF in hybrid coordinate representation using power mismatch equations, as presented in Chapter 2.

All relevant formulations are presented for bus *i* and branch *ij* where the non-diagonal parts are considered. The system elements are identical for all system buses and branches.

Newton Matrix Elements:

Equations (2.37) - (2.43) where,

Non-functional constraints are $h_j = \left[P_{g_i}^{+}, P_{g_i}^{-}, Q_{g_i}, V_i, V_j, t_i \right]$

Functional constraint is S_{ij}^2

$$x = \left[P_{g_i}^{+}, P_{g_i}^{-}, Q_{g_i}, \theta_i, V_i, \theta_j, V_j, t_i \right]$$

$$x_\alpha = \left[x_i, sl_j, su_j, \pi l_j, \pi u_j, \lambda_{p_i}, \lambda_{q_i}, \lambda_{p_j}, \lambda_{q_j} \right]$$

α is the system variable number $\alpha = 1, 2, ..., 2N + 3N_g + N_t$,

N is the total number of buses,

N_g is the total number of generators,

N_t is the total number of transformers on the system,

N_h is the total number of inequality constraints.

Left-Hand-Side Formulation

For equation (2.42): $-\nabla_{sl_j} L_\mu = -sl_j \Delta\pi l_j - \pi l_j \Delta sl_j$

$$-\nabla_{sl_{P_{g_i}^{+}}} L_\mu = -sl_{P_{g_i}^{+}} \Delta\pi l_{P_{g_i}^{+}} - \pi l_{P_{g_i}^{+}} \Delta sl_{P_{g_i}^{+}} \tag{A.I-1}$$

$$-\nabla_{sl_{P_{g_i}^{-}}} L_\mu = -sl_{P_{g_i}^{-}} \Delta\pi l_{P_{g_i}^{-}} - \pi l_{P_{g_i}^{-}} \Delta sl_{P_{g_i}^{-}} \tag{A.I-2}$$

$$-\nabla_{sl_{Q_{g_i}}} L_\mu = -sl_{Q_{g_i}} \Delta\pi l_{Q_{g_i}} - \pi l_{Q_{g_i}} \Delta sl_{Q_{g_i}} \tag{A.I-3}$$

$$-\nabla_{sl_{V_i}} L_\mu = -sl_{V_i} \Delta\pi l_{V_i} - \pi l_{V_i} \Delta sl_{V_i} \tag{A.I-4}$$

$$-\nabla_{sl_{V_j}} L_\mu = -sl_{V_j} \Delta\pi l_{V_j} - \pi l_{V_j} \Delta sl_{V_j} \tag{A.I-5}$$

$$-\nabla_{sl_t} L_\mu = -sl_t \Delta\pi l_t - \pi l_t \Delta sl_t \tag{A.I-6}$$

For equation (2.43): $-\nabla_{su_j} L_\mu = su_j \Delta\pi u_j + \pi u_j \Delta su_j$

$$-\nabla_{su_{P_{g_i}^+}} L_\mu = su_{P_{g_i}^+} \Delta\pi u_{P_{g_i}^+} + \pi u_{P_{g_i}^+} \Delta su_{P_{g_i}^+} \tag{A.I-7}$$

$$-\nabla_{su_{P_{g_i}^-}} L_\mu = su_{P_{g_i}^-} \Delta\pi u_{P_{g_i}^-} + \pi u_{P_{g_i}^-} \Delta su_{P_{g_i}^-} \tag{A.I-8}$$

$$-\nabla_{su_{Q_{g_i}}} L_\mu = su_{Q_{g_i}} \Delta\pi u_{Q_{g_i}} + \pi u_{Q_{g_i}} \Delta su_{Q_{g_i}} \tag{A.I-9}$$

$$-\nabla_{su_{V_i}} L_\mu = su_{V_i} \Delta\pi u_{V_i} + \pi u_{V_i} \Delta su_{V_i} \tag{A.I-10}$$

$$-\nabla_{su_{V_j}} L_\mu = su_{V_j} \Delta\pi u_{V_j} + \pi u_{V_j} \Delta su_{V_j} \tag{A.I-11}$$

$$-\nabla_{su_{s_{ij}^2}} L_\mu = su_{s_{ij}^2} \Delta\pi u_{s_{ij}^2} + \pi u_{s_{ij}^2} \Delta su_{s_{ij}^2} \tag{A.I-12}$$

$$-\nabla_{su_t} L_\mu = su_t \Delta\pi u_t + \pi u_t \Delta su_t \tag{A.I-13}$$

For equation (2.40): $-\nabla_{\pi l_j} L_\mu = -\sum_{j=1}^{N_h} \nabla_{x_k} h_j \Delta x_k + \Delta sl_j$

$$-\nabla_{\pi l_{P_{g_i}^+}} L_\mu = -\nabla_{P_{g_i}^+} h_{P_{g_i}^+} \Delta P_{g_i}^+ + \Delta sl_{P_{g_i}^+} \tag{A.I-14}$$

$$-\nabla_{\pi l_{P_{g_i}^-}} L_\mu = -\nabla_{P_{g_i}^-} h_{P_{g_i}^-} \Delta P_{g_i}^- + \Delta sl_{P_{g_i}^-} \tag{A.I-15}$$

$$-\nabla_{\pi l_{Q_{g_i}}} L_\mu = -\nabla_{Q_{g_i}} h_{Q_{g_i}} \Delta Q_{g_i} + \Delta sl_{Q_{g_i}} \tag{A.I-16}$$

$$-\nabla_{\pi l_{V_i}} L_\mu = -\nabla_{V_i} h_{V_i} \Delta V_i + \Delta sl_{V_i} \tag{A.I-17}$$

$$-\nabla_{\pi l_{V_j}} L_\mu = -\nabla_{V_j} h_{V_j} \Delta V_j + \Delta sl_{V_j} \tag{A.I-18}$$

$$-\nabla_{\pi l_t} L_\mu = -\nabla_t h_t \Delta t + \Delta sl_t \tag{A.I-19}$$

For equation (2.41): $-\nabla_{\pi u_j} L_\mu = -\sum_{j=1}^{N_h} \nabla_{x_k} h_j \Delta x_k - \Delta su_j$

$$-\nabla_{\pi u_{P_{g_i}^+}} L_\mu = -\nabla_{P_{g_i}^+} h_{P_{g_i}^+} \Delta P_{g_i}^+ - \Delta su_{P_{g_i}^+} \tag{A.I-20}$$

$$-\nabla_{\pi u_{P_{g_i}^-}} L_\mu = -\nabla_{P_{g_i}^-} h_{P_{g_i}^-} \Delta P_{g_i}^- - \Delta su_{P_{g_i}^-} \tag{A.I-21}$$

$$-\nabla_{\pi u_{Q_{gi}}} L_\mu = -\nabla_{Q_{gi}} h_{Q_{gi}} \Delta Q_{g_i} - \Delta su_{Q_{gi}} \tag{A.I-22}$$

$$-\nabla_{\pi u_{V_i}} L_\mu = -\nabla_{V_i} h_{V_i} \Delta V_i - \Delta su_{V_i} \tag{A.I-23}$$

$$-\nabla_{\pi u_{V_j}} L_\mu = -\nabla_{V_j} h_{V_j} \Delta V_j - \Delta su_{V_j} \tag{A.I-24}$$

$$-\nabla_{\pi u_{S_{ij}^2}} L_\mu = -\nabla_{\theta_i} h_{S_{ij}^2} \Delta\theta_i - \nabla_{V_i} h_{S_{ij}^2} \Delta V_i - \nabla_{\theta_j} h_{S_{ij}^2} \Delta\theta_j - \nabla_{V_j} h_{S_{ij}^2} \Delta V_j - \Delta su_{S_{ij}^2} \tag{A.I-25}$$

$$-\nabla_{\pi u_t} L_\mu = -\nabla_t h_t \Delta t - \Delta su_t \tag{A.I-26}$$

For equation (2.37) with consideration of power mismatch at bus i and bus j:

$$-\nabla_x L_\mu = \left[-\sum_{i=1}^{N} \nabla_x (\nabla_x \Delta P_i) \lambda_{p_i} - \sum_{i=1}^{N} \nabla_x (\nabla_x \Delta Q_i) \lambda_{q_i} - \sum_{j=1}^{N_h} \nabla_x (\nabla_x h_j) \pi l_j - \sum_{j=1}^{N_h} \nabla_x (\nabla_x h_j) \pi u_j \right] \Delta x$$
$$-\sum_{i=1}^{N} \nabla_{x_k} \Delta P_i \Delta\lambda_{p_i} - \sum_{i=1}^{N} \nabla_{x_k} \Delta Q_i \Delta\lambda_{q_i} - \sum_{j=1}^{N_h} \nabla_{x_k} h_j \Delta\pi l_j - \sum_{j=1}^{N_h} \nabla_{x_k} h_j \Delta\pi u_j$$
$$+\sum_{i=1}^{N_g} \nabla x \nabla x f(x) \Delta x$$

$$-\nabla_{P_{g_i}^+} L_\mu = -\sum_{i=1}^{N} \nabla_{P_{g_i}^+} \Delta P_i \Delta\lambda_{p_i} - \sum_{j=1}^{N_h} \nabla_{P_{g_i}^+} h_{P_{g_i}^+} \Delta\pi l_{P_{g_i}^+} - \sum_{j=1}^{N_h} \nabla_{P_{g_i}^+} h_{P_{g_i}^+} \Delta\pi u_{P_{g_i}^+} \tag{A.I-27}$$

$$-\nabla_{P_{g_i}^-} L_\mu = -\sum_{i=1}^{N} \nabla_{P_{g_i}^-} \Delta P_i \Delta\lambda_{p_i} - \sum_{j=1}^{N_h} \nabla_{P_{g_i}^-} h_{P_{g_i}^-} \Delta\pi l_{P_{g_i}^-} - \sum_{j=1}^{N_h} \nabla_{P_{g_i}^-} h_{P_{g_i}^-} \Delta\pi u_{P_{g_i}^-} \tag{A.I-28}$$

$$-\nabla_{Q_{g_i}} L_\mu = -\sum_{i=1}^{N} \nabla_{Q_{g_i}} \Delta Q_i \Delta\lambda_{q_i} - \sum_{j=1}^{N_h} \nabla_{Q_{g_i}} h_{Q_{g_i}} \Delta\pi l_{Q_{g_i}} - \sum_{j=1}^{N_h} \nabla_{Q_{g_i}} h_{Q_{g_i}} \Delta\pi u_{Q_{g_i}} \tag{A.I-29}$$

$$-\nabla_{\theta_i} L_\mu = \left[-\nabla_{\theta_i} (\nabla_{\theta_i} \Delta P_i) \lambda_{p_i} - \nabla_{\theta_i} (\nabla_{\theta_i} \Delta Q_i) \lambda_{q_i} - \nabla_{\theta_i} (\nabla_{\theta_i} \Delta P_j) \lambda_{p_j} - \nabla_{\theta_i} (\nabla_{\theta_i} \Delta Q_j) \lambda_{q_j} - \nabla_{\theta_i} (\nabla_{\theta_i} h_{S_{ij}^2}) \pi u_{S_{ij}^2} \right] \Delta\theta_i$$
$$+\left[-\nabla_{V_i} (\nabla_{\theta_i} \Delta P_i) \lambda_{p_i} - \nabla_{V_i} (\nabla_{\theta_i} \Delta Q_i) \lambda_{q_i} - \nabla_{V_i} (\nabla_{\theta_i} \Delta P_j) \lambda_{p_j} - \nabla_{V_i} (\nabla_{\theta_i} \Delta Q_j) \lambda_{q_j} - \nabla_{V_i} (\nabla_{\theta_i} h_{S_{ij}^2}) \pi u_{S_{ij}^2} \right] \Delta V_i$$
$$+\left[-\nabla_{\theta_j} (\nabla_{\theta_i} \Delta P_i) \lambda_{p_i} - \nabla_{\theta_j} (\nabla_{\theta_i} \Delta Q_i) \lambda_{q_i} - \nabla_{\theta_j} (\nabla_{\theta_i} \Delta P_j) \lambda_{p_j} - \nabla_{\theta_j} (\nabla_{\theta_i} \Delta Q_j) \lambda_{q_j} - \nabla_{\theta_j} (\nabla_{\theta_i} h_{S_{ij}^2}) \pi u_{S_{ij}^2} \right] \Delta\theta_j$$
$$+\left[-\nabla_{V_j} (\nabla_{\theta_i} \Delta P_i) \lambda_{p_i} - \nabla_{V_j} (\nabla_{\theta_i} \Delta Q_i) \lambda_{q_i} - \nabla_{V_j} (\nabla_{\theta_i} \Delta P_j) \lambda_{p_j} - \nabla_{V_j} (\nabla_{\theta_i} \Delta Q_j) \lambda_{q_j} - \nabla_{V_j} (\nabla_{\theta_i} h_{S_{ij}^2}) \pi u_{S_{ij}^2} \right] \Delta V_j$$
$$+\left[-\nabla_{t_i} (\nabla_{\theta_i} \Delta P_i) \lambda_{p_i} - \nabla_{t_i} (\nabla_{\theta_i} \Delta Q_i) \lambda_{q_i} - \nabla_{t_i} (\nabla_{\theta_i} \Delta P_j) \lambda_{p_j} - \nabla_{t_i} (\nabla_{\theta_i} \Delta Q_j) \lambda_{q_j} \right] \Delta t_i$$
$$-\nabla_{\theta_i} \Delta P_i \Delta\lambda_{p_i} - \nabla_{\theta_i} \Delta Q_i \Delta\lambda_{q_i} - \nabla_{\theta_i} \Delta P_j \Delta\lambda_{p_j} - \nabla_{\theta_i} \Delta Q_j \Delta\lambda_{q_j} - \nabla_{\theta_i} h_{S_{ij}^2} \Delta\pi u_{S_{ij}^2} \tag{A.I-30}$$

$$-\nabla_{V_i} L_\mu = \Big[-\nabla_{V_i}(\nabla_{V_i}\Delta P_i)\lambda_{p_i} - \nabla_{V_i}(\nabla_{V_i}\Delta Q_i)\lambda_{q_i} - \nabla_{V_i}(\nabla_{V_i}\Delta P_j)\lambda_{p_j} - \nabla_{V_i}(\nabla_{V_i}\Delta Q_j)\lambda_{q_j} - \nabla_{V_i}(\nabla_{V_i} h_{S_{ij}^2})\pi u_{S_{ij}^2}\Big]\Delta V_i$$
$$+\Big[-\nabla_{\theta_i}(\nabla_{V_i}\Delta P_i)\lambda_{p_i} - \nabla_{\theta_i}(\nabla_{V_i}\Delta Q_i)\lambda_{q_i} - \nabla_{\theta_i}(\nabla_{V_i}\Delta P_j)\lambda_{p_j} - \nabla_{\theta_i}(\nabla_{V_i}\Delta Q_j)\lambda_{q_j} - \nabla_{\theta_i}(\nabla_{V_i} h_{S_{ij}^2})\pi u_{S_{ij}^2}\Big]\Delta\theta_i$$
$$+\Big[-\nabla_{V_j}(\nabla_{V_i}\Delta P_i)\lambda_{p_i} - \nabla_{V_j}(\nabla_{V_i}\Delta Q_i)\lambda_{q_i} - \nabla_{V_j}(\nabla_{V_i}\Delta P_j)\lambda_{p_j} - \nabla_{V_j}(\nabla_{V_i}\Delta Q_j)\lambda_{q_j} - \nabla_{V_j}(\nabla_{V_i} h_{S_{ij}^2})\pi u_{S_{ij}^2}\Big]\Delta V_j$$
$$+\Big[-\nabla_{\theta_j}(\nabla_{V_i}\Delta P_i)\lambda_{p_i} - \nabla_{\theta_j}(\nabla_{V_i}\Delta Q_i)\lambda_{q_i} - \nabla_{\theta_j}(\nabla_{V_i}\Delta P_j)\lambda_{p_j} - \nabla_{\theta_j}(\nabla_{V_i}\Delta Q_j)\lambda_{q_j} - \nabla_{\theta_j}(\nabla_{V_i} h_{S_{ij}^2})\pi u_{S_{ij}^2}\Big]\Delta\theta_j$$
$$+\Big[-\nabla_{t_i}(\nabla_{V_i}\Delta P_i)\lambda_{p_i} - \nabla_{t_i}(\nabla_{V_i}\Delta Q_i)\lambda_{q_i} - \nabla_{t_i}(\nabla_{V_i}\Delta P_j)\lambda_{p_j} - \nabla_{t_i}(\nabla_{V_i}\Delta Q_j)\lambda_{q_j}\Big]\Delta t_i$$
$$-\nabla_{V_i}\Delta P_i\Delta\lambda_{p_i} - \nabla_{V_i}\Delta Q_i\Delta\lambda_{q_i} - \nabla_{V_i}\Delta P_j\Delta\lambda_{p_j} - \nabla_{V_i}\Delta Q_j\Delta\lambda_{q_i} - \nabla_{V_i} h_{V_i}\Delta\pi l_{V_i} - \nabla_{V_i} h_{V_i}\Delta\pi u_{V_i} - \nabla_{V_i} h_{S_{ij}^2}\Delta\pi u_{S_{ij}^2} \quad \text{(A.I-31)}$$

$$-\nabla_{\theta_j} L_\mu = \Big[-\nabla_{\theta_j}(\nabla_{\theta_j}\Delta P_i)\lambda_{p_i} - \nabla_{\theta_j}(\nabla_{\theta_j}\Delta Q_i)\lambda_{q_i} - \nabla_{\theta_j}(\nabla_{\theta_j}\Delta P_j)\lambda_{p_j} - \nabla_{\theta_j}(\nabla_{\theta_j}\Delta Q_j)\lambda_{q_j} - \nabla_{\theta_j}(\nabla_{\theta_j} h_{S_{ij}^2})\pi u_{S_{ij}^2}\Big]\Delta\theta_j$$
$$+\Big[-\nabla_{\theta_i}(\nabla_{\theta_j}\Delta P_i)\lambda_{p_i} - \nabla_{\theta_i}(\nabla_{\theta_j}\Delta Q_i)\lambda_{q_i} - \nabla_{\theta_i}(\nabla_{\theta_j}\Delta P_j)\lambda_{p_j} - \nabla_{\theta_i}(\nabla_{\theta_j}\Delta Q_j)\lambda_{q_j} - \nabla_{\theta_i}(\nabla_{\theta_j} h_{S_{ij}^2})\pi u_{S_{ij}^2}\Big]\Delta\theta_i$$
$$+\Big[-\nabla_{V_i}(\nabla_{\theta_j}\Delta P_i)\lambda_{p_i} - \nabla_{V_i}(\nabla_{\theta_j}\Delta Q_i)\lambda_{q_i} - \nabla_{V_i}(\nabla_{\theta_j}\Delta P_j)\lambda_{p_j} - \nabla_{V_i}(\nabla_{\theta_j}\Delta Q_j)\lambda_{q_j} - \nabla_{V_i}(\nabla_{\theta_j} h_{S_{ij}^2})\pi u_{S_{ij}^2}\Big]\Delta V_i$$
$$+\Big[-\nabla_{V_j}(\nabla_{\theta_j}\Delta P_i)\lambda_{p_i} - \nabla_{V_j}(\nabla_{\theta_j}\Delta Q_i)\lambda_{q_i} - \nabla_{V_j}(\nabla_{\theta_j}\Delta P_j)\lambda_{p_j} - \nabla_{V_j}(\nabla_{\theta_j}\Delta Q_j)\lambda_{q_j} - \nabla_{V_j}(\nabla_{\theta_j} h_{S_{ij}^2})\pi u_{S_{ij}^2}\Big]\Delta V_j$$
$$+\Big[-\nabla_{t_i}(\nabla_{\theta_j}\Delta P_i)\lambda_{p_i} - \nabla_{t_i}(\nabla_{\theta_j}\Delta Q_i)\lambda_{q_i} - \nabla_{t_i}(\nabla_{\theta_j}\Delta P_j)\lambda_{p_j} - \nabla_{t_i}(\nabla_{\theta_j}\Delta Q_j)\lambda_{q_j}\Big]\Delta t_i$$
$$-\nabla_{\theta_j}\Delta P_i\Delta\lambda_{p_i} - \nabla_{\theta_j}\Delta Q_i\Delta\lambda_{q_i} - \nabla_{\theta_j}\Delta P_j\Delta\lambda_{p_j} - \nabla_{\theta_j}\Delta Q_j\Delta\lambda_{q_j} - \nabla_{\theta_j} h_{S_{ij}^2}\Delta\pi u_{S_{ij}^2} \quad \text{(A.I-32)}$$

$$-\nabla_{V_j} L_\mu = \Big[-\nabla_{V_j}(\nabla_{V_j}\Delta P_i)\lambda_{p_i} - \nabla_{V_j}(\nabla_{V_j}\Delta Q_i)\lambda_{q_i} - \nabla_{V_j}(\nabla_{V_j}\Delta P_j)\lambda_{p_j} - \nabla_{V_j}(\nabla_{V_j}\Delta Q_j)\lambda_{q_j} - \nabla_{V_j}(\nabla_{V_j} h_{S_{ij}^2})\pi u_{S_{ij}^2}\Big]\Delta V_j$$
$$+\Big[-\nabla_{\theta_i}(\nabla_{V_j}\Delta P_i)\lambda_{p_i} - \nabla_{\theta_i}(\nabla_{V_j}\Delta Q_i)\lambda_{q_i} - \nabla_{\theta_i}(\nabla_{V_j}\Delta P_j)\lambda_{p_j} - \nabla_{\theta_i}(\nabla_{V_j}\Delta Q_j)\lambda_{q_j} - \nabla_{\theta_i}(\nabla_{V_j} h_{S_{ij}^2})\pi u_{S_{ij}^2}\Big]\Delta\theta_i$$
$$+\Big[-\nabla_{V_i}(\nabla_{V_j}\Delta P_i)\lambda_{p_i} - \nabla_{V_i}(\nabla_{V_j}\Delta Q_i)\lambda_{q_i} - \nabla_{V_i}(\nabla_{V_j}\Delta P_j)\lambda_{p_j} - \nabla_{V_i}(\nabla_{V_j}\Delta Q_j)\lambda_{q_j} - \nabla_{V_i}(\nabla_{V_j} h_{S_{ij}^2})\pi u_{S_{ij}^2}\Big]\Delta V_i$$
$$+\Big[-\nabla_{\theta_j}(\nabla_{V_j}\Delta P_i)\lambda_{p_i} - \nabla_{\theta_j}(\nabla_{V_j}\Delta Q_i)\lambda_{q_i} - \nabla_{\theta_j}(\nabla_{V_j}\Delta P_j)\lambda_{p_j} - \nabla_{\theta_j}(\nabla_{V_j}\Delta Q_j)\lambda_{q_j} - \nabla_{\theta_j}(\nabla_{V_j} h_{S_{ij}^2})\pi u_{S_{ij}^2}\Big]\Delta\theta_j$$
$$+\Big[-\nabla_{t_i}(\nabla_{V_j}\Delta P_i)\lambda_{p_i} - \nabla_{t_i}(\nabla_{V_j}\Delta Q_i)\lambda_{q_i} - \nabla_{t_i}(\nabla_{V_j}\Delta P_j)\lambda_{p_j} - \nabla_{t_i}(\nabla_{V_j}\Delta Q_j)\lambda_{q_j}\Big]\Delta t_i$$
$$-\nabla_{V_j}\Delta P_i\Delta\lambda_{p_i} - \nabla_{V_j}\Delta Q_i\Delta\lambda_{q_i} - \nabla_{V_j}\Delta P_j\Delta\lambda_{p_j} - \nabla_{V_j}\Delta Q_j\Delta\lambda_{q_i} - \nabla_{V_j} h_{V_j}\Delta\pi l_{V_j} - \nabla_{V_j} h_{V_j}\Delta\pi u_{V_j} - \nabla_{V_j} h_{S_{ij}^2}\Delta\pi u_{S_{ij}^2} \quad \text{(A.I-33)}$$

$$-\nabla_{t_i} L_\mu = \Big[-\nabla_{t_i}(\nabla_{t_i}\Delta P_i)\lambda_{p_i} - \nabla_{t_i}(\nabla_{t_i}\Delta Q_i)\lambda_{q_i} - \nabla_{t_i}(\nabla_{t_i}\Delta P_j)\lambda_{p_j} - \nabla_{t_i}(\nabla_{t_i}\Delta Q_j)\lambda_{q_j}\Big]\Delta t_i$$
$$+\Big[-\nabla_{\theta_i}(\nabla_{t_i}\Delta P_i)\lambda_{p_i} - \nabla_{\theta_i}(\nabla_{t_i}\Delta Q_i)\lambda_{q_i} - \nabla_{\theta_i}(\nabla_{t_i}\Delta P_j)\lambda_{p_j} - \nabla_{\theta_i}(\nabla_{t_i}\Delta Q_j)\lambda_{q_j}\Big]\Delta\theta_i$$
$$+\Big[-\nabla_{V_i}(\nabla_{t_i}\Delta P_i)\lambda_{p_i} - \nabla_{V_i}(\nabla_{t_i}\Delta Q_i)\lambda_{q_i} - \nabla_{V_i}(\nabla_{t_i}\Delta P_j)\lambda_{p_j} - \nabla_{V_i}(\nabla_{t_i}\Delta Q_j)\lambda_{q_j}\Big]\Delta V_i \quad \text{(A.I-34)}$$
$$+\Big[-\nabla_{\theta_j}(\nabla_{t_i}\Delta P_i)\lambda_{p_i} - \nabla_{\theta_j}(\nabla_{t_i}\Delta Q_i)\lambda_{q_i} - \nabla_{\theta_j}(\nabla_{t_i}\Delta P_j)\lambda_{p_j} - \nabla_{\theta_j}(\nabla_{t_i}\Delta Q_j)\lambda_{q_j}\Big]\Delta\theta_j$$
$$+\Big[-\nabla_{V_j}(\nabla_{t_i}\Delta P_i)\lambda_{p_i} - \nabla_{V_j}(\nabla_{t_i}\Delta Q_i)\lambda_{q_i} - \nabla_{V_j}(\nabla_{t_i}\Delta P_j)\lambda_{p_j} - \nabla_{V_j}(\nabla_{t_i}\Delta Q_j)\lambda_{q_j}\Big]\Delta V_j$$
$$-\nabla_{t_i}\Delta P_i\Delta\lambda_{p_i} - \nabla_{t_i}\Delta Q_i\Delta\lambda_{q_i} - \nabla_{t_i}\Delta P_j\Delta\lambda_{p_i} - \nabla_{t_i}\Delta Q_j\Delta\lambda_{q_i} - \nabla_{t_i} h_{t_i}\Delta\pi l_{t_i} - \nabla_{t_i} h_{t_i}\Delta\pi u_{t_i}$$

For equation (2.38): $-\nabla_{\lambda p_i} L_\mu = -\sum_{i=1}^{N} \nabla_x \Delta P_i \Delta x = -\sum_{i=1}^{N} J_{p_i}(x)\Delta x$

$$-\nabla_{\lambda p_i} L_\mu = -\Big[\nabla_{P_{g_i}^+} \Delta P_i \Delta P_{g_i}^+ + \nabla_{P_{g_i}^-} \Delta P_i \Delta P_{g_i}^- + \nabla_{\theta_i} \Delta P_i \Delta \theta_i + \nabla_{V_i} \Delta P_i \Delta V_i + \nabla_{\theta_j} \Delta P_i \Delta \theta_j + \nabla_{V_j} \Delta P_i \Delta V_j + \nabla_{t_i} \Delta P_i \Delta t_i \Big] \quad \text{(A.I-35)}$$

$$-\nabla_{\lambda p_j} L_\mu = -\Big[\nabla_{\theta_i} \Delta P_j \Delta \theta_i + \nabla_{V_i} \Delta P_j \Delta V_i + \nabla_{t_i} \Delta P_j \Delta t_i \Big] \quad \text{(A.I-36)}$$

For equation (2.39): $-\nabla_{\lambda_{q_i}} L_\mu = -\sum_{i=1}^{N} \nabla_x \Delta Q_i \Delta x = -\sum_{i=1}^{N} J_{q_i}(x) \Delta x$

$$-\nabla_{\lambda q_i} L_\mu = -\Big[\nabla_{Q_{g_i}} \Delta Q_i \Delta Q_{g_i} + \nabla_{\theta_i} \Delta Q_i \Delta \theta_i + \nabla_{V_i} \Delta Q_i \Delta V_i + \nabla_{\theta_j} \Delta Q_i \Delta \theta_j + \nabla_{V_j} \Delta Q_i \Delta V_j + \nabla_{t_i} \Delta Q_i \Delta t_i \Big] \quad \text{(A.I-37)}$$

$$-\nabla_{\lambda q_j} L_\mu = -\Big[\nabla_{\theta_i} \Delta Q_j \Delta \theta_i + \nabla_{V_i} \Delta Q_j \Delta V_i + \nabla_{\theta_j} \Delta Q_j \Delta \theta_j + \nabla_{V_j} \Delta Q_j \Delta V_j + \nabla_{t_i} \Delta Q_j \Delta t_i \Big] \quad \text{(A.I-38)}$$

Right-Hand-Side Formulation

From 1st order KKT condition equations, (2.26) – (2.32).

From equation (2.31) $\nabla_{sl_j} L_\mu = \mu - sl_j \pi l_j$

$$\nabla_{sl_{P_{g_i}^+}} L_\mu = \mu - sl_{P_{g_i}^+} \pi l_{P_{g_i}^+} \quad \text{(A.I-39)}$$

$$\nabla_{sl_{P_{g_i}^-}} L_\mu = \mu - sl_{P_{g_i}^-} \pi l_{P_{g_i}^-} \quad \text{(A.I-40)}$$

$$\nabla_{sl_{Q_{g_i}}} L_\mu = \mu - sl_{Q_{g_i}} \pi l_{Q_{g_i}} \quad \text{(A.I-41)}$$

$$\nabla_{sl_{V_i}} L_\mu = \mu - sl_{V_i} \pi l_{V_i} \quad \text{(A.I-42)}$$

s_{ij}^2 has no lower limit

$$\nabla_{sl_{t_i}} L_\mu = \mu - sl_{t_i} \pi l_{t_i} \quad \text{(A.I-43)}$$

From equation (2.32) $\nabla_{su_j} L_\mu = \mu + su_j \pi u_j$

$$\nabla_{su_{P_{g_i}^+}} L_\mu = \mu + su_{P_{g_i}^+} \pi u_{P_{g_i}^+} \quad \text{(A.I-44)}$$

$$\nabla_{su_{P_{g_i}^-}} L_\mu = \mu + su_{P_{g_i}^-} \pi u_{P_{g_i}^-} \quad \text{(A.I-45)}$$

$$\nabla_{su_{Q_{g_i}}} L_\mu = \mu + su_{Q_{g_i}} \pi u_{Q_{g_i}} \quad \text{(A.I-46)}$$

$$\nabla_{su_{V_i}} L_\mu = \mu + su_{V_i}\ \pi u_{V_i} \tag{A.I-47}$$

$$\nabla_{su_{s_{ij}^2}} L_\mu = \mu + su_{s_{ij}^2}\ \pi u_{s_{ij}^2} \tag{A.I-48}$$

$$\nabla_{su_{t_i}} L_\mu = \mu + su_{t_i}\ \pi u_{t_i} \tag{A.I-49}$$

From equation (2.29) $\nabla_{\pi l_j} L_\mu = -\left(h_j - sl_j - h_j^{\min}\right)$

$$\nabla_{\pi l_{P_{g_i}^+}} L_\mu = -\left(P_{g_i}^+ - sl_{P_{g_i}^+} - P_{g_i}^{+\min}\right) \tag{A.I-50}$$

$$\nabla_{\pi l_{P_{g_i}^-}} L_\mu = -\left(P_{g_i}^- - sl_{P_{g_i}^-} - P_{g_i}^{-\min}\right) \tag{A.I-51}$$

$$\nabla_{\pi l_{Q_{g_i}}} L_\mu = -\left(Q_{g_i} - sl_{Q_{g_i}} - Q_{g_i}^{\min}\right) \tag{A.I-52}$$

$$\nabla_{\pi l_{V_i}} L_\mu = -\left(V_i - sl_{V_i} - V_i^{\min}\right) \tag{A.I-53}$$

s_{ij}^2 has no lower limit

$$\nabla_{\pi l_{t_i}} L_\mu = -\left(t_i - sl_{t_i} - t_i^{\min}\right) \tag{A.I-54}$$

From equation (2.30) $\nabla_{\pi u_j} L_\mu = -\left(h_j + su_j - h_j^{\max}\right)$

$$\nabla_{\pi u_{P_{g_i}^+}} L_\mu = -\left(P_{g_i}^+ + su_{P_{g_i}^+} - P_{g_i}^{+\max}\right) \tag{A.I-55}$$

$$\nabla_{\pi u_{P_{g_i}^-}} L_\mu = -\left(P_{g_i}^- + su_{P_{g_i}^-} - P_{g_i}^{-\max}\right) \tag{A.I-56}$$

$$\nabla_{\pi u_{Q_{g_i}}} L_\mu = -\left(Q_{g_i} + su_{Q_{g_i}} - Q_{g_i}^{\max}\right) \tag{A.I-57}$$

$$\nabla_{\pi u_{V_i}} L_\mu = -\left(V_i + su_{V_i} - V_i^{\max}\right) \tag{A.I-58}$$

$$\nabla_{\pi u_{s_{ij}^2}} L_\mu = -\left(s_{ij}^2 + su_{s_{ij}^2} - s_{ij}^{2\max}\right) \tag{A.I-59}$$

$$\nabla_{\pi u_{t_i}} L_\mu = -\left(t_i + su_{t_i} - t_i^{\max}\right) \tag{A.I-60}$$

From equation (2.26) $\nabla_x L_\mu = \nabla x f(x) - \sum_{i=1}^{N} \nabla_x \Delta P_i \lambda_{p_i} - \sum_{i=1}^{N} \nabla_x \Delta Q_i \lambda_{q_i} - \sum_{j=1}^{N_h} \nabla_x h_j \pi l_j - \sum_{j=1}^{N_h} \nabla_x h_j \pi u_j$

$$\nabla_{\substack{P^+\\g_i}} L_\mu = \nabla_{\substack{P^+\\g_i}} f(x) - \nabla_{\substack{P^+\\g_i}} \Delta P_i \lambda_{p_i} - \nabla_{\substack{P^+\\g_i}} h_{\substack{P^+\\g_i}} \pi l_{\substack{P^+\\g_i}} - \nabla_{\substack{P^+\\g_i}} h_{\substack{P^+\\g_i}} \pi u_{\substack{P^+\\g_i}} \tag{A.I-61}$$

$$\nabla_{P_{g_i}^-} L_\mu = \nabla_{P_{g_i}^-} f(x) - \nabla_{P_{g_i}^-} \Delta P_i \lambda_{p_i} - \nabla_{P_{g_i}^-} h_{P_{g_i}^-} \pi l_{P_{g_i}^-} - \nabla_{P_{g_i}^-} h_{P_{g_i}^-} \pi u_{P_{g_i}^-} \tag{A.I-62}$$

$$\nabla_{Q_{g_i}} L_\mu = \nabla_{Q_{g_i}} f(x) - \nabla_{Q_{g_i}} \Delta Q_i \lambda_{q_i} - \nabla_{Q_{g_i}} h_{Q_{g_i}} \pi l_{Q_{g_i}} - \nabla_{Q_{g_i}} h_{Q_{g_i}} \pi u_{Q_{g_i}} \tag{A.I-63}$$

$$\begin{aligned}\nabla_{\theta_i} L_\mu = &-\nabla_{\theta_i} \Delta P_i \lambda_{p_i} - \nabla_{\theta_i} \Delta Q_i \lambda_{q_i} - \nabla_{\theta_i} \Delta P_j \lambda_{p_j} - \nabla_{\theta_i} \Delta Q_j \lambda_{q_j} - \nabla_{\theta_i} h_{\theta_i} \pi l_{\theta_i} \\ &- \nabla_{\theta_i} h_{\theta_i} \pi u_{\theta_i} - \nabla_{\theta_i} h_{S_{ij}^2} \pi u_{S_{ij}^2}\end{aligned} \tag{A.I-64}$$

$$\begin{aligned}\nabla_{V_i} L_\mu = &-\nabla_{V_i} \Delta P_i \lambda_{p_i} - \nabla_{V_i} \Delta Q_i \lambda_{q_i} - \nabla_{V_i} \Delta P_j \lambda_{p_j} - \nabla_{V_i} \Delta Q_j \lambda_{q_j} - \nabla_{V_i} h_{V_i} \pi l_{V_i} \\ &- \nabla_{V_i} h_{V_i} \pi u_{V_i} - \nabla_{V_i} h_{S_{ij}^2} \pi u_{S_{ij}^2}\end{aligned} \tag{A.I-65}$$

$$\nabla_{t_i} L_\mu = -\nabla_{t_i} \Delta P_i \lambda_{p_i} - \nabla_{t_i} \Delta Q_i \lambda_{q_i} - \nabla_{t_i} \Delta P_j \lambda_{p_j} - \nabla_{t_i} \Delta Q_j \lambda_{q_j} - \nabla_{t_i} h_{t_i} \pi l_t - \nabla_{t_i} h_{t_i} \pi u_{t_i} \tag{A.I-66}$$

From equation (2.27)

$$\nabla_{\lambda p_i} L_\mu = -\Delta P_i = -\left(P_{g_i} + P_{g_i}^+ - P_{g_i}^- - P_{d_i} - P_i \right) \tag{A.I-67}$$

From equation (2.28)

$$\nabla_{\lambda q_i} L_\mu = -\Delta Q_i = -\left(Q_{g_i} - Q_{d_i} - Q_i \right) \tag{A.I-68}$$

Appendix II

Derivation of power mismatch equations as presented in Chapter 2 and Appendix I

The derivation of the power mismatch equations for the following components of the transmission system in hybrid equation representation are presented in this appendix,

- Transmission line
- Transformer

The power mismatch equations are derived first using a single-line system with one generator and one load. Where, hybrid representation uses polar coordinates for voltages and rectangular coordinates for admittances.

Derivation of power mismatch equations for hybrid equation representation

Steady-state model of a two-bus system with one generator bus, one load bus and one transmission line (branch *ij*).

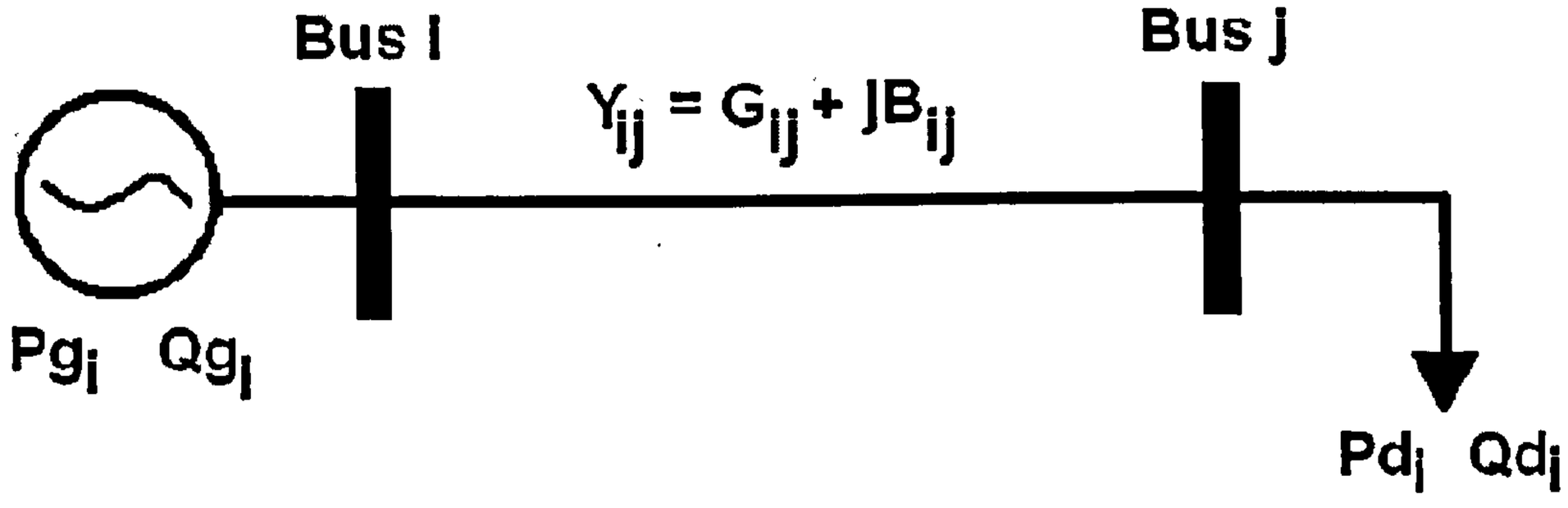

Figure AII-1: 2 bus system.

where,

P_{g_i} is the real power generated at bus *i*,

Q_{g_i} is the reactive power generated at bus *i*,

P_{d_j} is the real power demand at bus *j*,

Q_{d_j} is the reactive power demand at bus *j*,

Y_{ij} is the admittance of the transmission line equal to $Y_{ij} = G_{ij} + jB_{ij}$.

Complex power S_{ij} flows from bus i to bus j. The complex power at bus i is [Gronen (1988)],

$$S_i = P_i + jQ_i = V_i I_i^* = V_i \left[\sum_{j=1}^{N} Y_{ij} V_j \right] \tag{A.II-1}$$

where,

i and j are the bus index numbers,

V_i is the voltage at bus i, $V_i\left(\cos\theta_i + j\sin\theta_i\right)$,

V_j is the voltage at bus j, $V_j\left(\cos\theta_j + j\sin\theta_j\right)$,

I_i is the current at bus i,

Y_{ij} is the admittance of branch ij between buses i and j,

N is the total number of system buses.

In hybrid representation the voltage is represented in polar coordinates and admittance in rectangular coordinates.

$$P_i + jQ_i = V_i\left(\cos\theta_i + j\sin\theta_i\right)\left[\sum_{j=1}^{N} (G_{ij} + jB_{ij})\left(V_j\left(\cos\theta_j + j\sin\theta_j\right)\right) \right]^* \tag{A.II-2}$$

where,

θ_i is the voltage angle at bus i,

θ_j is the voltage angle at bus j,

G_{ij} is the conductance or real part of the branch admittance Y_{ij},

B_{ij} is the susceptance or the imaginary part of the branch admittance Y_{ij}.

Expand terms in the parenthesis, substitute the complex conjugate and separate real and imaginary parts. Complex power in hybrid equation representation.

$$P_i + jQ_i = V_i\left(\cos\theta_i + j\sin\theta_i\right)\left[\sum_{j=1}^{N} V_j\left(G_{ij}\cos\theta_j - B_{ij}\sin\theta_j\right) - jV_j\left(G_{ij}\sin\theta_j + B_{ij}\cos\theta_j\right) \right] \tag{A.II-3}$$

Include voltage at bus i, and group real and imaginary components.

$$\begin{aligned} P_i + jQ_i = \sum_{j=1}^{N} \Big\{ & V_i V_j \left[G_{ij}\left(\cos\left(\theta_i - \theta_j\right) + B_{ij}\sin\left(\theta_i - \theta_j\right)\right)\right] \\ & + jV_i V_j \left[G_{ij}\left(\sin\left(\theta_i - \theta_j\right) - B_{ij}\cos\left(\theta_i - \theta_j\right)\right)\right] \Big\} \end{aligned} \tag{A.II-4}$$

Real and reactive power mismatch equations are,

$$\Delta P_i = P_{g_i} - P_{d_i} - P_i \tag{A.II-5}$$

$$\Delta Q_i = Q_{g_i} - Q_{d_i} - Q_i \tag{A.II-6}$$

where,

P_i is the real power injection at bus i,

Q_i is the reactive power injection at bus i.

The general form of the power injection equations is,

$$P_i = \sum_{j=1}^{N} P_{ij} = \sum_{j=1}^{N} \left\{ V_i V_j \left[G_{ij} \left(\cos\left(\theta_i - \theta_j\right) + B_{ij} \sin\left(\theta_i - \theta_j\right) \right) \right] \right\} \tag{A.II-7}$$

$$Q_i = \sum_{j=1}^{N} Q_{ij} = \sum_{j=1}^{N} \left\{ V_i V_j \left[G_{ij} \left(\sin\left(\theta_i - \theta_j\right) - B_{ij} \cos\left(\theta_i - \theta_j\right) \right) \right] \right\} \tag{A.II-8}$$

where,

N is the total number of branches connected to bus i.

Modelling and derivation of transmission line power flow equations

A transmission line can be represented by the following equivalent circuit,

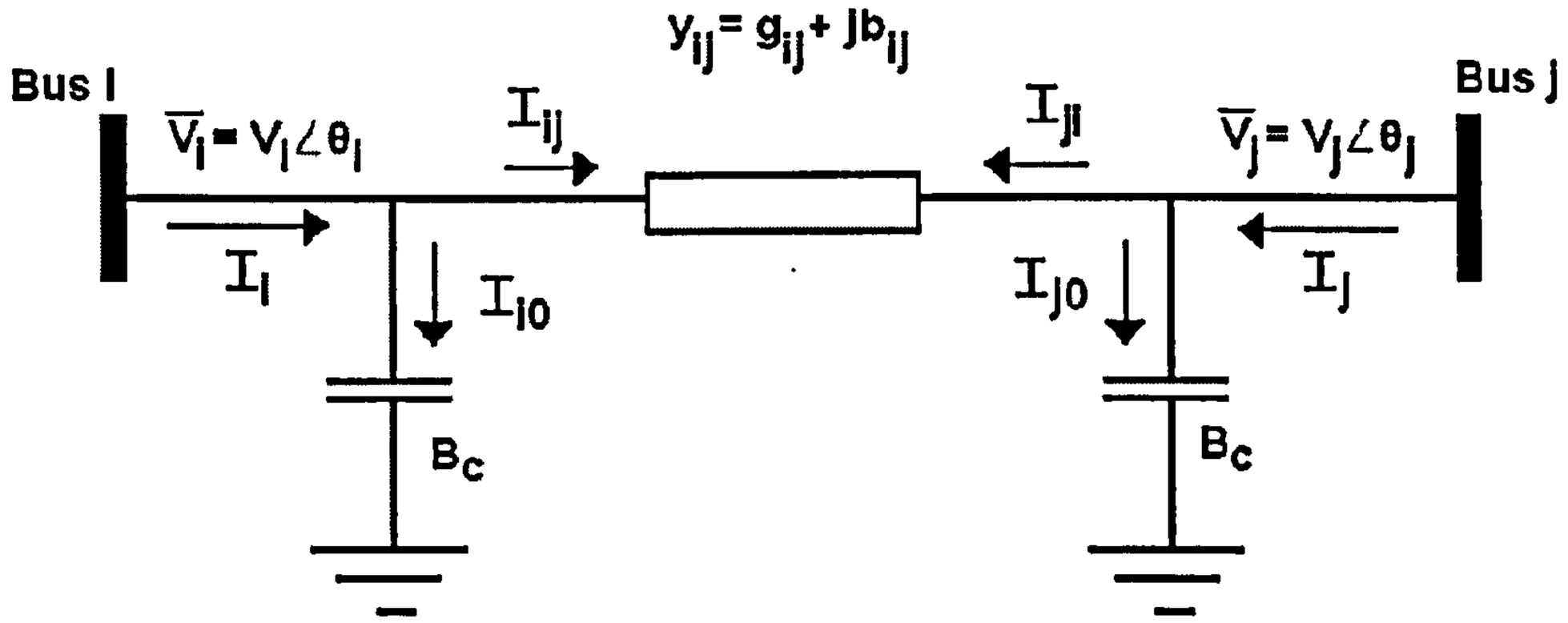

Figure AII-2: Transmission line model.

where,

$$I_{io} = jB_c V_i \tag{A.II-9}$$

$$I_{ij} = (g_{ij} + jb_{ij})(V_i - V_j) \tag{A.II-10}$$

$y_{ij} = g_{ij} + jb_{ij}$ is the branch admittance element.

The current at bus i is,

$$I_i = I_{io} + I_{ij} \tag{A.II-11}$$

Substitute (A.II-9) and (A.II-10),

$$I_i = (g_{ij} + jb_{ij})(V_i - V_j) + jB_c V_i \tag{A.II-12}$$

Group terms with respect to voltages and bus i and j,

$$I_i = \left[g_{ij} + j(b_{ij} + B_c)\right]V_i - (g_{ij} + jb_{ij})V_j \tag{A.II-13}$$

In matrix form,

$$\begin{bmatrix} I_i \\ I_j \end{bmatrix} = \begin{bmatrix} Y_{ii} & Y_{ij} \\ Y_{ji} & Y_{jj} \end{bmatrix}\begin{bmatrix} V_i \\ V_j \end{bmatrix} = \begin{bmatrix} g_{ij} + j(b_{ij} + B_c) & -(g_{ij} + jb_{ij}) \\ -(g_{ij} + jb_{ij}) & g_{ij} + j(b_{ij} + B_c) \end{bmatrix}\begin{bmatrix} V_i \\ V_j \end{bmatrix} \tag{A.II-14}$$

Note that $Y_{ij} = Y_{ji}$.

Substitute voltages and group real and imaginary parts the currents at buses i and j become,

$$\begin{aligned} I_i = {} & V_i\left[g_{ij}\cos\theta_i - (b_{ij} + B_c)\sin\theta_i\right] - V_j\left[g_{ij}\cos\theta_j - b_{ij}\sin\theta_j\right] \\ & + j\left\{V_i\left[g_{ij}\sin\theta_i + (b_{ij} + B_c)\cos\theta_i\right] - V_j\left[g_{ij}\sin\theta_j + b_{ij}\cos\theta_j\right]\right\} \end{aligned} \tag{A.II-15}$$

$$\begin{aligned} I_j = {} & V_j\left[g_{ij}\cos\theta_j - (b_{ij} + B_c)\sin\theta_j\right] - V_i\left[g_{ij}\cos\theta_i - b_{ij}\sin\theta_i\right] \\ & + j\left\{V_j\left[g_{ij}\sin\theta_j + (b_{ij} + B_c)\cos\theta_j\right] - V_i\left[g_{ij}\sin\theta_i + b_{ij}\cos\theta_i\right]\right\} \end{aligned} \tag{A.II-16}$$

The complex power S_{ij} flows from bus i to bus j, equation (A.II-1),

$$S_{ij} = P_{ij} + jQ_{ij} = V_i I_i^* = \left[V_i(\cos\theta_i + j\sin\theta_i)\right]I_i^* \tag{A.II-17}$$

Substitute I_i^*, the real and reactive power flow equations are,

$$P_{ij} = V_i^2 g_{ij} - V_i V_j\left[g_{ij}\cos\left(\theta_i - \theta_j\right) + b_{ij}\sin\left(\theta_i - \theta_j\right)\right] \tag{A.II-18}$$

$$Q_{ij} = -V_i^2\left(b_{ij} - B_c\right) - V_i V_j\left[g_{ij}\sin\left(\theta_i - \theta_j\right) - b_{ij}\cos\left(\theta_i - \theta_j\right)\right] \tag{A.II-19}$$

Substitute admittance elements g_{ij} and b_{ij} with the equivalent $-G_{ij}$ and $-B_{ij}$ for the off-diagonal terms respectively, the real and reactive power flows in general terms are obtained:

$$P_{ij} = V_i^2 g_{ij} + V_i V_j\left[G_{ij}\cos\left(\theta_i - \theta_j\right) + B_{ij}\sin\left(\theta_i - \theta_j\right)\right] \tag{A.II-20}$$

$$Q_{ij} = -V_i^2\left(b_{ij} - B_c\right) + V_i V_j\left[G_{ij}\sin\left(\theta_i - \theta_j\right) - B_{ij}\cos\left(\theta_i - \theta_j\right)\right] \tag{A.II-21}$$

where, $g_{ij} = -G_{ij}$ and $b_{ij} = -B_{ij}$.

G_{ij} is the short form for $\sum_{j=1}^{N} g_{ij}$,

B_{ij} is the short form for $\sum_{j=1}^{N} b_{ij}$,

N is the total number of branches connected to bus i.

The transmission line capacity is given by,

$$S_{ij}^2 = \left(P_{ij}^2 + jQ_{ij}^2\right) \tag{A.II-22}$$

Where P_{ij} and Q_{ij} are given by equations (A.II-18 and A.II-20) and (A.II-19 and A.II-21) respectively.

Modelling and derivation of transformer with tap ratio control power flow equations

Steady state transformer model with tap ratio control at primary side bus i.

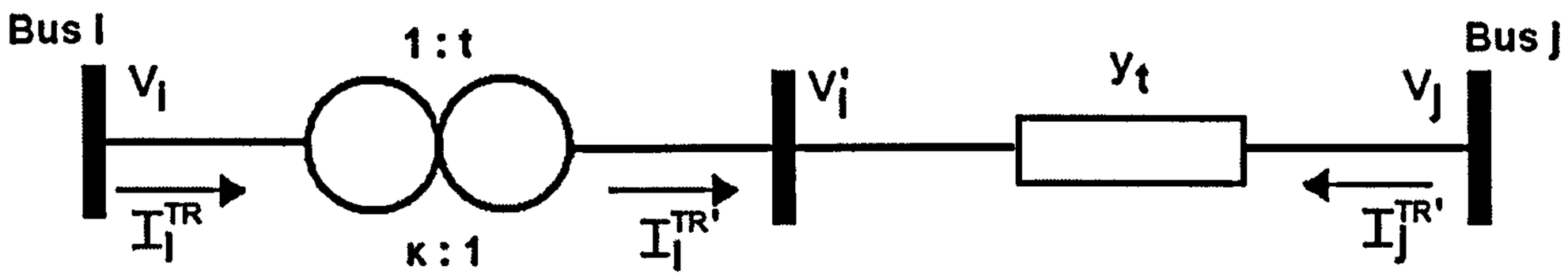

Figure AII-3: Transformer model.

where,

V_i and I_i^{TR} are the primary side voltage and current respectively,

$V_i^{'}$ and $I_i^{TR'}$ are the secondary side voltage and current respectively,

V_j and I_j^{TR} are the voltage and current at bus j,

t is the tap value,

κ is the tap-ratio, related to t as defined below,

y_t is the transformer admittance.

Note that $\frac{1}{t} = \frac{V_i}{V_i^{'}} = \frac{I_i^{TR'}}{I_i^{TR}} = \kappa$, and the tap-ratio control is assumed to be at the same side as bus i.

The secondary current is equivalent to, $I_i^{TR'} = \frac{I_i^{TR}}{t}$ and is be calculated by, $I_i^{TR'} = \left(V_i^{'} - V_j\right) y_t$. The secondary voltage is equivalent to $V_i^{'} = tV_i$. Substitute the secondary side values to obtain current on primary side of transformer,

$$I_i^{TR} = t\left(tV_i - V_j\right) y_t = t^2 y_t V_i - t y_t V_j \tag{A.II-23}$$

The current at bus j is equal to,

$$I_j^{TR} = \left(V_j - V_i^{'}\right) y_t = \left(V_j - tV_i^{'}\right) y_t = -t y_t V_i - y_t V_j \tag{A.II-24}$$

The current equations in matrix form are,

$$\begin{bmatrix} I_i^{TR} \\ I_j^{TR} \end{bmatrix} = \begin{bmatrix} Y_{ii} & Y_{ij} \\ Y_{ji} & Y_{jj} \end{bmatrix} \begin{bmatrix} V_i \\ V_j \end{bmatrix} = \begin{bmatrix} t^2 y_t & -t y_t \\ -t y_t & y_t \end{bmatrix} \begin{bmatrix} V_i \\ V_j \end{bmatrix}$$

The transformer equivalent circuit,

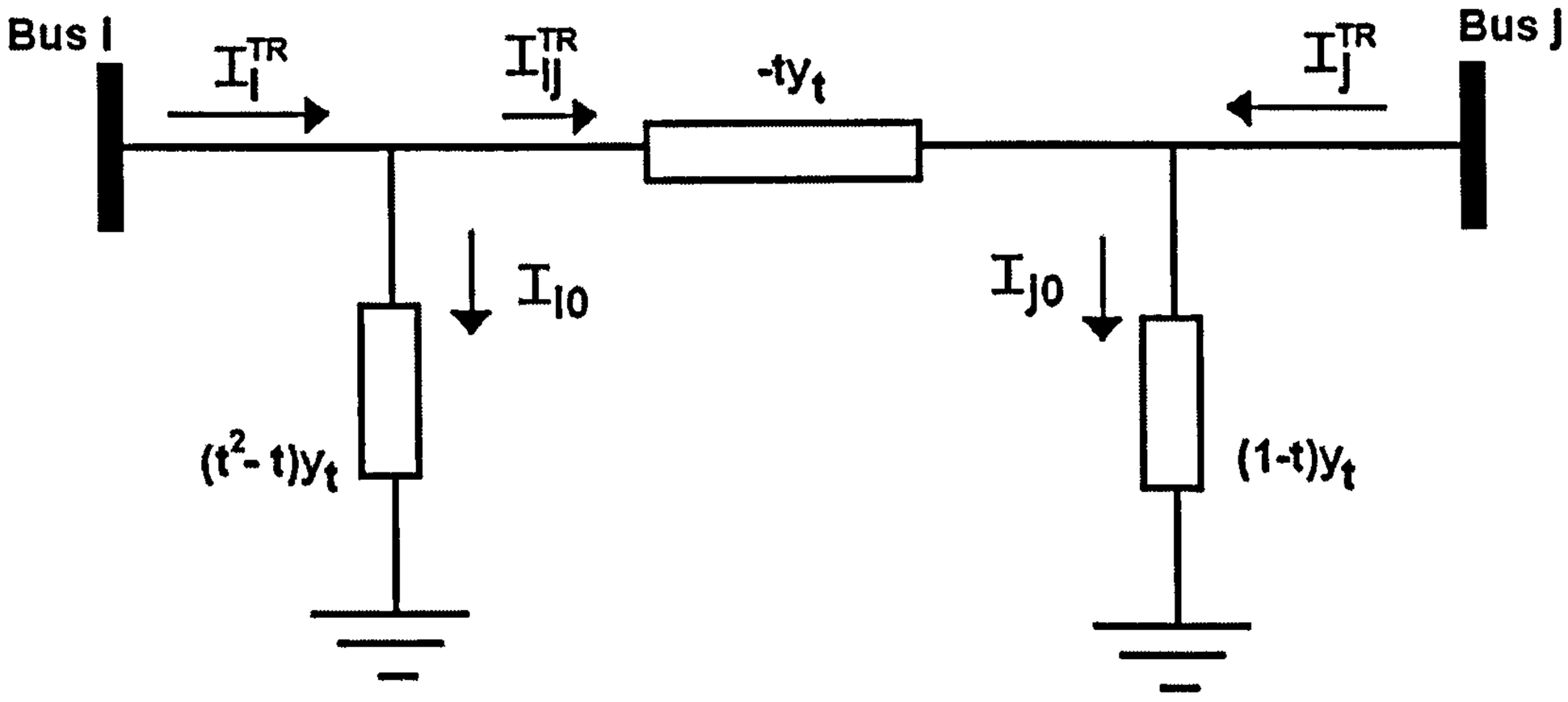

Figure AII-4: Transformer equivalent circuit.

where, y_t is the transformer admittance, equal to, $y_t = g_{ij} + jb_{ij}$. Substitute transformer admittance and voltages into equations (A.II-23) and (A.II-24),

$$\begin{aligned} I_i^{TR} = {} & V_i t^2 \left[g_{ij} \cos\theta_i - b_{ij} \sin\theta_i + j\left(g_{ij} \sin\theta_i + b_{ij} \cos\theta_i\right)\right] \\ & - V_j t \left[g_{ij} \cos\theta_j - b_{ij} \sin\theta_j + j\left(g_{ij} \sin\theta_j + b_{ij} \cos\theta_j\right)\right] \end{aligned} \tag{A.II-25}$$

$$\begin{aligned} I_j^{TR} = {} & -V_i t \left[g_{ij} \cos\theta_i - b_{ij} \sin\theta_i + j\left(g_{ij} \sin\theta_i + b_{ij} \cos\theta_i\right)\right] \\ & + V_j \left[g_{ij} \cos\theta_j - b_{ij} \sin\theta_j + j\left(g_{ij} \sin\theta_j + b_{ij} \cos\theta_j\right)\right] \end{aligned} \tag{A.II-26}$$

The complex power between buses i and j is $S_{ij} = V_i I_i^{TR*}$. By substituting equation (A.II-25) the complex power flow of a transmission line with a transformer with tap ratio control on bus side i is,

$$P_{ij}^{TR} = V_i^2 t^2 g_{ij} - V_i V_j t\left[g_{ij}\cos\left(\theta_i - \theta_j\right) + b_{ij}\sin\left(\theta_i - \theta_j\right)\right] \quad \text{(A.II-27)}$$

$$Q_{ij}^{TR} = -V_i^2 t^2 b_{ij} - V_i V_j t\left[g_{ij}\sin\left(\theta_i - \theta_j\right) - b_{ij}\cos\left(\theta_i - \theta_j\right)\right] \quad \text{(A.II-28)}$$

Signs should match (A.II-18) and (A.II-19).

$$S_{ij}^{TR} = P_{ij}^{TR} + jQ_{ij}^{TR}$$

The corresponding complex power flow from bus j to bus i with transformer tap ratio control on side i,

$$P_{ji}^{TR} = V_i^2 g_{ij} - V_i V_j t\left[g_{ij}\cos\left(\theta_i - \theta_j\right) - b_{ij}\sin\left(\theta_i - \theta_j\right)\right] \quad \text{(A.II-29)}$$

$$Q_{ji}^{TR} = -V_j^2 b_{ij} + V_i V_j t\left[g_{ij}\sin\left(\theta_i - \theta_j\right) + b_{ij}\cos\left(\theta_i - \theta_j\right)\right] \quad \text{(A.II-30)}$$

$$S_{ji}^{TR} = V_j I_j^{TR*} = P_{ji}^{TR} + jQ_{ji}^{TR}$$

The transformer tap value t is represented in the real and reactive power mismatch equations as follows,

$$\Delta P_i = P_{g_i} - P_{d_i} - P_i \quad \text{(A.II-31)}$$

$$\Delta Q_i = Q_{g_i} - Q_{d_i} - Q_i \quad \text{(A.II-32)}$$

where,

$$P_i = \sum_{j=1}^{N} P_{ij} + \sum_{j=1}^{Nt} P_{ij}^{TR} \quad \text{(A.II-33)}$$

$$Q_i = \sum_{j=1}^{N} Q_{ij} + \sum_{j=1}^{Nt} Q_{ij}^{TR} \quad \text{(A.II-34)}$$

where,

N is the total number of branches connected to bus i,

Nt is the total number of transformers connected to bus i.

System variables, x

- At all buses, N, there are two system variables, θ_i, V_i.
- At all generator buses, N_g, there are three system variables, $\Delta P_{g_i}^{+}, \Delta P_{g_i}^{-}, Q_{g_i}$.

- At all buses with transformer tap ratio control, N_t, there is one system variable, t.
- At all buses with a FACTS controller, N_F, there are four system variables, $\theta_{se}, V_{se}, \theta_{sh}, V_{sh}$.

S_{ij}^2 Functional constrain equation of transmission line

The transmission line capacity S_{ij}^2 is a functional constraint of the system variables x.

$$S_{ij}^2 = P_{ij}^2 + Q_{ij}^2 \tag{A.II-35}$$

$$P_{ij} = V_i^2 g_{ii} - V_i V_j \left(g_{ij} \cos(\theta_i - \theta_j) + b_{ij} \sin(\theta_i - \theta_j) \right) \tag{A.II-36}$$

$$Q_{ij} = -V_i^2 b_{ii} - V_i V_j \left(g_{ij} \sin(\theta_i - \theta_j) - b_{ij} \cos(\theta_i - \theta_j) \right) \tag{A.II-37}$$

When $h(x) = S_{ij}^2$ and $h_j^{\max}(x) = S_{ij}^{2\max}$, the single sided inequality is,

$$S_{ij}^2 < S_{ij}^{2\max} \tag{A.II-38}$$

The associated slack and dual variables are, $su_{S_{ij}^2}$ and $\pi u_{S_{ij}^2}$.

The Lagrange function only concerning S_{ij}^2, $S_{ij}^{2\max}$, $su_{S_{ij}^2}$ and $\pi u_{S_{ij}^2}$ is,

$$L_{\mu, S_{ij}^2} = -\mu \sum_{j=1}^{N_h} \ln(su_j) - \sum_{j=1}^{N_h} \pi u_j (h_j + su_j - h_j^{\max}) \tag{A.II-39}$$

First derivative,

$$\frac{\partial L_{\mu, S_{ij}^2}}{\partial x} = -\pi u_j \left(\frac{\partial S_{ij}^2}{\partial x} \right) \tag{A.II-40}$$

Second derivative,

$$\frac{\partial^2 L_{\mu, S_{ij}^2}}{\partial x \partial x} = -\pi u_j \left(\frac{\partial^2 S_{ij}^2}{\partial x \partial x} \right) \tag{A.II-41}$$

Where the term on the right hand side in the brackets are,

$$\frac{\partial S_{ij}^2}{\partial x} = 2P_{ij} \frac{\partial P_{ij}}{\partial x} + 2Q_{ij} \frac{\partial Q_{ij}}{\partial x} \tag{A.II-42}$$

$$\frac{\partial^2 S_{ij}^2}{\partial x \partial x} = 2 \frac{\partial P_{ij}}{\partial x} \frac{\partial P_{ij}}{\partial x} + 2 \frac{\partial Q_{ij}}{\partial x} \frac{\partial Q_{ij}}{\partial x} 2P_{ij} \frac{\partial^2 P_{ij}}{\partial x \partial x} + 2Q_{ij} \frac{\partial^2 Q_{ij}}{\partial x \partial x} \tag{A.II-43}$$

Transformer tap ratio constraint t

The transformer tap ratio is a double-sided inequality constraint,

$$t^{\min} < t < t^{\max}$$

where $h(x) = t$, $h_j^{\min}(x) = t^{\min}$ and $h_j^{\max}(x) = t^{\max}$. The associated slack and dual variables are, $sl_t, \pi l_t, su_t$ and πu_t. The Lagrange function only concerning, t, $t^{\min}$, $t^{\max}$, $sl_t, \pi l_t, su_t$ and πu_t is,

$$\begin{aligned} L_{\mu,t} = &-\mu \sum_{j=1}^{N_h} \ln(sl_j) - \mu \sum_{j=1}^{N_h} \ln(su_j) - \sum_{j=1}^{N_h} \pi l_j (h_j - sl_j - h_j^{\min}) \\ &- \sum_{j=1}^{N_h} \pi u_j (h_j + su_j - h_j^{\max}) \end{aligned} \tag{A.II-44}$$

First derivative,

$$\frac{\partial L_{\mu,t}}{\partial t} = -\left(\pi l_j + \pi u_j\right)\left(\frac{\partial h_j(x)}{\partial t}\right) \tag{A.II-45}$$

where, $\frac{\partial h_j(x)}{\partial t} = 1$.

Second derivative,

$$\frac{\partial^2 L_{\mu,t}}{\partial t^2} = 0 \tag{A.II-46}$$

Reference

Gronen, T., (1988) "Modern Power System Analysis", *John Wiley & Sons, Inc.*

APPENDIX III

Formulation for FACTS controllers for the interior point OPF using hybrid coordinate representation of the power mismatch equations, as presented in Chapter 3.

All relevant formulations are presented for bus *i* and branch *ij* where the non-diagonal parts are considered.

Additional Newton matrix elements for FACTS controllers only:

Equations (3.27) - (3.36) where,

$$h_j^{FACTS} = \left[\theta_{se}, V_{se}, \theta_{sh}, V_{sh}\right]$$

$$x^{FACTS} = \left[\theta_i, V_i, \theta_j, V_j, \theta_{se}, V_{se}, \theta_{sh}, V_{sh}\right]$$

$$x_{k_\alpha}^{FACTS} = \left[x^{FACTS}, sl_j^{FACTS}, su_j^{FACTS}, \pi l_j^{FACTS}, \pi u_j^{FACTS}, \lambda_{p_i}, \lambda_{q_i}, \lambda_{p_j}, \lambda_{q_j}, \lambda_{PE}, \lambda_{PC}, \lambda_{QC}\right]$$

$$sl_j^{FACTS} = \left[sl_{\theta_{se}}, sl_{V_{se}}, sl_{\theta_{sh}}, sl_{V_{sh}}\right]$$

$$su_j^{FACTS} = \left[su_{\theta_{se}}, su_{V_{se}}, su_{\theta_{sh}}, su_{V_{sh}}\right]$$

$$\pi l_j^{FACTS} = \left[\pi l_{\theta_{se}}, \pi l_{V_{se}}, \pi l_{\theta_{sh}}, \pi l_{V_{sh}}\right]$$

$$\pi u_j^{FACTS} = \left[\pi u_{\theta_{se}}, \pi u_{V_{se}}, \pi u_{\theta_{sh}}, \pi u_{V_{sh}}\right]$$

N is the total number of buses on the system,

N_g is the total number of generators on the system,

N_t is the total number of transformers on the system,

N_F is the total number of FACTS controllers on the system,

N_h is the total number of inequality constraints.

Left-hand-side formulation

For equation (3.35): $-\nabla_{sl_j} L_\mu = -sl_j \Delta\pi l_j - \pi l_j \Delta sl_j$

$$-\nabla_{sl_{\theta_{se}}} L_\mu = -sl_{\theta_{se}} \Delta\pi l_{\theta_{se}} - \pi l_{\theta_{se}} \Delta sl_{\theta_{se}} \qquad \text{(A.III-1)}$$

$$-\nabla_{sl_{V_{se}}} L_\mu = -sl_{V_{se}} \Delta\pi l_{V_{se}} - \pi l_{V_{se}} \Delta sl_{V_{se}} \qquad \text{(A.III-2)}$$

$$-\nabla_{sl_{\theta_{sh}}} L_\mu = -sl_{\theta_{sh}} \Delta\pi l_{\theta_{sh}} - \pi l_{\theta_{sh}} \Delta sl_{\theta_{sh}} \quad \text{(A.III-3)}$$

$$-\nabla_{sl_{V_{sh}}} L_\mu = -sl_{V_{sh}} \Delta\pi l_{V_{sh}} - \pi l_{V_{sh}} \Delta sl_{V_{sh}} \quad \text{(A.III-4)}$$

For equation (3.36): $-\nabla_{su_j} L_\mu = su_j \Delta\pi u_j + \pi u_j \Delta su_j$

$$-\nabla_{su_{\theta_{se}}} L_\mu = su_{\theta_{se}} \Delta\pi u_{\theta_{se}} + \pi u_{\theta_{se}} \Delta su_{\theta_{se}} \quad \text{(A.III-5)}$$

$$-\nabla_{su_{V_{se}}} L_\mu = su_{V_{se}} \Delta\pi u_{V_{se}} + \pi u_{V_{se}} \Delta su_{V_{se}} \quad \text{(A.III-6)}$$

$$-\nabla_{su_{\theta_{sh}}} L_\mu = su_{\theta_{sh}} \Delta\pi u_{\theta_{sh}} + \pi u_{\theta_{sh}} \Delta su_{\theta_{sh}} \quad \text{(A.III-7)}$$

$$-\nabla_{su_{V_{sh}}} L_\mu = su_{V_{sh}} \Delta\pi u_{V_{sh}} + \pi u_{V_{sh}} \Delta su_{V_{sh}} \quad \text{(A.III-8)}$$

For equation (3.33): $-\nabla_{\pi l_j} L_\mu = -\sum_{j=1}^{N_h} \nabla_x h_j \Delta x + \Delta sl_j$

$$-\nabla_{\pi l_{\theta_{se}}} L_\mu = -\nabla_{\theta_{se}} h_{\theta_{se}} \Delta\theta_{se} + \Delta sl_{\theta_{se}} \quad \text{(A.III-9)}$$

$$-\nabla_{\pi l_{V_{se}}} L_\mu = -\nabla_{V_{se}} h_{V_{se}} \Delta V_{se} + \Delta sl_{V_{se}} \quad \text{(A.III-10)}$$

$$-\nabla_{\pi l_{\theta_{sh}}} L_\mu = -\nabla_{\theta_{sh}} h_{\theta_{sh}} \Delta\theta_{sh} + \Delta sl_{\theta_{sh}} \quad \text{(A.III-11)}$$

$$-\nabla_{\pi l_{V_{sh}}} L_\mu = -\nabla_{V_{sh}} h_{V_{sh}} \Delta V_{sh} + \Delta sl_{V_{sh}} \quad \text{(A.III-12)}$$

For equation (3.34): $-\nabla_{\pi u_j} L_\mu = -\sum_{j=1}^{N_h} \nabla_x h_j \Delta x - \Delta su_j$

$$-\nabla_{\pi u_{\theta_{se}}} L_\mu = -\nabla_{\theta_{se}} h_{\theta_{se}} \Delta\theta_{se} - \Delta su_{\theta_{se}} \quad \text{(A.III-13)}$$

$$-\nabla_{\pi u_{V_{se}}} L_\mu = -\nabla_{V_{se}} h_{V_{se}} \Delta V_{se} - \Delta su_{V_{se}} \quad \text{(A.III-14)}$$

$$-\nabla_{\pi u_{\theta_{sh}}} L_\mu = -\nabla_{\theta_{sh}} h_{\theta_{sh}} \Delta\theta_{sh} - \Delta su_{\theta_{sh}} \quad \text{(A.III-15)}$$

$$-\nabla_{\pi u_{V_{sh}}} L_\mu = -\nabla_{V_{sh}} h_{V_{sh}} \Delta V_{sh} - \Delta su_{V_{sh}} \quad \text{(A.III-16)}$$

For equation (2.37) with consideration of power mismatch at bus i and bus j:

$$-\nabla_x L_\mu = \left[-\sum_{i=1}^{N} \nabla_x (\nabla_x \Delta P_i) \lambda_{p_i} - \sum_{i=1}^{N} \nabla_x (\nabla_x \Delta Q_i) \lambda_{q_i} - \sum_{j=1}^{N_h} \nabla_x (\nabla_x h_j) \pi l_j - \sum_{j=1}^{N_h} \nabla_x (\nabla_x h_j) \pi u_j \right] \Delta x$$
$$-\sum_{i=1}^{N} \nabla_{x_k} \Delta P_i \Delta \lambda_{p_i} - \sum_{i=1}^{N} \nabla_{x_k} \Delta Q_i \Delta \lambda_{q_i} - \sum_{j=1}^{N_h} \nabla_{x_k} h_j \Delta \pi l_j - \sum_{j=1}^{N_h} \nabla_{x_k} h_j \Delta \pi u_j \qquad \text{(A.III-17)}$$
$$+\sum_{i=1}^{N_g} \nabla x \nabla x f(x) \Delta x$$

$$-\nabla_{\theta_{se}} L_\mu = \left[-\nabla_{\theta_{se}} (\nabla_{\theta_{se}} \Delta P_i) \lambda_{p_i} - \nabla_{\theta_{se}} (\nabla_{\theta_{se}} \Delta Q_i) \lambda_{q_i} - \nabla_{\theta_{se}} (\nabla_{\theta_{se}} \Delta P_j) \lambda_{p_j} - \nabla_{\theta_{se}} (\nabla_{\theta_{se}} \Delta Q_j) \lambda_{q_j} \right.$$
$$\left. - \nabla_{\theta_{se}} (\nabla_{\theta_{se}} \Delta PE_{UPFC}) \lambda_{PE_{UPFC}} \right] \Delta \theta_{se}$$
$$+ \left[-\nabla_{V_{se}} (\nabla_{\theta_{se}} \Delta P_i) \lambda_{p_i} - \nabla_{V_{se}} (\nabla_{\theta_{se}} \Delta Q_i) \lambda_{q_i} - \nabla_{V_{se}} (\nabla_{\theta_{se}} \Delta P_j) \lambda_{p_j} - \nabla_{V_{se}} (\nabla_{\theta_{se}} \Delta Q_j) \lambda_{q_j} \right.$$
$$\left. - \nabla_{V_{se}} (\nabla_{\theta_{se}} \Delta PE_{UPFC}) \lambda_{PE_{UPFC}} \right] \Delta V_{se} \qquad \text{(A.III-18)}$$
$$+ \left[-\nabla_{\theta_i} (\nabla_{\theta_{se}} \Delta P_i) \lambda_{p_i} - \nabla_{\theta_i} (\nabla_{\theta_{se}} \Delta Q_i) \lambda_{q_i} - \nabla_{\theta_i} (\nabla_{\theta_{se}} \Delta PE_{UPFC}) \lambda_{PE_{UPFC}} \right] \Delta \theta_i$$
$$+ \left[-\nabla_{V_i} (\nabla_{\theta_{se}} \Delta P_i) \lambda_{p_i} - \nabla_{V_i} (\nabla_{\theta_{se}} \Delta Q_i) \lambda_{q_i} - \nabla_{V_i} (\nabla_{\theta_{se}} \Delta PE_{UPFC}) \lambda_{PE_{UPFC}} \right] \Delta V_i$$
$$+ \left[-\nabla_{\theta_j} (\nabla_{\theta_{se}} \Delta P_j) \lambda_{p_j} - \nabla_{\theta_j} (\nabla_{\theta_{se}} \Delta Q_j) \lambda_{q_j} - \nabla_{\theta_j} (\nabla_{\theta_{se}} \Delta PE_{UPFC}) \lambda_{PE_{UPFC}} \right] \Delta \theta_j$$
$$+ \left[-\nabla_{V_j} (\nabla_{\theta_{se}} \Delta P_j) \lambda_{p_j} - \nabla_{V_j} (\nabla_{\theta_{se}} \Delta Q_j) \lambda_{q_j} - \nabla_{V_j} (\nabla_{\theta_{se}} \Delta PE_{UPFC}) \lambda_{PE_{UPFC}} \right] \Delta V_j$$
$$-\nabla_{\theta_{se}} \Delta P_i \Delta \lambda_{p_i} - \nabla_{\theta_{se}} \Delta Q_i \Delta \lambda_{q_i} - \nabla_{\theta_{se}} h_{\theta_{se}} \Delta \pi u_{\theta_{se}}$$

$$-\nabla_{V_{se}} L_\mu = \left[-\nabla_{V_{se}} \left(\nabla_{V_{se}} PE_{UPFC} \right) \lambda_{PE_{UPFC}} \right] \Delta V_{se}$$
$$+ \left[-\nabla_{\theta_{se}} (\nabla_{V_{se}} \Delta P_i) \lambda_{p_i} - \nabla_{\theta_{se}} (\nabla_{V_{se}} \Delta Q_i) \lambda_{q_i} - \nabla_{\theta_{se}} (\nabla_{V_{se}} \Delta P_j) \lambda_{p_j} - \nabla_{\theta_{se}} (\nabla_{V_{se}} \Delta Q_j) \lambda_{q_j} \right.$$
$$\left. - \nabla_{\theta_{se}} (\nabla_{V_{se}} \Delta PE_{UPFC}) \lambda_{PE_{UPFC}} \right] \Delta \theta_{se}$$
$$+ \left[-\nabla_{\theta_i} (\nabla_{V_{se}} \Delta P_i) \lambda_{p_i} - \nabla_{\theta_i} (\nabla_{V_{se}} \Delta Q_i) \lambda_{q_i} - \nabla_{\theta_i} (\nabla_{V_{se}} \Delta PE_{UPFC}) \lambda_{PE_{UPFC}} \right] \Delta \theta_i \qquad \text{(A.III-19)}$$
$$+ \left[-\nabla_{V_i} (\nabla_{V_{se}} \Delta P_i) \lambda_{p_i} - \nabla_{V_i} (\nabla_{V_{se}} \Delta Q_i) \lambda_{q_i} - \nabla_{V_i} (\nabla_{V_{se}} \Delta PE_{UPFC}) \lambda_{PE_{UPFC}} \right] \Delta V_i$$
$$+ \left[-\nabla_{\theta_j} (\nabla_{V_{se}} \Delta P_j) \lambda_{p_j} - \nabla_{\theta_j} (\nabla_{V_{se}} \Delta Q_j) \lambda_{q_j} - \nabla_{\theta_j} (\nabla_{V_{se}} \Delta PE_{UPFC}) \lambda_{PE_{UPFC}} \right] \Delta \theta_j$$
$$+ \left[-\nabla_{V_j} (\nabla_{V_{se}} \Delta P_j) \lambda_{p_j} - \nabla_{V_j} (\nabla_{V_{se}} \Delta Q_j) \lambda_{q_j} - \nabla_{V_j} (\nabla_{V_{se}} \Delta PE_{UPFC}) \lambda_{PE_{UPFC}} \right] \Delta V_j$$
$$-\nabla_{V_{se}} \Delta P_i \Delta \lambda_{p_i} - \nabla_{V_{se}} \Delta Q_i \Delta \lambda_{q_i} - \nabla_{V_{se}} \Delta P_j \Delta \lambda_{p_j} - \nabla_{V_{se}} \Delta Q_j \Delta \lambda_{q_j} - \nabla_{V_{se}} h_{V_{se}} \Delta \pi u_{V_{se}}$$

$$-\nabla_{\theta_{sh}} L_\mu = \left[-\nabla_{\theta_{sh}} (\nabla_{\theta_{sh}} \Delta P_i) \lambda_{p_i} - \nabla_{\theta_{sh}} (\nabla_{\theta_{sh}} \Delta Q_i) \lambda_{q_i} - \nabla_{\theta_{sh}} (\nabla_{\theta_{sh}} \Delta PE_{UPFC}) \lambda_{PE_{UPFC}} \right] \Delta \theta_{sh}$$
$$+ \left[-\nabla_{V_{sh}} (\nabla_{\theta_{sh}} \Delta P_i) \lambda_{p_i} - \nabla_{V_{sh}} (\nabla_{\theta_{sh}} \Delta Q_i) \lambda_{q_i} - \nabla_{V_{sh}} (\nabla_{\theta_{sh}} \Delta PE_{UPFC}) \lambda_{PE_{UPFC}} \right] \Delta V_{sh}$$
$$+ \left[-\nabla_{\theta_i} (\nabla_{\theta_{sh}} \Delta P_i) \lambda_{p_i} - \nabla_{\theta_i} (\nabla_{\theta_{sh}} \Delta Q_i) \lambda_{q_i} - \nabla_{\theta_i} (\nabla_{\theta_{sh}} \Delta PE_{UPFC}) \lambda_{PE_{UPFC}} \right] \Delta \theta_i \qquad \text{(A.III-20)}$$
$$+ \left[-\nabla_{V_i} (\nabla_{\theta_{sh}} \Delta P_i) \lambda_{p_i} - \nabla_{V_i} (\nabla_{\theta_{sh}} \Delta Q_i) \lambda_{q_i} - \nabla_{V_i} (\nabla_{\theta_{sh}} \Delta PE_{UPFC}) \lambda_{PE_{UPFC}} \right] \Delta V_i$$
$$-\nabla_{\theta_{sh}} \Delta P_i \Delta \lambda_{p_i} - \nabla_{\theta_{sh}} \Delta Q_i \Delta \lambda_{q_i} - \nabla_{\theta_{sh}} h_{\theta_{sh}} \Delta \pi u_{\theta_{sh}}$$

$$
\begin{aligned}
-\nabla V_{sh} L_{\mu} = & \left[-\nabla V_{sh} (\nabla \theta_{sh} \Delta PE_{UPFC}) \lambda_{PE_{UPFC}}\right] \Delta V_{sh} \\
& + \left[-\nabla \theta_{sh} (\nabla V_{sh} \Delta P_i) \lambda_{p_i} - \nabla \theta_{sh} (\nabla V_{sh} \Delta Q_i) \lambda_{q_i} - \nabla \theta_{sh} (\nabla V_{sh} \Delta PE_{UPFC}) \lambda_{PE_{UPFC}}\right] \Delta \theta_{sh} \\
& + \left[-\nabla \theta_i (\nabla V_{sh} \Delta P_i) \lambda_{p_i} - \nabla \theta_i (\nabla V_{sh} \Delta Q_i) \lambda_{q_i} - \nabla \theta_i (\nabla V_{sh} \Delta PE_{UPFC}) \lambda_{PE_{UPFC}}\right] \Delta \theta_i \\
& + \left[-\nabla V_i (\nabla \theta_{sh} \Delta P_i) \lambda_{p_i} - \nabla V_i (\nabla V_{sh} \Delta Q_i) \lambda_{q_i} - \nabla V_i (\nabla V_{sh} \Delta PE_{UPFC}) \lambda_{PE_{UPFC}}\right] \Delta V_i \\
& - \nabla V_{sh} \Delta P_i \Delta \lambda_{p_i} - \nabla V_{sh} \Delta Q_i \Delta \lambda_{q_i} - \nabla V_{sh} h_{V_{sh}} \Delta \pi u_{V_{sh}}
\end{aligned}
\tag{A.III-21}
$$

$$
\begin{aligned}
-\nabla \theta_i L_{\mu} = & \left[-\nabla \theta_i (\nabla \theta_i \Delta P_i) \lambda_{p_i} - \nabla \theta_i (\nabla \theta_i \Delta Q_i) \lambda_{q_i} - \nabla \theta_i (\nabla \theta_i \Delta PE_{UPFC}) \lambda_{PE_{UPFC}}\right] \Delta \theta_i \\
& + \left[-\nabla V_i (\nabla \theta_i \Delta P_i) \lambda_{p_i} - \nabla V_i (\nabla \theta_i \Delta Q_i) \lambda_{q_i} - \nabla V_i (\nabla \theta_i \Delta PE_{UPFC}) \lambda_{PE_{UPFC}}\right] \Delta V_i \\
& + \left[-\nabla \theta_{se} (\nabla \theta_i \Delta P_i) \lambda_{p_i} - \nabla \theta_{se} (\nabla \theta_i \Delta Q_i) \lambda_{q_i} - \nabla \theta_{se} (\nabla \theta_i \Delta PE_{UPFC}) \lambda_{PE_{UPFC}}\right] \Delta \theta_{se} \\
& + \left[-\nabla V_{se} (\nabla \theta_i \Delta P_i) \lambda_{p_i} - \nabla V_{se} (\nabla \theta_i \Delta Q_i) \lambda_{q_i} - \nabla V_{se} (\nabla \theta_i \Delta PE_{UPFC}) \lambda_{PE_{UPFC}}\right] \Delta V_{se} \\
& + \left[-\nabla \theta_{sh} (\nabla \theta_i \Delta P_i) \lambda_{p_i} - \nabla \theta_{sh} (\nabla \theta_i \Delta Q_i) \lambda_{q_i} - \nabla \theta_{sh} (\nabla \theta_i \Delta PE_{UPFC}) \lambda_{PE_{UPFC}}\right] \Delta \theta_{sh} \\
& + \left[-\nabla V_{sh} (\nabla \theta_i \Delta P_i) \lambda_{p_i} - \nabla V_{sh} (\nabla \theta_i \Delta Q_i) \lambda_{q_i} - \nabla V_{sh} (\nabla \theta_i \Delta PE_{UPFC}) \lambda_{PE_{UPFC}}\right] \Delta V_{sh} \\
& - \nabla \theta_i \Delta P_i \Delta \lambda_{p_i} - \nabla \theta_i \Delta Q_i \Delta \lambda_{q_i}
\end{aligned}
\tag{A.III-22}
$$

$$
\begin{aligned}
-\nabla V_i L_{\mu} = & \left[-\nabla \theta_i (\nabla V_i \Delta P_i) \lambda_{p_i} - \nabla \theta_i (\nabla V_i \Delta Q_i) \lambda_{q_i} - \nabla \theta_i (\nabla V_i PE_{UPFC}) \lambda_{PE_{UPFC}}\right] \Delta \theta_i \\
& + \left[-\nabla \theta_{se} (\nabla V_i \Delta P_i) \lambda_{p_i} - \nabla \theta_{se} (\nabla V_i \Delta Q_i) \lambda_{q_i} - \nabla \theta_{se} (\nabla V_i PE_{UPFC}) \lambda_{PE_{UPFC}}\right] \Delta \theta_{se} \\
& + \left[-\nabla V_{se} (\nabla V_i \Delta P_i) \lambda_{p_i} - \nabla V_{se} (\nabla V_i \Delta Q_i) \lambda_{q_i} - \nabla V_{se} (\nabla V_i PE_{UPFC}) \lambda_{PE_{UPFC}}\right] \Delta V_{se} \\
& + \left[-\nabla \theta_{sh} (\nabla V_i \Delta P_i) \lambda_{p_i} - \nabla \theta_{sh} (\nabla V_i \Delta Q_i) \lambda_{q_i} - \nabla \theta_{sh} (\nabla V_i PE_{UPFC}) \lambda_{PE_{UPFC}}\right] \Delta \theta_{sh} \\
& + \left[-\nabla V_{sh} (\nabla V_i \Delta P_i) \lambda_{p_i} - \nabla V_{sh} (\nabla V_i \Delta Q_i) \lambda_{q_i} - \nabla V_{sh} (\nabla V_i PE_{UPFC}) \lambda_{PE_{UPFC}}\right] \Delta V_{sh} \\
& - \nabla V_i \Delta P_i \Delta \lambda_{p_i} - \nabla V_i \Delta Q_i \Delta \lambda_{q_i}
\end{aligned}
\tag{A.III-23}
$$

$$
\begin{aligned}
-\nabla \theta_j L_{\mu} = & \left[-\nabla \theta_j (\nabla \theta_j \Delta P_j) \lambda_{p_j} - \nabla \theta_j (\nabla \theta_j \Delta Q_j) \lambda_{q_j} - \nabla \theta_j (\nabla \theta_j \Delta PE_{UPFC}) \lambda_{PE_{UPFC}}\right] \Delta \theta_j \\
& + \left[-\nabla V_j (\nabla \theta_j \Delta P_j) \lambda_{p_j} - \nabla V_j (\nabla \theta_j \Delta Q_j) \lambda_{q_j} - \nabla V_j (\nabla \theta_j \Delta PE_{UPFC}) \lambda_{PE_{UPFC}}\right] \Delta V_j \\
& + \left[-\nabla \theta_{se} (\nabla \theta_j \Delta P_j) \lambda_{p_j} - \nabla \theta_{se} (\nabla \theta_j \Delta Q_j) \lambda_{q_j} - \nabla \theta_{se} (\nabla \theta_j \Delta PE_{UPFC}) \lambda_{PE_{UPFC}}\right] \Delta \theta_{se} \\
& + \left[-\nabla V_{se} (\nabla \theta_j \Delta P_j) \lambda_{p_j} - \nabla V_{se} (\nabla \theta_j \Delta Q_j) \lambda_{q_j} - \nabla V_{se} (\nabla \theta_j \Delta PE_{UPFC}) \lambda_{PE_{UPFC}}\right] \Delta V_{se} \\
& - \nabla \theta_j \Delta P_j \Delta \lambda_{p_j} - \nabla \theta_j \Delta Q_j \Delta \lambda_{q_j}
\end{aligned}
\tag{A.III-24}
$$

$$
\begin{aligned}
-\nabla V_j L_{\mu} = & \left[-\nabla \theta_j (\nabla V_j \Delta P_j) \lambda_{p_j} - \nabla \theta_j (\nabla V_j \Delta Q_j) \lambda_{q_j} - \nabla \theta_j (\nabla V_j \Delta PE_{UPFC}) \lambda_{PE_{UPFC}}\right] \Delta \theta_j \\
& + \left[-\nabla \theta_{se} (\nabla V_j \Delta P_j) \lambda_{p_j} - \nabla \theta_{se} (\nabla V_j \Delta Q_j) \lambda_{q_j} - \nabla \theta_{se} (\nabla V_j \Delta PE_{UPFC}) \lambda_{PE_{UPFC}}\right] \Delta \theta_{se} \\
& + \left[-\nabla V_{se} (\nabla V_j \Delta P_j) \lambda_{p_j} - \nabla V_{se} (\nabla V_j \Delta Q_j) \lambda_{q_j} - \nabla V_{se} (\nabla V_j \Delta PE_{UPFC}) \lambda_{PE_{UPFC}}\right] \Delta V_{se} \\
& - \nabla V_j \Delta P_j \Delta \lambda_{p_j} - \nabla V_j \Delta Q_j \Delta \lambda_{q_j}
\end{aligned}
\tag{A.III-25}
$$

For equation (3.28): $-\nabla \lambda_{p_i} L_{\mu} = -\sum_{i=1}^{N} \nabla_x \Delta P_i \Delta x = -\sum_{i=1}^{N} J_{p_i}(x) \Delta x$ and

$$
-\nabla \lambda_{p_j} L_{\mu} = -\sum_{j=1}^{N} \nabla_x \Delta P_j \Delta x = -\sum_{j=1}^{N} J_{p_j}(x) \Delta x \tag{A.III-26}
$$

$$-\nabla\lambda_{p_i}L_\mu=-\Big[\nabla_{\theta_{se}}\Delta P_i\Delta\theta_{se}+\nabla_{V_{se}}\Delta P_i\Delta V_{se}+\nabla_{\theta_{sh}}\Delta P_i\Delta\theta_{sh}+\nabla_{V_{sh}}\Delta P_i\Delta V_{sh}+\nabla_{\theta_i}\Delta P_i\Delta\theta_i+\nabla_{V_i}\Delta P_i\Delta V_i\ \Delta V_i\Big] \quad \text{(A.III-27)}$$

$$-\nabla\lambda_{p_j}L_\mu=-\Big[\nabla_{\theta_{se}}\Delta P_j\Delta\theta_{se}+\nabla_{V_{se}}\Delta P_j\Delta V_{se}+\nabla_{\theta_j}\Delta P_j\Delta\theta_j+\nabla_{V_j}\Delta P_j\Delta V_j\Big] \quad \text{(A.III-28)}$$

For equation (3.29): $-\nabla\lambda_{q_i}L_\mu=-\sum_{i=1}^{N}\nabla_x\Delta Q_i\Delta x=-\sum_{i=1}^{N}J_{q_i}(x)\Delta x$ and

$$-\nabla\lambda_{q_j}L_\mu=-\sum_{j=1}^{N}\nabla_x\Delta Q_j\Delta x=-\sum_{j=1}^{N}J_{q_j}(x)\Delta x \quad \text{(A.III-29)}$$

$$-\nabla\lambda_{q_i}L_\mu=-\Big[\nabla_{\theta_{se}}\Delta Q_i\Delta\theta_{se}+\nabla_{V_{se}}\Delta Q_i\Delta V_{se}+\nabla_{\theta_{sh}}\Delta Q_i\Delta\theta_{sh}+\nabla_{V_{sh}}\Delta Q_i\Delta V_{sh}+\nabla_{\theta_i}\Delta Q_i\Delta\theta_i+\nabla_{V_i}\Delta Q_i\Delta V_i\Big] \quad \text{(A.III-30)}$$

$$-\nabla\lambda_{q_j}L_\mu=-\Big[\nabla_{\theta_{se}}\Delta Q_j\Delta\theta_{se}+\nabla_{V_{se}}\Delta Q_j\Delta V_{se}+\nabla_{\theta_j}\Delta Q_j\Delta\theta_j+\nabla_{V_j}\Delta Q_j\Delta V_j\Big] \quad \text{(A.III-31)}$$

For equation (3.30): $-\nabla\lambda_{PE_i}L_\mu=-\sum_{i=1}^{N_F}\nabla_x PE_i\Delta x$

$$-\nabla\lambda_{PE_i}L_\mu=-\Big[\nabla\theta_{se}PE_i\Delta\theta_{se}+\nabla V_{se}PE_i\Delta V_{se}+\nabla\theta_{sh}PE_i\Delta\theta_{sh}+\nabla V_{sh}PE_i\Delta V_{sh}+\nabla\theta_i PE_i\Delta\theta_i+\nabla V_i PE_i\Delta V_i+\nabla\theta_j PE_i\Delta\theta_j+\nabla V_j PE_i\Delta V_j\Big] \quad \text{(A.III-32)}$$

For equation (3.31): $-\nabla\lambda_{PC_i}L_\mu=-\sum_{i=1}^{N_F}\nabla_x PC_i\Delta x$

$$-\nabla\lambda_{PC_i}L_\mu=-\Big[\nabla_{\theta_{se}}PC_i\Delta\theta_{se}+\nabla_{V_{se}}PC_i\Delta V_{se}+\nabla_{\theta_i}PC_i\Delta\theta_i+\nabla_{V_i}PC_i\Delta V_i+\nabla_{\theta_j}PC_j\Delta\theta_j+\nabla_{V_j}PC_j\Delta V_j\Big] \quad \text{(A.III-33)}$$

For equation (3.32): $-\nabla\lambda_{QC_i}L_\mu=-\sum_{i=1}^{N_F}\nabla_x QC_i\Delta x$

$$-\nabla\lambda_{QC_i}L_\mu=-\Big[\nabla_{\theta_{se}}QC_i\Delta\theta_{se}+\nabla_{V_{se}}QC_i\Delta V_{se}+\nabla_{\theta_i}QC_i\Delta\theta_i+\nabla_{V_i}QC_i\Delta V_i+\nabla_{\theta_j}QC_i\Delta\theta_j+\nabla_{V_j}QC_i\Delta V_j\Big] \quad \text{(A.III-34)}$$

Right-hand-side formulation

From 1st order KKT condition equations, (3.17) – (3.26).

From equation (3.25) $\nabla_{sl_j} L_\mu = \mu - sl_j \pi l_j$

$$\nabla_{sl_{\theta_{se}}} L_\mu = \mu - sl_{\theta_{se}} \pi l_{\theta_{se}} \tag{A.III-35}$$

$$\nabla_{sl_{V_{se}}} L_\mu = \mu - sl_{V_{se}} \pi l_{V_{se}} \tag{A.III-36}$$

$$\nabla_{sl_{\theta_{sh}}} L_\mu = \mu - sl_{\theta_{sh}} \pi l_{\theta_{sh}} \tag{A.III-37}$$

$$\nabla_{sl_{V_{sh}}} L_\mu = \mu - sl_{V_{sh}} \pi l_{V_{sh}} \tag{A.III-38}$$

From equation (3.26) $\nabla_{su_j} L_\mu = \mu + su_j \pi u_j$

$$\nabla_{su_{\theta_{se}}} L_\mu = \mu + su_{\theta_{se}} \pi u_{\theta_{se}} \tag{A.III-39}$$

$$\nabla_{su_{V_{se}}} L_\mu = \mu + su_{V_{se}} \pi u_{V_{se}} \tag{A.III-40}$$

$$\nabla_{su_{\theta_{sh}}} L_\mu = \mu + su_{\theta_{sh}} \pi u_{\theta_{sh}} \tag{A.III-41}$$

$$\nabla_{su_{V_{sh}}} L_\mu = \mu + su_{V_{sh}} \pi u_{V_{sh}} \tag{A.III-42}$$

From equation (3.23) $\nabla_{\pi l_j} L_\mu = -\left(h_j - sl_j - h_j^{\min}\right)$

$$\nabla_{\pi l_{\theta_{se}}} L_\mu = -\left(\theta_{se} - sl_{\theta_{se}} - \theta_{se}^{\min}\right) \tag{A.III-43}$$

$$\nabla_{\pi l_{V_{se}}} L_\mu = -\left(V_{se} - sl_{V_{se}} - V_{se}^{\min}\right) \tag{A.III-44}$$

$$\nabla_{\pi l_{\theta_{sh}}} L_\mu = -\left(\theta_{sh} - sl_{\theta_{sh}} - \theta_{sh}^{\min}\right) \tag{A.III-45}$$

$$\nabla_{\pi l_{V_{sh}}} L_\mu = -\left(V_{sh} - sl_{V_{sh}} - V_{sh}^{\min}\right) \tag{A.III-46}$$

From equation (3.24) $\nabla_{\pi u_j} L_\mu = -\left(h_j + su_j - h_j^{\max}\right)$

$$\nabla_{\pi u_{\theta_{se}}} L_\mu = -\left(\theta_{se} + su_{\theta_{se}} - \theta_{se}^{\max}\right) \tag{A.III-47}$$

$$\nabla_{\pi u_{V_{se}}} L_\mu = -\left(V_{se} + su_{V_{se}} - V_{se}^{\max}\right) \tag{A.III-48}$$

$$\nabla_{\pi u_{\theta_{sh}}} L_\mu = -\left(\theta_{sh} + su_{\theta_{sh}} - \theta_{sh}^{\max}\right) \tag{A.III-49}$$

$$\nabla_{\pi u_{V_{sh}}} L_\mu = -\left(V_{sh} + su_{V_{sh}} - V_{sh}^{\max} \right) \tag{A.III-50}$$

From equation (3.17) $\nabla_x L_\mu = \nabla x f(x) - \sum_{i=1}^{N} \nabla_x \Delta P_i \lambda_{p_i} - \sum_{i=1}^{N} \nabla_x \Delta Q_i \lambda_{q_i} - \sum_{j=1}^{N_h} \nabla_x h_j \pi l_j - \sum_{j=1}^{N_h} \nabla_x h_j \pi u_j$

$$\nabla_{\theta_{se}} L_\mu = -\nabla_{\theta_{se}} \Delta P_i \lambda_{p_i} - \nabla_{\theta_{se}} \Delta Q_i \lambda_{q_i} - \nabla_{\theta_{se}} \Delta P_j \lambda_{p_j} - \nabla_{\theta_{se}} \Delta Q_j \lambda_{q_j} - \nabla_{\theta_{se}} PE_{UPFC} \lambda_{PE_{UPFC}} - \nabla_{\theta_{se}} h_{\theta_{se}} \pi l_{\theta_{se}} - \nabla_{\theta_{se}} h_{\theta_{se}} \pi u_{\theta_{se}} \tag{A.III-51}$$

$$\nabla_{V_{se}} L_\mu = -\nabla_{V_{se}} \Delta P_i \lambda_{p_i} - \nabla_{V_{se}} \Delta Q_i \lambda_{q_i} - \nabla_{V_{se}} \Delta P_j \lambda_{p_j} - \nabla_{V_{se}} \Delta Q_j \lambda_{q_j} - \nabla_{V_{se}} PE_{UPFC} \lambda_{PE_{UPFC}} - \nabla_{V_{se}} h_{V_{se}} \pi l_{V_{se}} - \nabla_{V_{se}} h_{V_{se}} \pi u_{V_{se}} \tag{A.III-52}$$

$$\nabla_{\theta_{sh}} L_\mu = -\nabla_{\theta_{sh}} \Delta P_i \lambda_{p_i} - \nabla_{\theta_{sh}} \Delta Q_i \lambda_{q_i} - \nabla_{\theta_{sh}} PE_{UPFC} \lambda_{PE_{UPFC}} - \nabla_{\theta_{sh}} h_{\theta_{sh}} \pi l_{\theta_{sh}} - \nabla_{\theta_{sh}} h_{\theta_{sh}} \pi u_{\theta_{sh}} \tag{A.III-53}$$

$$\nabla_{V_{sh}} L_\mu = -\nabla_{V_{sh}} \Delta P_i \lambda_{p_i} - \nabla_{V_{sh}} \Delta Q_i \lambda_{q_i} - \nabla_{V_{sh}} PE_{UPFC} \lambda_{PE_{UPFC}} - \nabla_{V_{sh}} h_{V_{sh}} \pi l_{V_{sh}} - \nabla_{V_{sh}} h_{V_{sh}} \pi u_{V_{sh}} \tag{A.III-54}$$

$$\nabla_{\theta_i} L_\mu = -\nabla_{\theta_i} \Delta P_i \lambda_{p_i} - \nabla_{\theta_i} \Delta Q_i \lambda_{q_i} - \nabla_{\theta_i} PE_{UPFC} \lambda_{PE_{UPFC}} \tag{A.III-55}$$

$$\nabla_{V_i} L_\mu = -\nabla_{V_i} \Delta P_i \lambda_{p_i} - \nabla_{V_i} \Delta Q_i \lambda_{q_i} - \nabla_{V_i} PE_{UPFC} \lambda_{PE_{UPFC}} \tag{A.III-56}$$

$$\nabla_{\theta_j} L_\mu = -\nabla_{\theta_j} \Delta P_j \lambda_{p_j} - \nabla_{\theta_j} \Delta Q_j \lambda_{q_j} - \nabla_{\theta_j} PE_{UPFC} \lambda_{PE_{UPFC}} \tag{A.III-57}$$

$$\nabla_{V_j} L_\mu = -\nabla_{V_j} \Delta P_j \lambda_{p_j} - \nabla_{V_j} \Delta Q_j \lambda_{q_j} - \nabla_{V_j} PE_{UPFC} \lambda_{PE_{UPFC}} \tag{A.III-58}$$

From equation (3.18) $\nabla_{\lambda p_i} L_\mu = -\Delta P_i$

$$\nabla_{\lambda p_i} L_\mu = -\Delta P_i = -\left(P_{g_i} + P_{g_i}^{+} - P_{g_i}^{-} - P_{d_i} - P_i^{LINE} - P_i^{TRANS} - P_i^{UPFC} \right) \tag{A.III-59}$$

$$\nabla_{\lambda p_j} L_\mu = -\Delta P_j = -\left(P_{g_j} + P_{g_j}^{+} - P_{g_j}^{-} - P_{d_j} - P_j^{LINE} - P_j^{TRANS} - P_j^{UPFC} \right) \tag{A.III-60}$$

From equation (3.19) $\nabla_{\lambda q_i} L_\mu = -\Delta Q_i$

$$\nabla_{\lambda q_i} L_\mu = -\Delta Q_i = -\left(Q_{g_i} - Q_{d_i} - Q_i^{LINE} - Q_i^{TRANS} - Q_i^{UPFC} \right) \tag{A.III-61}$$

$$\nabla_{\lambda q_j} L_\mu = -\Delta Q_j = -\left(Q_{g_j} - Q_{d_j} - Q_j^{LINE} - Q_j^{TRANS} - Q_j^{UPFC} \right) \tag{A.III-62}$$

Appendix IV

Derivation of power flow equations, constraint equations and controller ratings for FACTS controller steady state equivalent circuit models, as presented in Chapter 3 and Appendix III.

STATCOM controller model: Derivation of power mismatch equations

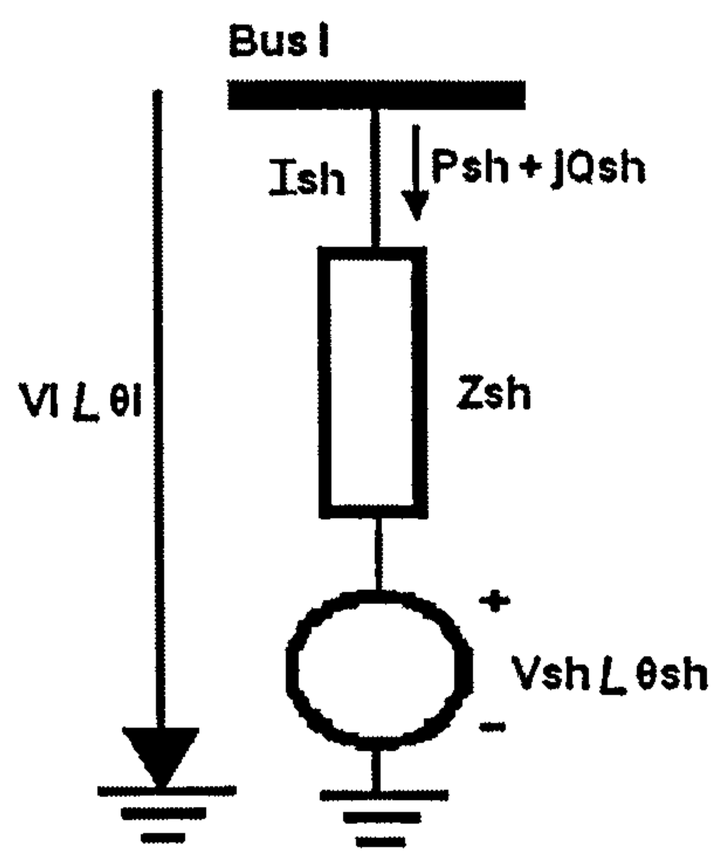

Figure AIV-1: STATCOM equivalent circuit model.

where,

$\overline{V_{sh}} = V_{sh}\angle\theta_{sh}$ is the voltage source from the shunt branch,

$g_{sh} + jb_{sh} = 1/Z_{sh} = Y_{sh}$ is the impedance from the shunt branch,

$g_{sh} = g_{ii}$ and $b_{sh} = b_{ii}$ are the bus conductances and susceptances,

Branch current equation

$$I_{sh} = \left(\overline{V}_i - \overline{V}_{sh}\right)\left(g_{sh} + jb_{sh}\right) \tag{A.IV-1}$$

$$\begin{aligned} I_{sh} = {} & V_i\left(g_{sh}\cos\theta_i - b_{sh}\sin\theta_i + j\left[g_{sh}\sin\theta_i + b_{sh}\cos\theta_i\right]\right) \\ & -V_{sh}\left(g_{sh}\cos\theta_{sh} - b_{sh}\sin\theta_{sh} + j\left[g_{sh}\sin\theta_{sh} + b_{sh}\cos\theta_{sh}\right]\right) \end{aligned} \tag{A.IV-2}$$

Branch power flow constraint equations

$$S_{sh} = V_i I_{sh}^{*} = P_{sh} + jQ_{sh} \tag{A.IV-3}$$

$$\begin{aligned} S_{sh} = {} & V_i^2\left(g_{sh} - jb_{sh}\right) - V_i V_{sh}\left(g_{sh}\cos\left(\theta_i - \theta_{sh}\right) + b_{sh}\sin\left(\theta_i - \theta_{sh}\right)\right) \\ & + jV_i V_{sh}\left(g_{sh}\sin\left(\theta_{sh} - \theta_i\right) + b_{sh}\cos\left(\theta_i - \theta_{sh}\right)\right) \end{aligned} \tag{A.IV-4}$$

$$P_{sh} = V_i^2 g_{sh} - V_i V_{sh}\left(g_{sh}\cos(\theta_i - \theta_{sh}) + b_{sh}\sin(\theta_i - \theta_{sh})\right) \quad \text{(A.IV-5)}$$

$$Q_{sh} = -V_i^2 b_{sh} - V_i V_{sh}\left(g_{sh}\sin(\theta_i - \theta_{sh}) - b_{sh}\cos(\theta_i - \theta_{sh})\right) \quad \text{(A.IV-6)}$$

Active power exchange operating constraint

The operating constraint of the STATCOM is the active power exchange via the DC link,

$$PE_{sh} = \mathrm{Re}\left(V_{sh} I_{sh}^*\right) = 0$$

where, $\mathrm{Re}\left(V_{sh} I_{sh}^*\right) = V_{sh}^2 g_{sh} - V_{sh} V_i\left(g_{sh}\cos(\theta_i - \theta_{sh}) - b_{sh}\sin(\theta_i - \theta_{sh})\right)$ (A.IV-7)

Controller rating

$$S_{sh}^R = V_{sh} I_{sh}^* = \mathrm{Re}\left(V_{sh} I_{sh}^*\right) + \mathrm{Im}\left(V_{sh} I_{sh}^*\right) = \sqrt{\left(P_{sh}^R\right)^2 + \left(jQ_{sh}^R\right)^2} \quad \text{(A.IV-8)}$$

where,

$$P_{sh}^R = \mathrm{Re}\left(V_{sh} I_{sh}^*\right) = V_{sh}^2 g_{sh} - V_{sh} V_i\left(g_{sh}\cos(\theta_i - \theta_{sh}) - b_{sh}\sin(\theta_i - \theta_{sh})\right) \quad \text{(A.IV-9)}$$

$$Q_{sh}^R = \mathrm{Im}\left(V_{sh} I_{sh}^*\right) = -V_{sh}^2 b_{sh} + V_{sh} V_i\left(g_{sh}\sin(\theta_i - \theta_{sh}) + b_{sh}\cos(\theta_i - \theta_{sh})\right) \quad \text{(A.IV-10)}$$

or,

$$\left|S_{sh}^R\right| = |V_{sh}||I_{sh}| \quad \text{(A.IV-11)}$$

where,

$$|I_{sh}| = \left|\frac{\left(\bar{V}_i - \bar{V}_{sh}\right)}{\bar{Z}_{sh}}\right| \quad \text{(A.IV-12)}$$

$$|I_{sh}| = \sqrt{V_i^2 + V_{sh}^2 - 2V_i V_{sh}\cos(\theta_i - \theta_{sh})}\,/\,Z_{sh} \quad \text{(A.IV-13)}$$

SSSC controller model: Derivation of power mismatch equations

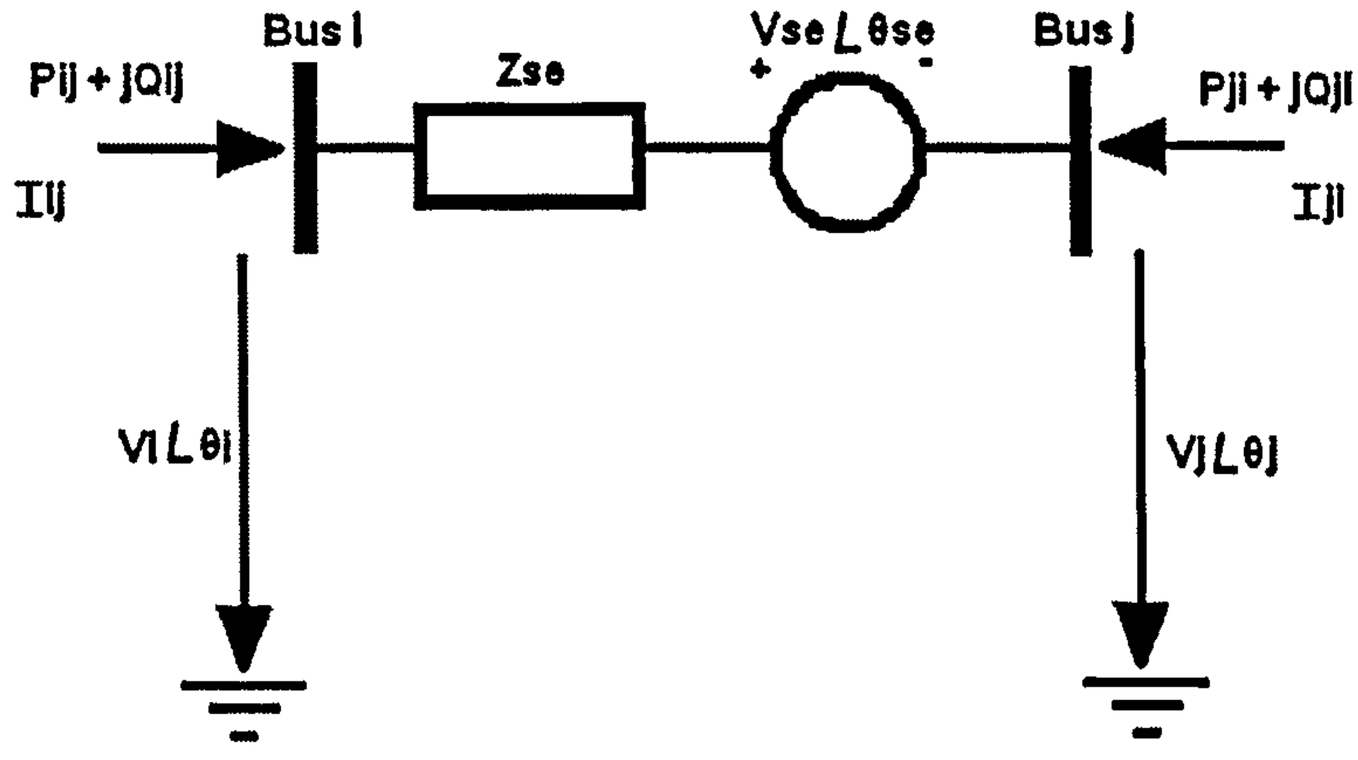

Figure AIV-2: SSSC equivalent circuit model.

where,

$\overline{V_{se}} = V_{se}\angle\theta_{se}$ is the voltage source from the series branch,

$g_{ij} + jb_{ij} = 1/Z_{se} = Y_{se}$ is the impedance from the series branch,

$g_{se} = g_{ij} = g_{ji}$ and $b_{se} = b_{ij} = b_{ji}$ are the branch conductances and susceptances.

Branch current equations

$$I_{ij} = \left(\bar{V}_i - \bar{V}_{se} - \bar{V}_j\right)\left(g_{ij} + jb_{ij}\right) \tag{A.IV-14}$$

$$\begin{aligned} I_{ij} &= V_i\left(g_{ii}\cos\theta_i - b_{ii}\sin\theta_i\right) + jV_i\left(g_{ii}\sin\theta_i + b_{ii}\cos\theta_i\right) \\ &\quad -V_{se}\left(g_{ij}\cos\theta_{se} - b_{ij}\sin\theta_{se}\right) - jV_{se}\left(g_{ij}\sin\theta_{se} + b_{ij}\cos\theta_{se}\right) \\ &\quad -V_j\left(g_{ij}\cos\theta_j - b_{ij}\sin\theta_j\right) - jV_j\left(g_{ij}\sin\theta_j + b_{ij}\cos\theta_j\right) \end{aligned} \tag{A.IV-15}$$

where, $g_{ij} = g_{se} = g_{ii}$ and $b_{ij} = b_{se} = b_{ii}$.

$$\begin{aligned} I_{ji} &= -I_{ij} \\ &= -\left\{\left(\bar{V}_i - \bar{V}_{se} - \bar{V}_j\right)\left(g_{ij} + jb_{ij}\right)\right\} = \left(-\bar{V}_i + \bar{V}_{se} + \bar{V}_j\right)\left(g_{ij} + jb_{ij}\right) \end{aligned} \tag{A.IV-16}$$

$$\begin{aligned} I_{ji} &= -V_i\left(g_{ij}\cos\theta_i - b_{ij}\sin\theta_i\right) - jV_i\left(g_{ij}\sin\theta_i + b_{ij}\cos\theta_i\right) \\ &\quad +V_{se}\left(g_{ij}\cos\theta_{se} - b_{ij}\sin\theta_{se}\right) + jV_{se}\left(g_{ij}\sin\theta_{se} + b_{ij}\cos\theta_{se}\right) \\ &\quad +V_j\left(g_{jj}\cos\theta_j - b_{jj}\sin\theta_j\right) + jV_j\left(g_{jj}\sin\theta_j + b_{jj}\cos\theta_j\right) \end{aligned} \tag{A.IV-17}$$

Branch power flow constraint equations

$$S_{ij} = V_i I_{ij}^* \tag{A.IV-18}$$

$$\begin{aligned} P_{ij} &= V_i^2 g_{ii} - V_i V_{se}\left(g_{ij}\cos\left(\theta_i - \theta_{se}\right) + b_{ij}\sin\left(\theta_i - \theta_{se}\right)\right) \\ &\quad -V_i V_j\left(g_{ij}\cos\left(\theta_i - \theta_j\right) + b_{ij}\sin\left(\theta_i - \theta_j\right)\right) \end{aligned} \tag{A.IV-19}$$

$$\begin{aligned} Q_{ij} &= -V_i^2 b_{ii} - V_i V_{se}\left(g_{ij}\sin\left(\theta_i - \theta_{se}\right) - b_{ij}\cos\left(\theta_i - \theta_{se}\right)\right) \\ &\quad -V_i V_j\left(g_{ij}\sin\left(\theta_i - \theta_j\right) - b_{ij}\cos\left(\theta_i - \theta_j\right)\right) \end{aligned} \tag{A.IV-20}$$

$$S_{ji} = V_j I_{ji}^* \tag{A.IV-21}$$

$$\begin{aligned} P_{ji} &= V_j^2 g_{jj} + V_j V_{se}\left(g_{ij}\cos\left(\theta_j - \theta_{se}\right) + b_{ij}\sin\left(\theta_j - \theta_{se}\right)\right) \\ &\quad -V_j V_i\left(g_{ij}\cos\left(\theta_j - \theta_i\right) + b_{ij}\sin\left(\theta_j - \theta_i\right)\right) \end{aligned} \tag{A.IV-22}$$

$$\begin{aligned} Q_{ji} &= -V_j^2 b_{jj} + V_j V_{se}\left(g_{ij}\sin\left(\theta_j - \theta_{se}\right) - b_{ij}\cos\left(\theta_j - \theta_{se}\right)\right) \\ &\quad -V_j V_i\left(g_{ij}\sin\left(\theta_j - \theta_i\right) - b_{ij}\cos\left(\theta_j - \theta_i\right)\right) \end{aligned} \tag{A.IV-23}$$

Active power exchange operating constraint

The operating constraint of the SSSC is the active power exchange via the DC link,

$$PE_{se} = \mathrm{Re}\left(V_{se} I_{ji}^{*}\right) = 0$$

where,

$$\begin{aligned}\mathrm{Re}\left(V_{se} I_{ji}^{*}\right) = {} & V_{se}^{2} g_{ij} - V_i V_{se}\left[g_{ij}\cos\left(\theta_i - \theta_{se}\right) - b_{ij}\sin\left(\theta_i - \theta_{se}\right)\right] \\ & + V_j V_{se}\left[g_{ij}\cos\left(\theta_j - \theta_{se}\right) - b_{ij}\sin\left(\theta_j - \theta_{se}\right)\right]\end{aligned} \tag{A.IV-24}$$

Controller rating

$$S_{se}^{R} = V_{se} I_{ji}^{*} = \mathrm{Re}\left(V_{se} I_{ji}^{*}\right) + \mathrm{Im}\left(V_{se} I_{ji}^{*}\right) = \sqrt{\left(P_{se}^{R}\right)^{2} + \left(jQ_{se}^{R}\right)^{2}} \tag{A.IV-25}$$

where,

$$\begin{aligned}P_{se}^{R} = \mathrm{Re}\left(V_{se} I_{ji}^{*}\right) = {} & V_{se}^{2} g_{ij} - V_i V_{se}\left[g_{ij}\cos\left(\theta_i - \theta_{se}\right) - b_{ij}\sin\left(\theta_i - \theta_{se}\right)\right] \\ & + V_j V_{se}\left[g_{ij}\cos\left(\theta_j - \theta_{se}\right) - b_{ij}\sin\left(\theta_j - \theta_{se}\right)\right]\end{aligned} \tag{A.IV-26}$$

$$\begin{aligned}Q_{se}^{R} = \mathrm{Im}\left(V_{se} I_{ji}^{*}\right) = {} & -V_{se}^{2} b_{ij} + V_i V_{se}\left[g_{ij}\sin\left(\theta_i - \theta_{se}\right) + b_{ij}\cos\left(\theta_i - \theta_{se}\right)\right] \\ & - V_j V_{se}\left[g_{ij}\sin\left(\theta_j - \theta_{se}\right) + b_{ij}\cos\left(\theta_j - \theta_{se}\right)\right]\end{aligned} \tag{A.IV-27}$$

or,

$$\left|S_{se}^{R}\right| = \left|V_{se}\right|\left|I_{se}\right| \tag{A.IV-28}$$

where,

$$\left|I_{se}\right| = \left|I_{ij}\right| = \left|\frac{\left(\bar{V}_i - \bar{V}_{se} - \bar{V}_j\right)}{\bar{Z}_{se}}\right| \tag{A.IV-29}$$

$$\left|I_{se}\right| = \sqrt{V_i^2 + V_{se}^2 + V_j^2 - 2V_i V_{se}\cos\left(\theta_i - \theta_{se}\right) + 2V_j V_{se}\cos\left(\theta_j - \theta_{se}\right) - 2V_i V_j \cos\left(\theta_i - \theta_j\right)} \Big/ Z_{se} \tag{A.IV-30}$$

UPFC controller model: Derivation of power mismatch equations

$\overline{V_{sh}} = V_{sh}\angle\theta_{sh}$ is the voltage source from the shunt branch,

$\overline{V_{se}} = V_{se}\angle\theta_{se}$ is the voltage source from the series branch,

$g_{sh} + jb_{sh} = 1/Z_{sh} = Y_{sh}$ is the impedance from the shunt branch,

$g_{ij} + jb_{ij} = 1/Z_{se} = Y_{se}$ is the impedance from the series branch,

$g_{sh} = g_{ii}$ and $b_{sh} = b_{ii}$ are the bus conductances and susceptances,

$g_{se} = g_{ij} = g_{ji}$ and $b_{se} = b_{ij} = b_{ji}$ are the branch conductances and susceptances.

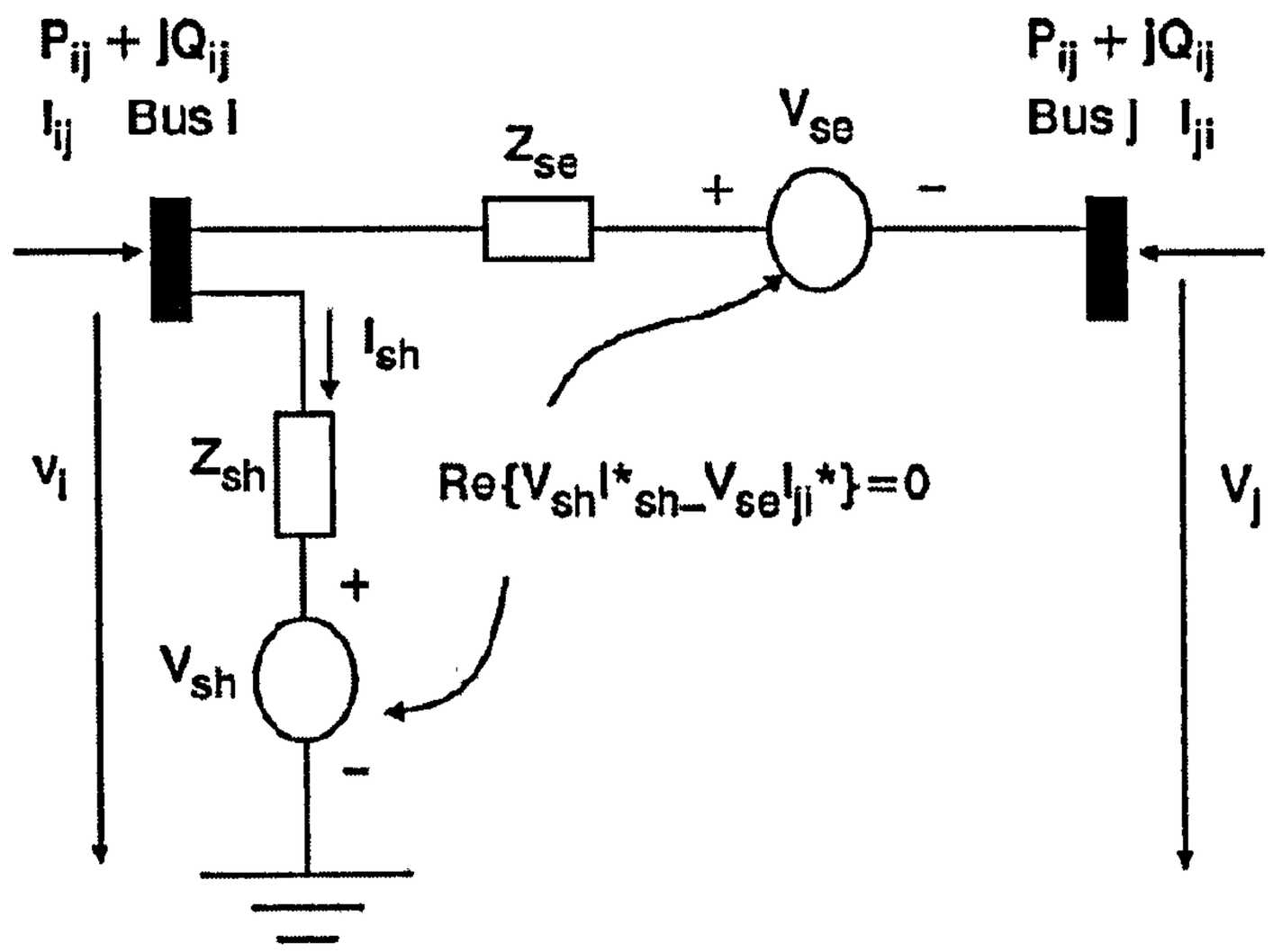

Figure AIV-3: UPFC equivalent circuit model.

Branch current equations

$$I_{sh} = \left(\bar{V}_i - \bar{V}_{sh}\right)\left(g_{sh} + jb_{sh}\right) \tag{A.IV-31}$$

$$\begin{aligned} I_{sh} = {} & V_i\left(g_{sh}\cos\theta_i - b_{sh}\sin\theta_i + j\left[g_{sh}\sin\theta_i + b_{sh}\cos\theta_i\right]\right) \\ & -V_{sh}\left(g_{sh}\cos\theta_{sh} - b_{sh}\sin\theta_{sh} + j\left[g_{sh}\sin\theta_{sh} + b_{sh}\cos\theta_{sh}\right]\right) \end{aligned} \tag{A.IV-32}$$

$$I_{ij} = \left(\bar{V}_i - \bar{V}_{se} - \bar{V}_j\right)\left(g_{ij} + jb_{ij}\right) \tag{A.IV-33}$$

$$\begin{aligned} I_{ij} = {} & V_i\left(g_{ii}\cos\theta_i - b_{ii}\sin\theta_i\right) + jV_i\left(g_{ii}\sin\theta_i + b_{ii}\cos\theta_i\right) \\ & -V_{se}\left(g_{ij}\cos\theta_{se} - b_{ij}\sin\theta_{se}\right) - jV_{se}\left(g_{ij}\sin\theta_{se} + b_{ij}\cos\theta_{se}\right) \\ & -V_j\left(g_{ij}\cos\theta_j - b_{ij}\sin\theta_j\right) - jV_j\left(g_{ij}\sin\theta_j + b_{ij}\cos\theta_j\right) \end{aligned} \tag{A.IV-34}$$

where, $g_{ij} = g_{se} = g_{ii}$ and $b_{ij} = b_{se} = b_{ii}$.

$$\begin{aligned} I_{ji} &= -I_{ij} \\ &= -\left\{\left(\bar{V}_i - \bar{V}_{se} - \bar{V}_j\right)\left(g_{ij} + jb_{ij}\right)\right\} = \left(-\bar{V}_i + \bar{V}_{se} + \bar{V}_j\right)\left(g_{ij} + jb_{ij}\right) \end{aligned} \tag{A.IV-35}$$

$$\begin{aligned} I_{ji} = {} & -V_i\left(g_{ij}\cos\theta_i - b_{ij}\sin\theta_i\right) - jV_i\left(g_{ij}\sin\theta_i + b_{ij}\cos\theta_i\right) \\ & +V_{se}\left(g_{ij}\cos\theta_{se} - b_{ij}\sin\theta_{se}\right) + jV_{se}\left(g_{ij}\sin\theta_{se} + b_{ij}\cos\theta_{se}\right) \\ & +V_j\left(g_{jj}\cos\theta_j - b_{jj}\sin\theta_j\right) + jV_j\left(g_{jj}\sin\theta_j + b_{jj}\cos\theta_j\right) \end{aligned} \tag{A.IV-36}$$

where, $g_{ij} = g_{jj}$ and $b_{ij} = b_{jj}$.

Branch power flow constraint equations

$$S_{sh} = V_i I_{sh}^* = P_{sh} + jQ_{sh} \tag{A.IV-37}$$

$$P_{sh} = V_i^2 g_{sh} - V_i V_{sh}\left(g_{sh}\cos\left(\theta_i - \theta_{sh}\right) + b_{sh}\sin\left(\theta_i - \theta_{sh}\right)\right) \quad \text{(A.IV-38)}$$

$$Q_{sh} = -V_i^2 b_{sh} - V_i V_{sh}\left(g_{sh}\sin\left(\theta_i - \theta_{sh}\right) - b_{sh}\cos\left(\theta_i - \theta_{sh}\right)\right) \quad \text{(A.IV-39)}$$

$$S_{ij} = V_i I_{ij}^{*} = P_{ij} + jQ_{ij} \quad \text{(A.IV-40)}$$

$$\begin{aligned} P_{ij} = {} & V_i^2 g_{ii} - V_i V_{se}\left(g_{ij}\cos\left(\theta_i - \theta_{se}\right) + b_{ij}\sin\left(\theta_i - \theta_{se}\right)\right) \\ & - V_i V_j\left(g_{ij}\cos\left(\theta_i - \theta_j\right) + b_{ij}\sin\left(\theta_i - \theta_j\right)\right) \end{aligned} \quad \text{(A.IV-41)}$$

$$\begin{aligned} Q_{ij} = {} & -V_i^2 b_{ii} - V_i V_{se}\left(g_{ij}\sin\left(\theta_i - \theta_{se}\right) - b_{ij}\cos\left(\theta_i - \theta_{se}\right)\right) \\ & - V_i V_j\left(g_{ij}\sin\left(\theta_i - \theta_j\right) - b_{ij}\cos\left(\theta_i - \theta_j\right)\right) \end{aligned} \quad \text{(A.IV-42)}$$

$$S_{ji} = V_j I_{ji}^{*} = P_{ji} + jQ_{ji} \quad \text{(A.IV-43)}$$

$$\begin{aligned} P_{ji} = {} & V_j^2 g_{jj} + V_j V_{se}\left(g_{ij}\cos\left(\theta_j - \theta_{se}\right) + b_{ij}\sin\left(\theta_j - \theta_{se}\right)\right) \\ & - V_j V_i\left(g_{ij}\cos\left(\theta_j - \theta_i\right) + b_{ij}\sin\left(\theta_j - \theta_i\right)\right) \end{aligned} \quad \text{(A.IV-44)}$$

$$\begin{aligned} Q_{ji} = {} & -V_j^2 b_{jj} + V_j V_{se}\left(g_{ij}\sin\left(\theta_j - \theta_{se}\right) - b_{ij}\cos\left(\theta_j - \theta_{se}\right)\right) \\ & - V_j V_i\left(g_{ij}\sin\left(\theta_j - \theta_i\right) - b_{ij}\cos\left(\theta_j - \theta_i\right)\right) \end{aligned} \quad \text{(A.IV-45)}$$

Active power balance operating constraint

The operating constraint of the UPFC is the active power exchange between the two inverters via the common DC link,

$$PE_{UPFC} = PE_{sh} - PE_{se} = \mathrm{Re}\left(\bar{V}_{sh}\bar{I}_{sh}^{*}\right) - \mathrm{Re}\left(\bar{V}_{se}\bar{I}_{ji}^{*}\right) = 0 \quad \text{(A.IV-46)}$$

where, $PE_{sh} = \mathrm{Re}\left(\bar{V}_{sh}\bar{I}_{sh}^{*}\right)$ and $PE_{se} = \mathrm{Re}\left(\bar{V}_{se}\bar{I}_{ji}^{*}\right)$ are the active power exchanges of the shunt converter and the series converter to the DC link respectively.

$$\mathrm{Re}\left(\bar{V}_{sh}\bar{I}_{sh}^{*}\right) = V_{sh}^2 g_{sh} - V_{sh}V_i\left(g_{sh}\cos\left(\theta_i - \theta_{sh}\right) - b_{sh}\sin\left(\theta_i - \theta_{sh}\right)\right) \quad \text{(A.IV-47)}$$

$$\begin{aligned} \mathrm{Re}\left(\bar{V}_{se}\bar{I}_{ji}^{*}\right) = {} & V_{se}^2 g_{ij} - V_i V_{se}\left[g_{ij}\cos\left(\theta_i - \theta_{se}\right) - b_{ij}\sin\left(\theta_i - \theta_{se}\right)\right] \\ & + V_j V_{se}\left[g_{ij}\cos\left(\theta_j - \theta_{se}\right) - b_{ij}\sin\left(\theta_j - \theta_{se}\right)\right] \end{aligned} \quad \text{(A.IV-48)}$$

Controller Rating

$$S_{UPFC}^{R} = S_{sh}^{R} + S_{se}^{R} \quad \text{(A.IV-49)}$$

where,

Shunt Branch

$$S_{sh}^{R} = \bar{V}_{sh}\bar{I}_{sh}^{*} = P_{sh}^{R} + jQ_{sh}^{R}$$

$$P_{sh}^{R} = \mathrm{Re}\left(\bar{V}_{sh}\bar{I}_{sh}^{*}\right) = V_{sh}^{2}g_{sh} - V_{sh}V_{i}\left(g_{sh}\cos\left(\theta_{i}-\theta_{sh}\right) - b_{sh}\sin\left(\theta_{i}-\theta_{sh}\right)\right) \quad \text{(A.IV-50)}$$

$$Q_{sh}^{R} = \mathrm{Im}\left(\bar{V}_{sh}\bar{I}_{sh}^{*}\right) = -V_{sh}^{2}b_{sh} + V_{sh}V_{i}\left(g_{sh}\sin\left(\theta_{i}-\theta_{sh}\right) + b_{sh}\cos\left(\theta_{i}-\theta_{sh}\right)\right) \quad \text{(A.IV-51)}$$

Series Branch

$$S_{se}^{R} = \bar{V}_{se}\bar{I}_{ji}^{*} = P_{se}^{R} + jQ_{se}^{R} \quad \text{(A.IV-52)}$$

$$\begin{aligned} P_{se}^{R} = \mathrm{Re}\left(\bar{V}_{se}\bar{I}_{ji}^{*}\right) = {} & V_{se}^{2}g_{ij} - V_{i}V_{se}\left[g_{ij}\cos\left(\theta_{i}-\theta_{se}\right) - b_{ij}\sin\left(\theta_{i}-\theta_{se}\right)\right] \\ & + V_{j}V_{se}\left[g_{ij}\cos\left(\theta_{j}-\theta_{se}\right) - b_{ij}\sin\left(\theta_{j}-\theta_{se}\right)\right] \end{aligned} \quad \text{(A.IV-53)}$$

$$\begin{aligned} Q_{se}^{R} = \mathrm{Im}\left(\bar{V}_{se}\bar{I}_{ji}^{*}\right) = {} & -V_{se}^{2}b_{ij} + V_{i}V_{se}\left[g_{ij}\sin\left(\theta_{i}-\theta_{se}\right) + b_{ij}\cos\left(\theta_{i}-\theta_{se}\right)\right] \\ & - V_{j}V_{se}\left[g_{ij}\sin\left(\theta_{j}-\theta_{se}\right) + b_{ij}\cos\left(\theta_{j}-\theta_{se}\right)\right] \end{aligned} \quad \text{(A.IV-54)}$$

APPENDIX V

List of first and second derivatives for the interior point OPF problem presented in Chapter 2 and Appendix I.

List of transmission line power flow equations

At bus i

$$\bar{S}_i = \bar{V}_i \bar{I}_i^* = P_i + jQ_i \tag{A.V-1}$$

$$P_i = V_i^2 g_{ii} - V_i V_j \left(g_{ij} \cos\left(\theta_i - \theta_j\right) + b_{ij} \sin\left(\theta_i - \theta_j\right) \right) \tag{A.V-2}$$

$$Q_i = -V_i^2 b_{ii} - V_i V_j \left(g_{ij} \sin\left(\theta_i - \theta_j\right) - b_{ij} \cos\left(\theta_i - \theta_j\right) \right) \tag{A.V-3}$$

At bus j

$$\bar{S}_j = \bar{V}_j \bar{I}_j^* = P_j + jQ_j$$

$$P_j = V_j^2 g_{jj} - V_i V_j \left[g_{ij} \cos\left(\theta_i - \theta_j\right) - b_{ij} \sin\left(\theta_i - \theta_j\right) \right] \tag{A.V-4}$$

$$Q_j = -V_j^2 b_{jj} + V_i V_j \left[g_{ij} \sin\left(\theta_i - \theta_j\right) + b_{ij} \cos\left(\theta_i - \theta_j\right) \right] \tag{A.V-5}$$

Objective function,

$$f(x) = \sum_i^{N_g} \left[C_{g_i}^+ P_{g_i}^+ \right] + \sum_i^{N_g} \left[C_{g_i}^- P_{g_i}^- \right] \tag{A.V-6}$$

Transmission line functional constraint

$$\bar{S}_{ij} = \bar{V}_i \bar{I}_{ij}^*$$

$$S_{ij}^2 = P_{ij}^2 + Q_{ij}^2 \tag{A.V-7}$$

$$P_{ij} = V_i^2 g_{ii} - V_i V_j \left(g_{ij} \cos\left(\theta_i - \theta_j\right) + b_{ij} \sin\left(\theta_i - \theta_j\right) \right) \tag{A.V-8}$$

$$Q_{ij} = -V_i^2 b_{ii} - V_i V_j \left(g_{ij} \sin\left(\theta_i - \theta_j\right) - b_{ij} \cos\left(\theta_i - \theta_j\right) \right) \tag{A.V-9}$$

List of first derivatives

From equation (2.26):

$$\nabla_{P_{g_i}^+} f(x) = C_{g_i}^+ \tag{A.V-10}$$

$$\nabla_{P_{g_i}^-} f(x) = C_{g_i}^- \tag{A.V-11}$$

From equations (2.26), (2.37), (2.40) and (2.41):

$$\nabla_{P_{g_i}^+} h_{P_{g_i}^+} = 1 \tag{A.V-12}$$

$$\nabla_{P_{g_i}^-} h_{P_{g_i}^-} = 1 \tag{A.V-13}$$

$$\nabla_{Q_{g_i}} h_{Q_{g_i}} = 1 \tag{A.V-14}$$

$$\nabla_{V_i} h_{V_i} = 1 \tag{A.V-15}$$

$$\nabla_t h_t = 1 \tag{A.V-16}$$

From equations (2.26) and (2.41):

$$\nabla_{\theta_i} h_{S_{ij}^2} = 2P_{ij}\frac{\partial P_{ij}}{\partial \theta_i} + 2Q_{ij}\frac{\partial Q_{ij}}{\partial \theta_i} \tag{A.V-17}$$

$$\nabla_{V_i} h_{S_{ij}^2} = 2P_{ij}\frac{\partial P_{ij}}{\partial V_i} + 2Q_{ij}\frac{\partial Q_{ij}}{\partial V_i} \tag{A.V-18}$$

$$\nabla_{\theta_j} h_{S_{ij}^2} = 2P_{ij}\frac{\partial P_{ij}}{\partial \theta_j} + 2Q_{ij}\frac{\partial Q_{ij}}{\partial \theta_j} \tag{A.V-19}$$

$$\nabla_{V_j} h_{S_{ij}^2} = 2P_{ij}\frac{\partial P_{ij}}{\partial V_j} + 2Q_{ij}\frac{\partial Q_{ij}}{\partial V_j} \tag{A.V-20}$$

where,

$$\frac{\partial P_{ij}}{\partial \theta_i} = V_i V_j \left(g_{ij} \sin\left(\theta_i - \theta_j\right) - b_{ij} \cos\left(\theta_i - \theta_j\right)\right) \tag{A.V-21}$$

$$\frac{\partial Q_{ij}}{\partial \theta_i} = -V_i V_j \left(g_{ij} \cos\left(\theta_i - \theta_j\right) + b_{ij} \sin\left(\theta_i - \theta_j\right)\right) \tag{A.V-22}$$

$$\frac{\partial P_{ij}}{\partial V_i} = 2V_i\ g_{ii} - V_j \left(g_{ij} \cos\left(\theta_i - \theta_j\right) + b_{ij} \sin\left(\theta_i - \theta_j\right)\right) \tag{A.V-23}$$

$$\frac{\partial Q_{ij}}{\partial V_i} = -2V_i\ b_{ii} - V_j \left(g_{ij} \sin\left(\theta_i - \theta_j\right) - b_{ij} \cos\left(\theta_i - \theta_j\right)\right) \tag{A.V-24}$$

$$\frac{\partial P_{ij}}{\partial \theta_j} = -\frac{\partial P_{ij}}{\partial \theta_i} = -V_i V_j \left(g_{ij} \sin\left(\theta_i - \theta_j\right) - b_{ij} \cos\left(\theta_i - \theta_j\right)\right) \tag{A.V-25}$$

$$\frac{\partial Q_{ij}}{\partial \theta_j} = -\frac{\partial Q_{ij}}{\partial \theta_i} = V_i V_j \left(g_{ij} \cos\left(\theta_i - \theta_j\right) + b_{ij} \sin\left(\theta_i - \theta_j\right)\right) \tag{A.V-26}$$

$$\frac{\partial P_{ij}}{\partial V_j} = -V_i \left(g_{ij} \cos\left(\theta_i - \theta_j\right) + b_{ij} \sin\left(\theta_i - \theta_j\right)\right) \tag{A.V-27}$$

$$\frac{\partial Q_{ij}}{\partial V_j} = -V_i \left(g_{ij} \sin\left(\theta_i - \theta_j\right) - b_{ij} \cos\left(\theta_i - \theta_j\right)\right) \tag{A.V-28}$$

From equations (2.26), (2.37) - (2.39):

$$\nabla_{P_{g_i}^+} \Delta P_i = 1 \tag{A.V-29}$$

$$\nabla_{P_{g_i}^-} \Delta P_i = -1 \tag{A.V-30}$$

$$\nabla_{Q_{g_i}} \Delta Q_i = 1 \tag{A.V-31}$$

Active power mismatch equations at bus i

$$\nabla_{\theta_i} \Delta P_i = -\frac{\partial P_i}{\partial \theta_i} = -V_i V_j \left(g_{ij} \sin\left(\theta_i - \theta_j\right) - b_{ij} \cos\left(\theta_i - \theta_j\right) \right) \tag{A.V-32}$$

$$\nabla_{V_i} \Delta P_i = -\frac{\partial P_i}{\partial V_i} = -2V_i \; g_{ii} + V_j \left(g_{ij} \cos\left(\theta_i - \theta_j\right) + b_{ij} \sin\left(\theta_i - \theta_j\right) \right) \tag{A.V-33}$$

$$\nabla_{\theta_j} \Delta P_i = -\frac{\partial P_i}{\partial \theta_j} = V_i V_j \left(g_{ij} \sin\left(\theta_i - \theta_j\right) - b_{ij} \cos\left(\theta_i - \theta_j\right) \right) \tag{A.V-34}$$

$$\nabla_{V_j} \Delta P_i = -\frac{\partial P_i}{\partial V_j} = V_i \left(g_{ij} \cos\left(\theta_i - \theta_j\right) + b_{ij} \sin\left(\theta_i - \theta_j\right) \right) \tag{A.V-35}$$

Reactive power mismatch equations at bus i

$$\nabla_{\theta_i} \Delta Q_i = -\frac{\partial Q_i}{\partial \theta_i} = V_i V_j \left(g_{ij} \cos\left(\theta_i - \theta_j\right) + b_{ij} \sin\left(\theta_i - \theta_j\right) \right) \tag{A.V-36}$$

$$\nabla_{V_i} \Delta Q_i = -\frac{\partial Q_i}{\partial V_i} = 2V_i \; b_{ii} + V_j \left(g_{ij} \sin\left(\theta_i - \theta_j\right) - b_{ij} \cos\left(\theta_i - \theta_j\right) \right) \tag{A.V-37}$$

$$\nabla_{\theta_j} \Delta Q_i = -\frac{\partial Q_i}{\partial \theta_j} = -V_i V_j \left(g_{ij} \cos\left(\theta_i - \theta_j\right) + b_{ij} \sin\left(\theta_i - \theta_j\right) \right) \tag{A.V-38}$$

$$\nabla_{V_j} \Delta Q_i = -\frac{\partial Q_i}{\partial V_j} = V_i \left(g_{ij} \sin\left(\theta_i - \theta_j\right) - b_{ij} \cos\left(\theta_i - \theta_j\right) \right) \tag{A.V-39}$$

Active power mismatch equations at bus j

$$\nabla_{\theta_i} \Delta P_j = -\frac{\partial P_j}{\partial \theta_i} = -V_i V_j \left(g_{ij} \sin\left(\theta_i - \theta_j\right) + b_{ij} \cos\left(\theta_i - \theta_j\right) \right) \tag{A.V-40}$$

$$\nabla_{V_i} \Delta P_j = -\frac{\partial P_j}{\partial V_i} = V_j \left(g_{ij} \cos\left(\theta_i - \theta_j\right) - b_{ij} \sin\left(\theta_i - \theta_j\right) \right) \tag{A.V-41}$$

$$\nabla_{\theta_j} \Delta P_j = -\frac{\partial P_j}{\partial \theta_j} = V_i V_j \left(g_{ij} \sin\left(\theta_i - \theta_j\right) + b_{ij} \cos\left(\theta_i - \theta_j\right) \right) \tag{A.V-42}$$

$$\nabla_{V_j} \Delta P_j = -\frac{\partial P_j}{\partial V_j} = -2V_j \, g_{jj} + V_i \left(g_{ij} \cos\left(\theta_j - \theta_i\right) - b_{ij} \sin\left(\theta_j - \theta_i\right) \right) \tag{A.V-43}$$

Reactive power mismatch equation at bus j

$$\nabla_{\theta_i} \Delta Q_j = -\frac{\partial Q_j}{\partial \theta_i} = -V_i V_j \left(g_{ij} \cos\left(\theta_i - \theta_j\right) - b_{ij} \sin\left(\theta_i - \theta_j\right) \right) \tag{A.V-44}$$

$$\nabla_{V_i} \Delta Q_j = -\frac{\partial Q_j}{\partial V_i} = -V_j \left(g_{ij} \sin\left(\theta_i - \theta_j\right) + b_{ij} \cos\left(\theta_i - \theta_j\right) \right) \quad \text{(A.V-45)}$$

$$\nabla_{\theta_j} \Delta Q_j = -\frac{\partial Q_j}{\partial \theta_j} = V_i V_j \left(g_{ij} \cos\left(\theta_i - \theta_j\right) - b_{ij} \sin\left(\theta_i - \theta_j\right) \right) \quad \text{(A.V-46)}$$

$$\nabla_{V_j} \Delta Q_j = -\frac{\partial Q_j}{\partial V_j} = 2V_j b_{jj} - V_i \left(g_{ij} \sin\left(\theta_i - \theta_j\right) + b_{ij} \cos\left(\theta_i - \theta_j\right) \right) \quad \text{(A.V-47)}$$

List of second derivatives

From equation (2.37):

Active power mismatch equations at bus *i*:

$$\nabla_{\theta_i} (\nabla_{\theta_i} \Delta P_i) = -\frac{\partial^2 P_i}{\partial \theta_i \partial \theta_i} = -V_i V_j \left(g_{ij} \cos\left(\theta_i - \theta_j\right) + b_{ij} \sin\left(\theta_i - \theta_j\right) \right) \quad \text{(A.V-48)}$$

$$\nabla_{\theta_i} (\nabla_{V_i} \Delta P_i) = -\frac{\partial^2 P_i}{\partial \theta_i \partial V_i} = -V_j \left(g_{ij} \sin\left(\theta_i - \theta_j\right) - b_{ij} \cos\left(\theta_i - \theta_j\right) \right) \quad \text{(A.V-49)}$$

$$\nabla_{\theta_i} (\nabla_{\theta_j} \Delta P_i) = -\frac{\partial^2 P_i}{\partial \theta_i \partial \theta_j} = \frac{\partial^2 P_i}{\partial \theta_i \partial \theta_i} = V_i V_j \left(g_{ij} \cos\left(\theta_i - \theta_j\right) + b_{ij} \sin\left(\theta_i - \theta_j\right) \right) \quad \text{(A.V-50)}$$

$$\nabla_{\theta_i} (\nabla_{V_j} \Delta P_i) = -\frac{\partial^2 P_i}{\partial \theta_i \partial V_j} = -V_i \left(g_{ij} \sin\left(\theta_i - \theta_j\right) - b_{ij} \cos\left(\theta_i - \theta_j\right) \right) \quad \text{(A.V-51)}$$

$$\nabla_{V_i} (\nabla_{V_i} \Delta P_i) = -\frac{\partial^2 P_i}{\partial V_i \partial V_i} = -2 g_{ii} \quad \text{(A.V-52)}$$

$$\nabla_{V_i} (\nabla_{\theta_j} \Delta P_i) = -\frac{\partial^2 P_i}{\partial V_i \partial \theta_j} = V_j \left(g_{ij} \sin\left(\theta_i - \theta_j\right) - b_{ij} \cos\left(\theta_i - \theta_j\right) \right) \quad \text{(A.V-53)}$$

$$\nabla_{V_i} (\nabla_{V_j} \Delta P_i) = -\frac{\partial^2 P_i}{\partial V_i \partial V_j} = \left(g_{ij} \cos\left(\theta_i - \theta_j\right) + b_{ij} \sin\left(\theta_i - \theta_j\right) \right) \quad \text{(A.V-54)}$$

$$\nabla_{\theta_j} (\nabla_{\theta_j} \Delta P_i) = -\frac{\partial^2 P_i}{\partial \theta_j \partial \theta_j} = -V_i V_j \left(g_{ij} \cos\left(\theta_i - \theta_j\right) + b_{ij} \sin\left(\theta_i - \theta_j\right) \right) \quad \text{(A.V-55)}$$

$$\nabla_{\theta_j} (\nabla_{V_j} \Delta P_i) = -\frac{\partial^2 P_i}{\partial \theta_j \partial V_j} = V_i \left(g_{ij} \sin\left(\theta_i - \theta_j\right) - b_{ij} \cos\left(\theta_i - \theta_j\right) \right) \quad \text{(A.V-56)}$$

$$\nabla_{V_j} (\nabla_{V_j} \Delta P_i) = -\frac{\partial^2 P_i}{\partial V_j \partial V_j} = 0 \quad \text{(A.V-57)}$$

Reactive power mismatch equations at bus *i*:

$$\nabla_{\theta_i} (\nabla_{\theta_i} \Delta Q_i) = -\frac{\partial^2 Q_i}{\partial \theta_i \partial \theta_i} = -V_i V_j \left(g_{ij} \sin\left(\theta_i - \theta_j\right) - b_{ij} \cos\left(\theta_i - \theta_j\right) \right) \quad \text{(A.V-58)}$$

$$\nabla_{\theta_i} (\nabla_{V_i} \Delta Q_i) = -\frac{\partial^2 Q_i}{\partial \theta_i \partial V_i} = V_j \left(g_{ij} \cos\left(\theta_i - \theta_j\right) + b_{ij} \sin\left(\theta_i - \theta_j\right) \right) \quad \text{(A.V-59)}$$

$$\nabla_{\theta_i}(\nabla_{\theta_j}\Delta Q_i) = -\frac{\partial^2 Q_i}{\partial\theta_i\partial\theta_j} = V_i V_j\left(g_{ij}\sin\left(\theta_i-\theta_j\right)-b_{ij}\cos\left(\theta_i-\theta_j\right)\right) \quad \text{(A.V-60)}$$

$$\nabla_{\theta_i}(\nabla_{V_j}\Delta Q_i) = -\frac{\partial^2 Q_i}{\partial\theta_i\partial V_j} = V_i\left(g_{ij}\cos\left(\theta_i-\theta_j\right)+b_{ij}\sin\left(\theta_i-\theta_j\right)\right) \quad \text{(A.V-61)}$$

$$\nabla_{V_i}(\nabla_{V_i}\Delta Q_i) = -\frac{\partial^2 Q_i}{\partial V_i\partial V_i} = 2b_{ii} \quad \text{(A.V-62)}$$

$$\nabla_{V_i}(\nabla_{\theta_j}\Delta Q_i) = -\frac{\partial^2 Q_i}{\partial V_i\partial\theta_j} = -V_j\left(g_{ij}\cos\left(\theta_i-\theta_j\right)+b_{ij}\sin\left(\theta_i-\theta_j\right)\right) \quad \text{(A.V-63)}$$

$$\nabla_{V_i}(\nabla_{V_j}\Delta Q_i) = -\frac{\partial^2 Q_i}{\partial V_i\partial V_j} = \left(g_{ij}\sin\left(\theta_i-\theta_j\right)-b_{ij}\cos\left(\theta_i-\theta_j\right)\right) \quad \text{(A.V-64)}$$

$$\nabla_{\theta_j}(\nabla_{\theta_j}\Delta Q_i) = -\frac{\partial^2 Q_i}{\partial\theta_j\partial\theta_j} = -V_i V_j\left(g_{ij}\sin\left(\theta_i-\theta_j\right)-b_{ij}\cos\left(\theta_i-\theta_j\right)\right) \quad \text{(A.V-65)}$$

$$\nabla_{\theta_j}(\nabla_{V_j}\Delta Q_i) = -\frac{\partial^2 Q_i}{\partial\theta_j\partial V_j} = -V_i\left(g_{ij}\cos\left(\theta_i-\theta_j\right)+b_{ij}\sin\left(\theta_i-\theta_j\right)\right) \quad \text{(A.V-66)}$$

$$\nabla_{V_j}(\nabla_{V_j}\Delta Q_i) = -\frac{\partial^2 Q_i}{\partial V_j\partial V_j} = 0 \quad \text{(A.V-67)}$$

Active power mismatch equations at bus *j*:

$$\nabla_{\theta_i}(\nabla_{\theta_i}\Delta P_j) = -\frac{\partial^2 P_j}{\partial\theta_i\partial\theta_i} = -V_i V_j\left(g_{ij}\cos\left(\theta_i-\theta_j\right)-b_{ij}\sin\left(\theta_i-\theta_j\right)\right) \quad \text{(A.V-68)}$$

$$\nabla_{\theta_i}(\nabla_{V_i}\Delta P_j) = -\frac{\partial^2 P_j}{\partial\theta_i\partial V_i} = -V_j\left(g_{ij}\sin\left(\theta_i-\theta_j\right)+b_{ij}\cos\left(\theta_i-\theta_j\right)\right) \quad \text{(A.V-69)}$$

$$\nabla_{\theta_i}(\nabla_{\theta_j}\Delta P_j) = -\frac{\partial^2 P_j}{\partial\theta_i\partial\theta_j} = V_i V_j\left(g_{ij}\cos\left(\theta_i-\theta_j\right)-b_{ij}\sin\left(\theta_i-\theta_j\right)\right) \quad \text{(A.V-70)}$$

$$\nabla_{\theta_i}(\nabla_{V_j}\Delta P_j) = -\frac{\partial^2 P_j}{\partial\theta_i\partial V_j} = -V_i\left(g_{ij}\sin\left(\theta_i-\theta_j\right)+b_{ij}\cos\left(\theta_i-\theta_j\right)\right) \quad \text{(A.V-71)}$$

$$\nabla_{V_i}(\nabla_{V_i}\Delta P_j) = -\frac{\partial^2 P_j}{\partial V_i\partial V_i} = 0 \quad \text{(A.V-72)}$$

$$\nabla_{V_i}(\nabla_{\theta_j}\Delta P_j) = -\frac{\partial^2 P_j}{\partial V_i\partial\theta_j} = V_j\left(g_{ij}\sin\left(\theta_i-\theta_j\right)+b_{ij}\cos\left(\theta_i-\theta_j\right)\right) \quad \text{(A.V-73)}$$

$$\nabla_{V_i}(\nabla_{V_j}\Delta P_j) = -\frac{\partial^2 P_j}{\partial V_i\partial V_j} = \left(g_{ij}\cos\left(\theta_i-\theta_j\right)-b_{ij}\sin\left(\theta_i-\theta_j\right)\right) \quad \text{(A.V-74)}$$

$$\nabla_{\theta_j}(\nabla_{\theta_j}\Delta P_j) = -\frac{\partial^2 P_j}{\partial\theta_j\partial\theta_j} = -V_iV_j\left(g_{ij}\cos\left(\theta_i-\theta_j\right)-b_{ij}\sin\left(\theta_i-\theta_j\right)\right) \quad \text{(A.V-75)}$$

$$\nabla_{\theta_j}(\nabla_{V_j}\Delta P_j) = -\frac{\partial^2 P_j}{\partial\theta_i\partial V_j} = V_i\left(g_{ij}\sin\left(\theta_i-\theta_j\right)+b_{ij}\cos\left(\theta_i-\theta_j\right)\right) \quad \text{(A.V-76)}$$

$$\nabla_{V_j}(\nabla_{V_j}\Delta P_j) = -\frac{\partial^2 P_j}{\partial V_j\partial V_j} = 0 \quad \text{(A.V-77)}$$

Reactive power mismatch equations at bus j:

$$\nabla_{\theta_i}(\nabla_{\theta_i}\Delta Q_j) = -\frac{\partial^2 Q_j}{\partial\theta_i\partial\theta_i} = V_iV_j\left(g_{ij}\sin\left(\theta_i-\theta_j\right)+b_{ij}\cos\left(\theta_i-\theta_j\right)\right) \quad \text{(A.V-78)}$$

$$\nabla_{\theta_i}(\nabla_{V_i}\Delta Q_j) = -\frac{\partial^2 Q_j}{\partial\theta_i\partial V_i} = -V_j\left(g_{ij}\cos\left(\theta_i-\theta_j\right)-b_{ij}\sin\left(\theta_i-\theta_j\right)\right) \quad \text{(A.V-79)}$$

$$\nabla_{\theta_i}(\nabla_{\theta_j}\Delta Q_j) = -\frac{\partial^2 Q_j}{\partial\theta_i\partial\theta_j} = -V_iV_j\left(g_{ij}\sin\left(\theta_i-\theta_j\right)+b_{ij}\cos\left(\theta_i-\theta_j\right)\right) \quad \text{(A.V-80)}$$

$$\nabla_{\theta_i}(\nabla_{V_j}\Delta Q_j) = -\frac{\partial^2 Q_j}{\partial\theta_i\partial V_j} = -V_i\left(g_{ij}\cos\left(\theta_i-\theta_j\right)-b_{ij}\sin\left(\theta_i-\theta_j\right)\right) \quad \text{(A.V-81)}$$

$$\nabla_{V_i}(\nabla_{V_i}\Delta Q_j) = -\frac{\partial^2 Q_j}{\partial V_i\partial V_i} = 0 \quad \text{(A.V-82)}$$

$$\nabla_{V_i}(\nabla_{\theta_j}\Delta Q_j) = -\frac{\partial^2 Q_j}{\partial V_i\partial\theta_j} = V_j\left(g_{ij}\cos\left(\theta_i-\theta_j\right)-b_{ij}\sin\left(\theta_i-\theta_j\right)\right) \quad \text{(A.V-83)}$$

$$\nabla_{V_i}(\nabla_{V_j}\Delta Q_j) = -\frac{\partial^2 Q_j}{\partial V_i\partial V_j} = -\left(g_{ij}\sin\left(\theta_i-\theta_j\right)+b_{ij}\cos\left(\theta_i-\theta_j\right)\right) \quad \text{(A.V-84)}$$

$$\nabla_{\theta_j}(\nabla_{\theta_j}\Delta Q_j) = -\frac{\partial^2 Q_j}{\partial\theta_j\partial\theta_j} = V_iV_j\left(g_{ij}\sin\left(\theta_i-\theta_j\right)+b_{ij}\cos\left(\theta_i-\theta_j\right)\right) \quad \text{(A.V-85)}$$

$$\nabla_{\theta_j}(\nabla_{V_j}\Delta Q_j) = -\frac{\partial^2 Q_j}{\partial\theta_j\partial V_j} = V_i\left(g_{ij}\cos\left(\theta_i-\theta_j\right)-b_{ij}\sin\left(\theta_i-\theta_j\right)\right) \quad \text{(A.V-86)}$$

$$\nabla_{V_j}(\nabla_{V_j}\Delta Q_j) = -\frac{\partial^2 Q_j}{\partial V_j\partial V_j} = 2b_{jj} \quad \text{(A.V-87)}$$

Transmission line functional constraint, from equation (2.37),

$$\nabla_{\theta_i}(\nabla_{\theta_i}h_{S_{ij}^2}) = 2\left[\frac{\partial P_{ij}}{\partial\theta_i}\frac{\partial P_{ij}}{\partial\theta_i}+P_{ij}\frac{\partial^2 P_{ij}}{\partial\theta_i\partial\theta_i}+\frac{\partial Q_{ij}}{\partial\theta_i}\frac{\partial Q_{ij}}{\partial\theta_i}+Q_{ij}\frac{\partial^2 Q_{ij}}{\partial\theta_i\partial\theta_i}\right] \quad \text{(A.V-88)}$$

$$\nabla_{\theta_i}(\nabla_{V_i} h_{S_{ij}^2}) = 2\left[\frac{\partial P_{ij}}{\partial \theta_i}\frac{\partial P_{ij}}{\partial V_i} + P_{ij}\frac{\partial^2 P_{ij}}{\partial \theta_i \partial V_i} + \frac{\partial Q_{ij}}{\partial \theta_i}\frac{\partial Q_{ij}}{\partial V_i} + Q_{ij}\frac{\partial^2 Q_{ij}}{\partial \theta_i \partial V_i}\right] \quad \text{(A.V-89)}$$

$$\nabla_{\theta_i}(\nabla_{\theta_j} h_{S_{ij}^2}) = 2\left[\frac{\partial P_{ij}}{\partial \theta_i}\frac{\partial P_{ij}}{\partial \theta_j} + P_{ij}\frac{\partial^2 P_{ij}}{\partial \theta_i \partial \theta_j} + \frac{\partial Q_{ij}}{\partial \theta_i}\frac{\partial Q_{ij}}{\partial \theta_j} + Q_{ij}\frac{\partial^2 Q_{ij}}{\partial \theta_i \partial \theta_j}\right] \quad \text{(A.V-90)}$$

$$\nabla_{\theta_i}(\nabla_{V_j} h_{S_{ij}^2}) = 2\left[\frac{\partial P_{ij}}{\partial \theta_i}\frac{\partial P_{ij}}{\partial V_j} + P_{ij}\frac{\partial^2 P_{ij}}{\partial \theta_i \partial V_j} + \frac{\partial Q_{ij}}{\partial \theta_i}\frac{\partial Q_{ij}}{\partial V_j} + Q_{ij}\frac{\partial^2 Q_{ij}}{\partial \theta_i \partial V_j}\right] \quad \text{(A.V-91)}$$

where,

$$\frac{\partial P_{ij}}{\partial \theta_i} = V_i V_j\left(g_{ij}\sin\left(\theta_i - \theta_j\right) - b_{ij}\cos\left(\theta_i - \theta_j\right)\right) \quad \text{(A.V-92)}$$

$$\frac{\partial^2 P_i}{\partial \theta_i \partial \theta_i} = V_i V_j\left(g_{ij}\cos\left(\theta_i - \theta_j\right) + b_{ij}\sin\left(\theta_i - \theta_j\right)\right) \quad \text{(A.V-93)}$$

$$\frac{\partial^2 P_i}{\partial \theta_i \partial V_i} = V_j\left(g_{ij}\sin\left(\theta_i - \theta_j\right) - b_{ij}\cos\left(\theta_i - \theta_j\right)\right) \quad \text{(A.V-94)}$$

$$\frac{\partial^2 P_i}{\partial \theta_i \partial \theta_j} = -V_i V_j\left(g_{ij}\cos\left(\theta_i - \theta_j\right) + b_{ij}\sin\left(\theta_i - \theta_j\right)\right) \quad \text{(A.V-95)}$$

$$\frac{\partial^2 P_i}{\partial \theta_i \partial V_j} = V_i\left(g_{ij}\sin\left(\theta_i - \theta_j\right) - b_{ij}\cos\left(\theta_i - \theta_j\right)\right) \quad \text{(A.V-96)}$$

$$\frac{\partial Q_{ij}}{\partial \theta_i} = -V_i V_j\left(g_{ij}\cos\left(\theta_i - \theta_j\right) + b_{ij}\sin\left(\theta_i - \theta_j\right)\right) \quad \text{(A.V-97)}$$

$$\frac{\partial^2 Q_i}{\partial \theta_i \partial \theta_i} = V_i V_j\left(g_{ij}\sin\left(\theta_i - \theta_j\right) - b_{ij}\cos\left(\theta_i - \theta_j\right)\right) \quad \text{(A.V-98)}$$

$$\frac{\partial^2 Q_i}{\partial \theta_i \partial V_i} = -V_j\left(g_{ij}\cos\left(\theta_i - \theta_j\right) + b_{ij}\sin\left(\theta_i - \theta_j\right)\right) \quad \text{(A.V-99)}$$

$$\frac{\partial^2 Q_i}{\partial \theta_i \partial \theta_j} = -V_i V_j\left(g_{ij}\sin\left(\theta_i - \theta_j\right) - b_{ij}\cos\left(\theta_i - \theta_j\right)\right) \quad \text{(A.V-100)}$$

$$\frac{\partial^2 Q_i}{\partial \theta_i \partial V_j} = -V_i\left(g_{ij}\cos\left(\theta_i - \theta_j\right) + b_{ij}\sin\left(\theta_i - \theta_j\right)\right) \quad \text{(A.V-101)}$$

$$\nabla_{V_i}(\nabla_{V_i} h_{S_{ij}^2}) = 2\left[\frac{\partial P_{ij}}{\partial V_i}\frac{\partial P_{ij}}{\partial V_i} + P_{ij}\frac{\partial^2 P_{ij}}{\partial V_i \partial V_i} + \frac{\partial Q_{ij}}{\partial V_i}\frac{\partial Q_{ij}}{\partial V_i} + Q_{ij}\frac{\partial^2 Q_{ij}}{\partial V_i \partial V_i}\right] \quad \text{(A.V-102)}$$

$$\nabla_{V_i}(\nabla_{\theta_j} h_{S_{ij}^2}) = 2\left[\frac{\partial P_{ij}}{\partial V_i}\frac{\partial P_{ij}}{\partial \theta_j} + P_{ij}\frac{\partial^2 P_{ij}}{\partial V_i \partial \theta_j} + \frac{\partial Q_{ij}}{\partial V_i}\frac{\partial Q_{ij}}{\partial \theta_j} + Q_{ij}\frac{\partial^2 Q_{ij}}{\partial V_i \partial \theta_j}\right] \quad \text{(A.V-103)}$$

$$\nabla_{V_i}(\nabla_{V_j} h_{S_{ij}^2}) = 2\left[\frac{\partial P_{ij}}{\partial V_i}\frac{\partial P_{ij}}{\partial V_j} + P_{ij}\frac{\partial^2 P_{ij}}{\partial V_i \partial V_j} + \frac{\partial Q_{ij}}{\partial V_i}\frac{\partial Q_{ij}}{\partial V_j} + Q_{ij}\frac{\partial^2 Q_{ij}}{\partial V_i \partial V_j}\right] \quad \text{(A.V-104)}$$

where,

$$\frac{\partial P_{ij}}{\partial V_i} = 2V_i\ g_{ii} - V_j\left(g_{ij}\cos\left(\theta_i - \theta_j\right) + b_{ij}\sin\left(\theta_i - \theta_j\right)\right) \quad \text{(A.V-105)}$$

$$\frac{\partial^2 P_i}{\partial V_i \partial V_i} = 2g_{ii} \quad \text{(A.V-106)}$$

$$\frac{\partial^2 P_i}{\partial V_i \partial \theta_j} = -V_j\left(g_{ij}\sin\left(\theta_i - \theta_j\right) - b_{ij}\cos\left(\theta_i - \theta_j\right)\right) \quad \text{(A.V-107)}$$

$$\frac{\partial^2 P_i}{\partial V_i \partial V_j} = -\left(g_{ij}\cos\left(\theta_i - \theta_j\right) + b_{ij}\sin\left(\theta_i - \theta_j\right)\right) \quad \text{(A.V-108)}$$

$$\frac{\partial Q_{ij}}{\partial V_i} = -2V_i\ b_{ii} - V_j\left(g_{ij}\sin\left(\theta_i - \theta_j\right) - b_{ij}\cos\left(\theta_i - \theta_j\right)\right) \quad \text{(A.V-109)}$$

$$\frac{\partial^2 Q_i}{\partial V_i \partial V_i} = -2b_{ii} \quad \text{(A.V-110)}$$

$$\frac{\partial^2 Q_i}{\partial V_i \partial \theta_j} = V_j\left(g_{ij}\cos\left(\theta_i - \theta_j\right) + b_{ij}\sin\left(\theta_i - \theta_j\right)\right) \quad \text{(A.V-111)}$$

$$\frac{\partial^2 Q_i}{\partial V_i \partial V_j} = -\left(g_{ij}\sin\left(\theta_i - \theta_j\right) - b_{ij}\cos\left(\theta_i - \theta_j\right)\right) \quad \text{(A.V-112)}$$

$$\nabla_{\theta_j}(\nabla_{\theta_j} h_{S_{ij}^2}) = 2\left[\frac{\partial P_{ij}}{\partial \theta_j}\frac{\partial P_{ij}}{\partial \theta_j} + P_{ij}\frac{\partial^2 P_{ij}}{\partial \theta_j \partial \theta_j} + \frac{\partial Q_{ij}}{\partial \theta_j}\frac{\partial Q_{ij}}{\partial \theta_j} + Q_{ij}\frac{\partial^2 Q_{ij}}{\partial \theta_j \partial \theta_j}\right] \quad \text{(A.V-113)}$$

$$\nabla_{\theta_j}(\nabla_{V_j} h_{S_{ij}^2}) = 2\left[\frac{\partial P_{ij}}{\partial \theta_j}\frac{\partial P_{ij}}{\partial V_j} + P_{ij}\frac{\partial^2 P_{ij}}{\partial \theta_j \partial V_j} + \frac{\partial Q_{ij}}{\partial \theta_j}\frac{\partial Q_{ij}}{\partial V_j} + Q_{ij}\frac{\partial^2 Q_{ij}}{\partial \theta_j \partial V_j}\right] \quad \text{(A.V-114)}$$

where,

$$\frac{\partial P_j}{\partial \theta_j} = -V_i V_j\left(g_{ij}\sin\left(\theta_i - \theta_j\right) + b_{ij}\cos\left(\theta_i - \theta_j\right)\right) \quad \text{(A.V-115)}$$

$$\frac{\partial^2 P_i}{\partial \theta_j \partial \theta_j} = V_i V_j\left(g_{ij}\cos\left(\theta_i - \theta_j\right) + b_{ij}\sin\left(\theta_i - \theta_j\right)\right) \quad \text{(A.V-116)}$$

$$\frac{\partial^2 P_i}{\partial \theta_j \partial V_j} = -V_i\left(g_{ij}\sin\left(\theta_i - \theta_j\right) - b_{ij}\cos\left(\theta_i - \theta_j\right)\right) \quad \text{(A.V-117)}$$

$$\frac{\partial Q_i}{\partial \theta_j} = V_i V_j\left(g_{ij}\cos\left(\theta_i - \theta_j\right) + b_{ij}\sin\left(\theta_i - \theta_j\right)\right) \quad \text{(A.V-118)}$$

$$\frac{\partial^2 Q_i}{\partial\theta_j\partial\theta_j} = V_i V_j\left(g_{ij}\sin\left(\theta_i-\theta_j\right)-b_{ij}\cos\left(\theta_i-\theta_j\right)\right) \quad \text{(A.V-119)}$$

$$\frac{\partial^2 Q_i}{\partial\theta_j\partial V_j} = V_i\left(g_{ij}\cos\left(\theta_i-\theta_j\right)+b_{ij}\sin\left(\theta_i-\theta_j\right)\right) \quad \text{(A.V-120)}$$

$$\nabla_{V_j}\left(\nabla_{V_j}h_{S_{ij}^2}\right) = 2\left[\frac{\partial P_{ij}}{\partial V_j}\frac{\partial P_{ij}}{\partial V_j}+\frac{\partial Q_{ij}}{\partial V_j}\frac{\partial Q_{ij}}{\partial V_j}\right] \quad \text{(A.V-121)}$$

where,

$$\frac{\partial P_i}{\partial V_j} = -V_i\left(g_{ij}\cos\left(\theta_i-\theta_j\right)+b_{ij}\sin\left(\theta_i-\theta_j\right)\right) \quad \text{(A.V-122)}$$

$$\frac{\partial^2 P_{ij}}{\partial V_j\partial V_j} = 0 \quad \text{(A.V-123)}$$

$$\frac{\partial Q_i}{\partial V_j} = -V_i\left(g_{ij}\sin\left(\theta_i-\theta_j\right)-b_{ij}\cos\left(\theta_i-\theta_j\right)\right) \quad \text{(A.V-124)}$$

$$\frac{\partial^2 Q_{ij}}{\partial V_j\partial V_j} = 0 \quad \text{(A.V-125)}$$

List of transmission line power flow equations with transformer tap-ratio control at bus *i*

Transmission line power flow from bus *i* with transformer tap-ratio control at bus *i*.

$$S_{ij}^{TR} = \bar{V}_i\bar{I}_{ij}^{TR*} = P_{ij}^{TR}+jQ_{ij}^{TR} \quad \text{(A.V-126)}$$

$$P_{ij}^{TR} = V_i^2 t^2 g_{ij} - V_i V_j t\left[g_{ij}\cos\left(\theta_i-\theta_j\right)+b_{ij}\sin\left(\theta_i-\theta_j\right)\right] \quad \text{(A.V-127)}$$

$$Q_{ij}^{TR} = -V_i^2 t^2 b_{ij} - V_i V_j t\left[g_{ij}\sin\left(\theta_i-\theta_j\right)-b_{ij}\cos\left(\theta_i-\theta_j\right)\right] \quad \text{(A.V-128)}$$

Transmission line power flow from bus *j* with transformer tap-ratio control at bus *i*.

$$S_{ji}^{TR} = \bar{V}_j\bar{I}_{ji}^{TR*} = P_{ji}^{TR}+jQ_{ji}^{TR} \quad \text{(A.V-129)}$$

$$P_{ji}^{TR} = V_j^2 g_{ij} - V_i V_j t\left[g_{ij}\cos\left(\theta_i-\theta_j\right)-b_{ij}\sin\left(\theta_i-\theta_j\right)\right] \quad \text{(A.V-130)}$$

$$Q_{ji}^{TR} = -V_j^2 b_{ij} + V_i V_j t\left[g_{ij}\sin\left(\theta_i-\theta_j\right)+b_{ij}\cos\left(\theta_i-\theta_j\right)\right] \quad \text{(A.V-131)}$$

First derivative

From equations (2.26), (2.37), (2.40) and (2.41):

$$\nabla_t h_t = 1 \quad \text{(A.V-132)}$$

From equations (2.26), (2.37) - (2.39):

$$\nabla_{\theta_i} \Delta P_i = -\frac{\partial P_i^{TR}}{\partial \theta_i} = -V_i V_j t\left(g_{ij} \sin\left(\theta_i - \theta_j\right) - b_{ij} \cos\left(\theta_i - \theta_j\right)\right) \quad \text{(A.V-133)}$$

$$\nabla_{V_i} \Delta P_i = -\frac{\partial P_i^{TR}}{\partial V_i} = -2V_i\, t^2 g_{ii} + V_j t\left(g_{ij} \cos\left(\theta_i - \theta_j\right) + b_{ij} \sin\left(\theta_i - \theta_j\right)\right) \quad \text{(A.V-134)}$$

$$\nabla_{\theta_j} \Delta P_i = -\frac{\partial P_i^{TR}}{\partial \theta_j} = V_i V_j t\left(g_{ij} \sin\left(\theta_i - \theta_j\right) - b_{ij} \cos\left(\theta_i - \theta_j\right)\right) \quad \text{(A.V-135)}$$

$$\nabla_{V_j} \Delta P_i = -\frac{\partial P_i^{TR}}{\partial V_j} = V_i t\left(g_{ij} \cos\left(\theta_i - \theta_j\right) + b_{ij} \sin\left(\theta_i - \theta_j\right)\right) \quad \text{(A.V-136)}$$

$$\nabla_{t_i} \Delta P_i T = -\frac{\partial P_i^{TR}}{\partial t_i} = -2V_i^2 t g_{ij} + V_i V_j \left(g_{ij} \cos\left(\theta_i - \theta_j\right) + b_{ij} \sin\left(\theta_i - \theta_j\right)\right) \quad \text{(A.V-137)}$$

$$\nabla_{\theta_i} \Delta Q_i = -\frac{\partial Q_i^{TR}}{\partial \theta_i} = V_i V_j t\left(g_{ij} \cos\left(\theta_i - \theta_j\right) + b_{ij} \sin\left(\theta_i - \theta_j\right)\right) \quad \text{(A.V-138)}$$

$$\nabla_{V_i} \Delta Q_i = -\frac{\partial Q_i^{TR}}{\partial V_i} = 2V_i\, t^2 b_{ii} + V_j t\left(g_{ij} \sin\left(\theta_i - \theta_j\right) - b_{ij} \cos\left(\theta_i - \theta_j\right)\right) \quad \text{(A.V-139)}$$

$$\nabla_{\theta_j} \Delta Q_i = -\frac{\partial Q_i^{TR}}{\partial \theta_j} = -V_i V_j t\left(g_{ij} \cos\left(\theta_i - \theta_j\right) + b_{ij} \sin\left(\theta_i - \theta_j\right)\right) \quad \text{(A.V-140)}$$

$$\nabla_{V_j} \Delta Q_i = -\frac{\partial Q_i^{TR}}{\partial V_j} = V_i t\left(g_{ij} \sin\left(\theta_i - \theta_j\right) - b_{ij} \cos\left(\theta_i - \theta_j\right)\right) \quad \text{(A.V-141)}$$

$$\nabla_{t_i} \Delta Q_i = -\frac{\partial Q_i^{TR}}{\partial t_j} = 2V_i^2 t b_{ii} + V_i V_j \left(g_{ij} \sin\left(\theta_i - \theta_j\right) - b_{ij} \cos\left(\theta_i - \theta_j\right)\right) \quad \text{(A.V-142)}$$

$$\nabla_{\theta_i} \Delta P_j = -\frac{\partial P_j^{TR}}{\partial \theta_i} = -V_i V_j t\left(g_{ij} \sin\left(\theta_i - \theta_j\right) + b_{ij} \cos\left(\theta_i - \theta_j\right)\right) \quad \text{(A.V-143)}$$

$$\nabla_{V_i} \Delta P_j = -\frac{\partial P_j^{TR}}{\partial V_i} = V_j t\left(g_{ij} \cos\left(\theta_i - \theta_j\right) - b_{ij} \sin\left(\theta_i - \theta_j\right)\right) \quad \text{(A.V-144)}$$

$$\nabla_{\theta_j} \Delta P_j = -\frac{\partial P_j^{TR}}{\partial \theta_j} = V_i V_j t\left(g_{ij} \sin\left(\theta_i - \theta_j\right) + b_{ij} \cos\left(\theta_i - \theta_j\right)\right) \quad \text{(A.V-145)}$$

$$\nabla_{V_j} \Delta P_j = -\frac{\partial P_j^{TR}}{\partial V_j} = -2V_j\, g_{jj} + V_i t\left(g_{ij} \cos\left(\theta_i - \theta_j\right) - b_{ij} \sin\left(\theta_i - \theta_j\right)\right) \quad \text{(A.V-146)}$$

$$\nabla_{t_i} \Delta P_j T = -\frac{\partial P_j^{TR}}{\partial t_i} = V_i V_j \left(g_{ij} \cos\left(\theta_i - \theta_j\right) - b_{ij} \sin\left(\theta_i - \theta_j\right)\right) \quad \text{(A.V-147)}$$

$$\nabla_{\theta_i} \Delta Q_j = -\frac{\partial Q_j^{TR}}{\partial \theta_i} = -V_i V_j t\left(g_{ij}\cos\left(\theta_i-\theta_j\right)-b_{ij}\sin\left(\theta_i-\theta_j\right)\right) \quad \text{(A.V-148)}$$

$$\nabla_{V_i} \Delta Q_j = -\frac{\partial Q_j^{TR}}{\partial V_i} = -V_j t\left(g_{ij}\sin\left(\theta_i-\theta_j\right)+b_{ij}\cos\left(\theta_i-\theta_j\right)\right) \quad \text{(A.V-149)}$$

$$\nabla_{\theta_j} \Delta Q_j = -\frac{\partial Q_j^{TR}}{\partial \theta_j} = \frac{\partial Q_j^{TR}}{\partial \theta_i} = V_i V_j t\left(g_{ij}\cos\left(\theta_i-\theta_j\right)-b_{ij}\sin\left(\theta_i-\theta_j\right)\right) \quad \text{(A.V-150)}$$

$$\nabla_{V_j} \Delta Q_j = -\frac{\partial Q_j^{TR}}{\partial V_j} = 2V_j b_{jj} - V_i t\left(g_{ij}\sin\left(\theta_i-\theta_j\right)+b_{ij}\cos\left(\theta_i-\theta_j\right)\right) \quad \text{(A.V-151)}$$

$$\nabla_{t_i} \Delta Q_j T = -\frac{\partial Q_j^{TR}}{\partial t_i} = -V_i V_j\left(g_{ij}\sin\left(\theta_i-\theta_j\right)+b_{ij}\cos\left(\theta_i-\theta_j\right)\right) \quad \text{(A.V-152)}$$

Transformer non-functional constraint

$$\nabla_{t_i} h_{t_i} = 1,\ \nabla_{t_i}\left(\nabla_{t_i} h_{t_i}\right) = 0 \quad \text{(A.V-153)}$$

Transformer, list of second derivatives, from equation (2.37):

Active power mismatch equations at bus *i*:

$$\nabla_{\theta_i}\left(\nabla_{\theta_i} \Delta P_i\right) = -\frac{\partial^2 P_i^{TR}}{\partial \theta_i \partial \theta_i} = -V_i V_j t\left(g_{ij}\cos\left(\theta_i-\theta_j\right)+b_{ij}\sin\left(\theta_i-\theta_j\right)\right) \quad \text{(A.V-154)}$$

$$\nabla_{\theta_i}\left(\nabla_{V_i} \Delta P_i\right) = -\frac{\partial^2 P_i^{TR}}{\partial \theta_i \partial V_i} = -V_j t\left(g_{ij}\sin\left(\theta_i-\theta_j\right)-b_{ij}\cos\left(\theta_i-\theta_j\right)\right) \quad \text{(A.V-155)}$$

$$\nabla_{\theta_i}\left(\nabla_{\theta_j} \Delta P_i\right) = -\frac{\partial^2 P_i^{TR}}{\partial \theta_i \partial \theta_j} = \frac{\partial^2 P_i^{TR}}{\partial \theta_i \partial \theta_i} = V_i V_j t\left(g_{ij}\cos\left(\theta_i-\theta_j\right)-b_{ij}\sin\left(\theta_i-\theta_j\right)\right) \quad \text{(A.V-156)}$$

$$\nabla_{\theta_i}\left(\nabla_{V_j} \Delta P_i\right) = -\frac{\partial^2 P_i^{TR}}{\partial \theta_i \partial V_j} = -V_i t\left(g_{ij}\sin\left(\theta_i-\theta_j\right)-b_{ij}\cos\left(\theta_i-\theta_j\right)\right) \quad \text{(A.V-157)}$$

$$\nabla_{\theta_i}\left(\nabla_{t_i} \Delta P_i\right) = -\frac{\partial^2 P_i^{TR}}{\partial \theta_i \partial t_i} = -V_i V_j\left(g_{ij}\sin\left(\theta_i-\theta_j\right)-b_{ij}\cos\left(\theta_i-\theta_j\right)\right) \quad \text{(A.V-158)}$$

$$\nabla_{V_i}\left(\nabla_{V_i} \Delta P_i\right) = -\frac{\partial^2 P_i^{TR}}{\partial V_i \partial V_i} = -2t^2 g_{ii} \quad \text{(A.V-159)}$$

$$\nabla_{V_i}\left(\nabla_{\theta_j} \Delta P_i\right) = -\frac{\partial^2 P_i^{TR}}{\partial V_i \partial \theta_j} = V_j t\left(g_{ij}\sin\left(\theta_i-\theta_j\right)-b_{ij}\cos\left(\theta_i-\theta_j\right)\right) \quad \text{(A.V-160)}$$

$$\nabla_{V_i}\left(\nabla_{V_j} \Delta P_i\right) = -\frac{\partial^2 P_i^{TR}}{\partial V_i \partial V_j} = t\left(g_{ij}\cos\left(\theta_i-\theta_j\right)+b_{ij}\sin\left(\theta_i-\theta_j\right)\right) \quad \text{(A.V-161)}$$

$$\nabla_{V_i}(\nabla_{t_i}\Delta P_i) = -\frac{\partial^2 P_i^{TR}}{\partial V_i \partial t_i} = -4V_i t g_{ij} + V_j\left(g_{ij}\cos\left(\theta_i-\theta_j\right)+b_{ij}\sin\left(\theta_i-\theta_j\right)\right) \quad \text{(A.V-162)}$$

$$\nabla_{\theta_j}(\nabla_{\theta_j}\Delta P_i) = -\frac{\partial^2 P_i^{TR}}{\partial \theta_j \partial \theta_j} = -V_i V_j\left(g_{ij}\cos\left(\theta_i-\theta_j\right)+b_{ij}\sin\left(\theta_i-\theta_j\right)\right) \quad \text{(A.V-163)}$$

$$\nabla_{\theta_j}(\nabla_{V_j}\Delta P_i) = -\frac{\partial^2 P_i^{TR}}{\partial \theta_j \partial V_j} = V_i t\left(g_{ij}\sin\left(\theta_i-\theta_j\right)-b_{ij}\cos\left(\theta_i-\theta_j\right)\right) \quad \text{(A.V-164)}$$

$$\nabla_{\theta_j}(\nabla_{t_i}\Delta P_i) = -\frac{\partial^2 P_i^{TR}}{\partial \theta_j \partial t_i} = V_i V_j\left(g_{ij}\sin\left(\theta_i-\theta_j\right)-b_{ij}\cos\left(\theta_i-\theta_j\right)\right) \quad \text{(A.V-165)}$$

$$\nabla_{V_j}(\nabla_{V_j}\Delta P_i) = 0 \quad \text{(A.V-166)}$$

$$\nabla_{V_j}(\nabla_{t_i}\Delta P_i) = -\frac{\partial^2 P_i^{TR}}{\partial V_j \partial t_i} = V_i\left(g_{ij}\cos\left(\theta_i-\theta_j\right)+b_{ij}\sin\left(\theta_i-\theta_j\right)\right) \quad \text{(A.V-167)}$$

$$\nabla_{t_i}(\nabla_{t_i}\Delta P_i) = -\frac{\partial^2 P_i^{TR}}{\partial t_i \partial t_i} = -2V_i^2 g_{ij} \quad \text{(A.V-168)}$$

Reactive power mismatch equations at bus i:

$$\nabla_{\theta_i}(\nabla_{\theta_i}\Delta Q_i) = -\frac{\partial^2 Q_i^{TR}}{\partial \theta_i \partial \theta_i} = -V_i V_j t\left(g_{ij}\sin\left(\theta_i-\theta_j\right)-b_{ij}\cos\left(\theta_i-\theta_j\right)\right) \quad \text{(A.V-169)}$$

$$\nabla_{\theta_i}(\nabla_{V_i}\Delta Q_i) = -\frac{\partial^2 Q_i^{TR}}{\partial \theta_i \partial V_i} = V_j t\left(g_{ij}\cos\left(\theta_i-\theta_j\right)+b_{ij}\sin\left(\theta_i-\theta_j\right)\right) \quad \text{(A.V-170)}$$

$$\nabla_{\theta_i}(\nabla_{\theta_j}\Delta Q_i) = -\frac{\partial^2 Q_i^{TR}}{\partial \theta_i \partial \theta_j} = \frac{\partial^2 Q_i^{TR}}{\partial \theta_i \partial \theta_i} = V_i V_j t\left(g_{ij}\sin\left(\theta_i-\theta_j\right)-b_{ij}\cos\left(\theta_i-\theta_j\right)\right) \quad \text{(A.V-171)}$$

$$\nabla_{\theta_i}(\nabla_{V_j}\Delta Q_i) = -\frac{\partial^2 Q_i^{TR}}{\partial \theta_i \partial V_j} = V_i t\left(g_{ij}\cos\left(\theta_i-\theta_j\right)+b_{ij}\sin\left(\theta_i-\theta_j\right)\right) \quad \text{(A.V-172)}$$

$$\nabla_{\theta_i}(\nabla_{t_i}\Delta Q_i) = -\frac{\partial^2 Q_i^{TR}}{\partial \theta_i \partial t_i} = V_i V_j\left(g_{ij}\cos\left(\theta_i-\theta_j\right)+b_{ij}\sin\left(\theta_i-\theta_j\right)\right) \quad \text{(A.V-173)}$$

$$\nabla_{V_i}(\nabla_{V_i}\Delta Q_i) = -\frac{\partial^2 Q_i^{TR}}{\partial V_i \partial V_i} = 2t^2 b_{ij} \quad \text{(A.V-174)}$$

$$\nabla_{V_i}(\nabla_{\theta_j}\Delta Q_i) = -\frac{\partial^2 Q_i^{TR}}{\partial V_i \partial \theta_j} = -V_j t\left(g_{ij}\cos\left(\theta_i-\theta_j\right)+b_{ij}\sin\left(\theta_i-\theta_j\right)\right) \quad \text{(A.V-175)}$$

$$\nabla_{V_i}(\nabla_{V_j}\Delta Q_i) = -\frac{\partial^2 Q_i^{TR}}{\partial V_i \partial V_j} = t\left(g_{ij}\sin\left(\theta_i-\theta_j\right)-b_{ij}\cos\left(\theta_i-\theta_j\right)\right) \quad \text{(A.V-176)}$$

$$\nabla_{V_i}(\nabla_{t_i}\Delta Q_i) = -\frac{\partial^2 Q_i^{TR}}{\partial V_i \partial t_i} = 4V_i t b_{ij} + V_j\left(g_{ij}\sin\left(\theta_i-\theta_j\right)-b_{ij}\cos\left(\theta_i-\theta_j\right)\right) \quad \text{(A.V-177)}$$

$$\nabla_{\theta_j}(\nabla_{\theta_j}\Delta Q_i) = -\frac{\partial^2 Q_i^{TR}}{\partial\theta_j\partial\theta_j} = -V_i V_j t\left(g_{ij}\sin\left(\theta_i-\theta_j\right)-b_{ij}\cos\left(\theta_i-\theta_j\right)\right) \quad \text{(A.V-178)}$$

$$\nabla_{\theta_j}(\nabla_{V_j}\Delta Q_i) = -\frac{\partial^2 Q_i^{TR}}{\partial\theta_j\partial V_j} = -V_i t\left(g_{ij}\cos\left(\theta_i-\theta_j\right)+b_{ij}\sin\left(\theta_i-\theta_j\right)\right) \quad \text{(A.V-179)}$$

$$\nabla_{\theta_j}(\nabla_{t_i}\Delta Q_i) = -\frac{\partial^2 Q_i^{TR}}{\partial\theta_j\partial t_i} = -V_i V_j\left(g_{ij}\cos\left(\theta_i-\theta_j\right)+b_{ij}\sin\left(\theta_i-\theta_j\right)\right) \quad \text{(A.V-180)}$$

$$\nabla_{V_j}(\nabla_{V_j}\Delta Q_i) = -\frac{\partial^2 Q_i^{TR}}{\partial V_j\partial V_j} = 0 \quad \text{(A.V-181)}$$

$$\nabla_{V_j}(\nabla_{t_i}\Delta Q_i) = -\frac{\partial^2 Q_i^{TR}}{\partial V_j\partial t_i} = V_i\left(g_{ij}\sin\left(\theta_i-\theta_j\right)-b_{ij}\cos\left(\theta_i-\theta_j\right)\right) \quad \text{(A.V-182)}$$

$$\nabla_{t_i}(\nabla_{t_i}\Delta Q_i) = -\frac{\partial^2 Q_i^{TR}}{\partial t_i\partial t_i} = 2V_i^2 b_{ij} \quad \text{(A.V-183)}$$

Transformer, second derivatives

From equation (2.37):

Active power mismatch equations at bus *j*:

$$\nabla_{\theta_i}(\nabla_{\theta_i}\Delta P_j) = -\frac{\partial^2 P_j^{TR}}{\partial\theta_i\partial\theta_i} = -V_i V_j t\left(g_{ij}\cos\left(\theta_i-\theta_j\right)-b_{ij}\sin\left(\theta_i-\theta_j\right)\right) \quad \text{(A.V-184)}$$

$$\nabla_{\theta_i}(\nabla_{V_i}\Delta P_j) = -\frac{\partial^2 P_j^{TR}}{\partial\theta_i\partial V_i} = -V_j t\left(g_{ij}\sin\left(\theta_i-\theta_j\right)+b_{ij}\cos\left(\theta_i-\theta_j\right)\right) \quad \text{(A.V-185)}$$

$$\nabla_{\theta_i}(\nabla_{\theta_j}\Delta P_j) = -\frac{\partial^2 P_j^{TR}}{\partial\theta_i\partial\theta_j} = \frac{\partial^2 P_j^{TR}}{\partial\theta_i\partial\theta_i} = V_i V_j t\left(g_{ij}\cos\left(\theta_i-\theta_j\right)-b_{ij}\sin\left(\theta_i-\theta_j\right)\right) \quad \text{(A.V-186)}$$

$$\nabla_{\theta_i}(\nabla_{V_j}\Delta P_j) = -\frac{\partial^2 P_j^{TR}}{\partial\theta_i\partial V_j} = -V_i t\left(g_{ij}\sin\left(\theta_i-\theta_j\right)+b_{ij}\cos\left(\theta_i-\theta_j\right)\right) \quad \text{(A.V-187)}$$

$$\nabla_{\theta_i}(\nabla_{t_i}\Delta P_j) = -\frac{\partial^2 P_j^{TR}}{\partial\theta_i\partial t_i} = -V_i V_j\left(g_{ij}\sin\left(\theta_i-\theta_j\right)+b_{ij}\cos\left(\theta_i-\theta_j\right)\right) \quad \text{(A.V-188)}$$

$$\nabla_{V_i}(\nabla_{V_i}\Delta P_j) = -\frac{\partial^2 P_j^{TR}}{\partial V_i\partial V_i} = 0 \quad \text{(A.V-189)}$$

$$\nabla_{V_i}(\nabla_{\theta_j}\Delta P_j) = -\frac{\partial^2 P_j^{TR}}{\partial V_i\partial\theta_j} = V_j\left(g_{ij}\sin\left(\theta_i-\theta_j\right)+b_{ij}\cos\left(\theta_i-\theta_j\right)\right) \quad \text{(A.V-190)}$$

$$\nabla_{V_i}(\nabla_{V_j}\Delta P_j) = -\frac{\partial^2 P_j^{TR}}{\partial V_i\partial V_j} = t\left(g_{ij}\cos\left(\theta_i-\theta_j\right)-b_{ij}\sin\left(\theta_i-\theta_j\right)\right) \quad \text{(A.V-191)}$$

$$\nabla_{V_i}(\nabla_{t_i}\Delta P_j) = -\frac{\partial^2 P_j^{TR}}{\partial V_i \partial t_i} = V_j\left(g_{ij}\cos\left(\theta_i-\theta_j\right)-b_{ij}\sin\left(\theta_i-\theta_j\right)\right) \quad \text{(A.V-192)}$$

$$\nabla_{\theta_j}(\nabla_{\theta_j}\Delta P_j) = -\frac{\partial^2 P_j^{TR}}{\partial \theta_j \partial \theta_j} = -V_i V_j t\left(g_{ij}\cos\left(\theta_i-\theta_j\right)-b_{ij}\sin\left(\theta_i-\theta_j\right)\right) \quad \text{(A.V-193)}$$

$$\nabla_{\theta_j}(\nabla_{V_j}\Delta P_j) = -\frac{\partial^2 P_j^{TR}}{\partial \theta_j \partial V_j} = V_i t\left(g_{ij}\sin\left(\theta_i-\theta_j\right)+b_{ij}\cos\left(\theta_i-\theta_j\right)\right) \quad \text{(A.V-194)}$$

$$\nabla_{\theta_j}(\nabla_{t_i}\Delta P_j) = -\frac{\partial^2 P_j^{TR}}{\partial \theta_j \partial t_i} = V_i V_j\left(g_{ij}\sin\left(\theta_i-\theta_j\right)+b_{ij}\cos\left(\theta_i-\theta_j\right)\right) \quad \text{(A.V-195)}$$

$$\nabla_{V_j}(\nabla_{V_j}\Delta P_j) = -\frac{\partial^2 P_j^{TR}}{\partial V_j \partial V_j} = -2g_{ij} \quad \text{(A.V-196)}$$

$$\nabla_{V_j}(\nabla_{t_i}\Delta P_j) = -\frac{\partial^2 P_j^{TR}}{\partial V_j \partial t_i} = V_i\left(g_{ij}\cos\left(\theta_i-\theta_j\right)-b_{ij}\sin\left(\theta_i-\theta_j\right)\right) \quad \text{(A.V-197)}$$

$$\nabla_{t_i}(\nabla_{t_i}\Delta P_j) = -\frac{\partial^2 P_j^{TR}}{\partial t_i \partial t_i} = 0 \quad \text{(A.V-198)}$$

Reactive power mismatch equations at bus *j*:

$$\nabla_{\theta_i}(\nabla_{\theta_i}\Delta Q_j) = -\frac{\partial^2 Q_j^{TR}}{\partial \theta_i \partial \theta_i} = V_i V_j t\left(g_{ij}\sin\left(\theta_i-\theta_j\right)+b_{ij}\cos\left(\theta_i-\theta_j\right)\right) \quad \text{(A.V-199)}$$

$$\nabla_{\theta_i}(\nabla_{V_i}\Delta Q_j) = -\frac{\partial^2 Q_j^{TR}}{\partial \theta_i \partial V_i} = -V_j t\left(g_{ij}\cos\left(\theta_i-\theta_j\right)-b_{ij}\sin\left(\theta_i-\theta_j\right)\right) \quad \text{(A.V-200)}$$

$$\nabla_{\theta_i}(\nabla_{\theta_j}\Delta Q_j) = -\frac{\partial^2 Q_j^{TR}}{\partial \theta_i \partial \theta_j} = \frac{\partial^2 Q_j^{TR}}{\partial \theta_i \partial \theta_i} = -V_i V_j t\left(g_{ij}\sin\left(\theta_i-\theta_j\right)+b_{ij}\cos\left(\theta_i-\theta_j\right)\right) \quad \text{(A.V-201)}$$

$$\nabla_{\theta_i}(\nabla_{V_j}\Delta Q_j) = -\frac{\partial^2 Q_j^{TR}}{\partial \theta_i \partial V_j} = -V_i t\left(g_{ij}\cos\left(\theta_i-\theta_j\right)-b_{ij}\sin\left(\theta_i-\theta_j\right)\right) \quad \text{(A.V-202)}$$

$$\nabla_{\theta_i}(\nabla_{t_i}\Delta Q_j) = -\frac{\partial^2 Q_j^{TR}}{\partial \theta_i \partial t_i} = -V_i V_j\left(g_{ij}\cos\left(\theta_i-\theta_j\right)-b_{ij}\sin\left(\theta_i-\theta_j\right)\right) \quad \text{(A.V-203)}$$

$$\nabla_{V_i}(\nabla_{V_i}\Delta Q_j) = -\frac{\partial^2 Q_j^{TR}}{\partial V_i \partial V_i} = 0 \quad \text{(A.V-204)}$$

$$\nabla_{V_i}(\nabla_{\theta_j}\Delta Q_j) = -\frac{\partial^2 Q_j^{TR}}{\partial V_i \partial \theta_j} = V_j t\left(g_{ij}\cos\left(\theta_i-\theta_j\right)-b_{ij}\sin\left(\theta_i-\theta_j\right)\right) \quad \text{(A.V-205)}$$

$$\nabla_{V_i}(\nabla_{V_j}\Delta Q_j) = -\frac{\partial^2 Q_j^{TR}}{\partial V_i \partial V_j} = -t\left(g_{ij}\sin\left(\theta_i-\theta_j\right)+b_{ij}\cos\left(\theta_i-\theta_j\right)\right) \quad \text{(A.V-206)}$$

$$\nabla_{V_i}(\nabla_{t_i}\Delta Q_j) = -\frac{\partial^2 Q_j^{TR}}{\partial V_i \partial t_i} = -V_j\left(g_{ij}\sin\left(\theta_i-\theta_j\right)+b_{ij}\cos\left(\theta_i-\theta_j\right)\right) \quad \text{(A.V-207)}$$

$$\nabla_{\theta_j}(\nabla_{\theta_j}\Delta Q_j) = -\frac{\partial^2 Q_j^{TR}}{\partial \theta_j \partial \theta_j} = V_i V_j t\left(g_{ij}\sin\left(\theta_i-\theta_j\right)+b_{ij}\cos\left(\theta_i-\theta_j\right)\right) \quad \text{(A.V-208)}$$

$$\nabla_{\theta_j}(\nabla_{V_j}\Delta Q_j) = -\frac{\partial^2 Q_j^{TR}}{\partial \theta_j \partial V_j} = V_i t\left(g_{ij}\cos\left(\theta_i-\theta_j\right)-b_{ij}\sin\left(\theta_i-\theta_j\right)\right) \quad \text{(A.V-209)}$$

$$\nabla_{\theta_j}(\nabla_{t_i}\Delta Q_j) = -\frac{\partial^2 Q_j^{TR}}{\partial \theta_j \partial t_i} = V_i V_j\left(g_{ij}\cos\left(\theta_i-\theta_j\right)-b_{ij}\sin\left(\theta_i-\theta_j\right)\right) \quad \text{(A.V-210)}$$

$$\nabla_{V_j}(\nabla_{V_j}\Delta Q_j) = -\frac{\partial^2 Q_j^{TR}}{\partial V_j \partial V_j} = 2b_{ij} \quad \text{(A.V-211)}$$

$$\nabla_{V_j}(\nabla_{t_i}\Delta Q_j) = -\frac{\partial^2 Q_j^{TR}}{\partial V_j \partial t_i} = -V_i\left(g_{ij}\sin\left(\theta_i-\theta_j\right)+b_{ij}\cos\left(\theta_i-\theta_j\right)\right) \quad \text{(A.V-212)}$$

$$\nabla_{t_i}(\nabla_{t_i}\Delta Q_j) = -\frac{\partial^2 Q_j^{TR}}{\partial t_i \partial t_i} = 0 \quad \text{(A.V-213)}$$

APPENDIX VI

List of UPFC FACTS controller power flow equations and first and second order derivatives for the interior point OPF problem, as presented in Chapter 3 and Appendix IV.

At bus *i*: (shunt branch of the UPFC is connected to bus *i*)

$$\begin{aligned}\bar{S}_i^{UPFC} &= \bar{V}_i\left[\sum_{j=sh,se,j}^{N_F} \bar{Y}_{ij}^{UPFC} V_j\right]^* \\ &= \bar{V}_i\left[\bar{Y}_{sh}\left(\bar{V}_i - \bar{V}_{sh}\right) + \bar{Y}_{se}\left(\bar{V}_i - \bar{V}_{se} - \bar{V}_j\right)\right]^* \\ &= \bar{V}_i\left[\bar{I}_{sh} + \bar{I}_{se}\right]^* \\ &= P_i^{UPFC} + jQ_i^{UPFC}\end{aligned} \tag{A.VI-1}$$

where $j = sh$ and se.

$$P_i^{UPFC} = P_i^{sh} + P_i^{se} \tag{A.VI-2}$$

$$Q_i^{UPFC} = Q_i^{sh} + Q_i^{se} \tag{A.VI-3}$$

$$\Delta P_i = P_{g_i} + P_{g_i}^{+} - P_{g_i}^{-} - P_{d_i} - P_i^{LINE} - P_i^{TRANS} - P_i^{UPFC} \tag{A.VI-4}$$

$$\Delta Q_i = Q_{g_i} - Q_{d_i} - Q_i^{LINE} - Q_i^{TRANS} - Q_i^{UPFC} \tag{A.VI-5}$$

where,

$$P_i^{UPFC} = \sum_{i \neq j, j=sh,se}^{N_F} P_{ij}^{UPFC} \tag{A.VI-6}$$

$$Q_i^{UPFC} = \sum_{i \neq j, j=sh,se}^{N_F} Q_{ij}^{UPFC} \tag{A.VI-7}$$

$$\begin{aligned}P_i^{UPFC} = &-V_i V_{sh}\left[g_{sh}\cos\left(\theta_{sh} - \theta_i\right) - b_{sh}\sin\left(\theta_{sh} - \theta_i\right)\right] \\ &-V_i V_{se}\left[g_{ij}\cos\left(\theta_{se} - \theta_i\right) - b_{ij}\sin\left(\theta_{se} - \theta_i\right)\right]\end{aligned} \tag{A.VI-8}$$

$$\begin{aligned}Q_i^{UPFC} = &V_i V_{sh}\left[g_{sh}\sin\left(\theta_{sh} - \theta_i\right) + b_{sh}\cos\left(\theta_{sh} - \theta_i\right)\right] \\ &+V_i V_{se}\left[g_{ij}\sin\left(\theta_{se} - \theta_i\right) + b_{ij}\cos\left(\theta_{se} - \theta_i\right)\right]\end{aligned} \tag{A.VI-9}$$

At bus j : (shunt branch of the UPFC is connected to bus i)

$$\begin{aligned}\bar{S}_j^{UPFC} &= \bar{V}_j\left[\sum_{i=se,j}^{N_F}\bar{Y}_{ij}^{UPFC}V_i\right]^* \\ &= \bar{V}_j\left[\bar{Y}_{se}\left(\bar{V}_j-\bar{V}_{se}-\bar{V}_i\right)\right]^* \\ &= \bar{V}_i\bar{I}_{ji}^* \\ &= P_j^{UPFC}+jQ_j^{UPFC}\end{aligned} \tag{A.VI-10}$$

$$P_j^{UPFC} = P_j^{se} \tag{A.VI-11}$$

$$Q_j^{UPFC} = Q_j^{se} \tag{A.VI-12}$$

$$\Delta P_j = P_{g_j}+P_{g_j}^{+}-P_{g_j}^{-}-P_{d_j}-P_j^{LINE}-P_j^{TRANS}-P_j^{UPFC} \tag{A.VI-13}$$

$$\Delta Q_j = Q_{g_j}-Q_{d_j}-Q_j^{LINE}-Q_j^{TRANS}-Q_j^{UPFC} \tag{A.VI-14}$$

where,

$$P_j^{UPFC} = \sum_{j\neq i,i=se}^{N_F} P_{ji}^{UPFC} \tag{A.VI-15}$$

$$Q_j^{UPFC} = \sum_{j\neq i,i=se}^{N_F} Q_{ji}^{UPFC} \tag{A.VI-16}$$

$$P_j^{UPFC} = V_jV_{se}\left(g_{ij}\cos\left(\theta_{se}-\theta_j\right)-b_{ij}\sin\left(\theta_{se}-\theta_j\right)\right) \tag{A.VI-17}$$

$$Q_j^{UPFC} = -V_jV_{se}\left(g_{ij}\sin\left(\theta_{se}-\theta_j\right)+b_{ij}\cos\left(\theta_{se}-\theta_j\right)\right) \tag{A.VI-18}$$

List of first derivatives

From equations (2.26), (2.37), (2.40) and (2.41)

$$\nabla_{\theta_{se}}h_{\theta_{se}} = 1 \tag{A.VI-19}$$

$$\nabla_{V_{se}}h_{V_{se}} = 1 \tag{A.VI-20}$$

$$\nabla_{\theta_{sh}}h_{\theta_{sh}} = 1 \tag{A.VI-21}$$

$$\nabla_{V_{sh}}h_{V_{sh}} = 1 \tag{A.VI-22}$$

Active power mismatch equation at bus i

$$\nabla_{\theta_{se}}\Delta P_i = -\frac{\partial P_i^{UPFC}}{\partial\theta_{se}} = -\frac{\partial P_i^{se}}{\partial\theta_{se}} = -V_iV_{se}\left[g_{ij}\sin\left(\theta_{se}-\theta_i\right)+b_{ij}\cos\left(\theta_{se}-\theta_i\right)\right] \tag{A.VI-23}$$

$$\nabla_{V_{se}}\Delta P_i = -\frac{\partial P_i^{UPFC}}{\partial V_{se}} = -\frac{\partial P_i^{se}}{\partial V_{se}} = V_i\left[g_{ij}\cos\left(\theta_{se}-\theta_i\right)-b_{ij}\sin\left(\theta_{se}-\theta_i\right)\right] \tag{A.VI-24}$$

$$\nabla_{\theta_{sh}}\Delta P_i = -\frac{\partial P_i^{UPFC}}{\partial \theta_{sh}} = -\frac{\partial P_i^{sh}}{\partial \theta_{sh}} = -V_i V_{sh}\left[g_{sh}\sin(\theta_{sh}-\theta_i)+b_{sh}\cos(\theta_{sh}-\theta_i)\right] \quad \text{(A.VI-25)}$$

$$\nabla_{V_{sh}}\Delta P_i = -\frac{\partial P_i^{UPFC}}{\partial V_{sh}} = -\frac{\partial P_i^{se}}{\partial V_{sh}} = V_i\left[g_{sh}\cos(\theta_{sh}-\theta_i)-b_{sh}\sin(\theta_{sh}-\theta_i)\right] \quad \text{(A.VI-26)}$$

$$\nabla_{\theta_i}\Delta P_i = -\frac{\partial P_i^{UPFC}}{\partial \theta_i} = V_i V_{sh}\left[g_{sh}\sin(\theta_{sh}-\theta_i)+b_{sh}\cos(\theta_{sh}-\theta_i)\right] + V_i V_{se}\left[g_{ij}\sin(\theta_{se}-\theta_i)+b_{ij}\cos(\theta_{se}-\theta_i)\right] \quad \text{(A.VI-27)}$$

$$\nabla_{V_i}\Delta P_i = -\frac{\partial P_i^{UPFC}}{\partial V_i} = V_{sh}\left[g_{sh}\cos(\theta_{sh}-\theta_i)-b_{sh}\sin(\theta_{sh}-\theta_i)\right] + V_{se}\left[g_{ij}\cos(\theta_{se}-\theta_i)-b_{ij}\sin(\theta_{se}-\theta_i)\right] \quad \text{(A.VI-28)}$$

$$\nabla_{\theta_j}\Delta P_i = -\frac{\partial P_i^{UPFC}}{\partial \theta_j} = 0 \quad \text{(A.VI-29)}$$

$$\nabla_{V_j}\Delta P_i = -\frac{\partial P_i^{UPFC}}{\partial V_j} = 0 \quad \text{(A.VI-30)}$$

Reactive power mismatch equations at bus i

$$\nabla_{\theta_{se}}\Delta Q_i = -\frac{\partial Q_i^{UPFC}}{\partial \theta_{se}} = -\frac{\partial Q_i^{se}}{\partial \theta_{se}} = -V_i V_{se}\left[g_{ij}\cos(\theta_{se}-\theta_i)-b_{ij}\sin(\theta_{se}-\theta_i)\right] \quad \text{(A.VI-31)}$$

$$\nabla_{V_{se}}\Delta Q_i = -\frac{\partial Q_i^{UPFC}}{\partial V_{se}} = -\frac{\partial Q_i^{se}}{\partial V_{se}} = -V_i\left[g_{ij}\sin(\theta_{se}-\theta_i)+b_{ij}\cos(\theta_{se}-\theta_i)\right] \quad \text{(A.VI-32)}$$

$$\nabla_{\theta_{sh}}\Delta Q_i = -\frac{\partial Q_i^{UPFC}}{\partial \theta_{sh}} = -\frac{\partial Q_i^{sh}}{\partial \theta_{sh}} = -V_i V_{sh}\left[g_{sh}\cos(\theta_{sh}-\theta_i)-b_{sh}\sin(\theta_{sh}-\theta_i)\right] \quad \text{(A.VI-33)}$$

$$\nabla_{V_{sh}}\Delta Q_i = -\frac{\partial Q_i^{UPFC}}{\partial V_{sh}} = -\frac{\partial Q_i^{sh}}{\partial V_{sh}} = -V_i\left[g_{sh}\sin(\theta_{sh}-\theta_i)+b_{sh}\cos(\theta_{sh}-\theta_i)\right] \quad \text{(A.VI-34)}$$

$$\nabla_{\theta_i}\Delta Q_i = -\frac{\partial Q_i^{UPFC}}{\partial \theta_i} = V_i V_{sh}\left[g_{sh}\cos(\theta_{sh}-\theta_i)-b_{sh}\sin(\theta_{sh}-\theta_i)\right] + V_i V_{se}\left[g_{ij}\cos(\theta_{se}-\theta_i)-b_{ij}\sin(\theta_{se}-\theta_i)\right] \quad \text{(A.VI-35)}$$

$$\nabla_{V_i}\Delta Q_i = -\frac{\partial Q_i^{UPFC}}{\partial V_i} = -V_{sh}\left[g_{sh}\sin(\theta_{sh}-\theta_i)+b_{sh}\cos(\theta_{sh}-\theta_i)\right] - V_{se}\left[g_{ij}\sin(\theta_{se}-\theta_i)+b_{ij}\cos(\theta_{se}-\theta_i)\right] \quad \text{(A.VI-36)}$$

$$\nabla_{\theta_j}\Delta Q_i = -\frac{\partial Q_i^{UPFC}}{\partial \theta_j} = 0 \quad \text{(A.VI-37)}$$

$$\nabla_{V_j}\Delta Q_i = -\frac{\partial Q_i^{UPFC}}{\partial V_j} = 0 \quad \text{(A.VI-38)}$$

Active power mismatch equations at bus j

$$\nabla_{\theta_{se}}\Delta P_j = -\frac{\partial P_j^{UPFC}}{\partial \theta_{se}} = -\frac{\partial P_j^{se}}{\partial \theta_{se}} = V_j V_{se}\left[g_{ij}\sin\left(\theta_{se}-\theta_j\right)+b_{ij}\cos\left(\theta_{se}-\theta_j\right)\right] \quad \text{(A.VI-39)}$$

$$\nabla_{V_{se}}\Delta P_j = -\frac{\partial P_j^{UPFC}}{\partial V_{se}} = -\frac{\partial P_j^{se}}{\partial V_{se}} = -V_j\left[g_{ij}\cos\left(\theta_{se}-\theta_j\right)-b_{ij}\sin\left(\theta_{se}-\theta_j\right)\right] \quad \text{(A.VI-40)}$$

$$\nabla_{\theta_{sh}}\Delta P_j = -\frac{\partial P_j^{UPFC}}{\partial \theta_{sh}} = 0 \quad \text{(A.VI-41)}$$

$$\nabla_{V_{sh}}\Delta P_j = -\frac{\partial P_j^{UPFC}}{\partial V_{sh}} = 0 \quad \text{(A.VI-42)}$$

$$\nabla_{\theta_i}\Delta P_j = -\frac{\partial P_j^{UPFC}}{\partial \theta_i} = 0 \quad \text{(A.VI-43)}$$

$$\nabla_{V_i}\Delta P_j = -\frac{\partial P_j^{UPFC}}{\partial V_i} = 0 \quad \text{(A.VI-44)}$$

$$\nabla_{\theta_j}\Delta P_j = -\frac{\partial P_j^{UPFC}}{\partial \theta_j} = -\frac{\partial P_j^{se}}{\partial \theta_{se}} = -V_j V_{se}\left[g_{ij}\sin\left(\theta_{se}-\theta_j\right)+b_{ij}\cos\left(\theta_{se}-\theta_j\right)\right] \quad \text{(A.VI-45)}$$

$$\nabla_{V_j}\Delta P_j = -\frac{\partial P_j^{UPFC}}{\partial V_j} = -\frac{\partial P_j^{se}}{\partial V_j} = -V_{se}\left[g_{ij}\cos\left(\theta_{se}-\theta_j\right)-b_{ij}\sin\left(\theta_{se}-\theta_j\right)\right] \quad \text{(A.VI-46)}$$

Reactive power mismatch equations at bus j

$$\nabla_{\theta_{se}}\Delta Q_j = -\frac{\partial Q_j^{UPFC}}{\partial \theta_{se}} = -\frac{\partial Q_j^{se}}{\partial \theta_{se}} = V_j V_{se}\left[g_{ij}\cos\left(\theta_{se}-\theta_j\right)-b_{ij}\sin\left(\theta_{se}-\theta_j\right)\right] \quad \text{(A.VI-47)}$$

$$\nabla_{V_{se}}\Delta Q_j = -\frac{\partial Q_j^{UPFC}}{\partial V_{se}} = -\frac{\partial Q_j^{se}}{\partial V_{se}} = V_j\left[g_{ij}\sin\left(\theta_{se}-\theta_j\right)+b_{ij}\cos\left(\theta_{se}-\theta_j\right)\right] \quad \text{(A.VI-48)}$$

$$\nabla_{\theta_{sh}}\Delta Q_j = -\frac{\partial Q_j^{UPFC}}{\partial \theta_{sh}} = 0 \quad \text{(A.VI-49)}$$

$$\nabla_{V_{sh}}\Delta Q_j = -\frac{\partial Q_j^{UPFC}}{\partial V_{sh}} = 0 \quad \text{(A.VI-50)}$$

$$\nabla_{\theta_i}\Delta Q_j = -\frac{\partial Q_j^{UPFC}}{\partial \theta_i} = 0 \quad \text{(A.VI-51)}$$

$$\nabla_{V_i}\Delta Q_j = -\frac{\partial Q_j^{UPFC}}{\partial V_i} = 0 \quad \text{(A.VI-52)}$$

$$\nabla_{\theta_j}\Delta Q_j = -\frac{\partial Q_j^{UPFC}}{\partial \theta_j} = -\frac{\partial Q_j^{se}}{\partial \theta_j} = -V_j V_{se}\left[g_{ij}\cos\left(\theta_{se}-\theta_j\right) - b_{ij}\sin\left(\theta_{se}-\theta_j\right)\right] \quad \text{(A.VI-53)}$$

$$\nabla_{V_j}\Delta Q_j = -\frac{\partial Q_j^{UPFC}}{\partial V_j} = -\frac{\partial Q_j^{se}}{\partial V_j} = V_{se}\left[g_{ij}\sin\left(\theta_{se}-\theta_j\right) + b_{ij}\cos\left(\theta_{se}-\theta_j\right)\right] \quad \text{(A.VI-54)}$$

FACTS controller, list of second derivatives

From equation (2.37):

Active power mismatch equations at bus *i*:

$$\nabla_{\theta_{se}}\left(\nabla_{\theta_{se}}\Delta P_i\right) = -\frac{\partial^2 P_i^{UPFC}}{\partial\theta_{se}\partial\theta_{se}} = -\frac{\partial^2 P_i^{se}}{\partial\theta_{se}\partial\theta_{se}} = -V_i V_{se}\left[g_{ij}\cos\left(\theta_{se}-\theta_i\right) - b_{ij}\sin\left(\theta_{se}-\theta_i\right)\right] \quad \text{(A.VI-55)}$$

$$\nabla_{V_{se}}\left(\nabla_{\theta_{se}}\Delta P_i\right) = -\frac{\partial^2 P_i^{UPFC}}{\partial\theta_{se}\partial V_{se}} = -\frac{\partial^2 P_i^{se}}{\partial\theta_{se}\partial V_{se}} = -V_i\left[g_{ij}\sin\left(\theta_{se}-\theta_i\right) + b_{ij}\cos\left(\theta_{se}-\theta_i\right)\right] \quad \text{(A.VI-56)}$$

$$\nabla_{\theta_{sh}}\left(\nabla_{\theta_{se}}\Delta P_i\right) = -\frac{\partial^2 P_i^{UPFC}}{\partial\theta_{se}\partial\theta_{sh}} = 0 \quad \text{(A.VI-57)}$$

$$\nabla_{V_{sh}}\left(\nabla_{\theta_{se}}\Delta P_i\right) = -\frac{\partial^2 P_i^{UPFC}}{\partial\theta_{se}\partial V_{sh}} = 0 \quad \text{(A.VI-58)}$$

$$\nabla_{\theta_i}\left(\nabla_{\theta_{se}}\Delta P_i\right) = -\frac{\partial^2 P_i^{UPFC}}{\partial\theta_{se}\partial\theta_i} = -\frac{\partial^2 P_i^{se}}{\partial\theta_{se}\partial\theta_i} = V_i V_{se}\left[g_{ij}\cos\left(\theta_{se}-\theta_i\right) - b_{ij}\sin\left(\theta_{se}-\theta_i\right)\right] \quad \text{(A.VI-59)}$$

$$\nabla_{V_i}\left(\nabla_{\theta_{se}}\Delta P_i\right) = -\frac{\partial^2 P_i^{UPFC}}{\partial\theta_{se}\partial V_i} = -\frac{\partial^2 P_i^{se}}{\partial\theta_{se}\partial V_i} = -V_{se}\left[g_{ij}\sin\left(\theta_{se}-\theta_i\right) + b_{ij}\cos\left(\theta_{se}-\theta_i\right)\right] \quad \text{(A.VI-60)}$$

$$\nabla_{\theta_j}\left(\nabla_{\theta_{se}}\Delta P_i\right) = -\frac{\partial^2 P_i^{UPFC}}{\partial\theta_{se}\partial\theta_j} = 0 \quad \text{(A.VI-61)}$$

$$\nabla_{V_j}\left(\nabla_{\theta_{se}}\Delta P_i\right) = -\frac{\partial^2 P_i^{UPFC}}{\partial\theta_{se}\partial V_j} = 0 \quad \text{(A.VI-62)}$$

$$\nabla_{V_{se}}\left(\nabla_{V_{se}}\Delta P_i\right) = -\frac{\partial^2 P_i^{UPFC}}{\partial V_{se}\partial V_{se}} = 0 \quad \text{(A.VI-63)}$$

$$\nabla_{\theta_{sh}}\left(\nabla_{V_{se}}\Delta P_i\right) = -\frac{\partial^2 P_i^{UPFC}}{\partial V_{se}\partial\theta_{sh}} = 0 \quad \text{(A.VI-64)}$$

$$\nabla_{V_{sh}}\left(\nabla_{V_{se}}\Delta P_i\right) = -\frac{\partial^2 P_i^{UPFC}}{\partial V_{se}\partial V_{sh}} = 0 \quad \text{(A.VI-65)}$$

$$\nabla_{\theta_i}\left(\nabla_{V_{se}}\Delta P_i\right)=-\frac{\partial^2 P_i^{UPFC}}{\partial V_{se}\partial\theta_i}=-\frac{\partial^2 P_i^{se}}{\partial V_{se}\partial\theta_i}=V_i\left[g_{ij}\sin\left(\theta_{se}-\theta_i\right)+b_{ij}\cos\left(\theta_{se}-\theta_i\right)\right] \quad \text{(A.VI-66)}$$

$$\nabla_{V_i}\left(\nabla_{V_{se}}\Delta P_i\right)=-\frac{\partial^2 P_i^{UPFC}}{\partial V_{se}\partial V_i}=-\frac{\partial^2 P_i}{\partial V_{se}\partial V_i}=\left[g_{ij}\cos\left(\theta_{se}-\theta_i\right)-b_{ij}\sin\left(\theta_{se}-\theta_i\right)\right] \quad \text{(A.VI-67)}$$

$$\nabla_{\theta_j}\left(\nabla_{V_{se}}\Delta P_i\right)=-\frac{\partial^2 P_i^{UPFC}}{\partial V_{se}\partial\theta_j}=0 \quad \text{(A.VI-68)}$$

$$\nabla_{V_j}\left(\nabla_{V_{se}}\Delta P_i\right)=-\frac{\partial^2 P_i^{UPFC}}{\partial V_{se}\partial V_j}=0 \quad \text{(A.VI-69)}$$

$$\begin{aligned}\nabla_{\theta_{sh}}\left(\nabla_{\theta_{sh}}\Delta P_i\right)&=-\frac{\partial^2 P_i^{UPFC}}{\partial\theta_{sh}\partial\theta_{sh}}\\&=-\frac{\partial^2 P_i^{sh}}{\partial\theta_{sh}\partial\theta_{sh}}=-V_iV_{sh}\left[g_{sh}\cos\left(\theta_{sh}-\theta_i\right)-b_{sh}\sin\left(\theta_{sh}-\theta_i\right)\right]\end{aligned} \quad \text{(A.VI-70)}$$

$$\nabla_{V_{sh}}\left(\nabla_{\theta_{sh}}\Delta P_i\right)=-\frac{\partial^2 P_i^{UPFC}}{\partial\theta_{sh}\partial V_{sh}}=-\frac{\partial^2 P_i^{sh}}{\partial\theta_{sh}\partial V_{sh}}=-V_i\left[g_{sh}\sin\left(\theta_{sh}-\theta_i\right)+b_{sh}\cos\left(\theta_{sh}-\theta_i\right)\right] \quad \text{(A.VI-71)}$$

$$\nabla_{\theta_i}\left(\nabla_{\theta_{sh}}\Delta P_i\right)=-\frac{\partial^2 P_i^{UPFC}}{\partial\theta_{sh}\partial\theta_i}=\frac{\partial^2 P_i^{sh}}{\partial\theta_{sh}\partial\theta_i}=V_iV_{sh}\left[g_{sh}\cos\left(\theta_{sh}-\theta_i\right)-b_{sh}\sin\left(\theta_{sh}-\theta_i\right)\right] \quad \text{(A.VI-72)}$$

$$\nabla_{V_i}\left(\nabla_{\theta_{sh}}\Delta P_i\right)=-\frac{\partial^2 P_i^{UPFC}}{\partial\theta_{sh}\partial V_i}=-\frac{\partial^2 P_i^{sh}}{\partial\theta_{sh}\partial V_i}=-V_{sh}\left[g_{sh}\sin\left(\theta_{sh}-\theta_i\right)+b_{sh}\cos\left(\theta_{sh}-\theta_i\right)\right] \quad \text{(A.VI-73)}$$

$$\nabla_{\theta_j}\left(\nabla_{\theta_{sh}}\Delta P_i\right)=-\frac{\partial^2 P_i^{UPFC}}{\partial\theta_{sh}\partial\theta_j}=0 \quad \text{(A.VI-74)}$$

$$\nabla_{V_j}\left(\nabla_{\theta_{sh}}\Delta P_i\right)=-\frac{\partial^2 P_i^{UPFC}}{\partial\theta_{sh}\partial V_j}=0 \quad \text{(A.VI-75)}$$

$$\nabla_{V_{sh}}\left(\nabla_{V_{sh}}\Delta P_i\right)=-\frac{\partial^2 P_i^{UPFC}}{\partial V_{sh}\partial V_{sh}}=0 \quad \text{(A.VI-76)}$$

$$\nabla_{\theta_i}\left(\nabla_{V_{sh}}\Delta P_i\right)=-\frac{\partial^2 P_i^{UPFC}}{\partial V_{sh}\partial\theta_i}=-\frac{\partial^2 P_i^{sh}}{\partial V_{sh}\partial\theta_i}=V_i\left[g_{sh}\sin\left(\theta_{sh}-\theta_i\right)+b_{sh}\cos\left(\theta_{sh}-\theta_i\right)\right] \quad \text{(A.VI-77)}$$

$$\nabla_{V_i}\left(\nabla_{V_{sh}}\Delta P_i\right)=-\frac{\partial^2 P_i^{UPFC}}{\partial V_{sh}\partial V_i}=-\frac{\partial^2 P_i^{sh}}{\partial V_{sh}\partial V_i}=\left[g_{sh}\cos\left(\theta_{sh}-\theta_i\right)-b_{sh}\sin\left(\theta_{sh}-\theta_i\right)\right] \quad \text{(A.VI-78)}$$

$$\nabla_{\theta_j}\left(\nabla_{V_{sh}}\Delta P_i\right)=-\frac{\partial^2 P_i^{UPFC}}{\partial V_{sh}\partial\theta_j}=0 \quad \text{(A.VI-79)}$$

$$\nabla_{V_j}\left(\nabla_{V_{sh}}\Delta P_i\right)=-\frac{\partial^2 P_i^{UPFC}}{\partial V_{sh}\partial V_j}=0 \quad \text{(A.VI-80)}$$

$$\nabla_{\theta_i}\left(\nabla_{\theta_i}\Delta P_i\right)=-\frac{\partial^2 P_i^{UPFC}}{\partial\theta_i\partial\theta_i}=-V_iV_{sh}\left[g_{sh}\cos\left(\theta_{sh}-\theta_i\right)-b_{sh}\sin\left(\theta_{sh}-\theta_i\right)\right]$$
$$-V_iV_{se}\left[g_{ij}\cos\left(\theta_{se}-\theta_i\right)-b_{ij}\sin\left(\theta_{se}-\theta_i\right)\right] \quad \text{(A.VI-81)}$$

$$\nabla_{V_i}\left(\nabla_{\theta_i}\Delta P_i\right)=-\frac{\partial^2 P_i^{UPFC}}{\partial\theta_i\partial V_i}=V_{sh}\left[g_{sh}\sin\left(\theta_{sh}-\theta_i\right)+b_{sh}\cos\left(\theta_{sh}-\theta_i\right)\right]$$
$$+V_{se}\left[g_{sh}\sin\left(\theta_{se}-\theta_i\right)+b_{sh}\cos\left(\theta_{se}-\theta_i\right)\right] \quad \text{(A.VI-82)}$$

$$\nabla_{\theta_j}\left(\nabla_{\theta_i}\Delta P_i\right)=-\frac{\partial^2 P_i^{UPFC}}{\partial\theta_i\partial\theta_j}=0 \quad \text{(A.VI-83)}$$

$$\nabla_{V_j}\left(\nabla_{\theta_i}\Delta P_i\right)=-\frac{\partial^2 P_i^{UPFC}}{\partial\theta_i\partial V_j}=0 \quad \text{(A.VI-84)}$$

$$\nabla_{V_i}\left(\nabla_{V_i}\Delta P_i\right)=-\frac{\partial^2 P_i^{UPFC}}{\partial V_i\partial V_i}=0 \quad \text{(A.VI-85)}$$

$$\nabla_{\theta_j}\left(\nabla_{V_i}\Delta P_i\right)=-\frac{\partial^2 P_i^{UPFC}}{\partial V_i\partial\theta_j}=0 \quad \text{(A.VI-86)}$$

$$\nabla_{V_j}\left(\nabla_{V_i}\Delta P_i\right)=-\frac{\partial^2 P_i^{UPFC}}{\partial V_i\partial V_j}=0 \quad \text{(A.VI-87)}$$

$$\nabla_{\theta_j}\left(\nabla_{\theta_j}\Delta P_i\right)=-\frac{\partial^2 P_i^{UPFC}}{\partial\theta_j\partial\theta_j}=0 \quad \text{(A.VI-88)}$$

$$\nabla_{V_j}\left(\nabla_{\theta_i}\Delta P_i\right)=-\frac{\partial^2 P_i^{UPFC}}{\partial\theta_j\partial V_j}=0 \quad \text{(A.VI-89)}$$

$$\nabla_{V_j}\left(\nabla_{V_j}\Delta P_i\right)=-\frac{\partial^2 P_i^{UPFC}}{\partial V_j\partial V_j}=0 \quad \text{(A.VI-90)}$$

Reactive power mismatch equations at bus i:

$$\nabla_{\theta_{se}}\left(\nabla_{\theta_{se}}\Delta Q_i\right)=-\frac{\partial^2 Q_i^{UPFC}}{\partial\theta_{se}\partial\theta_{se}}=-\frac{\partial^2 Q_i^{se}}{\partial\theta_{se}\partial\theta_{se}}=V_iV_{se}\left[g_{ij}\sin\left(\theta_{se}-\theta_i\right)+b_{ij}\cos\left(\theta_{se}-\theta_i\right)\right] \quad \text{(A.VI-91)}$$

$$\nabla_{V_{se}}\left(\nabla_{\theta_{se}}\Delta Q_i\right)=-\frac{\partial^2 Q_i^{UPFC}}{\partial\theta_{se}\partial V_{se}}=-\frac{\partial^2 Q_i^{se}}{\partial\theta_{se}\partial V_{se}}=-V_i\left[g_{ij}\cos\left(\theta_{se}-\theta_i\right)-b_{ij}\sin\left(\theta_{se}-\theta_i\right)\right] \quad \text{(A.VI-92)}$$

$$\nabla_{\theta_{sh}}\left(\nabla_{\theta_{se}}\Delta Q_i\right)=-\frac{\partial^2 Q_i^{UPFC}}{\partial\theta_{se}\partial\theta_{sh}}=0 \quad \text{(A.VI-93)}$$

$$\nabla_{V_{sh}}\left(\nabla_{\theta_{se}}\Delta Q_i\right)=-\frac{\partial^2 Q_i^{UPFC}}{\partial\theta_{se}\partial V_{sh}}=0 \quad \text{(A.VI-94)}$$

$$\nabla_{\theta_i}\left(\nabla_{\theta_{se}}\Delta Q_i\right)=-\frac{\partial^2 Q_i^{UPFC}}{\partial\theta_{se}\partial\theta_i}=-\frac{\partial^2 Q_i^{se}}{\partial\theta_{se}\partial\theta_i}=-V_iV_{se}\left[g_{ij}\sin\left(\theta_{se}-\theta_i\right)+b_{ij}\cos\left(\theta_{se}-\theta_i\right)\right] \quad \text{(A.VI-95)}$$

$$\nabla_{V_i}\left(\nabla_{\theta_{se}}\Delta Q_i\right)=-\frac{\partial^2 Q_i^{UPFC}}{\partial\theta_{se}\partial V_i}=-\frac{\partial^2 Q_i^{se}}{\partial\theta_{se}\partial V_i}=-V_{se}\left[g_{ij}\cos\left(\theta_{se}-\theta_i\right)-b_{ij}\sin\left(\theta_{se}-\theta_i\right)\right] \quad \text{(A.VI-96)}$$

$$\nabla_{\theta_j}\left(\nabla_{\theta_{se}}\Delta Q_i\right)=-\frac{\partial^2 Q_i^{UPFC}}{\partial\theta_{se}\partial\theta_j}=0 \quad \text{(A.VI-97)}$$

$$\nabla_{V_j}\left(\nabla_{\theta_{se}}\Delta Q_i\right)=-\frac{\partial^2 Q_i^{UPFC}}{\partial\theta_{se}\partial V_j}=0 \quad \text{(A.VI-98)}$$

$$\nabla_{V_{se}}\left(\nabla_{V_{se}}\Delta Q_i\right)=-\frac{\partial^2 Q_i^{UPFC}}{\partial V_{se}\partial V_{se}}=0 \quad \text{(A.VI-99)}$$

$$\nabla_{\theta_{sh}}\left(\nabla_{\theta_{se}}\Delta Q_i\right)=-\frac{\partial^2 Q_i^{UPFC}}{\partial\theta_{se}\partial\theta_{sh}}=0 \quad \text{(A.VI-100)}$$

$$\nabla_{V_{sh}}\left(\nabla_{\theta_{se}}\Delta Q_i\right)=-\frac{\partial^2 Q_i^{UPFC}}{\partial\theta_{se}\partial V_{sh}}=0 \quad \text{(A.VI-101)}$$

$$\nabla_{\theta_i}\left(\nabla_{V_{se}}\Delta Q_i\right)=-\frac{\partial^2 Q_i^{UPFC}}{\partial V_{se}\partial\theta_i}=-\frac{\partial^2 Q_i^{se}}{\partial V_{se}\partial\theta_i}=V_i\left[g_{ij}\cos\left(\theta_{se}-\theta_i\right)-b_{ij}\sin\left(\theta_{se}-\theta_i\right)\right] \quad \text{(A.VI-102)}$$

$$\nabla_{V_i}\left(\nabla_{V_{se}}\Delta Q_i\right)=-\frac{\partial^2 Q_i^{UPFC}}{\partial V_{se}\partial V_i}=-\frac{\partial^2 Q_i}{\partial V_{se}\partial V_i}=-\left[g_{ij}\sin\left(\theta_{se}-\theta_i\right)+b_{ij}\cos\left(\theta_{se}-\theta_i\right)\right] \quad \text{(A.VI-103)}$$

$$\nabla_{\theta_j}\left(\nabla_{V_{se}}\Delta Q_i\right)=-\frac{\partial^2 Q_i^{UPFC}}{\partial V_{se}\partial\theta_j}=0 \quad \text{(A.VI-104)}$$

$$\nabla_{V_j}\left(\nabla_{V_{se}}\Delta Q_i\right)=-\frac{\partial^2 Q_i^{UPFC}}{\partial V_{se}\partial V_j}=0 \quad \text{(A.VI-105)}$$

$$\nabla_{\theta_{sh}}\left(\nabla_{\theta_{sh}}\Delta Q_i\right)=-\frac{\partial^2 Q_i^{UPFC}}{\partial\theta_{sh}\partial\theta_{sh}}=-\frac{\partial^2 Q_i^{sh}}{\partial\theta_{sh}\partial\theta_{sh}}=V_iV_{sh}\left[g_{sh}\sin\left(\theta_{sh}-\theta_i\right)+b_{sh}\cos\left(\theta_{sh}-\theta_i\right)\right] \quad \text{(A.VI-106)}$$

$$\nabla_{V_{sh}}\left(\nabla_{\theta_{sh}}\Delta Q_i\right)=-\frac{\partial^2 Q_i^{UPFC}}{\partial\theta_{sh}\partial V_{sh}}=-\frac{\partial^2 Q_i^{sh}}{\partial\theta_{sh}\partial V_{sh}}=-V_i\left[g_{sh}\cos\left(\theta_{sh}-\theta_i\right)-b_{sh}\sin\left(\theta_{sh}-\theta_i\right)\right] \quad \text{(A.VI-107)}$$

$$\nabla_{\theta_i}\left(\nabla_{\theta_{sh}}\Delta Q_i\right)=-\frac{\partial^2 Q_i^{UPFC}}{\partial\theta_{sh}\partial\theta_i}$$
$$=-\frac{\partial^2 Q_i}{\partial\theta_{sh}\partial\theta_i}=-V_iV_{sh}\left[g_{sh}\sin\left(\theta_{sh}-\theta_i\right)+b_{sh}\cos\left(\theta_{sh}-\theta_i\right)\right] \quad \text{(A.VI-108)}$$

$$\nabla_{V_i}\left(\nabla_{\theta_{sh}}\Delta Q_i\right)=-\frac{\partial^2 Q_i^{UPFC}}{\partial\theta_{sh}\partial V_i}$$
$$=-\frac{\partial^2 Q_i^{sh}}{\partial\theta_{sh}\partial V_i}=-V_{sh}\left[g_{sh}\cos\left(\theta_{sh}-\theta_i\right)-b_{sh}\sin\left(\theta_{sh}-\theta_i\right)\right] \quad \text{(A.VI-109)}$$

$$\nabla_{\theta_j}\left(\nabla_{\theta_{sh}}\Delta Q_i\right)=-\frac{\partial^2 Q_i^{UPFC}}{\partial\theta_{sh}\partial\theta_j}=0 \quad \text{(A.VI-110)}$$

$$\nabla_{V_j}\left(\nabla_{\theta_{sh}}\Delta Q_i\right)=-\frac{\partial^2 Q_i^{UPFC}}{\partial\theta_{sh}\partial V_j}=0 \quad \text{(A.VI-111)}$$

$$\nabla_{V_{sh}}\left(\nabla_{V_{sh}}\Delta Q_i\right)=-\frac{\partial^2 Q_i^{UPFC}}{\partial V_{sh}\partial V_{sh}}=0 \quad \text{(A.VI-112)}$$

$$\nabla_{\theta_i}\left(\nabla_{V_{sh}}\Delta Q_i\right)=-\frac{\partial^2 Q_i^{UPFC}}{\partial V_{sh}\partial\theta_i}=-\frac{\partial^2 Q_i^{sh}}{\partial V_{sh}\partial\theta_i}=V_i\left[g_{sh}\cos\left(\theta_{sh}-\theta_i\right)-b_{sh}\sin\left(\theta_{sh}-\theta_i\right)\right] \quad \text{(A.VI-113)}$$

$$\nabla_{V_i}\left(\nabla_{V_{sh}}\Delta Q_i\right)=-\frac{\partial^2 Q_i^{UPFC}}{\partial V_{sh}\partial V_i}=-\frac{\partial^2 Q_i}{\partial V_{sh}\partial V_i}=-\left[g_{sh}\sin\left(\theta_{sh}-\theta_i\right)+b_{sh}\cos\left(\theta_{sh}-\theta_i\right)\right] \quad \text{(A.VI-114)}$$

$$\nabla_{\theta_j}\left(\nabla_{V_{sh}}\Delta Q_i\right)=-\frac{\partial^2 Q_i^{UPFC}}{\partial V_{sh}\partial\theta_j}=0 \quad \text{(A.VI-115)}$$

$$\nabla_{V_j}\left(\nabla_{V_{sh}}\Delta Q_i\right)=-\frac{\partial^2 Q_i^{UPFC}}{\partial V_{sh}\partial V_j}=0 \quad \text{(A.VI-116)}$$

$$\nabla_{\theta_i}\left(\nabla_{\theta_i}\Delta Q_i\right)=-\frac{\partial^2 Q_i^{UPFC}}{\partial\theta_i\partial\theta_i}=-\frac{\partial^2 Q_i}{\partial\theta_i\partial\theta_i}=V_iV_{sh}\left[g_{sh}\sin\left(\theta_{sh}-\theta_i\right)+b_{sh}\cos\left(\theta_{sh}-\theta_i\right)\right]$$
$$+V_iV_{se}\left[g_{ij}\sin\left(\theta_{se}-\theta_i\right)+b_{ij}\cos\left(\theta_{se}-\theta_i\right)\right] \quad \text{(A.VI-117)}$$

$$\nabla_{V_i}\left(\nabla_{\theta_i}\Delta Q_i\right)=-\frac{\partial^2 Q_i^{UPFC}}{\partial\theta_i\partial V_i}=-\frac{\partial^2 Q_i^{sh}}{\partial\theta_i\partial V_i}=V_{sh}\left[g_{sh}\cos\left(\theta_{sh}-\theta_i\right)-b_{sh}\sin\left(\theta_{sh}-\theta_i\right)\right]$$
$$+V_{se}\left[g_{ij}\cos\left(\theta_{se}-\theta_i\right)-b_{ij}\sin\left(\theta_{se}-\theta_i\right)\right] \quad \text{(A.VI-118)}$$

$$\nabla_{\theta_j}\left(\nabla_{\theta_i}\Delta Q_i\right)=-\frac{\partial^2 Q_i^{UPFC}}{\partial\theta_i\partial\theta_j}=0 \quad \text{(A.VI-119)}$$

$$\nabla_{V_j}\left(\nabla_{\theta_i}\Delta Q_i\right)=-\frac{\partial^2 Q_i^{UPFC}}{\partial\theta_i\partial V_j}=0 \quad \text{(A.VI-120)}$$

$$\nabla_{V_i}\left(\nabla_{V_i}\Delta Q_i\right)=-\frac{\partial^2 Q_i^{UPFC}}{\partial V_i\partial\theta_i}=0 \tag{A.VI-121}$$

$$\nabla_{\theta_j}\left(\nabla_{V_i}\Delta Q_i\right)=-\frac{\partial^2 Q_i^{UPFC}}{\partial V_i\partial\theta_j}=0 \tag{A.VI-122}$$

$$\nabla_{V_j}\left(\nabla_{V_i}\Delta Q_i\right)=-\frac{\partial^2 Q_i^{UPFC}}{\partial V_i\partial V_j}=0 \tag{A.VI-123}$$

$$\nabla_{\theta_j}\left(\nabla_{\theta_j}\Delta Q_i\right)=-\frac{\partial^2 Q_i^{UPFC}}{\partial\theta_j\partial\theta_j}=0 \tag{A.VI-124}$$

$$\nabla_{V_j}\left(\nabla_{\theta_j}\Delta Q_i\right)=-\frac{\partial^2 Q_i^{UPFC}}{\partial\theta_j\partial V_j}=0 \tag{A.VI-125}$$

$$\nabla_{V_j}\left(\nabla_{V_j}\Delta Q_i\right)=-\frac{\partial^2 Q_i^{UPFC}}{\partial V_j\partial V_j}=0 \tag{A.VI-126}$$

Active power mismatch equations at bus *j*:

$$\nabla_{\theta_{se}}\left(\nabla_{\theta_{se}}\Delta P_j\right)=-\frac{\partial^2 P_j^{UPFC}}{\partial\theta_{se}\partial\theta_{se}}$$
$$=-\frac{\partial^2 P_j^{se}}{\partial\theta_{se}\partial\theta_{se}}=V_jV_{se}\left[g_{ij}\cos\left(\theta_{se}-\theta_j\right)-b_{ij}\sin\left(\theta_{se}-\theta_j\right)\right] \tag{A.VI-127}$$

$$\nabla_{V_{se}}\left(\nabla_{\theta_{se}}\Delta P_j\right)=-\frac{\partial^2 P_j^{UPFC}}{\partial\theta_{se}\partial V_{se}}=-\frac{\partial^2 P_j^{se}}{\partial\theta_{se}\partial V_{se}}=V_j\left[g_{ij}\sin\left(\theta_{se}-\theta_j\right)+b_{ij}\cos\left(\theta_{se}-\theta_j\right)\right] \tag{A.VI-128}$$

$$\nabla_{\theta_{sh}}\left(\nabla_{\theta_{se}}\Delta P_j\right)=-\frac{\partial^2 P_j^{UPFC}}{\partial\theta_{se}\partial\theta_{sh}}=0 \tag{A.VI-129}$$

$$\nabla_{V_{sh}}\left(\nabla_{\theta_{se}}\Delta P_j\right)=-\frac{\partial^2 P_j^{UPFC}}{\partial\theta_{se}\partial V_{sh}}=0 \tag{A.VI-130}$$

$$\nabla_{\theta_i}\left(\nabla_{\theta_{se}}\Delta P_j\right)=-\frac{\partial^2 P_j^{UPFC}}{\partial\theta_{se}\partial\theta_i}=0 \tag{A.VI-131}$$

$$\nabla_{V_i}\left(\nabla_{\theta_{se}}\Delta P_j\right)=-\frac{\partial^2 P_j^{UPFC}}{\partial\theta_{se}\partial V_i}=0 \tag{A.VI-133}$$

$$\nabla_{\theta_j}\left(\nabla_{\theta_{se}}\Delta P_j\right)=-\frac{\partial^2 P_j^{UPFC}}{\partial\theta_{se}\partial\theta_j}$$
$$=-\frac{\partial^2 P_j^{se}}{\partial\theta_{se}\partial\theta_j}=-V_jV_{se}\left[g_{ij}\cos\left(\theta_{se}-\theta_j\right)-b_{ij}\sin\left(\theta_{se}-\theta_j\right)\right] \tag{A.VI-134}$$

$$\nabla V_j\left(\nabla\theta_{se}\Delta P_j\right)=-\frac{\partial^2 P_j^{UPFC}}{\partial\theta_{se}\partial V_j}=-\frac{\partial^2 P_j^{se}}{\partial\theta_{se}\partial V_j}=V_{se}\left[g_{ij}\sin\left(\theta_{se}-\theta_j\right)+b_{ij}\cos\left(\theta_{se}-\theta_j\right)\right] \quad \text{(A.VI-135)}$$

$$\nabla V_{se}\left(\nabla V_{se}\Delta P_j\right)=-\frac{\partial^2 P_j^{UPFC}}{\partial V_{se}\partial V_{se}}=0 \quad \text{(A.VI-136)}$$

$$\nabla\theta_{sh}\left(\nabla V_{se}\Delta P_j\right)=-\frac{\partial^2 P_j^{UPFC}}{\partial V_{se}\partial\theta_{sh}}=0 \quad \text{(A.VI-137)}$$

$$\nabla V_{sh}\left(\nabla V_{se}\Delta P_j\right)=-\frac{\partial^2 P_j^{UPFC}}{\partial V_{se}\partial V_{sh}}=0 \quad \text{(A.VI-138)}$$

$$\nabla\theta_i\left(\nabla V_{se}\Delta P_j\right)=-\frac{\partial^2 P_j^{UPFC}}{\partial V_{se}\partial\theta_i}=0 \quad \text{(A.VI-139)}$$

$$\nabla V_i\left(\nabla V_{se}\Delta P_j\right)=-\frac{\partial^2 P_j^{UPFC}}{\partial V_{se}\partial V_i}=0 \quad \text{(A.VI-140)}$$

$$\nabla\theta_j\left(\nabla V_{se}\Delta P_j\right)=-\frac{\partial^2 P_j^{UPFC}}{\partial V_{se}\partial\theta_j}=-\frac{\partial^2 P_j^{se}}{\partial V_{se}\partial\theta_j}=-V_j\left[g_{ij}\sin\left(\theta_{se}-\theta_j\right)+b_{ij}\cos\left(\theta_{se}-\theta_j\right)\right] \quad \text{(A.VI-141)}$$

$$\nabla V_j\left(\nabla V_{se}\Delta P_j\right)=-\frac{\partial^2 P_j^{UPFC}}{\partial V_{se}\partial V_j}=-\frac{\partial^2 P_j^{se}}{\partial V_{se}\partial V_j}=-\left[g_{ij}\cos\left(\theta_{se}-\theta_j\right)-b_{ij}\sin\left(\theta_{se}-\theta_j\right)\right] \quad \text{(A.VI-142)}$$

$$\nabla\theta_{sh}\left(\nabla\theta_{sh}\Delta P_j\right)=-\frac{\partial^2 P_j^{UPFC}}{\partial\theta_{sh}\partial\theta_{sh}}=0 \quad \text{(A.VI-143)}$$

$$\nabla V_{sh}\left(\nabla\theta_{sh}\Delta P_j\right)=-\frac{\partial^2 P_j^{UPFC}}{\partial\theta_{sh}\partial V_{sh}}=0 \quad \text{(A.VI-144)}$$

$$\nabla\theta_i\left(\nabla\theta_{sh}\Delta P_j\right)=-\frac{\partial^2 P_j^{UPFC}}{\partial\theta_{sh}\partial\theta_i}=0 \quad \text{(A.VI-145)}$$

$$\nabla V_i\left(\nabla\theta_{sh}\Delta P_j\right)=-\frac{\partial^2 P_j^{UPFC}}{\partial\theta_{sh}\partial V_i}=0 \quad \text{(A.VI-146)}$$

$$\nabla\theta_j\left(\nabla\theta_{sh}\Delta P_j\right)=-\frac{\partial^2 P_j^{UPFC}}{\partial\theta_{sh}\partial\theta_j}=0 \quad \text{(A.VI-147)}$$

$$\nabla V_j\left(\nabla\theta_{sh}\Delta P_j\right)=-\frac{\partial^2 P_j^{UPFC}}{\partial\theta_{sh}\partial V_j}=0 \quad \text{(A.VI-148)}$$

$$\nabla V_{sh}\left(\nabla V_{sh}\Delta P_j\right)=-\frac{\partial^2 P_j^{UPFC}}{\partial V_{sh}\partial V_{sh}}=0 \quad \text{(A.VI-149)}$$

$$\nabla_{\theta_i}\left(\nabla_{V_{sh}}\Delta P_j\right)=-\frac{\partial^2 P_j^{UPFC}}{\partial V_{sh}\partial\theta_i}=0 \quad \text{(A.VI-150)}$$

$$\nabla_{V_i}\left(\nabla_{V_{sh}}\Delta P_j\right)=-\frac{\partial^2 P_j^{UPFC}}{\partial V_{sh}\partial V_i}=0 \quad \text{(A.VI-151)}$$

$$\nabla_{\theta_j}\left(\nabla_{V_{sh}}\Delta P_j\right)=-\frac{\partial^2 P_j^{UPFC}}{\partial V_{sh}\partial\theta_j}=0 \quad \text{(A.VI-152)}$$

$$\nabla_{V_j}\left(\nabla_{V_{sh}}\Delta P_j\right)=-\frac{\partial^2 P_j^{UPFC}}{\partial V_{sh}\partial V_j}=0 \quad \text{(A.VI-153)}$$

$$\nabla_{\theta_i}\left(\nabla_{\theta_i}\Delta P_j\right)=-\frac{\partial^2 P_j^{UPFC}}{\partial\theta_i\partial\theta_i}=0 \quad \text{(A.VI-154)}$$

$$\nabla_{V_i}\left(\nabla_{\theta_i}\Delta P_j\right)=-\frac{\partial^2 P_j^{UPFC}}{\partial\theta_i\partial V_i}=0 \quad \text{(A.VI-155)}$$

$$\nabla_{\theta_j}\left(\nabla_{\theta_i}\Delta P_j\right)=-\frac{\partial^2 P_j^{UPFC}}{\partial\theta_i\partial\theta_j}=0 \quad \text{(A.VI-156)}$$

$$\nabla_{V_j}\left(\nabla_{\theta_i}\Delta P_j\right)=-\frac{\partial^2 P_j^{UPFC}}{\partial\theta_i\partial V_j}=0 \quad \text{(A.VI-157)}$$

$$\nabla_{V_i}\left(\nabla_{V_i}\Delta P_j\right)=-\frac{\partial^2 P_j^{UPFC}}{\partial V_i\partial V_i}=0 \quad \text{(A.VI-158)}$$

$$\nabla_{\theta_j}\left(\nabla_{V_i}\Delta P_j\right)=-\frac{\partial^2 P_j^{UPFC}}{\partial V_i\partial\theta_j}=0 \quad \text{(A.VI-159)}$$

$$\nabla_{V_j}\left(\nabla_{V_i}\Delta P_j\right)=-\frac{\partial^2 P_j^{UPFC}}{\partial V_i\partial V_j}=0 \quad \text{(A.VI-160)}$$

$$\nabla_{\theta_j}\left(\nabla_{\theta_j}\Delta P_j\right)=-\frac{\partial^2 P_j^{UPFC}}{\partial\theta_j\partial\theta_j}=-\frac{\partial^2 P_j^{se}}{\partial\theta_j\partial\theta_j}=V_jV_{se}\left[g_{ij}\cos\left(\theta_{se}-\theta_j\right)-b_{ij}\sin\left(\theta_{se}-\theta_j\right)\right] \quad \text{(A.VI-161)}$$

$$\nabla_{V_j}\left(\nabla_{\theta_j}\Delta P_j\right)=-\frac{\partial^2 P_j^{UPFC}}{\partial\theta_j\partial V_j}=-\frac{\partial^2 P_j^{se}}{\partial\theta_j\partial V_j}=-V_{se}\left[g_{ij}\sin\left(\theta_{se}-\theta_j\right)+b_{ij}\cos\left(\theta_{se}-\theta_j\right)\right] \quad \text{(A.VI-162)}$$

$$\nabla_{V_j}\left(\nabla_{V_j}\Delta P_j\right)=-\frac{\partial^2 P_j^{UPFC}}{\partial V_j\partial V_j}=0 \quad \text{(A.VI-163)}$$

Reactive power mismatch equations at bus *j*:

$$\nabla_{\theta_{se}}\left(\nabla_{\theta_{se}}\Delta Q_j\right)=-\frac{\partial^2 Q_j^{UPFC}}{\partial\theta_{se}\partial\theta_{se}} \qquad \text{(A.VI-164)}$$
$$=-\frac{\partial^2 Q_j^{se}}{\partial\theta_{se}\partial\theta_{se}}=-V_jV_{se}\left[g_{ij}\sin\left(\theta_{se}-\theta_j\right)+b_{ij}\cos\left(\theta_{se}-\theta_j\right)\right]$$

$$\nabla_{V_{se}}\left(\nabla_{\theta_{se}}\Delta Q_j\right)=-\frac{\partial^2 Q_j^{UPFC}}{\partial\theta_{se}\partial V_{se}}=-\frac{\partial^2 Q_j^{se}}{\partial\theta_{se}\partial V_{se}}=V_j\left[g_{ij}\cos\left(\theta_{se}-\theta_j\right)-b_{ij}\sin\left(\theta_{se}-\theta_j\right)\right] \qquad \text{(A.VI-165)}$$

$$\nabla_{\theta_{sh}}\left(\nabla_{\theta_{se}}\Delta Q_j\right)=-\frac{\partial^2 Q_j^{UPFC}}{\partial\theta_{se}\partial\theta_{sh}}=0 \qquad \text{(A.VI-166)}$$

$$\nabla_{V_{sh}}\left(\nabla_{\theta_{se}}\Delta Q_j\right)=-\frac{\partial^2 Q_j^{UPFC}}{\partial\theta_{se}\partial V_{sh}}=0 \qquad \text{(A.VI-167)}$$

$$\nabla_{\theta_i}\left(\nabla_{\theta_{se}}\Delta Q_j\right)=-\frac{\partial^2 Q_j^{UPFC}}{\partial\theta_{se}\partial\theta_i}=0 \qquad \text{(A.VI-168)}$$

$$\nabla_{V_i}\left(\nabla_{\theta_{se}}\Delta Q_j\right)=-\frac{\partial^2 Q_j^{UPFC}}{\partial\theta_{se}\partial V_i}=0 \qquad \text{(A.VI-169)}$$

$$\nabla_{\theta_j}\left(\nabla_{\theta_{se}}\Delta Q_j\right)=-\frac{\partial^2 Q_j^{UPFC}}{\partial\theta_{se}\partial\theta_j} \qquad \text{(A.VI-170)}$$
$$=-\frac{\partial^2 Q_j^{se}}{\partial\theta_{se}\partial\theta_j}=V_jV_{se}\left[g_{ij}\sin\left(\theta_{se}-\theta_j\right)+b_{ij}\cos\left(\theta_{se}-\theta_j\right)\right]$$

$$\nabla_{V_j}\left(\nabla_{\theta_{se}}\Delta Q_j\right)=-\frac{\partial^2 Q_j^{UPFC}}{\partial\theta_{se}\partial V_j}=-\frac{\partial^2 Q_j^{se}}{\partial\theta_{se}\partial V_j}=V_{se}\left[g_{ij}\cos\left(\theta_{se}-\theta_j\right)-b_{ij}\sin\left(\theta_{se}-\theta_j\right)\right] \qquad \text{(A.VI-171)}$$

$$\nabla_{\theta_j}\left(\nabla_{V_{se}}\Delta Q_j\right)=-\frac{\partial^2 Q_j^{UPFC}}{\partial V_{se}\partial\theta_j}=-\frac{\partial^2 Q_j^{se}}{\partial V_{se}\partial\theta_j}=V_j\left[g_{ij}\cos\left(\theta_{se}-\theta_j\right)-b_{ij}\sin\left(\theta_{se}-\theta_j\right)\right] \qquad \text{(A.VI-172)}$$

$$\nabla_{\theta_{sh}}\left(\nabla_{V_{se}}\Delta Q_j\right)=-\frac{\partial^2 Q_j^{UPFC}}{\partial V_{se}\partial\theta_{sh}}=0 \qquad \text{(A.VI-173)}$$

$$\nabla_{V_{sh}}\left(\nabla_{V_{se}}\Delta Q_j\right)=-\frac{\partial^2 Q_j^{UPFC}}{\partial V_{se}\partial V_{sh}}=0 \qquad \text{(A.VI-174)}$$

$$\nabla_{\theta_i}\left(\nabla_{V_{se}}\Delta Q_j\right)=-\frac{\partial^2 Q_j^{UPFC}}{\partial V_{se}\partial\theta_i}=0 \qquad \text{(A.VI-175)}$$

$$\nabla_{V_i}\left(\nabla_{V_{se}}\Delta Q_j\right)=-\frac{\partial^2 Q_j^{UPFC}}{\partial V_{se}\partial V_i}=0 \qquad \text{(A.VI-176)}$$

$$\nabla_{V_j}\left(\nabla_{V_{se}}\Delta Q_j\right)=-\frac{\partial^2 Q_j^{UPFC}}{\partial V_{se}\partial V_j}=-\frac{\partial^2 Q_j^{se}}{\partial V_{se}\partial V_j}=\left[g_{ij}\sin\left(\theta_{se}-\theta_j\right)+b_{ij}\cos\left(\theta_{se}-\theta_j\right)\right] \quad \text{(A.VI-177)}$$

$$\nabla_{\theta_{sh}}\left(\nabla_{\theta_{sh}}\Delta Q_j\right)=-\frac{\partial^2 Q_j^{UPFC}}{\partial\theta_{sh}\partial\theta_{sh}}=0 \quad \text{(A.VI-178)}$$

$$\nabla_{V_{sh}}\left(\nabla_{\theta_{sh}}\Delta Q_j\right)=-\frac{\partial^2 Q_j^{UPFC}}{\partial\theta_{sh}\partial V_{sh}}=0 \quad \text{(A.VI-179)}$$

$$\nabla_{\theta_i}\left(\nabla_{\theta_{sh}}\Delta Q_j\right)=-\frac{\partial^2 Q_j^{UPFC}}{\partial\theta_{sh}\partial\theta_i}=0 \quad \text{(A.VI-180)}$$

$$\nabla_{V_i}\left(\nabla_{\theta_{sh}}\Delta Q_j\right)=-\frac{\partial^2 Q_j^{UPFC}}{\partial\theta_{sh}\partial V_i}=0 \quad \text{(A.VI-181)}$$

$$\nabla_{\theta_j}\left(\nabla_{\theta_{sh}}\Delta Q_j\right)=-\frac{\partial^2 Q_j^{UPFC}}{\partial\theta_{sh}\partial\theta_j}=0 \quad \text{(A.VI-182)}$$

$$\nabla_{V_j}\left(\nabla_{\theta_{sh}}\Delta Q_j\right)=-\frac{\partial^2 Q_j^{UPFC}}{\partial\theta_{sh}\partial V_j}=0 \quad \text{(A.VI-183)}$$

$$\nabla_{V_{sh}}\left(\nabla_{V_{sh}}\Delta Q_j\right)=-\frac{\partial^2 Q_j^{UPFC}}{\partial V_{sh}\partial V_{sh}}=0 \quad \text{(A.VI-184)}$$

$$\nabla_{\theta_i}\left(\nabla_{V_{sh}}\Delta Q_j\right)=-\frac{\partial^2 Q_j^{UPFC}}{\partial V_{sh}\partial\theta_i}=0 \quad \text{(A.VI-185)}$$

$$\nabla_{V_i}\left(\nabla_{V_{sh}}\Delta Q_j\right)=-\frac{\partial^2 Q_j^{UPFC}}{\partial V_{sh}\partial V_i}=0 \quad \text{(A.VI-186)}$$

$$\nabla_{\theta_j}\left(\nabla_{V_{sh}}\Delta Q_j\right)=-\frac{\partial^2 Q_j^{UPFC}}{\partial V_{sh}\partial\theta_j}=0 \quad \text{(A.VI-187)}$$

$$\nabla_{V_j}\left(\nabla_{V_{sh}}\Delta Q_j\right)=-\frac{\partial^2 Q_j^{UPFC}}{\partial V_{sh}\partial V_j}=0 \quad \text{(A.VI-188)}$$

$$\nabla_{\theta_i}\left(\nabla_{\theta_i}\Delta Q_j\right)=-\frac{\partial^2 Q_j^{UPFC}}{\partial\theta_i\partial\theta_i}=0 \quad \text{(A.VI-189)}$$

$$\nabla_{V_i}\left(\nabla_{\theta_i}\Delta Q_j\right)=-\frac{\partial^2 Q_j^{UPFC}}{\partial\theta_i\partial V_i}=0 \quad \text{(A.VI-190)}$$

$$\nabla_{\theta_j}\left(\nabla_{\theta_i}\Delta Q_j\right)=-\frac{\partial^2 Q_j^{UPFC}}{\partial\theta_i\partial\theta_j}=0 \quad \text{(A.VI-191)}$$

$$\nabla_{V_j}\left(\nabla_{\theta_i}\Delta Q_j\right)=-\frac{\partial^2 Q_j^{UPFC}}{\partial\theta_i\partial V_j}=0 \tag{A.VI-192}$$

$$\nabla_{V_i}\left(\nabla_{V_i}\Delta Q_j\right)=-\frac{\partial^2 Q_j^{UPFC}}{\partial V_i\partial V_i}=0 \tag{A.VI-193}$$

$$\nabla_{\theta_j}\left(\nabla_{V_i}\Delta Q_j\right)=-\frac{\partial^2 Q_j^{UPFC}}{\partial V_i\partial\theta_j}=0 \tag{A.VI-194}$$

$$\nabla_{V_j}\left(\nabla_{V_i}\Delta Q_j\right)=-\frac{\partial^2 Q_j^{UPFC}}{\partial V_i\partial V_j}=0 \tag{A.VI-195}$$

$$\begin{aligned}\nabla_{\theta_j}\left(\nabla_{\theta_j}\Delta Q_j\right)&=-\frac{\partial^2 Q_j^{UPFC}}{\partial\theta_j\partial\theta_j}\\&=-\frac{\partial^2 Q_j^{se}}{\partial\theta_j\partial\theta_j}=-V_jV_{se}\left[g_{ij}\sin\left(\theta_{se}-\theta_j\right)+b_{ij}\cos\left(\theta_{se}-\theta_j\right)\right]\end{aligned} \tag{A.VI-196}$$

$$\begin{aligned}\nabla_{V_j}\left(\nabla_{\theta_j}\Delta Q_j\right)&=-\frac{\partial^2 Q_j^{UPFC}}{\partial\theta_j\partial V_j}\\&=-\frac{\partial^2 Q_j}{\partial\theta_j\partial V_j}=-V_{se}\left[g_{ij}\cos\left(\theta_{se}-\theta_j\right)-b_{ij}\sin\left(\theta_{se}-\theta_j\right)\right]\end{aligned} \tag{A.VI-197}$$

$$\nabla_{V_j}\left(\nabla_{V_j}\Delta Q_j\right)=-\frac{\partial^2 Q_j^{UPFC}}{\partial\theta_j\partial\theta_j}=0 \tag{A.VI-198}$$

List of FACTS controller active power constraint equations

The operating constraint of the UPFC is the active power exchange between the two inverters via the common DC link, as presented in Appendix IV.

$$PE_{UPFC}=PE_i=PE_{sh}-PE_{se}=\mathrm{Re}\left(\bar{V}_{sh}\bar{I}_{sh}^{*}\right)-\mathrm{Re}\left(\bar{V}_{se}\bar{I}_{ji}^{*}\right)=0 \tag{A.IV-46}$$

where, $PE_{sh}=\mathrm{Re}\left(\bar{V}_{sh}\bar{I}_{sh}^{*}\right)$ and $PE_{se}=\mathrm{Re}\left(\bar{V}_{se}\bar{I}_{ji}^{*}\right)$ are the active power exchanges of the shunt converter and the series converter to the DC link respectively.

$$PE_{sh}=\mathrm{Re}\left(\bar{V}_{sh}\bar{I}_{sh}^{*}\right)=V_{sh}^2g_{sh}-V_{sh}V_i\left[g_{sh}\cos\left(\theta_{sh}-\theta_i\right)+b_{sh}\sin\left(\theta_{sh}-\theta_i\right)\right] \tag{A.IV-7}$$

$$\begin{aligned}PE_{se}=\mathrm{Re}\left(\bar{V}_{se}\bar{I}_{ji}^{*}\right)&=V_{se}^2g_{ij}-V_iV_{se}\left[g_{ij}\cos\left(\theta_{se}-\theta_i\right)+b_{ij}\sin\left(\theta_{se}-\theta_i\right)\right]\\&\quad+V_jV_{se}\left[g_{ij}\cos\left(\theta_{se}-\theta_j\right)+b_{ij}\sin\left(\theta_{se}-\theta_j\right)\right]\end{aligned} \tag{A.IV-24}$$

First differentials of the UPFC operating constraint

$$\nabla_{\theta_{se}} PE_{UPFC} = -\frac{\partial PE_{se}}{\partial \theta_{se}} = -V_i V_{se}\left[g_{ij}\sin\left(\theta_{se}-\theta_i\right)-b_{ij}\cos\left(\theta_{se}-\theta_i\right)\right] + V_j V_{se}\left[g_{ij}\sin\left(\theta_{se}-\theta_j\right)-b_{ij}\cos\left(\theta_{se}-\theta_j\right)\right] \quad \text{(A.VI-199)}$$

$$\nabla_{V_{se}} PE_{UPFC} = -\frac{\partial PE_{se}}{\partial V_{se}} = -2V_{se}g_{ij} + V_i\left[g_{ij}\cos\left(\theta_{se}-\theta_i\right)+b_{ij}\sin\left(\theta_{se}-\theta_i\right)\right] - V_j V_{se}\left[g_{ij}\cos\left(\theta_{se}-\theta_j\right)+b_{ij}\sin\left(\theta_{se}-\theta_j\right)\right] \quad \text{(A.VI-200)}$$

$$\nabla_{\theta_{sh}} PE_{UPFC} = \frac{\partial PE_{sh}}{\partial \theta_{sh}} = V_{sh}V_i\left[g_{sh}\sin\left(\theta_{sh}-\theta_i\right)-b_{sh}\cos\left(\theta_{sh}-\theta_i\right)\right] \quad \text{(A.VI-201)}$$

$$\nabla_{V_{sh}} PE_{UPFC} = \frac{\partial PE_{sh}}{\partial V_{sh}} = 2V_{sh}g_{sh} - V_i\left[g_{sh}\cos\left(\theta_{sh}-\theta_i\right)+b_{sh}\sin\left(\theta_{sh}-\theta_i\right)\right] \quad \text{(A.VI-202)}$$

$$\nabla_{\theta_i} PE_{UPFC} = \frac{\partial PE_{sh}}{\partial \theta_i} - \frac{\partial PE_{se}}{\partial \theta_i} \quad \text{(A.VI-203)}$$

$$\frac{\partial PE_{se}}{\partial \theta_i} = -V_i V_{se}\left[g_{ij}\sin\left(\theta_{se}-\theta_i\right)-b_{ij}\cos\left(\theta_{se}-\theta_i\right)\right] \quad \text{(A.VI-204)}$$

$$\frac{\partial PE_{sh}}{\partial \theta_i} = -V_{sh}V_i\left[g_{sh}\sin\left(\theta_{sh}-\theta_i\right)-b_{sh}\cos\left(\theta_{sh}-\theta_i\right)\right] \quad \text{(A.VI-205)}$$

$$\nabla_{V_i} PE_{UPFC} = \frac{\partial PE_{sh}}{\partial V_i} - \frac{\partial PE_{se}}{\partial V_i} \quad \text{(A.VI-206)}$$

$$\frac{\partial PE_{se}}{\partial V_i} = -V_{sh}\left[g_{ij}\cos\left(\theta_{se}-\theta_i\right)+b_{ij}\sin\left(\theta_{se}-\theta_i\right)\right] \quad \text{(A.VI-207)}$$

$$\frac{\partial PE_{sh}}{\partial V_i} = -V_{sh}\left[g_{sh}\cos\left(\theta_{sh}-\theta_i\right)+b_{sh}\sin\left(\theta_{sh}-\theta_i\right)\right] \quad \text{(A.VI-208)}$$

$$\nabla_{\theta_j} PE_{UPFC} = -\frac{\partial PE_{se}}{\partial \theta_j} \quad \text{(A.VI-209)}$$

$$\frac{\partial PE_{se}}{\partial \theta_j} = V_j V_{se}\left[g_{ij}\sin\left(\theta_{se}-\theta_i\right)-b_{ij}\cos\left(\theta_{se}-\theta_i\right)\right] \quad \text{(A.VI-210)}$$

$$\nabla_{V_j} PE_{UPFC} = -\frac{\partial PE_{se}}{\partial V_j} \quad \text{(A.VI-211)}$$

$$\frac{\partial PE_{se}}{\partial V_j} = V_{sh}\left[g_{ij}\cos\left(\theta_{se}-\theta_j\right)+b_{ij}\sin\left(\theta_{se}-\theta_j\right)\right] \quad \text{(A.VI-212)}$$

List of second differentials of the UPFC operating constraint

$$\nabla_{\theta_{se}}\left(\nabla_{\theta_{se}} PE_{UPFC}\right) = -\frac{\partial^2 PE_{se}}{\partial \theta_{se}\partial \theta_{se}} \quad \text{(A.VI-213)}$$

$$\frac{\partial^2 PE_{se}}{\partial\theta_{se}\partial\theta_{se}} = V_i V_{se}\left[g_{ij}\cos\left(\theta_{se}-\theta_i\right)+b_{ij}\sin\left(\theta_{se}-\theta_i\right)\right] - V_j V_{se}\left[g_{ij}\cos\left(\theta_{se}-\theta_j\right)+b_{ij}\sin\left(\theta_{se}-\theta_j\right)\right] \quad \text{(A.VI-214)}$$

$$\nabla_{V_{se}}\left(\nabla_{\theta_{se}} PE_{UPFC}\right) = -\frac{\partial^2 PE_{se}}{\partial\theta_{se}\partial V_{se}} \quad \text{(A.VI-215)}$$

$$\frac{\partial^2 PE_{se}}{\partial\theta_{se}\partial V_{se}} = V_i\left[g_{ij}\sin\left(\theta_{se}-\theta_i\right)-b_{ij}\cos\left(\theta_{se}-\theta_i\right)\right] - V_j\left[g_{ij}\sin\left(\theta_{se}-\theta_j\right)-b_{ij}\cos\left(\theta_{se}-\theta_j\right)\right] \quad \text{(A.VI-216)}$$

$$\frac{\partial^2 PE_{UPFC}}{\partial\theta_{se}\partial\theta_{sh}} = \frac{\partial^2 PE_{sh}}{\partial\theta_{se}\partial\theta_{sh}} - \frac{\partial^2 PE_{se}}{\partial\theta_{se}\partial\theta_{sh}} = 0 \quad \text{(A.VI-217)}$$

$$\frac{\partial^2 PE_{UPFC}}{\partial\theta_{se}\partial V_{sh}} = \frac{\partial^2 PE_{sh}}{\partial\theta_{se}\partial V_{sh}} - \frac{\partial^2 PE_{se}}{\partial\theta_{se}\partial V_{sh}} = 0 \quad \text{(A.VI-218)}$$

$$\nabla_{\theta_i}\left(\nabla_{\theta_{se}} PE_{UPFC}\right) = -\frac{\partial^2 PE_{se}}{\partial\theta_{se}\partial\theta_i} \quad \text{(A.VI-219)}$$

$$\frac{\partial^2 PE_{se}}{\partial\theta_{se}\partial\theta_i} = -V_i V_{se}\left[g_{ij}\cos\left(\theta_{se}-\theta_i\right)+b_{ij}\sin\left(\theta_{se}-\theta_i\right)\right] \quad \text{(A.VI-220)}$$

$$\nabla_{V_i}\left(\nabla_{\theta_{se}} PE_{UPFC}\right) = -\frac{\partial^2 PE_{se}}{\partial\theta_{se}\partial V_i} \quad \text{(A.VI-221)}$$

$$\frac{\partial^2 PE_{se}}{\partial\theta_{se}\partial V_i} = V_{se}\left[g_{ij}\sin\left(\theta_{se}-\theta_i\right)-b_{ij}\cos\left(\theta_{se}-\theta_i\right)\right] \quad \text{(A.VI-222)}$$

$$\nabla_{\theta_j}\left(\nabla_{\theta_{se}} PE_{UPFC}\right) = -\frac{\partial^2 PE_{se}}{\partial\theta_{se}\partial\theta_j} \quad \text{(A.VI-223)}$$

$$\frac{\partial^2 PE_{se}}{\partial\theta_{se}\partial\theta_j} = V_j V_{se}\left[g_{ij}\cos\left(\theta_{se}-\theta_j\right)+b_{ij}\sin\left(\theta_{se}-\theta_j\right)\right] \quad \text{(A.VI-224)}$$

$$\nabla_{V_j}\left(\nabla_{\theta_{se}} PE_{UPFC}\right) = -\frac{\partial^2 PE_{se}}{\partial\theta_{se}\partial V_j} \quad \text{(A.VI-225)}$$

$$\frac{\partial^2 PE_{se}}{\partial\theta_{se}\partial V_j} = -V_{se}\left[g_{ij}\sin\left(\theta_{se}-\theta_j\right)-b_{ij}\cos\left(\theta_{se}-\theta_j\right)\right] \quad \text{(A.VI-226)}$$

$$\nabla_{V_{se}}\left(\nabla_{V_{se}} PE_{UPFC}\right) = -\frac{\partial^2 PE_{se}}{\partial V_{se}\partial V_{se}} \quad \text{(A.VI-227)}$$

$$\frac{\partial^2 PE_{se}}{\partial V_{se}\partial V_{se}} = 2g_{ij} \quad \text{(A.VI-228)}$$

$$\nabla_{\theta_{sh}}\left(\nabla_{V_{se}} PE_{UPFC}\right)=\frac{\partial^2 PE_{sh}}{\partial V_{se}\partial\theta_{sh}}-\frac{\partial^2 PE_{se}}{\partial V_{se}\partial\theta_{sh}}=0 \quad \text{(A.VI-229)}$$

$$\nabla_{V_{sh}}\left(\nabla_{V_{se}} PE_{UPFC}\right)=\frac{\partial^2 PE_{sh}}{\partial V_{se}\partial V_{sh}}-\frac{\partial^2 PE_{se}}{\partial V_{se}\partial V_{sh}}=0 \quad \text{(A.VI-230)}$$

$$\nabla_{\theta_i}\left(\nabla_{V_{se}} PE_{UPFC}\right)=-\frac{\partial^2 PE_{se}}{\partial V_{se}\partial\theta_i} \quad \text{(A.VI-231)}$$

$$\frac{\partial^2 PE_{se}}{\partial V_{se}\partial\theta_i}=-V_i\left[g_{ij}\sin\left(\theta_{se}-\theta_i\right)-b_{ij}\cos\left(\theta_{se}-\theta_i\right)\right] \quad \text{(A.VI-233)}$$

$$\nabla_{V_i}\left(\nabla_{V_{se}} PE_{UPFC}\right)=-\frac{\partial^2 PE_{se}}{\partial V_{se}\partial V_i} \quad \text{(A.VI-234)}$$

$$\frac{\partial^2 PE_{se}}{\partial V_{se}\partial V_i}=-\left[g_{ij}\cos\left(\theta_{se}-\theta_i\right)+b_{ij}\sin\left(\theta_{se}-\theta_i\right)\right] \quad \text{(A.VI-235)}$$

$$\nabla_{\theta_j}\left(\nabla_{V_{se}} PE_{UPFC}\right)=-\frac{\partial^2 PE_{se}}{\partial V_{se}\partial\theta_j} \quad \text{(A.VI-236)}$$

$$\frac{\partial^2 PE_{se}}{\partial V_{se}\partial\theta_j}=V_j\left[g_{ij}\sin\left(\theta_{se}-\theta_j\right)-b_{ij}\cos\left(\theta_{se}-\theta_j\right)\right] \quad \text{(A.VI-237)}$$

$$\nabla_{V_j}\left(\nabla_{V_{se}} PE_{UPFC}\right)=-\frac{\partial^2 PE_{se}}{\partial V_{se}\partial V_j} \quad \text{(A.VI-238)}$$

$$\frac{\partial^2 PE_{se}}{\partial V_{se}\partial V_j}=\left[g_{ij}\cos\left(\theta_{se}-\theta_i\right)+b_{ij}\sin\left(\theta_{se}-\theta_i\right)\right] \quad \text{(A.VI-239)}$$

$$\nabla_{\theta_{sh}}\left(\nabla_{\theta_{sh}} PE_{UPFC}\right)=\frac{\partial^2 PE_{sh}}{\partial\theta_{sh}\partial\theta_{sh}}=V_{sh}V_i\left[g_{sh}\cos\left(\theta_{sh}-\theta_i\right)+b_{sh}\sin\left(\theta_{sh}-\theta_i\right)\right] \quad \text{(A.VI-240)}$$

$$\nabla_{V_{sh}}\left(\nabla_{\theta_{sh}} PE_{UPFC}\right)=\frac{\partial^2 PE_{sh}}{\partial\theta_{sh}\partial V_{sh}}=V_i\left[g_{sh}\sin\left(\theta_{sh}-\theta_i\right)-b_{sh}\cos\left(\theta_{sh}-\theta_i\right)\right] \quad \text{(A.VI-241)}$$

$$\nabla_{\theta_i}\left(\nabla_{\theta_{sh}} PE_{UPFC}\right)=\frac{\partial^2 PE_{sh}}{\partial\theta_{sh}\partial\theta_i}=-V_{sh}V_i\left[g_{sh}\cos\left(\theta_{sh}-\theta_i\right)+b_{sh}\sin\left(\theta_{sh}-\theta_i\right)\right] \quad \text{(A.VI-242)}$$

$$\nabla_{V_i}\left(\nabla_{\theta_{sh}} PE_{UPFC}\right)=\frac{\partial^2 PE_{sh}}{\partial\theta_{sh}\partial V_i}=V_{sh}\left[g_{sh}\sin\left(\theta_{sh}-\theta_i\right)-b_{sh}\cos\left(\theta_{sh}-\theta_i\right)\right] \quad \text{(A.VI-243)}$$

$$\nabla_{\theta_j}\left(\nabla_{\theta_{sh}} PE_{UPFC}\right)=\frac{\partial^2 PE_{sh}}{\partial\theta_{sh}\partial\theta_j}-\frac{\partial^2 PE_{se}}{\partial\theta_{sh}\partial\theta_j}=0 \quad \text{(A.VI-244)}$$

$$\nabla_{V_j}\left(\nabla_{\theta_{sh}} PE_{UPFC}\right)=\frac{\partial^2 PE_{sh}}{\partial\theta_{sh}\partial V_j}-\frac{\partial^2 PE_{se}}{\partial\theta_{sh}\partial V_j}=0 \quad \text{(A.VI-245)}$$

$$\nabla_{V_{sh}}\left(\nabla_{V_{sh}} PE_{UPFC}\right)=\frac{\partial^2 PE_{sh}}{\partial V_{sh}\partial V_{sh}}=2g_{sh} \tag{A.VI-246}$$

$$\nabla_{\theta_i}\left(\nabla_{V_{sh}} PE_{UPFC}\right)=\frac{\partial^2 PE_{sh}}{\partial V_{sh}\partial \theta_i}=-V_i\left[g_{sh}\sin\left(\theta_{sh}-\theta_i\right)-b_{sh}\cos\left(\theta_{sh}-\theta_i\right)\right] \tag{A.VI-247}$$

$$\nabla_{V_i}\left(\nabla_{V_{sh}} PE_{UPFC}\right)=\frac{\partial^2 PE_{sh}}{\partial V_{sh}\partial V_i}=-\left[g_{sh}\cos\left(\theta_{sh}-\theta_i\right)+b_{sh}\sin\left(\theta_{sh}-\theta_i\right)\right] \tag{A.VI-248}$$

$$\nabla_{\theta_j}\left(\nabla_{V_{sh}} PE_{UPFC}\right)=\frac{\partial^2 PE_{sh}}{\partial V_{sh}\partial \theta_j}-\frac{\partial^2 PE_{se}}{\partial V_{sh}\partial \theta_j}=0 \tag{A.VI-249}$$

$$\nabla_{V_j}\left(\nabla_{V_{sh}} PE_{UPFC}\right)=\frac{\partial^2 PE_{sh}}{\partial V_{sh}\partial V_j}-\frac{\partial^2 PE_{se}}{\partial V_{sh}\partial \theta j}=0 \tag{A.VI-250}$$

$$\nabla_{\theta_i}\left(\nabla_{\theta_i} PE_{UPFC}\right)=\frac{\partial^2 PE_{sh}}{\partial \theta_i\partial \theta_i}-\frac{\partial^2 PE_{se}}{\partial \theta_i\partial \theta_i} \tag{A.VI-251}$$

$$\frac{\partial^2 PE_{se}}{\partial \theta_i\partial \theta_i}=V_iV_{se}\left[g_{ij}\cos\left(\theta_{se}-\theta_i\right)+b_{ij}\sin\left(\theta_{se}-\theta_i\right)\right] \tag{A.VI-252}$$

$$\frac{\partial^2 PE_{sh}}{\partial \theta_i\partial \theta_i}=V_iV_{sh}\left[g_{ij}\cos\left(\theta_{sh}-\theta_i\right)+b_{ij}\sin\left(\theta_{sh}-\theta_i\right)\right] \tag{A.VI-253}$$

$$\nabla_{V_i}\left(\nabla_{\theta_i} PE_{UPFC}\right)=\frac{\partial^2 PE_{sh}}{\partial \theta_i\partial V_i}-\frac{\partial^2 PE_{se}}{\partial \theta_i\partial V_i} \tag{A.VI-254}$$

$$\frac{\partial^2 PE_{se}}{\partial \theta_i\partial V_i}=-V_{se}\left[g_{ij}\sin\left(\theta_{se}-\theta_i\right)-b_{ij}\cos\left(\theta_{se}-\theta_i\right)\right] \tag{A.VI-255}$$

$$\frac{\partial^2 PE_{sh}}{\partial \theta_i\partial V_i}=-V_{sh}\left[g_{sh}\sin\left(\theta_{sh}-\theta_i\right)-b_{sh}\cos\left(\theta_{sh}-\theta_i\right)\right] \tag{A.VI-256}$$

$$\nabla_{\theta_j}\left(\nabla_{\theta_i} PE_{UPFC}\right)=\frac{\partial^2 PE_{sh}}{\partial \theta_i\partial \theta_j}-\frac{\partial^2 PE_{se}}{\partial \theta_i\partial \theta_j}=0 \tag{A.VI-257}$$

$$\nabla_{V_j}\left(\nabla_{\theta_i} PE_{UPFC}\right)=\frac{\partial^2 PE_{sh}}{\partial \theta_i\partial V_j}-\frac{\partial^2 PE_{se}}{\partial \theta_i\partial V_j}=0 \tag{A.VI-258}$$

$$\nabla_{V_i}\left(\nabla_{V_i} PE_{UPFC}\right)=\frac{\partial^2 PE_{sh}}{\partial V_i\partial V_i}-\frac{\partial^2 PE_{se}}{\partial V_i\partial V_i}=0 \tag{A.VI-259}$$

$$\nabla_{\theta_j}\left(\nabla_{V_i} PE_{UPFC}\right)=\frac{\partial^2 PE_{sh}}{\partial V_i\partial \theta_j}-\frac{\partial^2 PE_{se}}{\partial V_i\partial \theta_j}=0 \tag{A.VI-260}$$

$$\nabla_{V_i}\left(\nabla_{V_j} PE_{UPFC}\right)=\frac{\partial^2 PE_{sh}}{\partial V_i\partial V_j}-\frac{\partial^2 PE_{se}}{\partial V_i\partial V_j}=0 \tag{A.VI-261}$$

$$\nabla_{\theta_j}\left(\nabla_{\theta_j} PE_{UPFC}\right) = -\frac{\partial^2 PE_{se}}{\partial\theta_j \partial\theta_j} \tag{A.VI-262}$$

$$\frac{\partial^2 PE_{se}}{\partial\theta_j \partial\theta_j} = -V_j V_{se}\left[g_{ij}\cos\left(\theta_{se}-\theta_i\right)+b_{ij}\sin\left(\theta_{se}-\theta_i\right)\right] \tag{A.VI-263}$$

$$\nabla_{\theta_j}\left(\nabla_{\theta_j} PE_{UPFC}\right) = -\frac{\partial^2 PE_{se}}{\partial\theta_j \partial\theta_j} \tag{A.VI-264}$$

$$\frac{\partial^2 PE_{se}}{\partial\theta_j \partial V_j} = V_{se}\left[g_{ij}\sin\left(\theta_{se}-\theta_j\right)-b_{ij}\cos\left(\theta_{se}-\theta_j\right)\right] \tag{A.VI-265}$$

$$\nabla_{V_j}\left(\nabla_{V_j} PE_{UPFC}\right) = \frac{\partial^2 PE_{sh}}{\partial V_j \partial V_j} - \frac{\partial^2 PE_{se}}{\partial V_j \partial V_j} = 0 \tag{A.VI-266}$$

Appendix VII

Formulation for shunt bus sensitivity and series branch sensitivity, and shunt bus sensitivity compared with midpoint STATCOM installation results, as presented in Chapter 5.

Lagrange equation

$$\begin{aligned} L(x) = f(x) &- \mu\left(\ln(sl_i) + \ln(sl_j)\right) - \mu\left(\ln(su_i) + \ln(su_j)\right) \\ &- \lambda_{p_i}\Delta P_i(x) - \lambda_{q_i}\Delta Q_i(x) - \lambda_{p_j}\Delta P_j(x) - \lambda_{q_j}\Delta Q_j(x) \\ &- \pi l_i\left(h_i - sl_i - h_i^{\min}\right) - \pi u_i\left(h_i - su_i - h_i^{\max}\right) \\ &- \pi l_j\left(h_j - sl_j - h_j^{\min}\right) - \pi u_j\left(h_j - su_j - h_j^{\max}\right) \end{aligned} \qquad \text{(2.25) and (5.1)}$$

with objective function,

$$f(x) = \sum_i^{N_g}\left[C_{g_i}^{+} P_{g_i}^{+}\right] + \sum_i^{N_g}\left[C_{g_i}^{-} P_{g_i}^{-}\right] \qquad (2.1)$$

Shunt bus sensitivity:

Shunt bus sensitivity, first order differential with respect to Q_i.

$$S_i^{sh} = \frac{\partial L(x)}{\partial Q_i} \qquad \text{(A.VII-1)}$$

$$\frac{\partial L(x)}{\partial Q_i} = \frac{\partial L(x)}{\partial \Delta Q_i(x)} \frac{\partial \Delta Q_i(x)}{\partial Q_i}$$

$$\frac{\partial L(x)}{\partial Q_i} = -\lambda_{q_i} \frac{\partial \Delta Q_i(x)}{\partial Q_i} \qquad \text{(A.VII-2)}$$

where, $\Delta Q_i(x)$ is the reactive power mismatch given by,

$$\Delta Q_i(x) = Q_{g_i} - Q_{d_i} - Q_i$$

Thus $$\frac{\partial \Delta Q_i(x)}{\partial Q_i} = -1 \qquad \text{(A.VII-3)}$$

and $$\frac{\partial L(x)}{\partial Q_i} = \lambda_{q_i} \qquad \text{(A.VII-4)}$$

Series branch sensitivity:

Series branch sensitivity, first order differential with respect to X_{ij}.

$$S_{ij} = \frac{\partial L(x)}{\partial X_{ij}} \tag{A.VII-5}$$

$$\frac{\partial L(x)}{\partial X_{ij}} = \frac{\partial L(x)}{\partial \Delta P_i(x)} \frac{\partial \Delta P_i(x)}{\partial X_{ij}} + \frac{\partial L(x)}{\partial \Delta Q_i(x)} \frac{\partial \Delta Q_i(x)}{\partial X_{ij}} + \frac{\partial L(x)}{\partial \Delta P_j(x)} \frac{\partial \Delta P_j(x)}{\partial X_{ij}} + \frac{\partial L(x)}{\partial \Delta Q_j(x)} \frac{\partial \Delta Q_j(x)}{\partial X_{ij}} \tag{A.VII-6}$$

where,

$$\frac{\partial \Delta P_i(x)}{\partial X_{ij}} = \frac{\partial \Delta P_i(x)}{\partial g_{ii}} \frac{\partial g_{ii}}{\partial X_{ij}} + \frac{\partial \Delta P_i(x)}{\partial g_{ij}} \frac{\partial g_{ij}}{\partial X_{ij}} + \frac{\partial \Delta P_i(x)}{\partial b_{ii}} \frac{\partial b_{ii}}{\partial X_{ij}} + \frac{\partial \Delta P_i(x)}{\partial b_{ij}} \frac{\partial b_{ij}}{\partial X_{ij}} \tag{A.VII-7}$$

$$\frac{\partial \Delta Q_i(x)}{\partial X_{ij}} = \frac{\partial \Delta Q_i(x)}{\partial g_{ii}} \frac{\partial g_{ii}}{\partial X_{ij}} + \frac{\partial \Delta Q_i(x)}{\partial g_{ij}} \frac{\partial g_{ij}}{\partial X_{ij}} + \frac{\partial \Delta Q_i(x)}{\partial b_{ii}} \frac{\partial b_{ii}}{\partial X_{ij}} + \frac{\partial \Delta Q_i(x)}{\partial b_{ij}} \frac{\partial b_{ij}}{\partial X_{ij}} \tag{A.VII-8}$$

$$\frac{\partial \Delta P_j(x)}{\partial X_{ij}} = \frac{\partial \Delta P_j(x)}{\partial g_{ii}} \frac{\partial g_{ii}}{\partial X_{ij}} + \frac{\partial \Delta P_j(x)}{\partial g_{ij}} \frac{\partial g_{ij}}{\partial X_{ij}} + \frac{\partial \Delta P_j(x)}{\partial b_{ii}} \frac{\partial b_{ii}}{\partial X_{ij}} + \frac{\partial \Delta P_j(x)}{\partial b_{ij}} \frac{\partial b_{ij}}{\partial X_{ij}} \tag{A.VII-9}$$

$$\frac{\partial \Delta Q_j(x)}{\partial X_{ij}} = \frac{\partial \Delta Q_j(x)}{\partial g_{ii}} \frac{\partial g_{ii}}{\partial X_{ij}} + \frac{\partial \Delta Q_j(x)}{\partial g_{ij}} \frac{\partial g_{ij}}{\partial X_{ij}} + \frac{\partial \Delta Q_j(x)}{\partial b_{ii}} \frac{\partial b_{ii}}{\partial X_{ij}} + \frac{\partial \Delta Q_j(x)}{\partial b_{ij}} \frac{\partial b_{ij}}{\partial X_{ij}} \tag{A.VII-10}$$

First derivatives of Lagrange equation with respect to power mismatch ($\Delta P_i, \Delta Q_i, \Delta P_j, \Delta Q_j$) equals the dual variable parameters:

$$\frac{\partial L(x)}{\partial \Delta P_i(x)} = -\lambda_{p_i} \tag{A.VII-11}$$

$$\frac{\partial L(x)}{\partial \Delta Q_i(x)} = -\lambda_{q_i} \tag{A.VII-12}$$

$$\frac{\partial L(x)}{\partial \Delta P_j(x)} = -\lambda_{p_j} \tag{A.VII-13}$$

$$\frac{\partial L(x)}{\partial \Delta Q_j(x)} = -\lambda_{q_j} \tag{A.VII-14}$$

Power mismatch equations and derivatives with respect to line admittance variables g_{ii}, b_{ii}, g_{jj}, b_{jj}, g_{ij} and b_{ij}.

$$\Delta P_i(x) = P_{g_i} - P_{d_i} - P_i \tag{A.VII-15}$$

$$\Delta Q_i(x) = Q_{g_i} - Q_{d_i} - Q_i \tag{A.VII-16}$$

$$\Delta P_j(x) = P_{g_j} - P_{d_j} - P_j \tag{A.VII-17}$$

$$\Delta Q_j(x) = Q_{g_j} - Q_{d_j} - Q_j \tag{A.VII-18}$$

Where power injection equations P_i, Q_i, P_j and Q_j are:

$$-P_i = -V_i^2 g_{ii} + V_i V_j \left[g_{ij} \cos\left(\theta_i - \theta_j\right) + b_{ij} \sin\left(\theta_i - \theta_j\right) \right] \tag{A.VII-19}$$

$$-Q_i = V_i^2 b_{ii} + V_i V_j \left[g_{ij} \sin\left(\theta_i - \theta_j\right) - b_{ij} \cos\left(\theta_i - \theta_j\right) \right] \tag{A.VII-20}$$

$$-P_j = -V_j^2 g_{jj} + V_i V_j \left[g_{ij} \cos\left(\theta_j - \theta_i\right) + b_{ij} \sin\left(\theta_j - \theta_i\right) \right] \tag{A.VII-21}$$

$$-Q_j = V_j^2 b_{jj} + V_i V_j \left[g_{ij} \sin\left(\theta_j - \theta_i\right) - b_{ij} \cos\left(\theta_j - \theta_i\right) \right] \tag{A.VII-22}$$

Derivatives of power injections with respect to line admittance variables g_{ii}, b_{ii}, g_{jj}, b_{jj}, g_{ij} and b_{ij}.

$$\frac{\partial \Delta P_i(x)}{\partial g_{ii}} = -V_i^2 \tag{A.VII-23}$$

$$\frac{\partial \Delta P_i(x)}{\partial g_{ij}} = V_i V_j \cos\left(\theta_i - \theta_j\right) \tag{A.VII-24}$$

$$\frac{\partial \Delta P_i(x)}{\partial b_{ij}} = V_i V_j \sin\left(\theta_i - \theta_j\right) \tag{A.VII-25}$$

$$\frac{\partial \Delta Q_i(x)}{\partial b_{ii}} = V_i^2 \tag{A.VII-26}$$

$$\frac{\partial \Delta Q_i(x)}{\partial g_{ij}} = V_i V_j \sin\left(\theta_i - \theta_j\right) \tag{A.VII-27}$$

$$\frac{\partial \Delta Q_i(x)}{\partial b_{ij}} = -V_i V_j \cos\left(\theta_i - \theta_j\right) \tag{A.VII-28}$$

$$\frac{\partial \Delta P_j(x)}{\partial g_{jj}} = -V_j^2 \tag{A.VII-29}$$

$$\frac{\partial \Delta P_j(x)}{\partial g_{ij}} = V_i V_j \cos\left(\theta_j - \theta_i\right) \tag{A.VII-30}$$

$$\frac{\partial \Delta P_j(x)}{\partial b_{ij}} = V_i\, V_j \sin\left(\theta_j - \theta_i\right) \tag{A.VII-31}$$

$$\frac{\partial \Delta Q_j(x)}{\partial b_{jj}} = V_j^2 \tag{A.VII-32}$$

$$\frac{\partial \Delta Q_j(x)}{\partial g_{ij}} = V_i\, V_j \sin\left(\theta_j - \theta_i\right) \tag{A.VII-33}$$

$$\frac{\partial \Delta Q_j(x)}{\partial b_{ij}} = -V_i\, V_j \cos\left(\theta_j - \theta_i\right) \tag{A.VII-34}$$

Line admittance variables g_{ii} , b_{ii} , g_{jj} , b_{jj} , g_{ij} and b_{ij} , derivatives with respect to transmission line impedance X_{ij} .

$$\frac{\partial g_{ii}}{\partial X_{ij}} = \frac{\partial g_{jj}}{\partial X_{ij}} = \frac{\partial g_{ij}}{\partial X_{ij}} = \frac{-2R_{ij}X_{ij}}{\left(R_{ij}^2 + X_{ij}^2\right)^2} \tag{A.VII-35}$$

$$\frac{\partial b_{ii}}{\partial X_{ij}} = \frac{\partial b_{jj}}{\partial X_{ij}} = \frac{\partial b_{ij}}{\partial X_{ij}} = \frac{X_{ij}^2 - R_{ij}^2}{\left(R_{ij}^2 + X_{ij}^2\right)^2} \tag{A.VII-36}$$

The control variable X_{ij} is an implicit variable of the objective function $f(x)$ through the Lagrange equation $L(x)$. Sensitivity of a transmission line *ij*,

$$\frac{\partial f(x)}{\partial X_{ij}} = S_{ij} \tag{A.VII-37}$$

$$\begin{aligned} S_{ij} = &-\lambda_{p_i}\left\{\left[-V_i^2 + V_iV_j\cos\left(\theta_i - \theta_j\right)\right]\frac{\partial g_{ii}}{\partial X_{ij}} + \left[V_iV_j\sin\left(\theta_i - \theta_j\right)\right]\frac{\partial b_{ij}}{\partial X_{ij}}\right\} \\ &-\lambda_{q_i}\left\{\left[V_iV_j\sin\left(\theta_i - \theta_j\right)\right]\frac{\partial g_{ij}}{\partial X_{ij}} + \left[V_i^2 - V_iV_j\cos\left(\theta_i - \theta_j\right)\right]\frac{\partial b_{ii}}{\partial X_{ij}}\right\} \\ &-\lambda_{p_j}\left\{\left[-V_j^2 + V_iV_j\cos\left(\theta_j - \theta_i\right)\right]\frac{\partial g_{ij}}{\partial X_{ij}} + \left[V_iV_j\sin\left(\theta_j - \theta_i\right)\right]\frac{\partial b_{ij}}{\partial X_{ij}}\right\} \\ &-\lambda_{q_j}\left\{\left[V_iV_j\sin\left(\theta_j - \theta_i\right)\right]\frac{\partial g_{ij}}{\partial X_{ij}} + \left[V_i^2 - V_iV_j\cos\left(\theta_j - \theta_i\right)\right]\frac{\partial b_{jj}}{\partial X_{ij}}\right\} \end{aligned} \tag{A.VII-38}$$

Shunt bus sensitivity and midpoint STATCOM installation results

Shunt bus sensitivity is measured at system buses, $i = 1, 2, \ldots, N$. It aims to test the change in the objective function $f(x)$ due to change in reactive power injected or absorbed at bus i, Q_i. For midpoint installation of a STATCOM the reactive power injection is in the middle of the line, therefore shunt bus sensitivity is not a suitable indicator. Tables A5-1 and A5-2 show no correlations between sensitivity and % RTC results.

Table A5-1: 14 bus system, top three sensitivity and % RTC when STATCOM installed at midpoint of transmission lines.

1	2	3	4	5	6	7	8	9	10
% $MW_k^{FullRange}$	Bus numbers with highest sensitivity			Locations *i-j* and corresponding % reduction in total cost					
	1st	2nd	3rd	1st		2nd		3rd	
16%	13	12	14	M:1-2	93%	M:2-5	33%	M:2-4	30%
55%	13	14	12	M:1-2	71%	M:2-5	12%	M:2-4	11%
94%	13	14	12	M:1-2	38%	M:2-5	9%	M:2-4	8%

Table A5-2: 30 bus system, top three sensitivity and % RTC when STATCOM installed at midpoint of transmission lines.

1	2	3	4	5	6	7	8	9	10
% $MW_k^{FullRange}$	Bus numbers with highest sensitivity			Locations *i-j* and corresponding % reductions in total cost					
	1st	2nd	3rd	1st		2nd		3rd	
16%	3	26	30	M:2-6	77%	M:2-4	76%	M:1-2	72%
55%	26	3	24	M:1-2	90%	M:2-6	15%	M:2-4	7%
94%	26	3	23	M:1-2	48%	M:2-6	10%	M:2-4	3%

APPENDIX VIII

Input system data; 4 bus system, IEEE 14 bus and 30 bus systems.

4 bus system input data, as used in Chapter 2.

Table AVIII.1: 4 bus system transmission line data (no transformers on system)

Line no.	Bus *i*	Bus *j*	Resistance R_{ij} (p.u.)	Reactance X_{ij} (p.u.)	Susceptance B_c (p.u.)	Power transfer limit S_{ij}^{max} (p.u.)	Tap ratio
1	1	2	0.02	0.08	0.00	5.00	1
2	1	3	0.03	0.12	0.00	5.00	1
3	4	3	0.02	0.10	0.00	6.00	1
4	4	2	0.03	0.12	0.00	6.00	1

Table AVIII.2: 4 bus system bus and demand data

Bus no.	Bus type	P demand (p.u.)	Q demand (p.u.)
1	0	5.00	1.00
2	2	3.00	0.86
3	1	1.000	0.30
4	2	0.00	0.00

* Bus Type: (0) swing bus, (1) generator bus (PV bus), and (2) load bus (PQ bus).

Table AVIII.3: 4 bus system generator data

Generator bus no. *i*	$C_{g_i}^{+}$ (p.u.)	$C_{g_i}^{-}$ (p.u)	Initial value Pg0 (p.u.)	Max Pg (p.u.)	Min Pg (p.u.)	Initial value Qg0 (p.u.)	Max Qg (p.u.)	Min Qg (p.u.)
1	20	10	5.00	7.00	1.00	1.93	4.5	-1.0
3	20	10	4.00	7.00	1.00	0.70	4.5	-1.0

IEEE 14 bus system input data, as used in Chapters 2, 3, 4, 5 and 6.

Table AVIII.4: 14 bus system transmission line and transformer data

Line no.	Bus *i*	Bus *j*	Resistance R_{ij} (p.u.)	Reactance X_{ij} (p.u.)	Susceptance B_c (p.u.)	Power transfer limit S_{ij}^{max} (p.u.)	Tap ratio
1	1	2	0.01938	0.05917	0.02640	1.50	1
2	1	5	0.05403	0.22304	0.02460	1.50	1
3	2	3	0.04699	0.19797	0.02190	1.30	1
4	2	4	0.05811	0.17632	0.01870	1.30	1
5	2	5	0.05695	0.17388	0.01700	0.90	1
6	3	4	0.06701	0.17103	0.01730	0.65	1
7	4	5	0.01335	0.04211	0.00640	1.30	1
8 T	4	7	0.00000	0.20912	0.00000	0.65	0.978
9 T	4	9	0.00000	0.55618	0.00000	0.65	0.969
10 T	5	6	0.00000	0.25202	0.00000	0.65	0.932
11	6	11	0.09498	0.19890	0.00000	0.65	1
12	6	12	0.12291	0.25581	0.00000	0.65	1
13	6	13	0.06615	0.13027	0.00000	0.32	1
14	7	8	0.00000	0.17615	0.00000	0.32	1
15	7	9	0.00000	0.11001	0.00000	0.65	1
16	9	10	0.03181	0.08450	0.00000	0.16	1
17	9	14	0.12711	0.27038	0.00000	0.32	1
18	10	11	0.08205	0.19207	0.00000	0.16	1
19	12	13	0.22092	0.19988	0.00000	0.65	1
20	13	14	0.17093	0.34802	0.00000	0.16	1

Table AVIII.5: 14 bus system bus and demand data

Bus no.	Bus type*	P demand (p.u.)	Q demand (p.u.)
1	0	0.000	0.000
2	1	0.217	0.127
3	1	0.942	0.190
4	2	0.478	-0.039
5	2	0.076	0.016
6	1	0.112	0.075
7	2	0.000	0.000
8	1	0.000	0.000
9	2	0.295	0.166
10	2	0.090	0.058
11	2	0.035	0.018
12	2	0.061	0.016
13	2	0.135	0.058
14	2	0.149	0.050

* Bus Type: (0) swing bus, (1) generator bus (PV bus), and (2) load bus (PQ bus).

Table ABIII.6: 14 bus system generator data

Generator bus no. *i*	$C_{g_i}^{+}$ (p.u.)	$C_{g_i}^{-}$ (p.u)	Initial value Pg0 (p.u.)	Max Pg (p.u.)	Min Pg (p.u.)	Initial value Qg0 (p.u.)	Max Qg (p.u.)	Min Qg (p.u.)
1	20	10	1.74	4.00	0.00	0.00	1.50	-1.00
2	20	10	0.40	1.00	0.00	0.00	0.5	-0.40
3	20	10	0.15	1.00	0.00	0.10	0.40	0.00
6	20	10	0.15	1.00	0.00	0.00	0.24	-0.06
8	20	10	0.15	1.00	0.00	0.00	0.24	-0.06

IEEE 30 bus system input data, as used in Chapters 3, 4, 5 and 6.

Table AVIII.7: 30 bus system transmission line and transformer data

Line no.	Bus *i*	Bus *j*	Resistance R_{ij} (p.u.)	Reactance X_{ij} (p.u.)	Susceptance B_c (p.u.)	Power transfer limit S_{ij}^{max} (p.u.)	Tap ratio
1	1	2	0.0192	0.0575	0.0528	1.30	1
2	1	3	0.0452	0.1852	0.0408	1.30	1
3	2	4	0.0570	0.1737	0.0368	0.65	1
4	3	4	0.0132	0.0379	0.0084	1.30	1
5	2	5	0.0472	0.1983	0.0418	1.30	1
6	2	6	0.0581	0.1763	0.0374	0.65	1
7	4	6	0.0119	0.0414	0.0090	0.90	1
8	5	7	0.0460	0.1160	0.0204	0.70	1
9	6	7	0.0267	0.0820	0.0170	1.30	1
10	6	8	0.0120	0.0420	0.0090	0.32	1
11T	6	9	0.0100	0.2080	0.0000	0.65	1.0155
12T	6	10	0.0100	0.5560	0.0000	0.32	0.9629
13	9	11	0.0000	0.2080	0.0000	0.65	1
14	9	10	0.0000	0.1100	0.0000	0.65	1
15T	4	12	0.0100	0.2560	0.0000	0.65	1.0129
16	12	13	0.0000	0.1400	0.0000	0.65	1
17	12	14	0.1231	0.2559	0.0000	0.32	1
18	12	15	0.0662	0.1304	0.0000	0.32	1
19	12	16	0.0945	0.1987	0.0000	0.32	1
20	14	15	0.2210	0.1997	0.0000	0.16	1
21	16	17	0.0824	0.1932	0.0000	0.16	1
22	15	18	0.1070	0.2185	0.0000	0.16	1
23	18	19	0.0639	0.1292	0.0000	0.16	1
24	19	20	0.0340	0.0680	0.0000	0.32	1

Table AVIII.7: continued.

Line no.	Bus *i*	Bus *j*	Resistance R_{ij} (p.u.)	Reactance X_{ij} (p.u.)	Susceptance B_c (p.u.)	Power transfer limit S_{ij}^{max} (p.u.)	Tap ratio
25	10	20	0.0936	0.2090	0.0000	0.32	1
26	10	17	0.0324	0.0845	0.0000	0.32	1
27	10	21	0.0348	0.0749	0.0000	0.32	1
28	10	22	0.0727	0.1499	0.0000	0.32	1
29	21	22	0.0116	0.0236	0.0000	0.32	1
30	15	23	0.1000	0.2020	0.0000	0.16	1
31	22	24	0.1150	0.1790	0.0000	0.16	1
32	23	24	0.1320	0.2700	0.0000	0.16	1
33	24	25	0.1885	0.3292	0.0000	0.16	1
34	25	26	0.2544	0.3800	0.0000	0.16	1
35	25	27	0.1093	0.2087	0.0000	0.16	1
36T	28	27	0.0100	0.3960	0.0000	0.65	0.9581
37	27	29	0.2198	0.4153	0.0000	0.16	1
38	27	30	0.3202	0.6027	0.0000	0.16	1
39	29	30	0.2399	0.4533	0.0000	0.16	1
40	8	28	0.0636	0.2000	0.0428	0.32	1
41	6	28	0.0169	0.0599	0.0130	0.32	1

Table AVIII.8: 30 bus system bus and demand data

Bus no.	Bus type*	P demand (p.u.)	Q demand (p.u.)
1	0	0.0000	0.000
2	1	0.2170	0.127
3	2	0.0240	0.012
4	2	0.0760	0.016
5	1	0.9420	0.190
6	2	0.0000	0.000
7	2	0.2280	0.109
8	1	0.3000	0.300
9	2	0.0000	0.000
10	2	0.0580	0.020
11	1	0.0000	0.000
12	2	0.1120	0.075
13	1	0.0000	0.000
14	2	0.0620	0.016
15	2	0.0820	0.025
16	2	0.0350	0.018
17	2	0.0900	0.058
18	2	0.0320	0.009
19	2	0.0950	0.034
20	2	0.0220	0.007
21	2	0.1750	0.112
22	2	0.0000	0.000
23	2	0.0320	0.016
24	2	0.0870	0.087
25	2	0.0000	0.000
26	2	0.0350	0.023
27	2	0.0000	0.000
28	2	0.0000	0.000
29	2	0.0240	0.009
30	2	0.1060	0.019
31	2	0.0000	0.000

* Bus Type: (0) swing bus, (1) generator bus (PV bus), and (2) load bus (PQ bus).

Table AVIII.9: 30 bus system generator data

Generator bus no. i	$C^{+}_{g_i}$ (p.u.)	$C^{-}_{g_i}$ (p.u)	Initial value Pg0 (p.u.)	Max Pg (p.u.)	Min Pg (p.u.)	Initial value Qg0 (p.u.)	Max Qg (p.u.)	Min Qg (p.u.)
1	20	10	1.770	2.00	0.50	0.0279	3.00	0.40
2	20	10	0.460	0.80	0.2	0.0247	1.00	0.20
5	20	10	0.190	0.50	0.15	0.2257	0.80	0.15
8	20	10	0.170	0.37	0.10	0.3484	0.60	0.15
11	20	10	0.122	0.30	0.10	0.3078	0.50	0.10
13	20	10	0.122	0.40	0.12	0.3783	0.60	0.15

IEEE 30 bus system setup

Table AVIII.10: 30 bus Systems I, II and III comparison with STATCOM and UPFC.

System number	I	II	IIIa	IIIb
System description (across) / Total system values (down) (units: p.u.)	No congestion	Congestion no FACTS 70% Load Rise	STATCOM at Bus 3 70% Load Rise	UPFC at Line 1-2 70% Load Rise
Demand $\sum_{i}^{N_d} P_{d_i}$	2.83	4.19	4.19	4.19
Scheduled generation $\sum_{i}^{N_g} P^{0}_{g_i}$	2.83	4.97	4.97	4.97
Generation increase $\sum_{i}^{N_g} \Delta P^{+}_{g_i}$	0.092	0.954	1.146	0.486
Generation decrease $\sum_{i}^{N_g} \Delta P^{-}_{g_i}$	0.000	0.939	1.120	0.411
Generation output $\sum_{i}^{N_g} P_{g_i OUT}$	2.93	4.99	5.00	5.05
Loss P_{LOSS}	0.09	0.17	0.18	0.23
% Ploss w.r.t. $\sum_{i}^{N_g} P^{0}_{g_i}$	3.2 %	3.4 %	3.7 %	4.7 %
P^{0}_{g} Excess P_{EXCESS}	0.00	0.16	0.16	0.16
Result type /Condition (Table. 3-3 and Table 3-4)	N/A	N/A	B(ii)/2	B(ii)/2
Total cost $f(x)$ \$/h	1.84	28.46	34.11	13.83
% Cost reduction wrt System II	N/A	N/A	-20 %	51 %
% Cost due to P_{LOSS}	100 %	67 %	67 %	70 %
% Cost due to congestion	0 %	33 %	33 %	30 %
% Cost due to P_{EXCESS}	None	N/A $P_{EXCESS} < P_{LOSS}$	N/A $P_{EXCESS} < P_{LOSS}$	N/A $P_{EXCESS} < P_{LOSS}$
Congested lines	None	1-2, 2-6, 6-8, 12-15	1-2, 2-6, 9-10, 12-13, 12-15, 25-27	1-2, 1-3, 6-8, 12-13, 12-15
FACTS Controller rating MVA	N/A	N/A	83.5	82.2